Highly effective yet simple transmembrane anion transporters based upon *ortho*-phenylenediamine bis-ureas

Louise E. Karagiannidis[a], Cally J. E. Haynes[a], Katie J. Holder[a], Isabelle L. Kirby[a], Stephen J. Moore[a], Neil J. Wells[a] and Philip A. Gale [a]*

[a]Chemistry, University of Southampton, Southampton SO17 1BJ, UK

Table of Contents

S1: Overview of Compounds

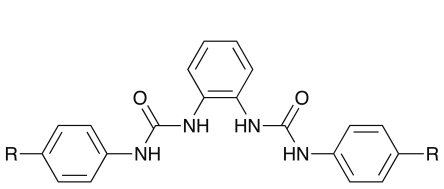

1 R = CF_3
2 R = SF_5

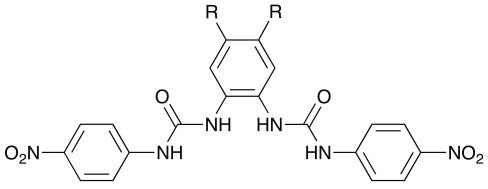

5 R = H
6 R = F

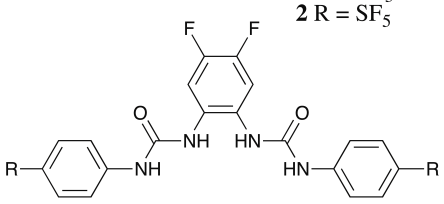

3 R = CF_3
4 R = SF_5

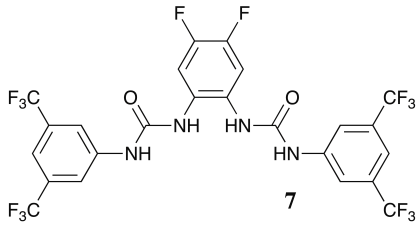

7

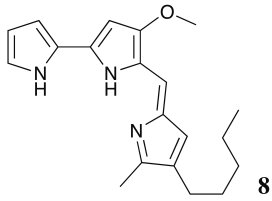

8

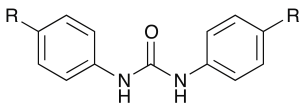

9 R = CF_3
10 R = SF_5

S2: General Procedures

All starting materials and solvents were purchased from commercial sources and used without further purification unless stated otherwise.

All NMR data were recorded on Bruker AVII400 or Bruker AV11HD400 FT-NMR spectrometers and referenced to the indicated solvent at 298 K. The $^{19}F\{^1H\}$ NMR were externally referenced to $CFCl_3$ in the corresponding solvent. Chemical shifts are reported on the delta scale and abbreviations used for spin multiplicity of peaks include: s = singlet, d = doublet, t = triplet, q = quartet, quin = quintet, m = multiplet, br = broad.

All receptor samples were submitted to the University of Southampton Institute for Applied Mass Spectrometry (**UoSIAMS**) for HRMS (ES). Samples were analysed using a MaXis (Bruker Daltonics, Bremen, Germany) mass spectrometer equipped with a Time of Flight (TOF) analyser. The sample was introduced via a Diones Ultimate 3000 autosampler and uHPLC pump. Gradient 20% acetonitrile (0.2% formic acid) to 100% acetonitrile (0.2% formic acid) in five minutes at a flow rate of 0.6 mL/min. High resolution was spectra were recorded using positive/negative electrospray ionization.

Melting point (Mp) analyses were carried out using a Barnstead Electrothermal IA9100 melting point machine.

S3: Synthesis

1,1'-(1,2-phenylene)bis(3-(4-(pentafluorosulfanyl)phenyl)urea) (**2**)

CDI (0.37 g, 2.30 mmol) was dissolved in DCM (12.5 mL). 4-Aminophenyl sulfur pentafluoride (0.50 g, 2.30 mmol) was also dissolved in DCM (2.5 mL) and added to the CDI solution. The reaction was stirred for 23.5 hrs at RT under N_2. *o*-Phenylene diamine (0.12 g, 1.15 mmol) was added to the reaction and the mixture stirred at RT under N_2 for 2 hrs. An off white precipitate was isolated from the organic phase, dissolved in MeOH and pushed through an SCX-2 column to remove impurities and unreacted amine. The solvent was removed to give a white solid (86% yield). ^{1}H NMR (DMSO-d_6, 400 MHz): δ (ppm) = 7.14 (dd, 2H, J = 6.0, 3.8 Hz), 7.60 (dd, 2H, J = 6.0, 3.7 Hz), 7.65 (d, 4H, J = 8.9 Hz), 7.80 (d, 4H, J = 8.9 Hz), 8.20 (s, 2H), 9.58 (s, 2H). ^{13}C{^{1}H} NMR (DMSO-d_6, 400 MHz): δ (ppm) = 117.44 (s, Ar CH), 124.31 (s, Ar CH), 124.53 (s, Ar CH), 126.77 (m, Ar CH), 131.05 (s, C-N), 143.24 (s, C-N), 145.96 (m, Ar C-SF_5), 152.86 (s, C=O). ^{19}F{^{1}H} NMR (DMSO-d_6, 500 MHz): δ (ppm) = 65.24 (d, 8F, J = 150.5 Hz), 89.39 (quin, 2F, J = 151.4 Hz). LRMS ESI$^-$ (m/z): 597.0 [M-H$^+$]$^-$. HRMS ESI$^+$ (m/z): 599.0628 [M+H$^+$]$^+$, err. (ppm) 2.4. Mp (°C): 238.1 – 239.4.

1,1'-(4,5-Difluoro-1,2-phenylene)bis(3-(4-(trifluoromethyl)phenyl)urea) (**3**)

4,5-Difluoro-*ortho*-phenylenediamine (373.6 mg, 2.59 mmol) was dissolved in DCM (20 mL) and pyridine (2.5 mL). 4-(trifluoromethyl)phenyl isocyanate (0.75 mL, 5.35 mmol) was added to the reaction. The reaction appeared a red colour and thickened immediately so additional DCM (20 mL) was added. The white precipitate was filtered off and washed with excess DCM. The precipitate was dissolved in MeOH with the aid of sonication and passed through an SCX-2 column to remove starting material amine and pyridine. The solid was dried *in vacuo* (68% yield). ^{1}H NMR (DMSO-d_6, 500 MHz): δ (ppm) = 7.64 (d, 4H, J = 11.2 Hz), 7.69 (d, 4H, J = 11.5 Hz), 7.72 (t, 2H, J = 10.5 Hz), 8.26 (s, 2H), 9.54 (s, 2H). ^{13}C{^{1}H} NMR (DMSO-d_6, 500 MHz): δ (ppm) = 112.59 (m, Ar CH), 117.96 (s, Ar CH), 122.02 (q, Ar C-CF_3, J = 31.9 Hz), 124.52 (q, CF_3, J = 270.9 Hz), 126.11 (q, Ar CH, J = 3.8 Hz), 127.86 (t, C-N, J = 5.6 Hz), 143.30 (s, C-N), 145.54 (dd, Ar C-F, J = 243.9, 15.7 Hz), 152.83 (s, C=O). ^{19}F{^{1}H} NMR (DMSO-d_6, 500 MHz): δ (ppm) = -142.44 (s, 2F), -60.18 (s, 6F). LRMS ESI$^-$ (m/z): 518.1 [M-H$^+$]$^-$. HRMS ESI$^+$ (m/z): 519.1062 [M+H$^+$]$^+$, err. (ppm) -0.5. Mp (°C): 216.5 – 217.5.

1,1'-(4,5- Difluoro-1,2-phenylene)bis(3-(4-(pentafluorosulfanyl)phenyl)urea) (**4**)

CDI (0.37 g, 2.30 mmol) was dissolved in DCM (5 mL). 4-Aminophenyl sulfur pentafluoride (0.50 g, 2.30 mmol) was also dissolved in DCM (5 mL) and added to the CDI solution. The reaction was stirred for 25 hrs at RT under N_2. 1,2-Diamino-4,5-difluorobenzene (0.16 g, 1.14 mmol) was dissolved in DCM (6 mL) and dry pyridine (1.5 mL) and added to the reaction. The mixture was stirred at RT under N_2 for 5 hrs. The resultant precipitate was collected by vacuum filtration and washed by sonication in DCM. The solvent was removed to give a white solid (23% yield). ^{1}H NMR (DMSO-d_6, 500 MHz): δ (ppm) = 7.65 (d, 4H, J = 9.2 Hz), 7.73 (t, 2H, J = 10.5 Hz), 7.80 (m, 4H, J = 9.3 Hz), 8.27 (s, 2H), 9.63 (s, 2H). ^{13}C{^{1}H} NMR (DMSO-d_6, 500 MHz): δ (ppm) = 112.65 (m, Ar CH), 117.58 (s, Ar CH), 126.79 (m, Ar CH), 127.81 (t, C-N, J = 5.6 Hz), 142.97 (s, C-N), 145.54 (dd, Ar C-F, J = 243.7, 16.7 Hz), 146.15 (m, Ar C-SF_5), 152.72 (s, C=O). ^{19}F{^{1}H} NMR (DMSO-d_6, 500 MHz): δ (ppm) = -142.26 (t, 2F, J = 10.0 Hz), 65.15 (d, 8F, J = 150.7 Hz), 89.20 (quin, 2F, J = 151.1 Hz). LRMS ESI^- (m/z): 632.8 $[M\text{-}H^+]^-$. HRMS ESI^+ (m/z): 635.0439 $[M+H^+]^+$, err. (ppm) -0.8. Mp (°C): 248.0 – 249.0.

1,1'-(4,5-Difluoro-1,2-phenylene)bis(3-(4-nitrophenyl)urea) (**6**)

To 4,5-Difluoro-*ortho*-phenylenediamine (223.8 mg, 1.55 mmol) and 4-nitrophenyl isocyanate (151.8 mg, 3.12 mmol) was added DCM (20 mL) and pyridine (5 mL). The reaction mixture was stirred for 2 hrs at RT under N_2. The resulting yellow precipitate was removed by filtration and sonicated in DCM (100 mL) for 1 hr. The precipitate was filtered and dried *in vacuo* to yield a yellow solid (59% yield). ^{1}H NMR (DMSO-d_6, 400 MHz): δ (ppm) = 7.73 (m, 6H), 8.20 (m, 4H), 8.35 (s, 2H), 9.86 (s, 2H). ^{13}C{^{1}H} NMR (DMSO-d_6, 500 MHz): δ (ppm) = 112.87 (m, Ar CH), 117.61 (s, Ar CH), 125.17 (s, Ar CH), 127.79 (t, C-N, J = 5.4 Hz), 141.21 (s, C-N), 145.68 (dd, Ar C-F, J = 244.5, 15.4 Hz), 146.13 (s, Ar C-NO_2), 152.55 (s, C=O). ^{19}F{^{1}H} NMR (DMSO-d_6, 500 MHz): δ (ppm) = -141.91 (s, 2F). LRMS ESI^- (m/z): 471.2 $[M\text{-}H^+]^-$. HRMS ESI^+ (m/z): 473.1016 $[M+H^+]^+$, err. (ppm) 1.4. Mp = 278.6–279.8 ° C.

1,1'-(4,5-Difluoro-1,2-phenylene)bis(3-(3,5-bis(trifluoromethyl)phenyl)urea) (**7**)

4,5-Difluoro-*ortho*-phenylenediamine (0.27 mg, 1.85 mmol) was dissolved in DCM (20 mL) and dry pyridine (5 mL). 3,5-bis(trifluoromethyl)isocyanate (0.64 mL, 3.70 mmol) was added and the reaction stirred for 4 hrs at RT under N_2. No change was observed hence the reaction was heated to reflux overnight. Again no change was observed. The solvent was removed *in vacuo* and the residues dissolved in EtOAc before washing with H_2O over $MgSO_4$. The resultant residues were passed through an SCX-2 column in MeOH and before the solvent was once again removed *in vacuo*. The product was then recrystallized from EtOAc (32% yield). ^{1}H NMR (DMSO-d_6, 500 MHz): δ (ppm) = 7.62 (s, 2H), 7.73 (t, 2H, J = 10.4 Hz), 8.11 (s, 4H), 8.38 (s, 2H), 9.82 (s, 2H). $^{13}C\{^1H\}$ NMR (DMSO-d_6, 500 MHz): δ (ppm) = 113.23 (m, Ar CH), 114.56 (m, Ar CH), 118.02 (m, Ar CH), 123.26 (q, CF_3, J = 272.6 Hz), 128.02 (m, C-N), 130.72 (q, C-CF_3, J = 32.7 Hz), 141.66 (s, C-N), 145.85 (dd, C-F, J = 244.4, 15.3 Hz), 152.98 (s, C=O) $^{19}F\{^1H\}$ NMR (DMSO-d_6, 500 MHz): δ (ppm) = -141.83 (s, 2F), -61.83 (s, 12F). LRMS ESI^- (m/z): 652.9 $[M-H^+]^-$. HRMS ESI^+ (m/z): 655.0809 $[M+H^+]^+$, err. (ppm) -1.3. Mp = 231.0–232.1 ° C.

(Bis(4-pentafluorosulfanyl)phenyl)urea (**10**)

1,1'-Carbonyl diimidazole (CDI) (1.03 g, 6.33 mmol) was dissolved in DCM (15 mL). 4-Aminophenyl sulfur pentafluoride (0.47 g, 2.16 mmol) was also dissolved in DCM (10 mL) and added to the CDI solution. The reaction was stirred for 23 hrs at room temperature (RT). The solvent was reduced *in vacuo* to 15 ml prior to washing with water (2 x 20 mL) to remove unreacted CDI. A white precipitate was isolated from the organic phase and washed with excess DCM (12% yield). ^{1}H NMR (DMSO-d_6, 400 MHz): δ (ppm) = 7.66 (d, 4H, J = 9.0 Hz), 7.82 (d, 4H, J = 9.4 Hz), 9.37 (s, 2H). $^{13}C\{^1H\}$ NMR (DMSO-d_6, 400 MHz): δ (ppm) = 117.84 (s, Ar CH), 126.81 (br s, Ar CH), 142.70 (s, C-N), 146.35 (m, Ar C-SF_5), 151.95 (s, C=O). $^{19}F\{^1H\}$ NMR (DMSO-d_6, 500 MHz): δ (ppm) = 65.13 (d, 8F, J = 150.7 Hz), 89.10 (quin, 2F, J = 150.9 Hz). LRMS ESI^- (m/z): 462.9 $[M-H^+]^-$. HRMS ESI^+ (m/z): 465.0148 $[M+H^+]^+$, err. (ppm) 1.0. Mp (°C): 285.9 – 287.6, followed by immediate decomposition.

S5: Characterisation

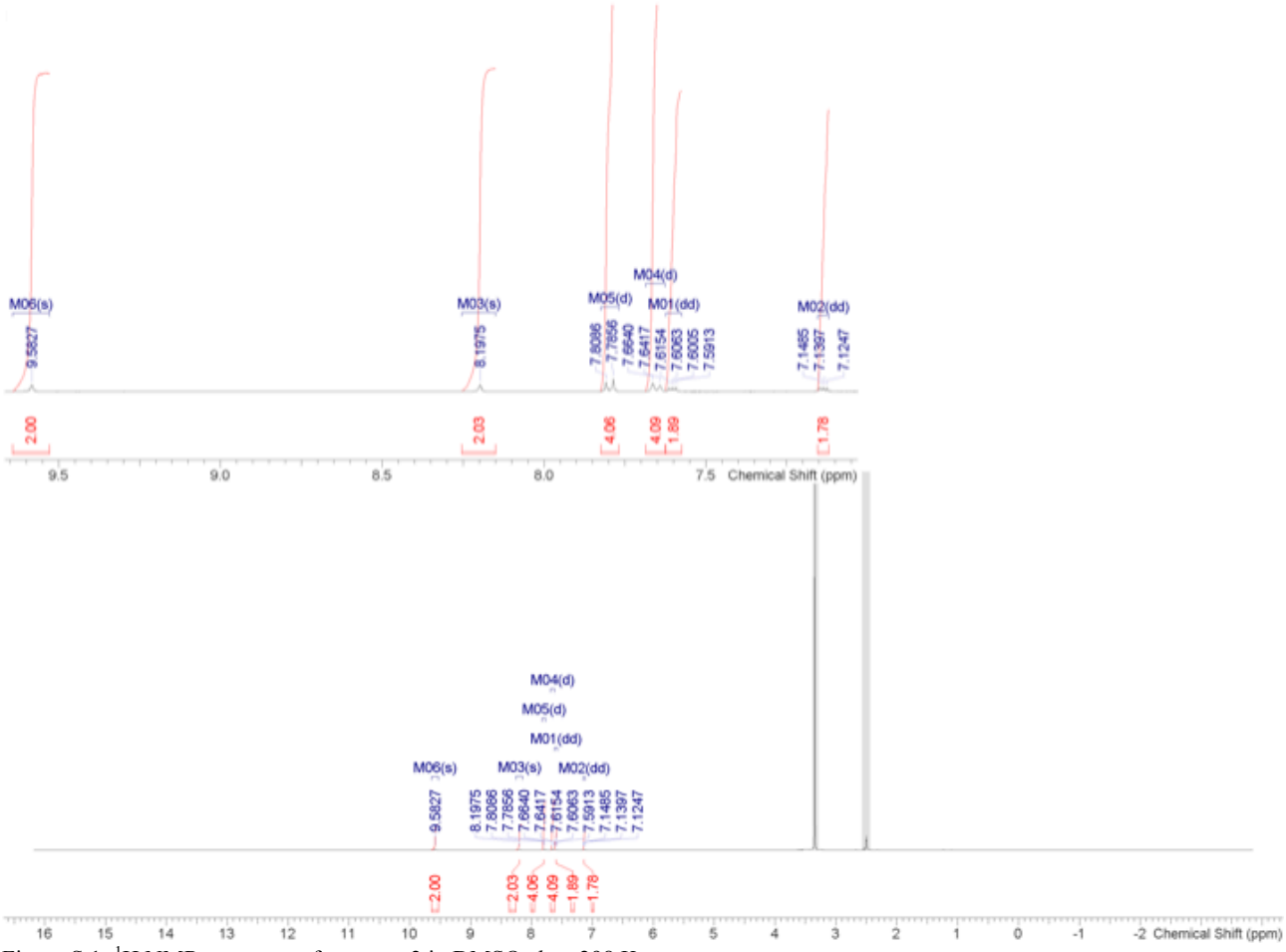

Figure S 1: ^{1}H NMR spectrum of receptor **2** in DMSO-d_6 at 298 K.

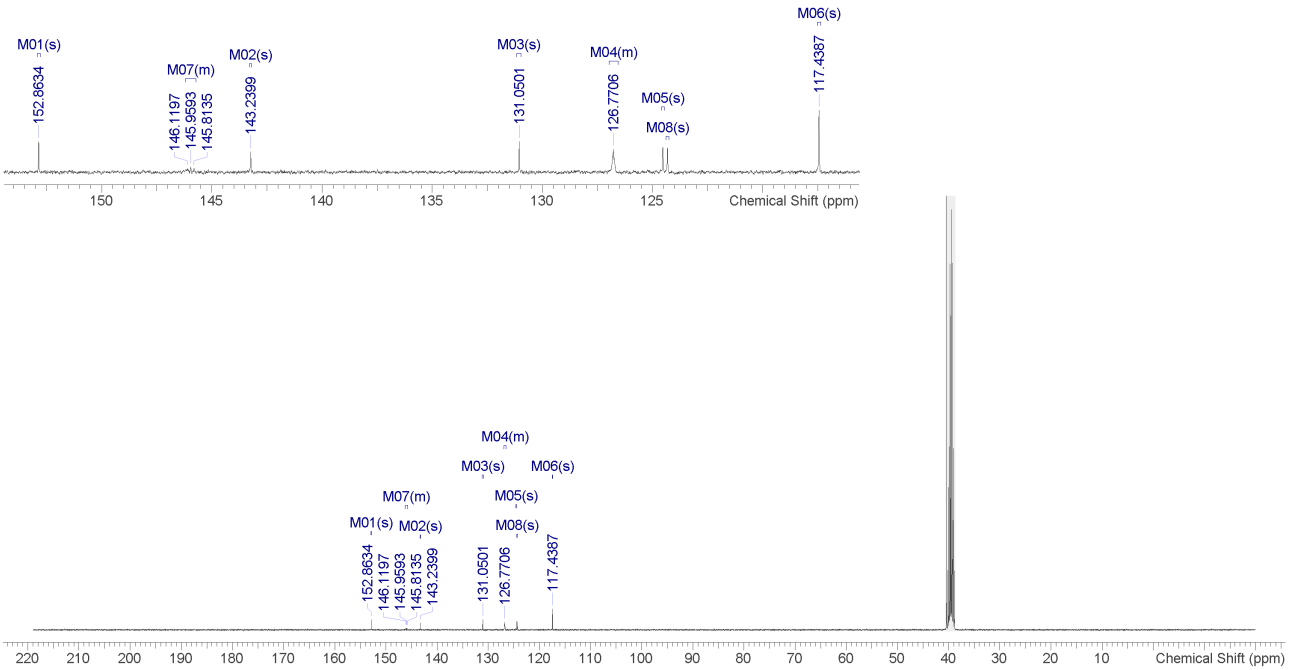

Figure S 2: :^{13}C{^{1}H} NMR spectrum of receptor **2** in DMSO-d_6 at 298 K.

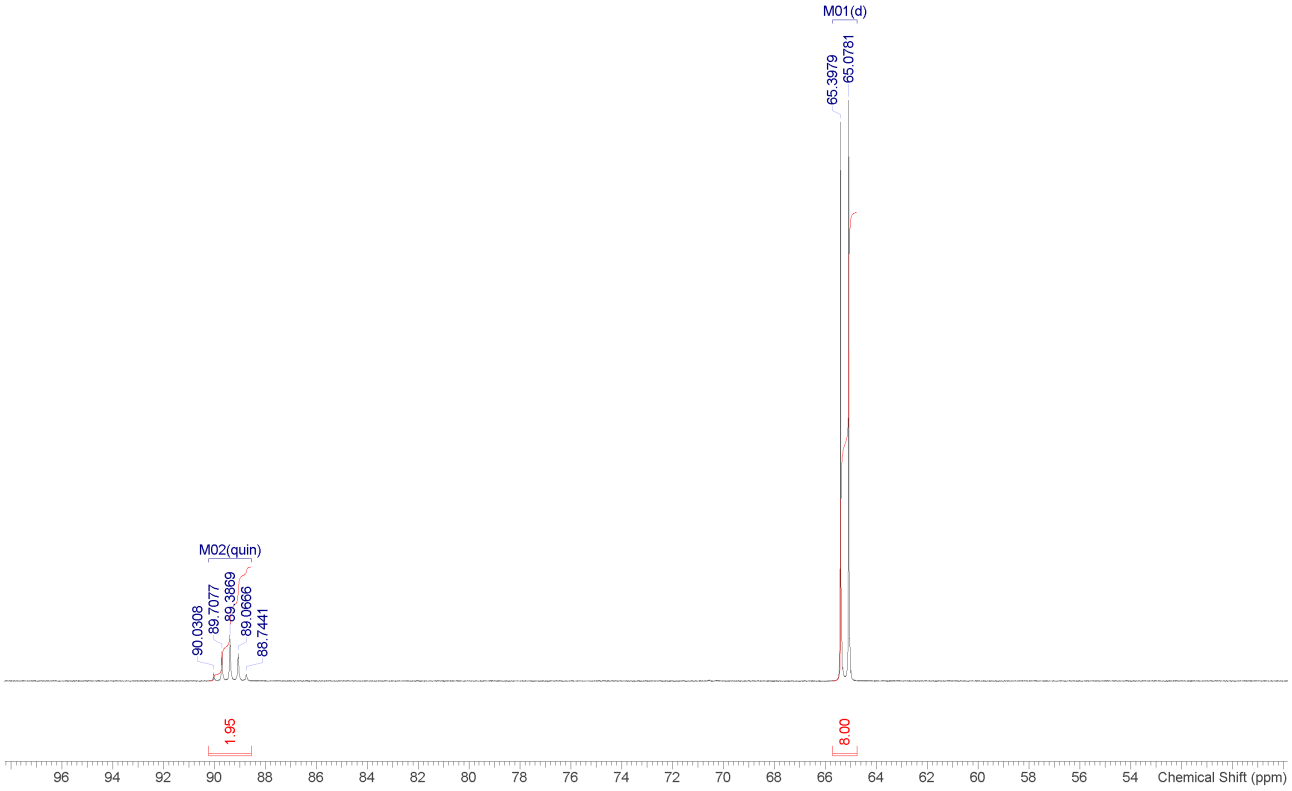

Figure S 3: $^{19}F\{^{1}H\}$ NMR spectrum of receptor **2** in DMSO-d_6 at 298 K.

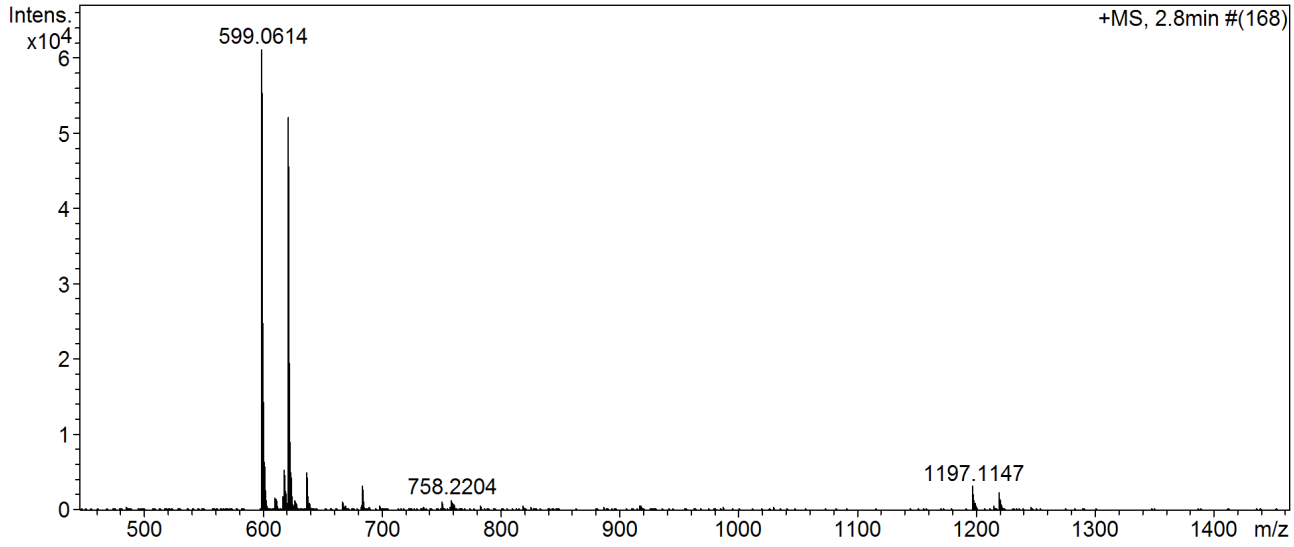

Meas. m/z	Formula	m/z	err [ppm]	err [mDa]	# Sigma	mSigma	rdb	e^- Conf	N-Rule
599.0614	C 24 H 18 F 7 O 8 S	599.0605	-1.4	-0.8	1	6.9	12.5	even	ok
	C 22 H 17 F 5 N 4 Na O 7 S	599.0630	2.8	1.7	2	7.6	13.5	even	ok
	C 22 H 15 F 8 N 4 O 5 S	599.0630	2.7	1.6	3	9.7	13.5	even	ok
	C 20 H 12 F 5 N 10 O 5 S	599.0628	2.3	1.4	4	9.7	17.5	even	ok
	C 18 H 14 F 7 N 10 O 2 S 2	599.0625	2.0	1.2	5	10.8	13.5	even	ok
	C 20 H 17 F 10 N 4 O 2 S 2	599.0628	2.4	1.4	6	11.0	9.5	even	ok
	C 21 H 21 F 5 Na O 11 S	599.0617	0.6	0.3	7	12.0	8.5	even	ok
	C 20 H 19 F 7 N 4 Na O 4 S 2	599.0628	2.4	1.5	8	12.8	9.5	even	ok
	C 20 H 17 F 6 N 6 O 5 S 2	599.0601	-2.2	-1.3	9	13.3	12.5	even	ok
	C 22 H 20 F 9 O 5 S 2	599.0603	-1.8	-1.1	10	13.3	8.5	even	ok
	C 21 H 12 F 8 N 8 Na O S	599.0619	1.0	0.6	11	14.7	15.5	even	ok
	C 23 H 16 F 9 N 4 O S 2	599.0616	0.5	0.3	12	14.9	13.5	even	ok
	C 19 H 16 F 5 N 6 O 9 S	599.0614	0.1	0.1	13	14.9	12.5	even	ok
	C 21 H 13 F 6 N 10 O S 2	599.0614	0.1	0.0	14	14.9	17.5	even	ok
	C 19 H 9 F 5 N 14 Na O S	599.0617	0.6	0.3	15	15.0	19.5	even	ok
	C 21 H 19 F 8 O 9 S	599.0617	0.5	0.3	16	15.2	8.5	even	ok
	C 22 H 22 F 6 Na O 7 S 2	599.0603	-1.7	-1.0	17	15.3	8.5	even	ok
	C 18 H 13 F 5 N 10 Na O 5 S	599.0603	-1.7	-1.0	18	16.1	14.5	even	ok
	C 20 H 16 F 8 N 4 Na O 5 S	599.0606	-1.3	-0.8	19	16.2	10.5	even	ok
	C 23 H 18 F 6 N 4 Na O 3 S 2	599.0617	0.5	0.3	20	17.4	13.5	even	ok
	C 18 H 11 F 8 N 10 O 3 S	599.0603	-1.7	-1.0	21	17.7	14.5	even	ok
	C 25 H 14 F 7 N 4 O 4 S	599.0618	0.8	0.5	22	17.8	17.5	even	ok
	C 18 H 18 F 10 N 4 Na O 2 S 2	599.0604	-1.6	-1.0	23	18.4	6.5	even	ok
	C 24 H 21 F 6 O 7 S 2	599.0627	2.3	1.4	24	19.6	11.5	even	ok
	C 26 H 14 F 10 N 2 Na S	599.0610	-0.6	-0.3	25	20.9	15.5	even	ok
	C 24 H 11 F 7 N 8 Na S	599.0608	-1.0	-0.6	26	21.1	19.5	even	ok
	C 18 H 13 F 9 N 8 Na O 2 S	599.0631	2.9	1.7	27	21.5	11.5	even	ok
	C 17 H 18 F 7 N 6 O 6 S 2	599.0612	-0.3	-0.2	28	21.5	8.5	even	ok
	C 19 H 21 F 10 O 6 S 2	599.0614	0.1	0.1	29	21.7	4.5	even	ok
	C 19 H 23 F 7 Na O 8 S 2	599.0615	0.2	0.1	30	22.8	4.5	even	ok
	C 18 H 20 F 5 N 2 O 13 S	599.0601	-2.1	-1.3	31	23.5	7.5	even	ok
	C 26 H 16 F 5 O 11	599.0607	-1.0	-0.6	32	26.6	16.5	even	ok
	C 23 H 17 F 6 O 12	599.0619	0.9	0.5	33	26.6	12.5	even	ok
	C 18 H 22 F 6 Na O 12 S	599.0628	2.5	1.5	34	27.8	4.5	even	ok
	C 18 H 20 F 9 O 10 S	599.0628	2.4	1.4	35	28.9	4.5	even	ok
	C 27 H 20 F 5 O 6 S 2	599.0616	0.4	0.2	36	29.4	15.5	even	ok
	C 25 H 13 F 5 N 4 Na O 7	599.0597	-2.8	-1.7	37	30.4	18.5	even	ok
	C 17 H 17 F 9 N 4 Na O 6 S	599.0617	0.6	0.4	38	30.6	6.5	even	ok
	C 26 H 15 F 8 N 4 S 2	599.0605	-1.4	-0.9	39	30.6	17.5	even	ok
	C 24 H 12 F 5 N 10 S 2	599.0602	-1.8	-1.1	40	30.8	21.5	even	ok
	C 22 H 14 F 6 N 4 Na O 8	599.0608	-0.9	-0.5	41	30.9	14.5	even	ok
	C 26 H 17 F 5 N 4 Na O 2 S 2	599.0605	-1.4	-0.8	42	31.7	17.5	even	ok
	C 28 H 13 F 6 N 4 O 3 S	599.0607	-1.1	-0.6	43	32.9	21.5	even	ok
	C 27 H 12 F 5 N 4 O 7	599.0621	1.2	0.7	44	33.5	21.5	even	ok
	C 20 H 18 F 7 O 13	599.0630	2.8	1.7	45	34.9	8.5	even	ok
	C 25 H 11 F 8 N 4 O 5	599.0596	-2.9	-1.7	46	35.7	18.5	even	ok
	C 25 H 13 F 9 N 2 Na O 4	599.0624	1.7	1.0	47	36.4	15.5	even	ok
	C 22 H 12 F 9 N 4 O 6	599.0608	-1.0	-0.6	48	36.5	14.5	even	ok
	C 23 H 10 F 6 N 8 Na O 4	599.0621	1.3	0.8	49	36.5	19.5	even	ok
	C 20 H 9 F 6 N 10 O 6	599.0605	-1.4	-0.8	50	36.7	18.5	even	ok
	C 28 H 12 F 8 N 2 Na O 3	599.0612	-0.2	-0.1	51	37.4	19.5	even	ok
	C 28 H 16 F 5 N 4 O 2 S 2	599.0629	2.6	1.6	52	38.6	20.5	even	ok
	C 19 H 15 F 7 N 4 Na O 9	599.0619	1.0	0.6	53	38.8	10.5	even	ok
	C 23 H 8 F 9 N 8 O 2	599.0621	1.3	0.7	54	38.8	19.5	even	ok
	C 21 H 5 F 6 N 14 O 2	599.0619	0.8	0.5	55	39.3	23.5	even	ok
	C 21 H 9 F 9 N 8 Na O 2	599.0597	-2.8	-1.7	56	40.7	16.5	even	ok
	C 18 H 6 F 7 N 14 O 3	599.0630	2.8	1.7	57	42.1	19.5	even	ok
	C 26 H 9 F 5 N 8 Na O 3	599.0610	-0.6	-0.4	58	42.5	23.5	even	ok
	C 18 H 19 F 7 Na O 13	599.0606	-1.2	-0.7	59	43.4	5.5	even	ok
	C 26 H 7 F 8 N 8 O	599.0610	-0.7	-0.4	60	45.1	23.5	even	ok
	C 18 H 17 F 10 O 11	599.0606	-1.3	-0.8	61	45.3	5.5	even	ok
	C 31 H 14 F 6 N 2 Na O S	599.0623	1.6	1.0	62	45.4	22.5	even	ok
	C 24 H 4 F 5 N 14 O	599.0607	-1.1	-0.6	63	45.6	27.5	even	ok
	C 19 H 13 F 10 N 4 O 7	599.0619	0.9	0.6	64	45.6	10.5	even	ok
	C 17 H 10 F 7 N 10 O 7	599.0617	0.5	0.3	65	45.6	14.5	even	ok
	C 31 H 11 F 7 N 2 Na O 2	599.0601	-2.1	-1.3	66	47.6	23.5	even	ok
	C 18 H 10 F 10 N 8 Na O 3	599.0608	-0.9	-0.5	67	48.4	12.5	even	ok
	C 31 H 9 F 10 N 2	599.0601	-2.2	-1.3	68	48.7	23.5	even	ok
	C 29 H 6 F 7 N 8	599.0598	-2.6	-1.5	69	49.0	27.5	even	ok
	C 31 H 12 F 5 N 4 O 2 S	599.0596	-3.0	-1.8	70	49.2	25.5	even	ok
	C 33 H 10 F 7 N 2 O 2	599.0625	1.9	1.1	71	55.8	26.5	even	ok
	C 34 H 13 F 5 N 2 Na S	599.0612	-0.3	-0.2	72	61.8	26.5	even	ok
	C 36 H 9 F 6 N 2 O	599.0614	0.0	0.0	73	70.2	30.5	even	ok
	C 39 H 8 F 5 N 2	599.0602	-1.9	-1.1	74	85.2	34.5	even	ok

Figure S 4: HRMS of receptor **2**.

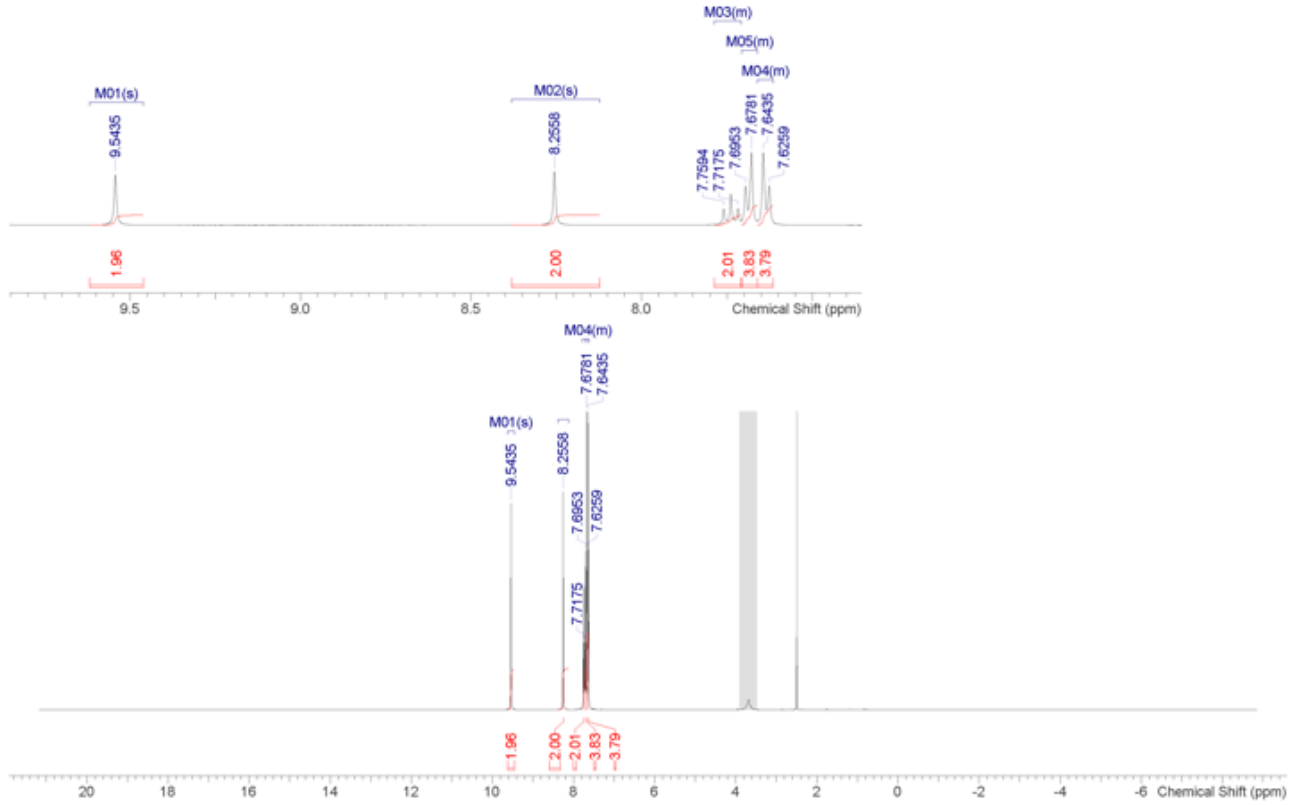

Figure S 5: ^{1}H NMR spectrum of receptor **3** in DMSO-d_6 at 298 K.

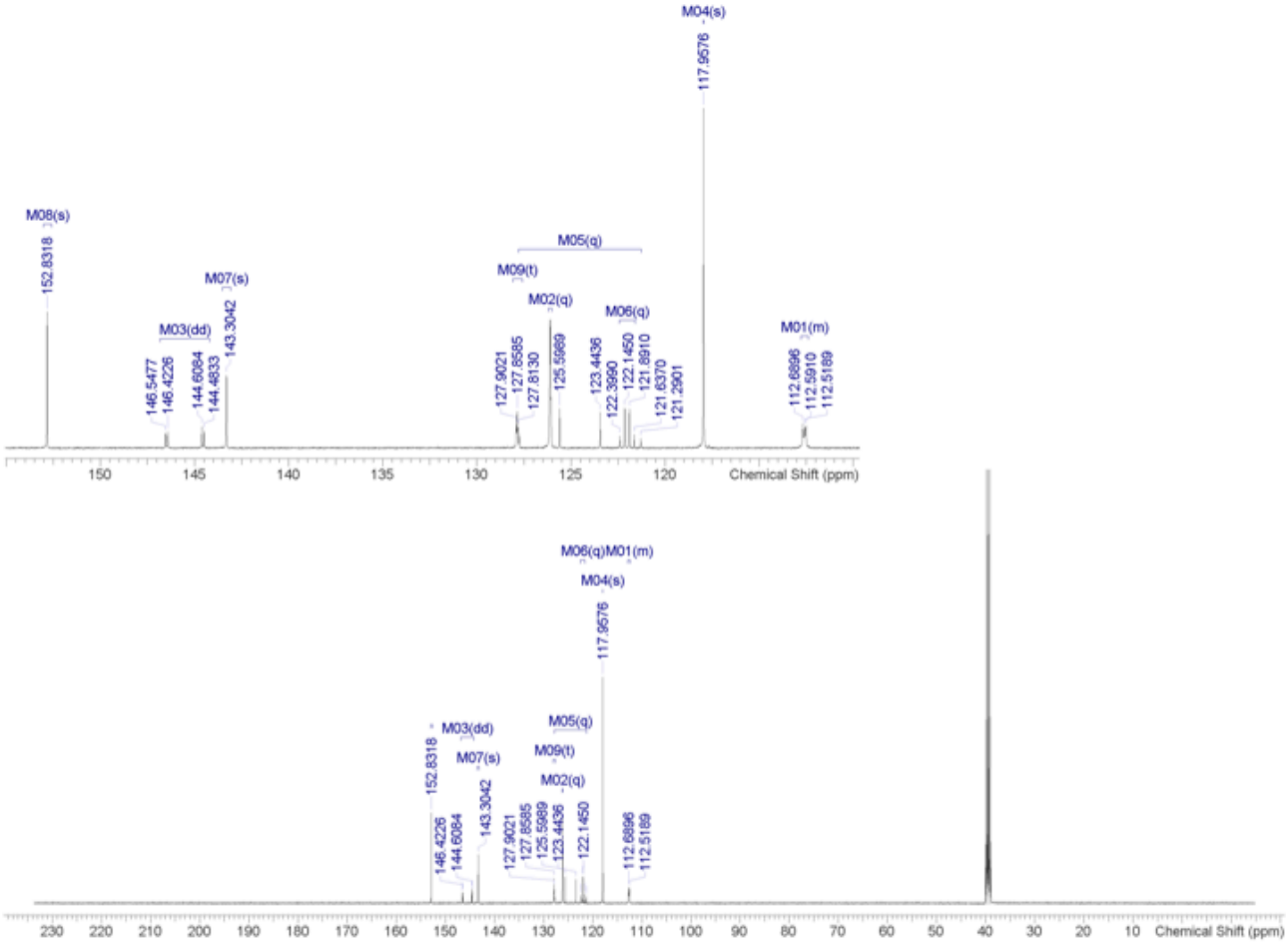

Figure S 6: $^{13}C\{^{1}H\}$ NMR spectrum of receptor **3** in DMSO-d_6 at 298 K.

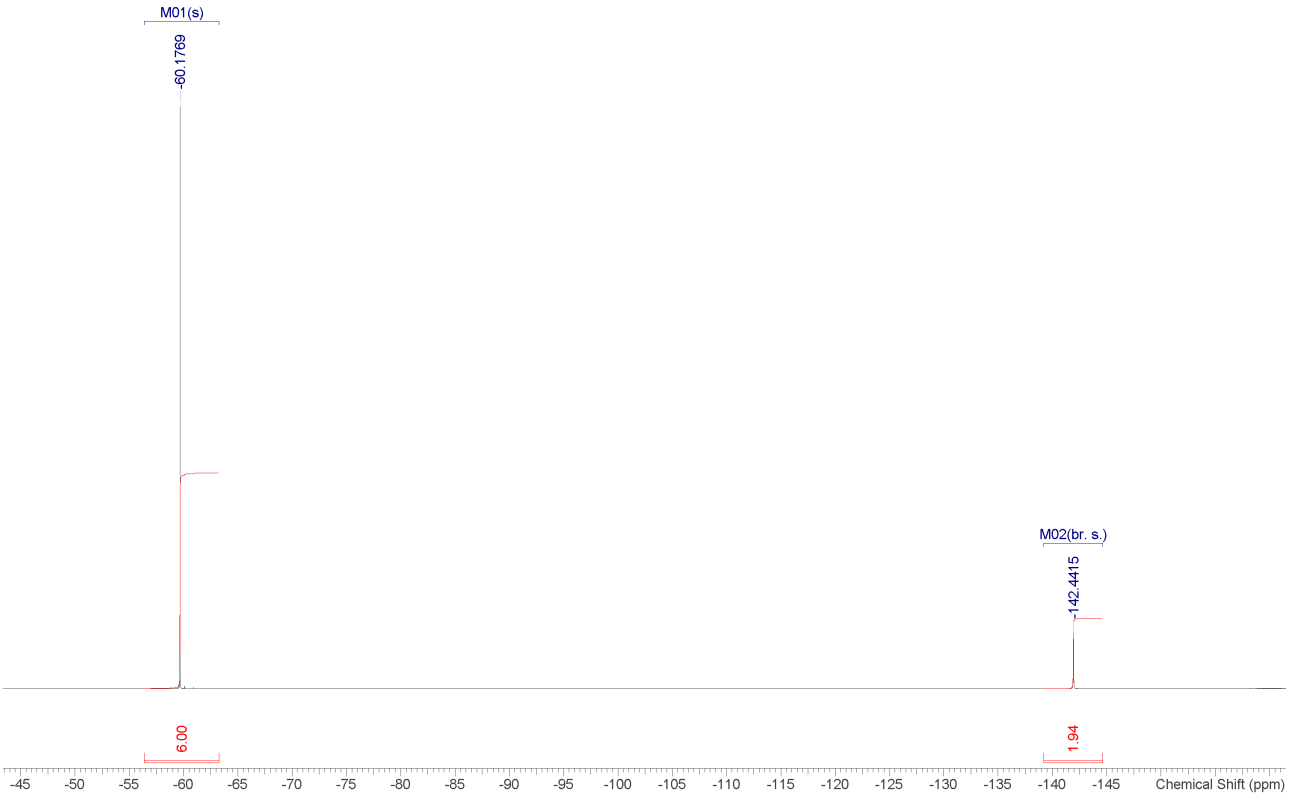

Figure S 7: $^{19}F\{^{1}H\}$ NMR spectrum of receptor **3** in DMSO-d_6 at 298 K.

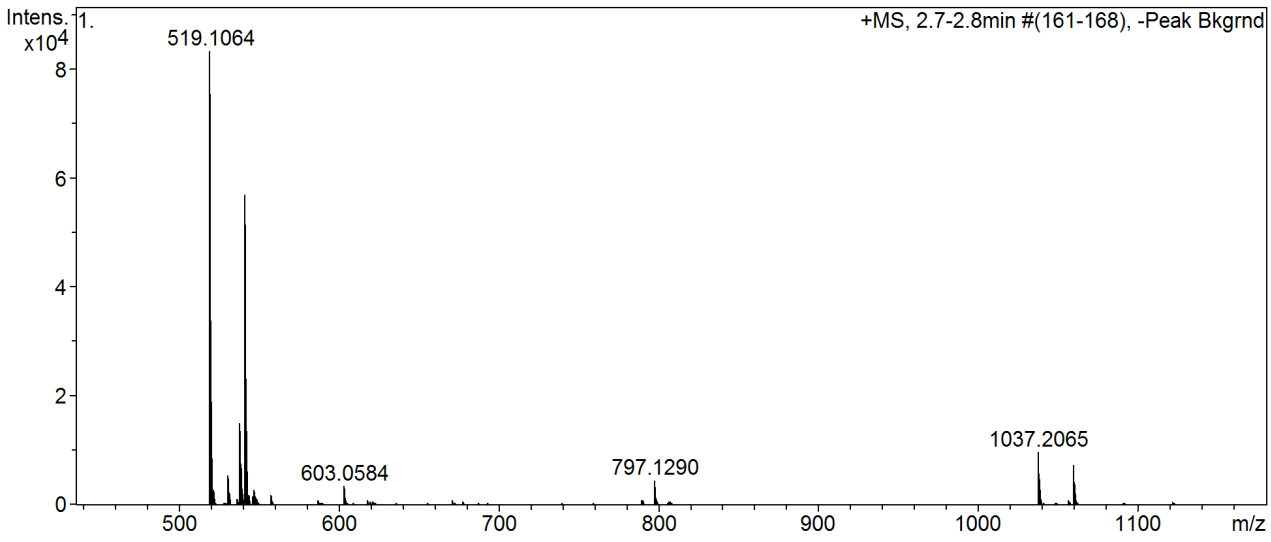

Meas. m/z	Formula	m/z	err [ppm]	err [mDa]	# Sigma	mSigma	rdb	e⁻ Conf	N-Rule
519.1064	C 22 H 15 F 8 N 4 O 2	519.1062	-0.5	-0.3	1	2.3	13.5	even	ok
	C 20 H 12 F 5 N 10 O 2	519.1059	-1.0	-0.5	2	2.4	17.5	even	ok
	C 22 H 17 F 5 N 4 Na O 4	519.1062	-0.4	-0.2	3	4.4	13.5	even	ok
	C 20 H 19 F 7 N 4 Na O S	519.1060	-0.9	-0.4	4	21.6	9.5	even	ok
	C 18 H 22 F 6 Na O 9	519.1060	-0.8	-0.4	5	27.8	4.5	even	ok
	C 24 H 21 F 6 O 4 S	519.1059	-1.0	-0.5	6	30.0	11.5	even	ok
	C 18 H 20 F 9 O 7	519.1060	-0.9	-0.5	7	32.0	4.5	even	ok
	C 17 H 21 F 6 N 6 O 2 S 2	519.1066	0.3	0.2	8	46.2	7.5	even	ok
	C 19 H 24 F 9 O 2 S 2	519.1069	0.8	0.4	9	46.2	3.5	even	ok
	C 19 H 26 F 6 Na O 4 S 2	519.1069	0.9	0.4	10	48.2	3.5	even	ok

Figure S 8: HRMS of receptor **3**.

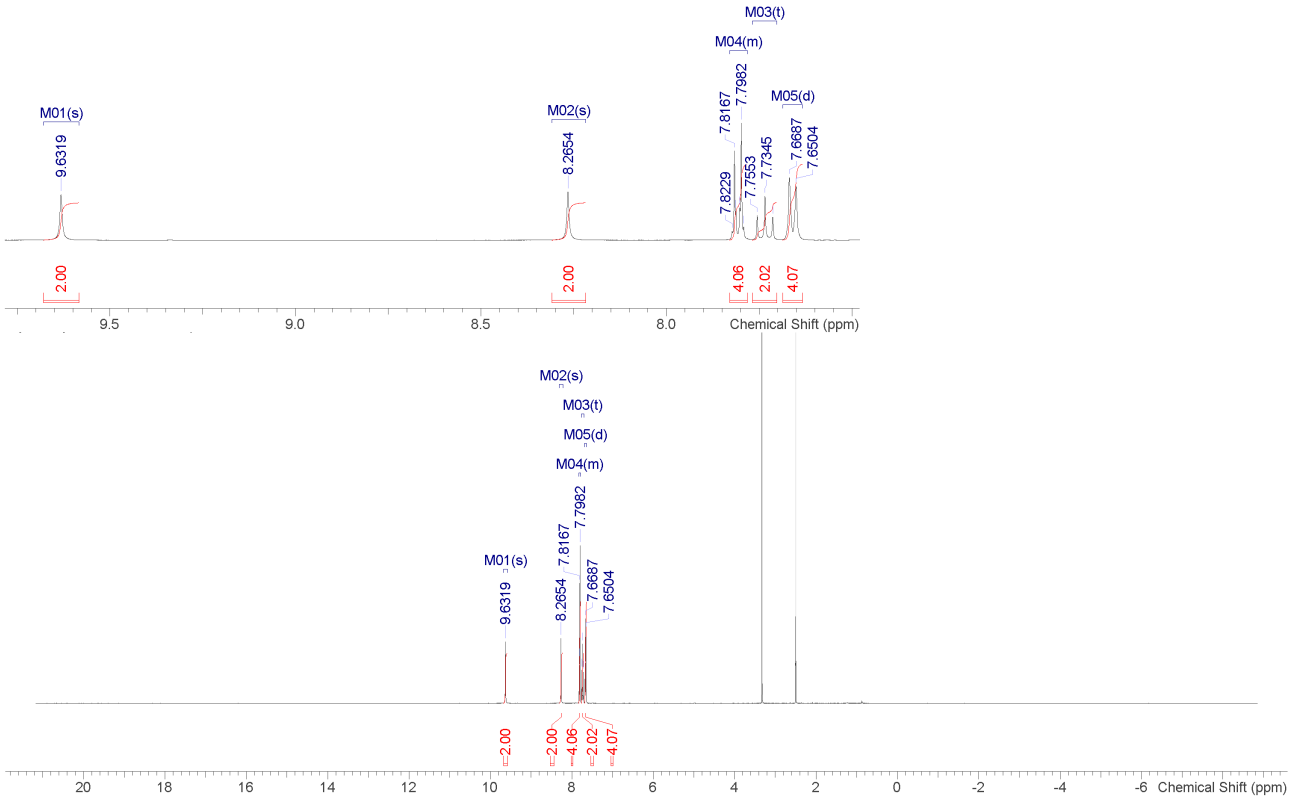

Figure S 9: ^{1}H NMR spectrum of receptor **4** in DMSO-d_6 at 298 K.

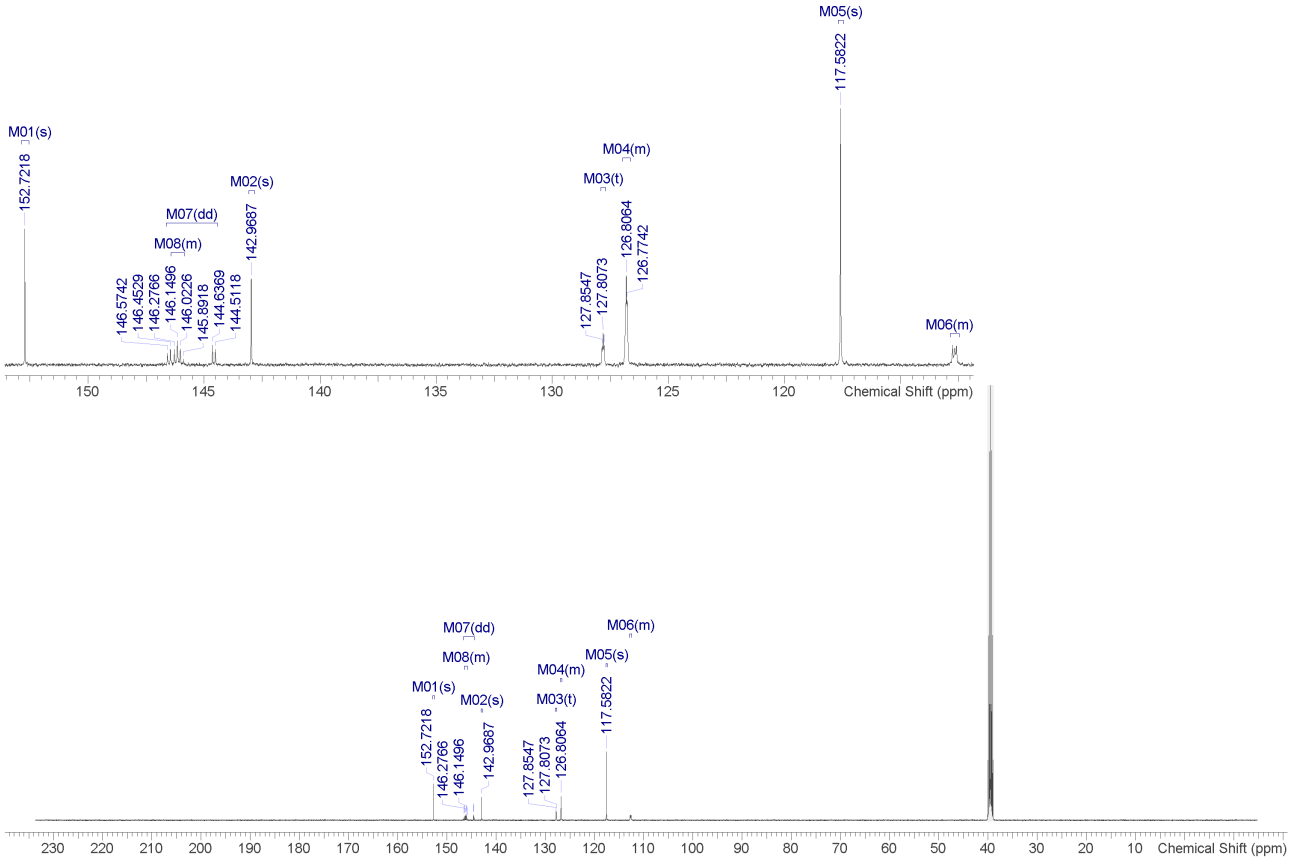

Figure S 10: ^{13}C{^{1}H} NMR spectrum of receptor **4** in DMSO-d_6 at 298 K.

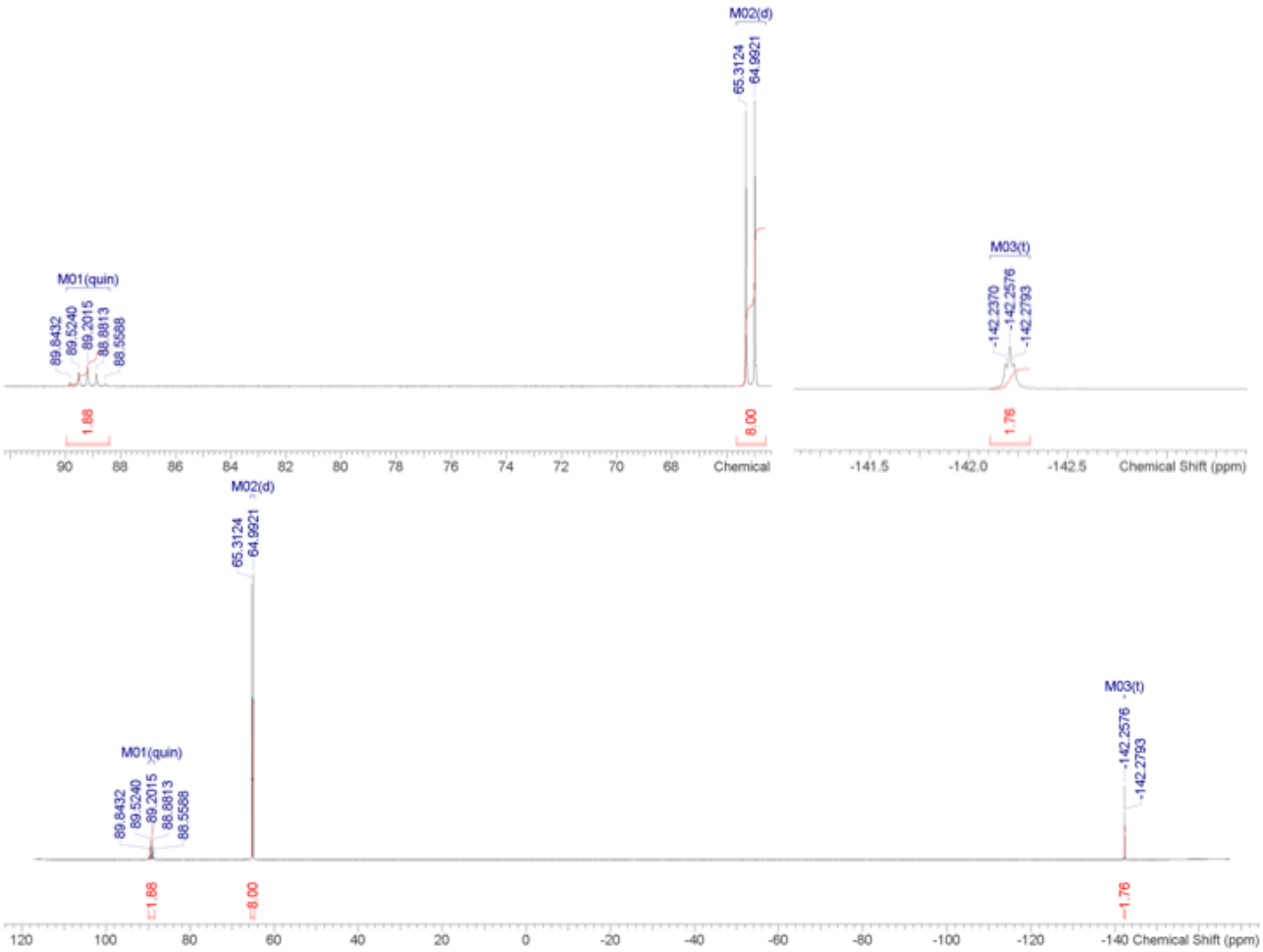

Figure S 11: $^{19}F\{^{1}H\}$ NMR spectrum of receptor **4** in DMSO-d_6 at 298 K.

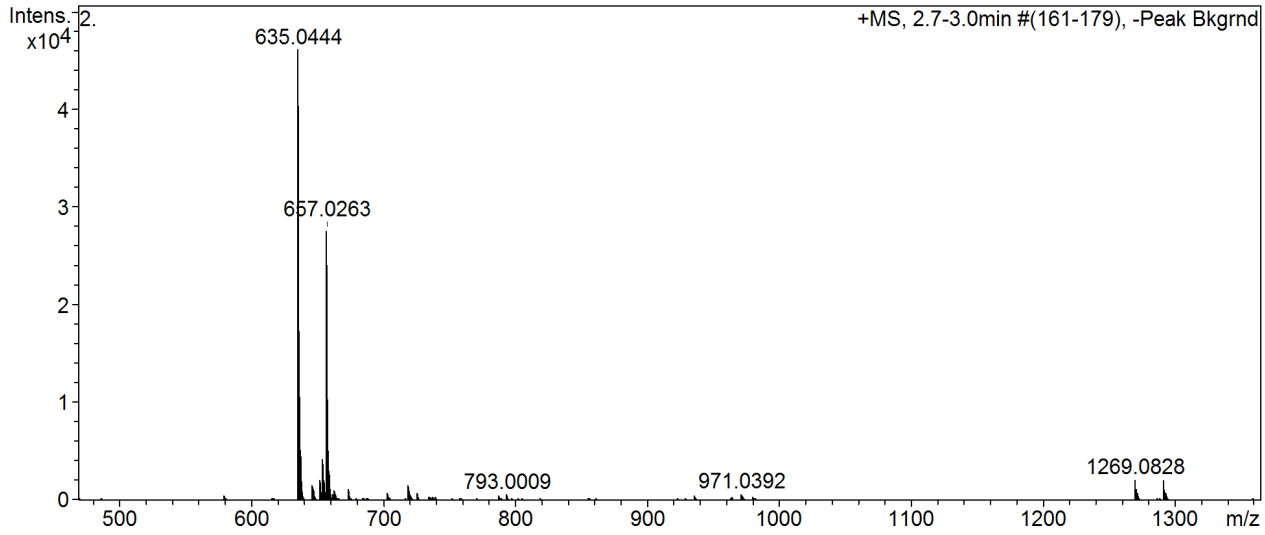

Meas. m/z	Formula	m/z	err [ppm]	err [mDa]	# Sigma	mSigma	rdb	e⁻ Conf	N-Rule
635.0444	C 19 H 10 F 6 N 14 Na S 2	635.0451	1.0	0.6	1	9.3	18.5	even	ok
	C 22 H 15 F 7 N 4 Na O 7 S	635.0442	-0.4	-0.2	2	9.7	13.5	even	ok
	C 20 H 15 F 12 N 4 O 2 S 2	635.0439	-0.8	-0.5	3	10.0	9.5	even	ok
	C 20 H 17 F 9 N 4 Na O 4 S 2	635.0440	-0.7	-0.5	4	11.5	9.5	even	ok
	C 22 H 13 F 10 N 4 O 5 S	635.0441	-0.5	-0.3	5	11.8	13.5	even	ok
	C 20 H 10 F 7 N 10 O 5 S	635.0439	-0.8	-0.5	6	11.9	17.5	even	ok
	C 19 H 17 F 6 N 6 O 8 S 2	635.0448	0.6	0.4	7	15.5	11.5	even	ok
	C 26 H 17 F 6 O 10 S	635.0441	-0.5	-0.3	8	15.6	15.5	even	ok
	C 21 H 20 F 9 O 8 S 2	635.0450	1.0	0.6	9	15.6	7.5	even	ok
	C 24 H 19 F 8 O 7 S 2	635.0439	-0.8	-0.5	10	17.1	11.5	even	ok
	C 24 H 21 F 5 Na O 9 S 2	635.0439	-0.8	-0.5	11	19.0	11.5	even	ok
	C 17 H 11 F 8 N 10 O 6 S	635.0451	1.0	0.6	12	22.3	13.5	even	ok
	C 18 H 11 F 11 N 8 Na O 2 S	635.0442	-0.3	-0.2	13	23.9	11.5	even	ok
	C 23 H 12 F 5 N 10 O 3 S 2	635.0450	0.9	0.6	14	24.9	20.5	even	ok
	C 24 H 13 F 5 N 4 Na O 10	635.0444	-0.0	-0.0	15	28.7	17.5	even	ok
	C 28 H 13 F 9 N 2 Na O 2 S	635.0446	0.3	0.2	16	28.7	18.5	even	ok
	C 26 H 10 F 6 N 8 Na O 2 S	635.0444	-0.1	-0.1	17	29.1	22.5	even	ok
	C 28 H 11 F 12 N 2 S	635.0446	0.2	0.1	18	29.2	18.5	even	ok
	C 17 H 20 F 5 N 2 O 16 S	635.0448	0.6	0.4	19	29.2	6.5	even	ok
	C 18 H 20 F 8 Na O 12 S	635.0440	-0.7	-0.4	20	29.5	4.5	even	ok
	C 26 H 8 F 9 N 8 S	635.0443	-0.1	-0.1	21	29.6	22.5	even	ok
	C 24 H 5 F 6 N 14 S	635.0441	-0.5	-0.3	22	29.9	26.5	even	ok
	C 18 H 18 F 11 O 10 S	635.0440	-0.8	-0.5	23	30.7	4.5	even	ok
	C 24 H 11 F 8 N 4 O 8	635.0444	-0.1	-0.1	24	30.8	17.5	even	ok
	C 22 H 8 F 5 N 10 O 8	635.0441	-0.5	-0.3	25	30.9	21.5	even	ok
	C 20 H 18 F 6 Na O 15	635.0442	-0.4	-0.2	26	35.4	8.5	even	ok
	C 28 H 14 F 7 N 4 O 2 S 2	635.0441	-0.5	-0.3	27	36.7	20.5	even	ok
	C 18 H 13 F 6 N 6 O 13	635.0439	-0.8	-0.5	28	37.2	12.5	even	ok
	C 20 H 16 F 9 O 13	635.0442	-0.4	-0.3	29	37.4	8.5	even	ok
	C 22 H 12 F 12 N 2 Na O 5	635.0447	0.4	0.2	30	42.4	11.5	even	ok
	C 20 H 9 F 9 N 8 Na O 5	635.0444	0.0	0.0	31	42.4	15.5	even	ok
	C 30 H 11 F 7 N 2 Na O 5	635.0448	0.6	0.4	32	42.5	22.5	even	ok
	C 30 H 12 F 5 N 4 O 5 S	635.0443	-0.2	-0.1	33	42.6	24.5	even	ok
	C 18 H 6 F 6 N 14 Na O 5	635.0442	-0.4	-0.2	34	42.7	19.5	even	ok
	C 30 H 9 F 10 N 2 O 3	635.0448	0.6	0.4	35	43.8	22.5	even	ok
	C 28 H 6 F 7 N 8 O 3	635.0446	0.2	0.1	36	44.0	26.5	even	ok
	C 20 H 7 F 12 N 8 O 3	635.0444	-0.1	-0.0	37	44.7	15.5	even	ok
	C 18 H 4 F 9 N 14 O 3	635.0442	-0.4	-0.3	38	45.0	19.5	even	ok
	C 26 H 7 F 11 N 6 Na	635.0449	0.7	0.4	39	45.0	20.5	even	ok
	C 24 H 4 F 8 N 12 Na	635.0446	0.3	0.2	40	45.4	24.5	even	ok
	C 22 H F 5 N 18 Na	635.0444	-0.1	-0.0	41	46.0	28.5	even	ok
	C 34 H 6 F 6 N 6 Na	635.0450	0.9	0.6	42	66.7	31.5	even	ok
	C 36 H 10 F 7 N 2 S	635.0447	0.5	0.3	43	71.7	29.5	even	ok
	C 38 H 8 F 5 N 2 O 3	635.0450	0.8	0.5	44	78.8	33.5	even	ok

Figure S 12: HRMS of receptor **4**.

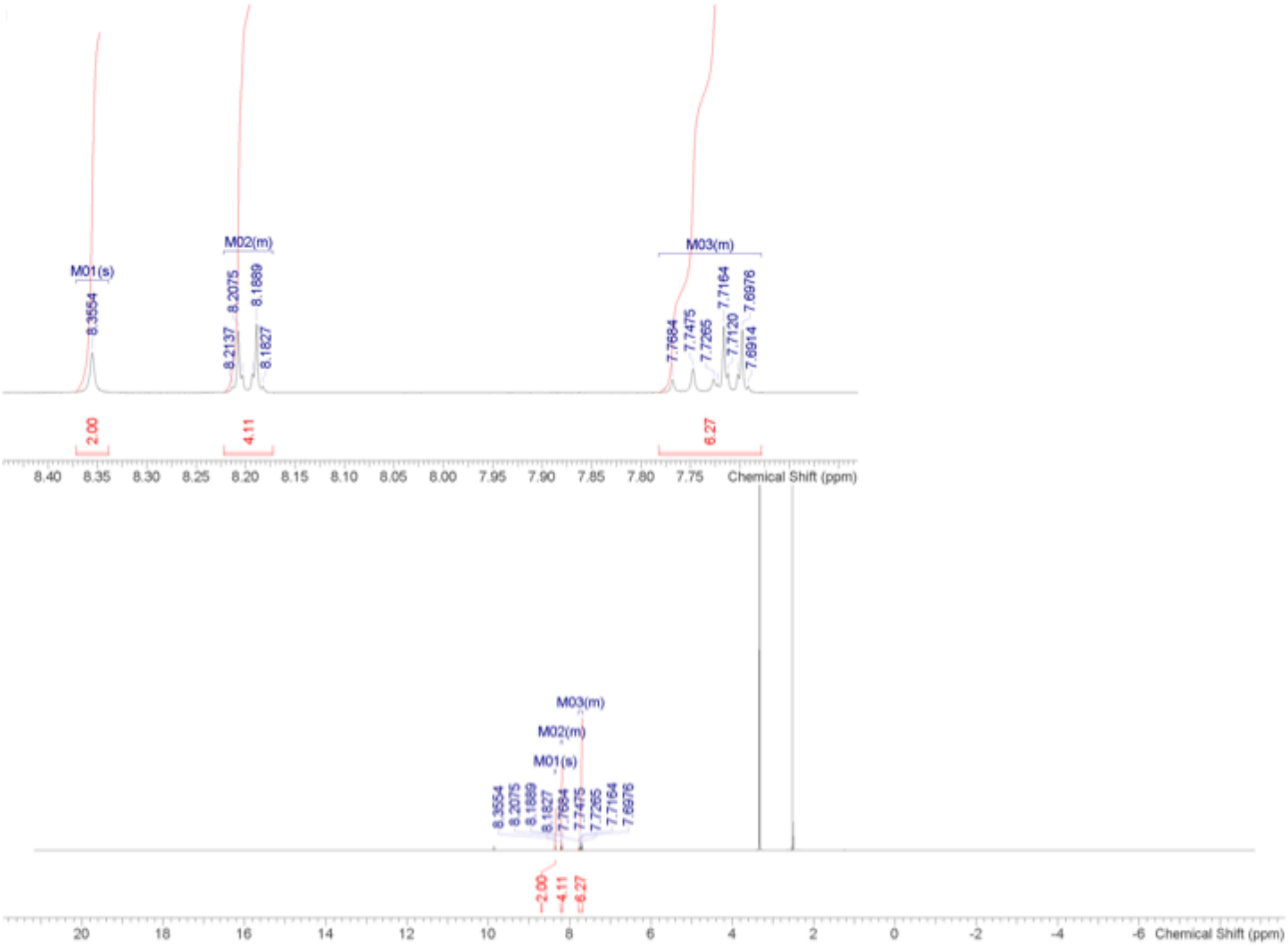

Figure S 13: ^{1}H NMR spectrum of receptor **6** in DMSO-d_6 at 298 K.

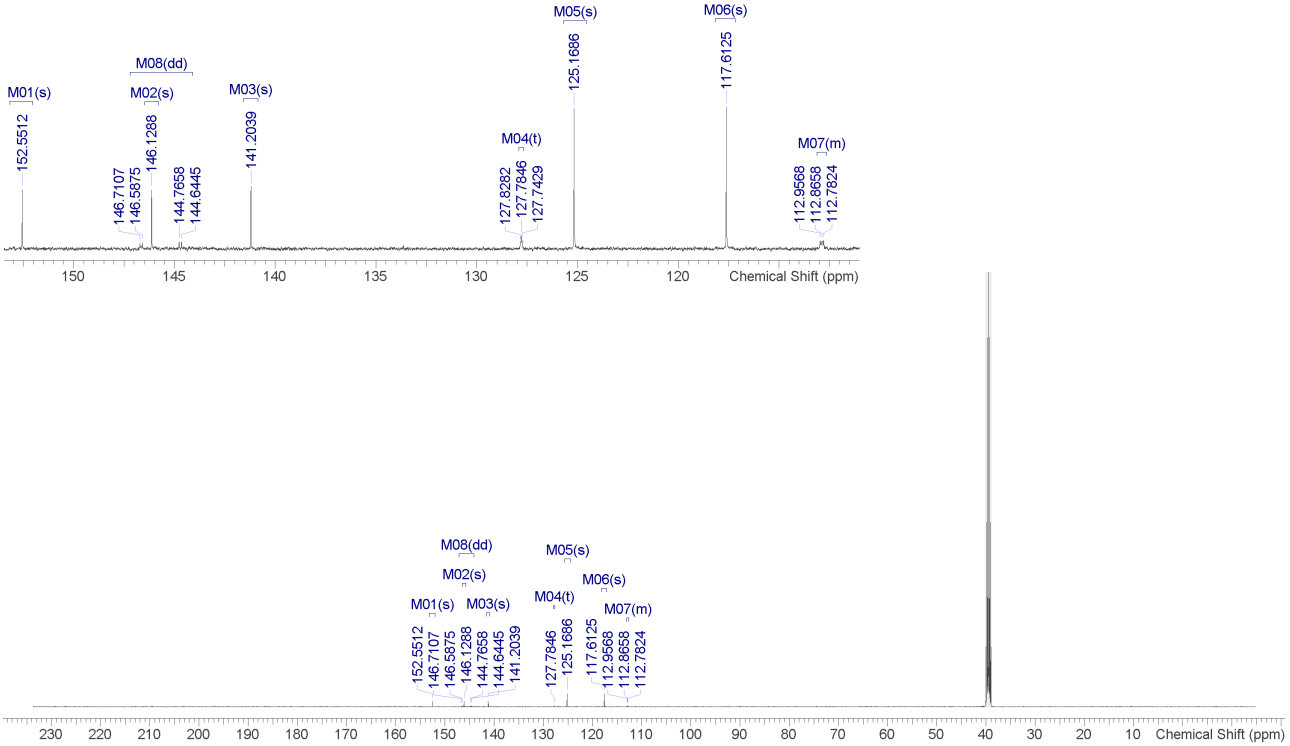

Figure S 14: ^{13}C{^{1}H} NMR spectrum of receptor **6** in DMSO-d_6 at 298 K.

Figure S 15: $^{19}F\{^{1}H\}$ NMR spectrum of receptor **6** in DMSO-d_6 at 298 K.

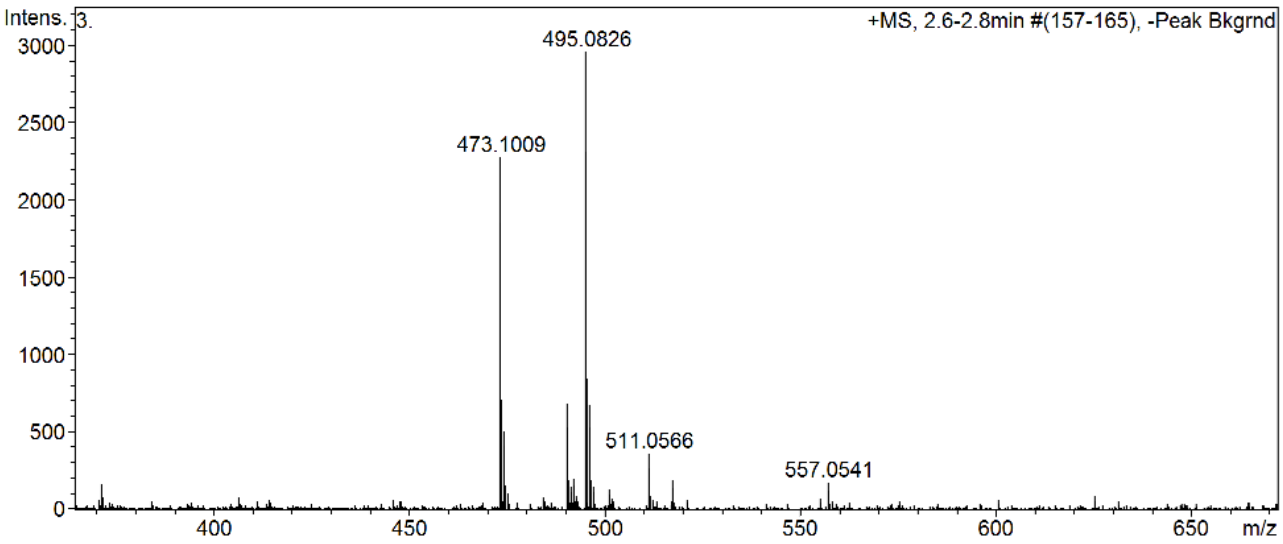

Meas. m/z	Formula	m/z	err [ppm]	err [mDa]	# Sigma	mSigma	rdb	e⁻ Conf	N-Rule
473.1009	C 19 H 19 F 2 N 2 O 10	473.1002	-1.4	-0.7	1	3.9	10.5	even	ok
	C 22 H 20 F 2 Na O 8	473.1018	2.0	0.9	2	8.1	11.5	even	ok
	C 20 H 15 F 2 N 6 O 6	473.1016	1.4	0.7	3	10.0	15.5	even	ok
	C 14 H 10 N 16 Na O 3	473.1014	1.1	0.5	4	13.4	17.5	even	ok
	C 19 H 12 F 2 N 10 Na O 2	473.1005	-0.9	-0.4	5	14.1	17.5	even	ok
	C 17 H 7 F 2 N 16	473.1002	-1.4	-0.7	6	16.1	21.5	even	ok
	C 16 H 22 N 2 Na O 13	473.1014	1.1	0.5	7	18.7	6.5	even	ok
	C 14 H 17 N 8 O 11	473.1011	0.5	0.2	8	21.9	10.5	even	ok
	C 25 H 19 F Na O 7	473.1007	-0.4	-0.2	9	24.1	15.5	even	ok
	C 23 H 14 F N 6 O 5	473.1004	-1.0	-0.5	10	28.0	19.5	even	ok
	C 24 H 10 F N 10 O	473.1018	1.8	0.9	11	42.8	24.5	even	ok
	C 29 H 14 N 4 Na O 2	473.1009	-0.0	-0.0	12	53.4	24.5	even	ok
	C 27 H 9 N 10	473.1006	-0.6	-0.3	13	53.4	28.5	even	ok
495.0826	C 19 H 18 F 2 N 2 Na O 10	495.0822	-0.8	-0.4	1	6.8	10.5	even	ok
	C 20 H 14 F 2 N 6 Na O 6	495.0835	1.9	0.9	2	8.9	15.5	even	ok
	C 17 H 13 F 2 N 8 O 8	495.0819	-1.4	-0.7	3	10.7	14.5	even	ok
	C 18 H 9 F 2 N 12 O 4	495.0832	1.3	0.6	4	11.1	19.5	even	ok
	C 17 H 6 F 2 N 16 Na	495.0822	-0.9	-0.4	5	16.2	21.5	even	ok
	C 24 H 16 F N 2 O 9	495.0834	1.7	0.8	6	20.0	17.5	even	ok
	C 23 H 13 F N 6 Na O 5	495.0824	-0.5	-0.2	7	25.3	19.5	even	ok
	C 14 H 16 N 8 Na O 11	495.0831	1.0	0.5	8	25.3	10.5	even	ok
	C 21 H 8 F N 12 O 3	495.0821	-1.0	-0.5	9	26.0	23.5	even	ok
	C 14 H 23 O 19	495.0828	0.4	0.2	10	34.5	3.5	even	ok
	C 27 H 15 N 2 O 8	495.0823	-0.6	-0.3	11	36.6	21.5	even	ok
	C 27 H 8 N 10 Na	495.0826	-0.1	-0.0	12	50.8	28.5	even	ok
	C 33 H 13 F 2 O 3	495.0827	0.3	0.1	13	65.5	26.5	even	ok

Figure S 16: HRMS of receptor **6**.

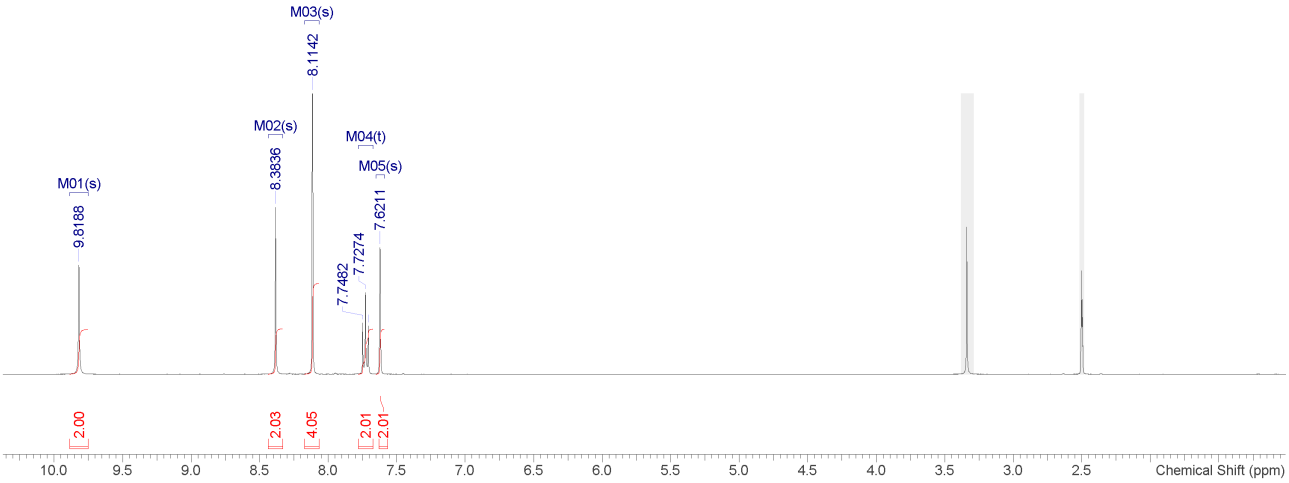

Figure S 17: ^{1}H NMR spectrum of receptor **7** in DMSO-d_6 at 298 K.

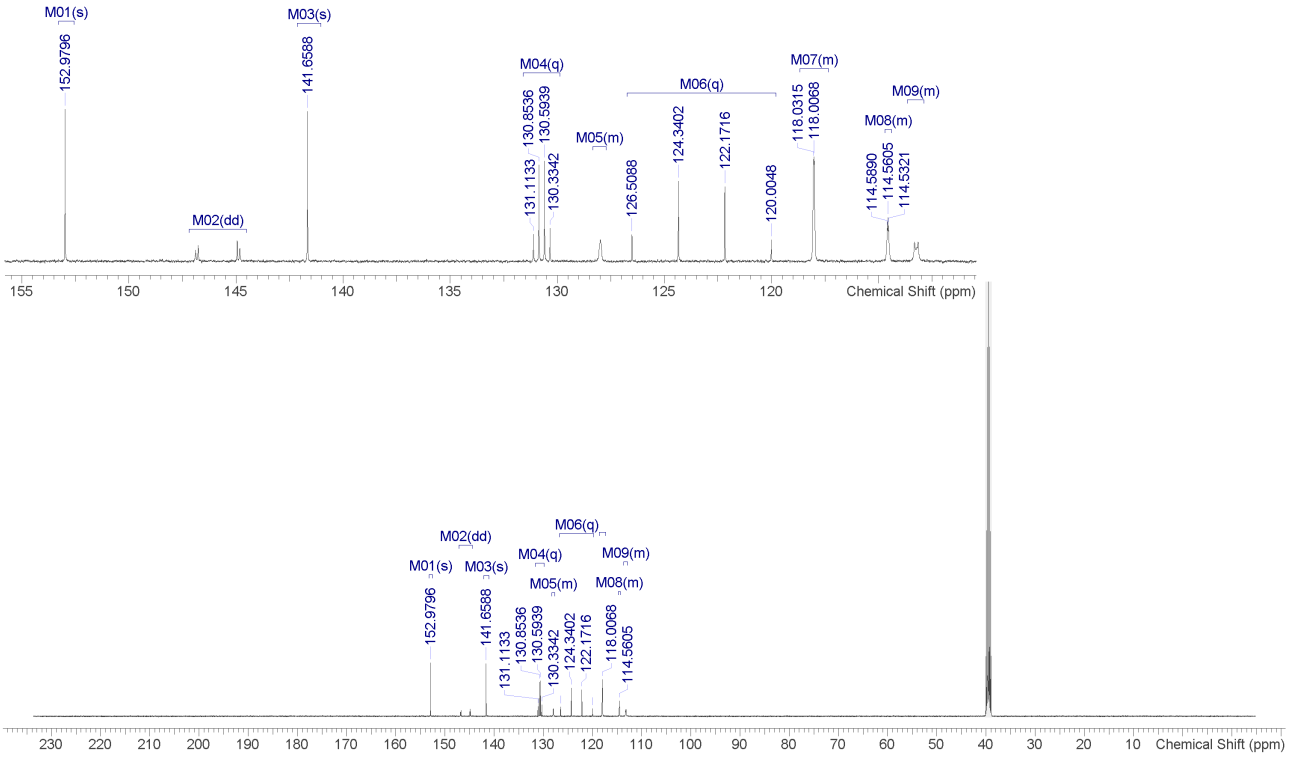

Figure S 18: $^{13}C\{^{1}H\}$ NMR spectrum of receptor **7** in DMSO-d_6 at 298 K.

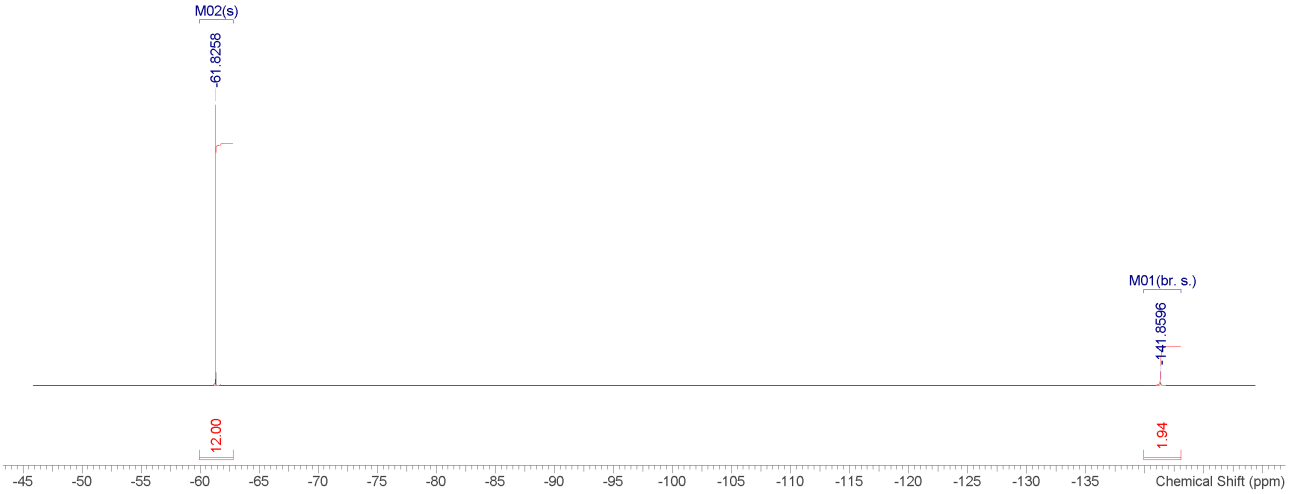

Figure S 19: $^{19}F\{^{1}H\}$ NMR spectrum of receptor **7** in DMSO-d_6 at 298 K.

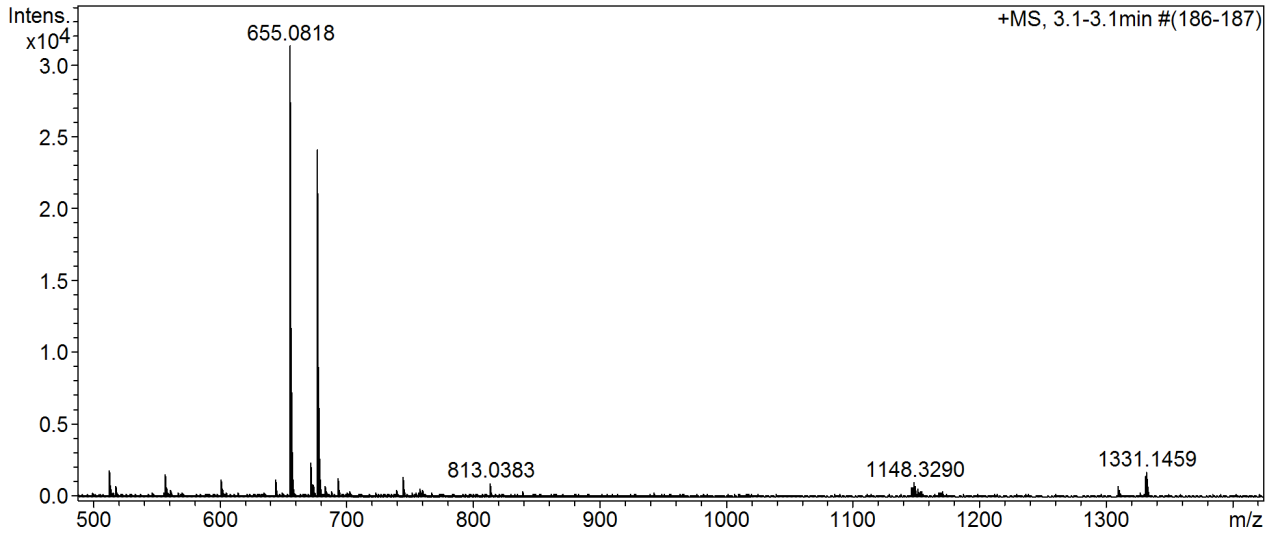

Meas. m/z	Formula	m/z	err [ppm]	err [mDa]	# Sigma	mSigma	rdb	e⁻ Conf	N-Rule
655.0818	C 24 H 13 F 14 N 4 O 2	655.0809	-1.3	-0.9	1	5.5	13.5	even	ok
	C 25 H 18 F 11 O 8	655.0821	0.4	0.2	2	5.7	11.5	even	ok
	C 24 H 15 F 11 N 4 Na O 4	655.0810	-1.3	-0.8	3	5.7	13.5	even	ok
	C 22 H 10 F 11 N 10 O 2	655.0807	-1.7	-1.1	4	5.9	17.5	even	ok
	C 21 H 16 F 12 N 4 Na O 5	655.0821	0.5	0.3	5	13.4	9.5	even	ok
	C 19 H 11 F 12 N 10 O 3	655.0818	0.1	0.0	6	13.7	13.5	even	ok
	C 27 H 14 F 14 N 2 Na	655.0826	1.2	0.8	7	17.3	14.5	even	ok
	C 25 H 11 F 11 N 8 Na	655.0823	0.8	0.5	8	20.3	18.5	even	ok
	C 28 H 17 F 10 O 7	655.0809	-1.4	-0.9	9	20.9	15.5	even	ok
	C 20 H 20 F 12 Na O 9	655.0808	-1.5	-1.0	10	24.3	4.5	even	ok
	C 18 H 15 F 12 N 6 O 7	655.0805	-2.0	-1.3	11	27.9	8.5	even	ok
	C 29 H 13 F 10 N 4 O 3	655.0822	0.7	0.4	12	32.9	20.5	even	ok

Figure S 20: HRMS of receptor **7**.

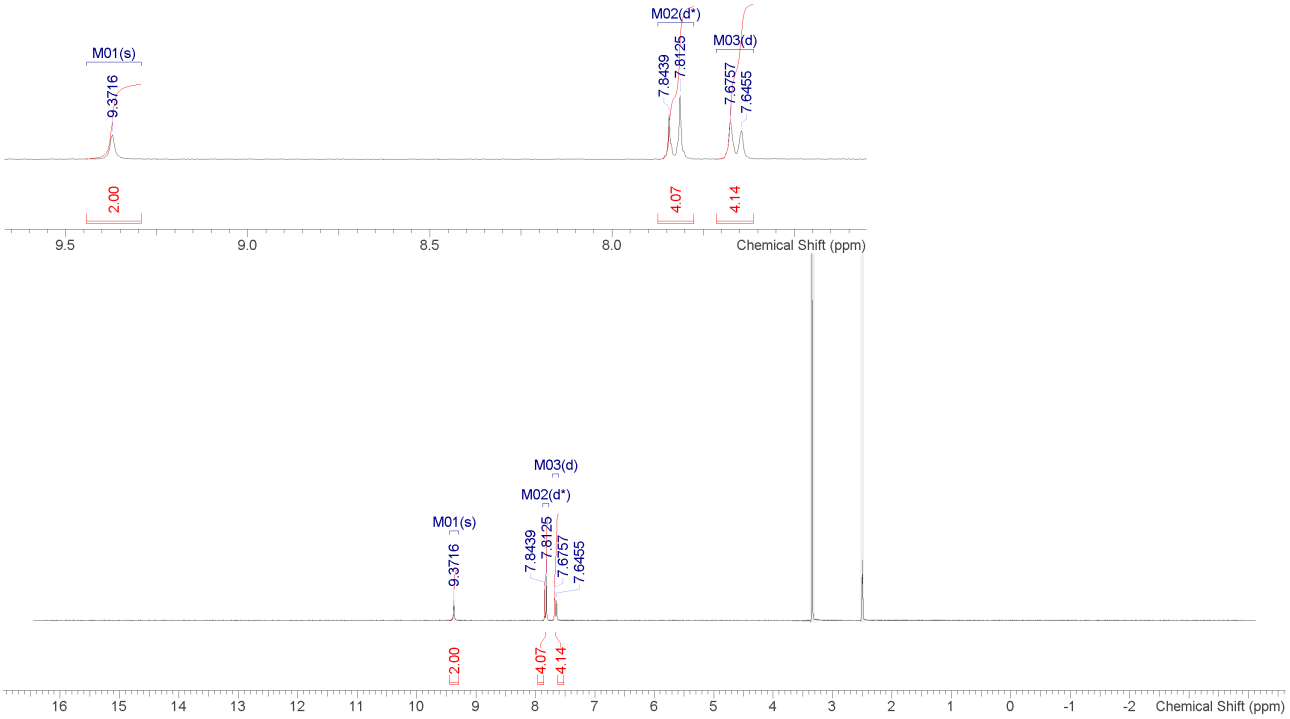

Figure S 21: ^{1}H NMR spectrum of receptor **10** in DMSO-d_6 at 298 K.

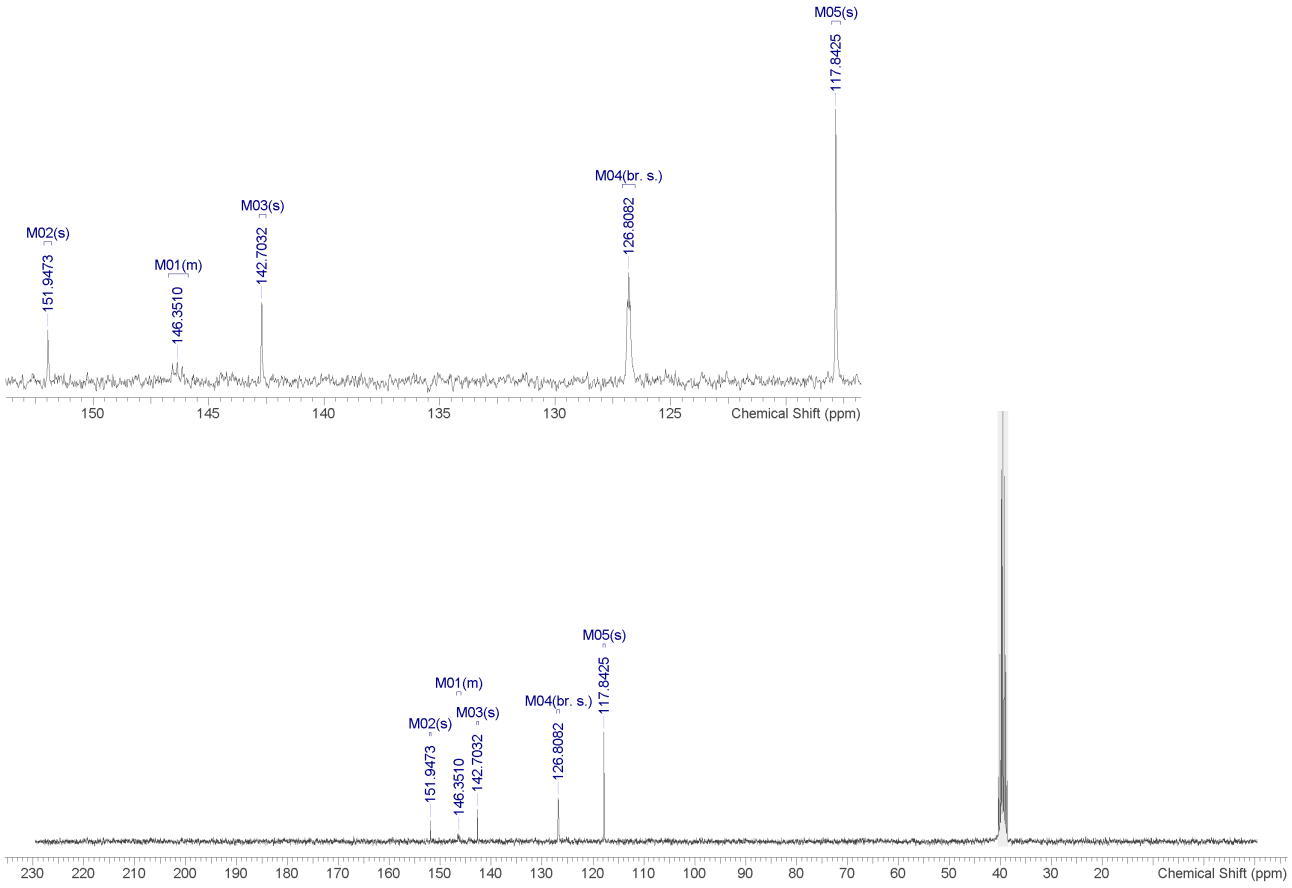

Figure S 22: $^{13}C\{^{1}H\}$ NMR spectrum of receptor **10** in DMSO-d_6 at 298 K.

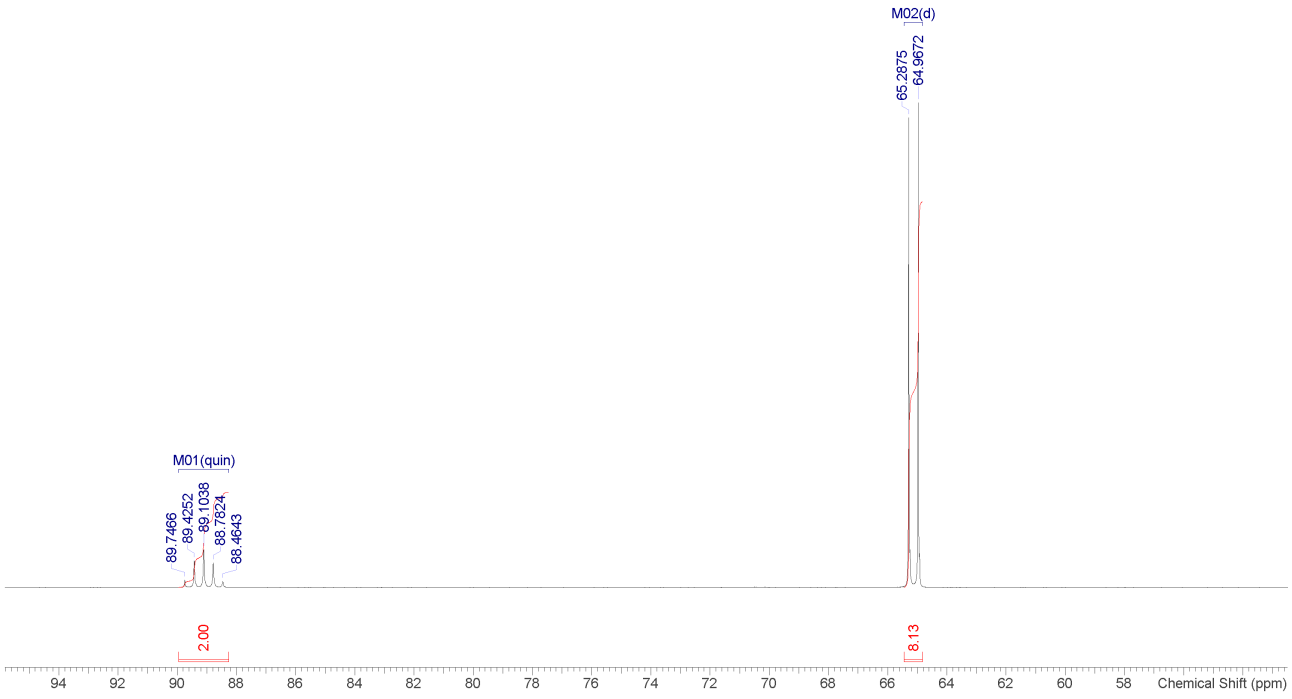

Figure S 23: $^{19}F\{^{1}H\}$ NMR spectrum of receptor **10** in DMSO-d_6 at 298 K.

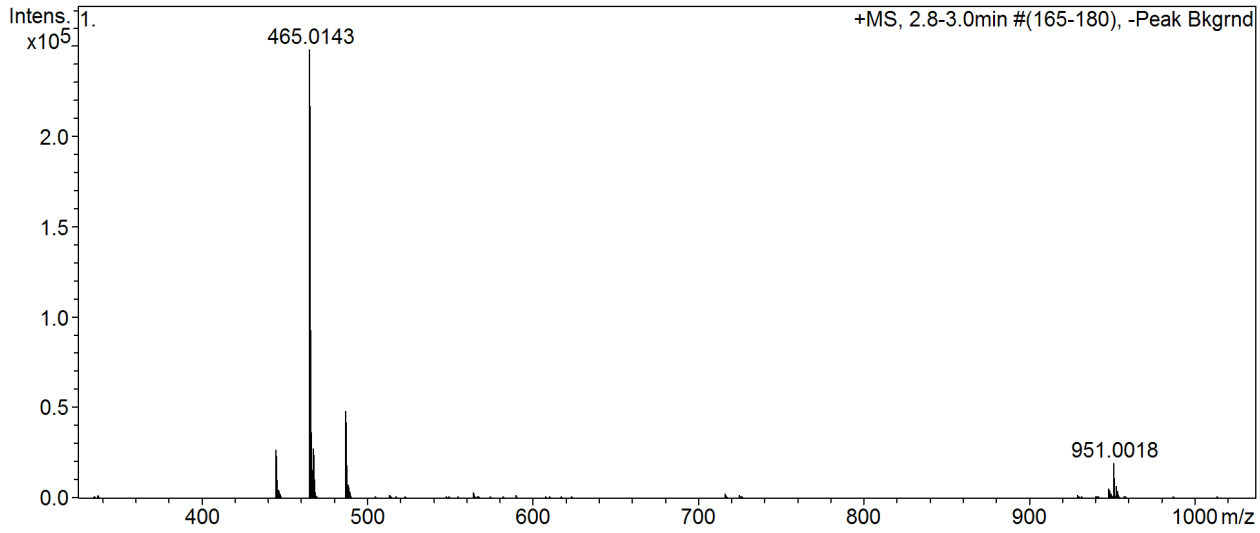

Meas. m/z	Formula	m/z	err [ppm]	err [mDa]	# Sigma	mSigma	rdb	e⁻ Conf	N-Rule
465.0143	C 13 H 13 F 7 N 2 Na O 3 S 2	465.0148	1.1	0.5	1	1.7	4.5	even	ok
	C 11 H 8 F 7 N 8 O S 2	465.0145	0.5	0.2	2	4.0	8.5	even	ok
	C 13 H 11 F 10 N 2 O S 2	465.0148	1.0	0.5	3	4.0	4.5	even	ok
	C 11 F 7 N 12 O 2	465.0150	1.5	0.7	4	9.4	14.5	even	ok
	C 16 H 10 F 9 N 2 S 2	465.0136	-1.4	-0.7	5	14.7	8.5	even	ok
	C 16 H 12 F 6 N 2 Na O 2 S 2	465.0137	-1.3	-0.6	6	14.8	8.5	even	ok
	C 14 H 7 F 6 N 8 S 2	465.0134	-1.9	-0.9	7	15.0	12.5	even	ok
	C 16 H 2 F 9 N 6 O	465.0141	-0.4	-0.2	8	19.3	14.5	even	ok
	C 15 H 11 F 5 N 2 Na O 6 S	465.0150	1.6	0.7	9	19.8	8.5	even	ok
	C 12 H 10 F 5 N 4 O 8 S	465.0134	-1.9	-0.9	10	20.4	7.5	even	ok
	C 18 H 7 F 9 Na O 3	465.0144	0.2	0.1	11	21.2	10.5	even	ok
	C 16 H 4 F 6 N 6 Na O 3	465.0141	-0.3	-0.2	12	21.4	14.5	even	ok
	C 15 H 9 F 8 N 2 O 4 S	465.0150	1.5	0.7	13	21.8	8.5	even	ok
	C 13 H 6 F 5 N 8 O 4 S	465.0147	1.0	0.5	14	22.0	12.5	even	ok
	C 17 H 7 F 6 N 2 O 7	465.0152	2.0	0.9	15	23.0	12.5	even	ok
	C 14 H 6 F 8 N 6 Na S	465.0139	-0.8	-0.4	16	26.1	10.5	even	ok
	C 12 H 3 F 5 N 12 Na S	465.0137	-1.3	-0.6	17	26.4	14.5	even	ok
	C 18 H 8 F 7 N 2 O 3 S	465.0138	-1.0	-0.4	18	28.7	12.5	even	ok
	C 11 H 7 F 9 N 6 Na O S	465.0151	1.7	0.8	19	29.1	6.5	even	ok
	C 9 H 4 F 6 N 12 Na O S	465.0148	1.1	0.5	20	29.3	10.5	even	ok
	C 9 H 11 F 6 N 4 O 9 S	465.0145	0.6	0.3	21	31.1	3.5	even	ok
	C 10 H 11 F 9 N 2 Na O 5 S	465.0137	-1.2	-0.6	22	32.6	1.5	even	ok
	C 20 H 6 F 5 N 2 O 6	465.0141	-0.5	-0.2	23	38.8	16.5	even	ok
	C 21 H 10 F 5 N 2 O S 2	465.0149	1.4	0.6	24	42.2	15.5	even	ok
	C 12 H 9 F 7 N 2 Na O 8	465.0139	-0.8	-0.4	25	52.0	5.5	even	ok
	C 24 H 8 F 6 Na S	465.0143	0.1	0.0	26	52.6	17.5	even	ok
	C 12 H 7 F 10 N 2 O 6	465.0139	-0.8	-0.4	27	54.2	5.5	even	ok
	C 10 H 4 F 7 N 8 O 6	465.0137	-1.4	-0.6	28	54.3	9.5	even	ok
	C 9 H 10 F 8 N 2 Na O 9	465.0151	1.7	0.8	29	61.6	1.5	even	ok
	C 26 H 4 F 7 O	465.0145	0.4	0.2	30	69.5	21.5	even	ok

Figure S 24: HRMS of receptor **10**.

S4: Anion Transport Studies

POPC was supplied by Genzyme. The vesicles used in all of the following studies were prepared according to literature procedures.[1] To prevent the vesicle membranes from bursting the ionic strength of the intra-vesicular and extra-vesicular solutions were made to be isotonic.

Vesicle preparation: POPC was dissolved in chloroform (approximately 29 mg mL^{-1}). A known volume (e.g. 1 mL) of the POPC solution was transferred to a RBF and the chloroform removed *in vacuo*. The resultant POPC thin film was dried under high vacuum for 4-24 hrs. The POPC was suspended in internal solution. The suspension was vortexed using a lab dancer to ensure that all POPC was removed from the sides of the flask. The volume of internal solution required to suspend the POPC is identical to that of the initial chloroform solution (e.g. 1 mL). The suspension was subjected to nine freeze-thaw cycles using liquid nitrogen and room temperature water alternately, after which the suspension was left to equilibrate to room temperature for thirty minutes. The resultant vesicles were extruded 25 times through a 200 nm polycarbonate membrane to generate vesicles of uniform size. The vesicles were dialysed in the external solution for 2-18 hrs to remove any unencapsulated "internal salts". The vesicle suspension was then diluted to a concentration of 1 mM using the external solution.

Test for Cl^-/NO_3^- antiport: Unilamellar POPC vesicles were loaded with aqueous internal solution containing 489 mM NaCl buffered to pH 7.2 with 5 mM sodium phosphate salts. The vesicles were dispersed in an aqueous external solution containing 489 mM $NaNO_3$ buffered to pH 7.2 with 5 mM sodium phosphate salts. The receptor was loaded as a percentage relative to the moles of lipid and in the form of a DMSO solution at 0 s. After 300 s, octaethylene glycol monododecyl ether detergent was added to lyse the vesicles (2.32 mM in 7:1 H_2O:DMSO v/v) and calibrate the chloride selective electrode to 100% chloride efflux at 420 s. All endpoint values are taken as of 270 s. Chloride concentrations were monitored using an Accumet solid-state combination chloride selective electrode. The lipid concentration per sample was 1 mM. Each data point represents the average of 3 runs. For the blank runs (pure DMSO) there is a minimum of 1 repeat and a maximum of 3. Error bars are shown where appropriate.

Test for Cl^-/HCO_3^- antiport: Unilamellar POPC vesicles were loaded with aqueous internal solution containing 451 mM NaCl buffered to pH 7.2 with 20 mM sodium phosphate salts. The vesicles were dispersed in an aqueous external solution containing 150 mM Na_2SO_4 buffered to pH 7.2 with 20 mM sodium phosphate salts. The receptor was loaded as a percentage relative to the moles of lipid and in the form of a DMSO solution at 0 s, and a spike of $NaHCO_3$ (33 mM) added at 120 s. After 420 s, octaethylene glycol monododecyl ether detergent was added to lyse the vesicles (2.32

mM in 7:1 H_2O:DMSO v/v) and calibrate the chloride selective electrode to 100% chloride efflux at 540 s. All endpoint values are taken as of 390 s. Chloride concentrations were monitored using an Accumet solid-state combination chloride selective electrode. The lipid concentration per sample was 1 mM. Each data point represents the average of 3 runs. For the blank runs (pure DMSO) there is a minimum of 1 repeat and a maximum of 3. Error bars are shown where appropriate.

Hill plot analysis was carried out using the above transport conditions, where each receptor is tested at multiple concentrations/loadings. Data points were taken at 270 s for Cl^-/NO_3^- transport and 390 s for Cl^-/HCO_3^- transport, and each point represents the average of at three runs.

S5: Anion Binding Studies

^{1}H NMR titrations: A 1.5 mL, 0.01 M d_6-DMSO/0.5% water solution of the receptor was prepared; 0.5 mL of which was added to an NMR tube and sealed with an airtight suba seal. The remaining 1 mL of receptor solution was used to make a 0.15 M solution of a guest anion, which was added as the TBA salt (TEA salt in the case of HCO_3^-). The receptor/anion solution was titrated into the NMR tube in small aliquots and a ^{1}H NMR spectrum was recorded after each addition. Using the receptor solution to make up the guest anion solution ensures that the receptor concentration remains constant as the anion/receptor solution is titrated into the NMR tube. Chemical shifts are reported on the delta scale in ppm and were referenced to residual solvent peaks. The data was then fitted to a 1:1 or 1:2 receptor:anion binding isotherm using WinEQNMR2.[2] d_6-DMSO is highly hygroscopic, hence adding 0.5% water to d_6-DMSO ensures that no additional moisture from the environment is absorbed by the d_6-DMSO, meaning the exact concentration of the receptor and receptor/anion solutions are known.

S6: Anion Transport Studies: Cl^-/NO_3^- Exchange

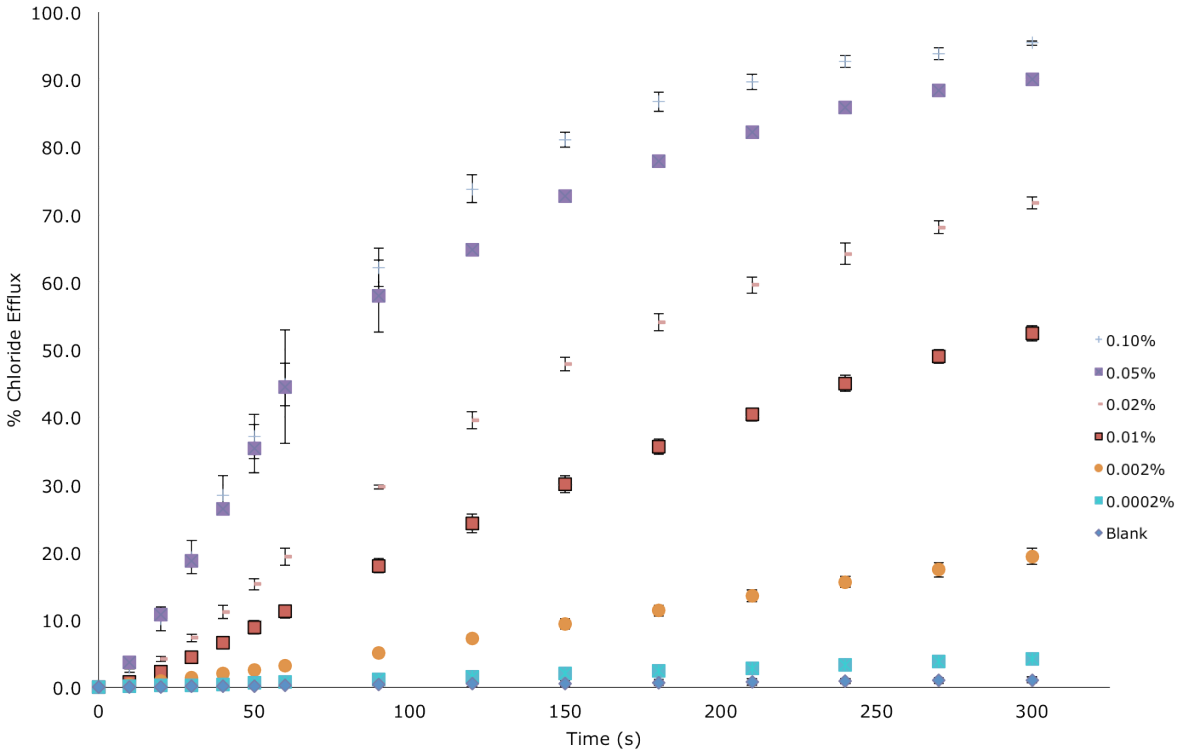

Figure S 25: Chloride efflux as a function of time, promoted by the addition of various concentrations of receptor **2**, from unilamellar POPC vesicles containing 489 mM NaCl buffered to pH 7.2 with 5 mM sodium phosphate salts. The vesicles were dispersed in 489 mM $NaNO_3$ buffered to pH 7.2 with 5 mM sodium phosphate salts. The receptor was loaded as a DMSO solution at 0 s. At the end of the experiment the vesicles were lysed to calibrate the chloride selective electrode to 100% chloride efflux.

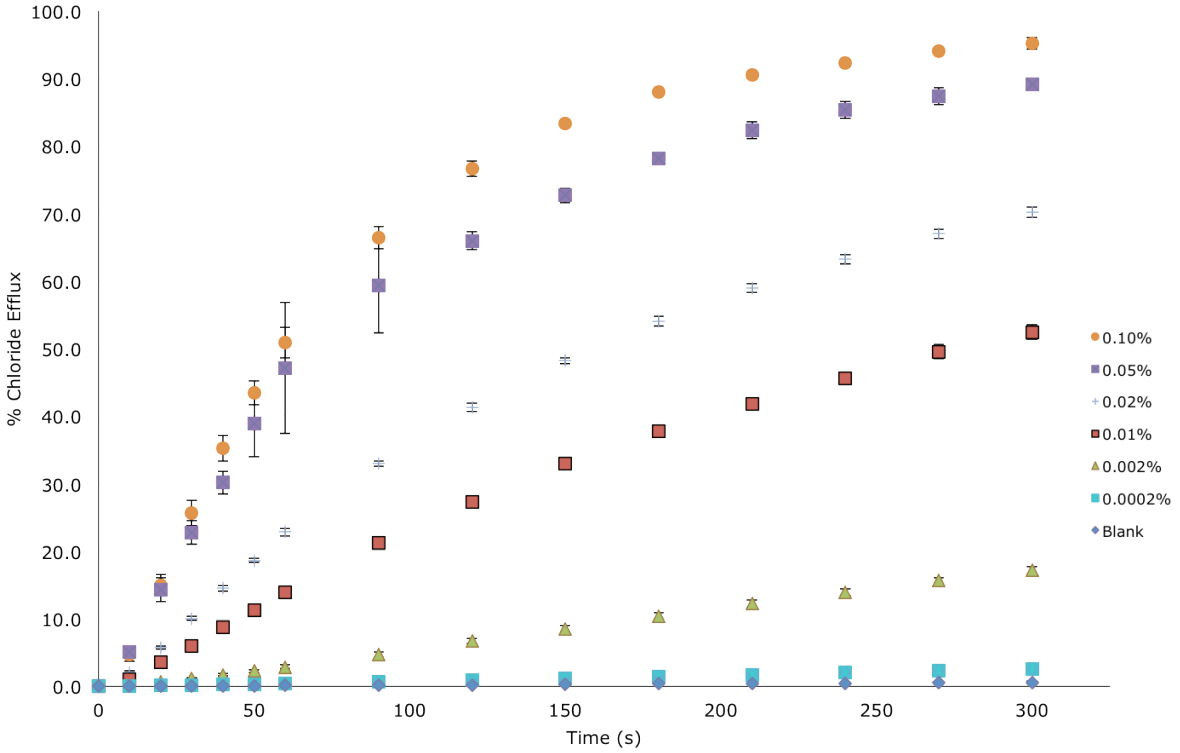

Figure S 26: Chloride efflux as a function of time, promoted by the addition of various concentrations of receptor **2,** from unilamellar POPC vesicles containing 489 mM NaCl buffered to pH 7.2 with 5 mM sodium phosphate salts. The vesicles were dispersed in 489 mM $NaNO_3$ buffered to pH 7.2 with 5 mM sodium phosphate salts. The receptor was loaded as a DMSO solution at 0 s. At the end of the experiment the vesicles were lysed to calibrate the chloride selective electrode to 100% chloride efflux.

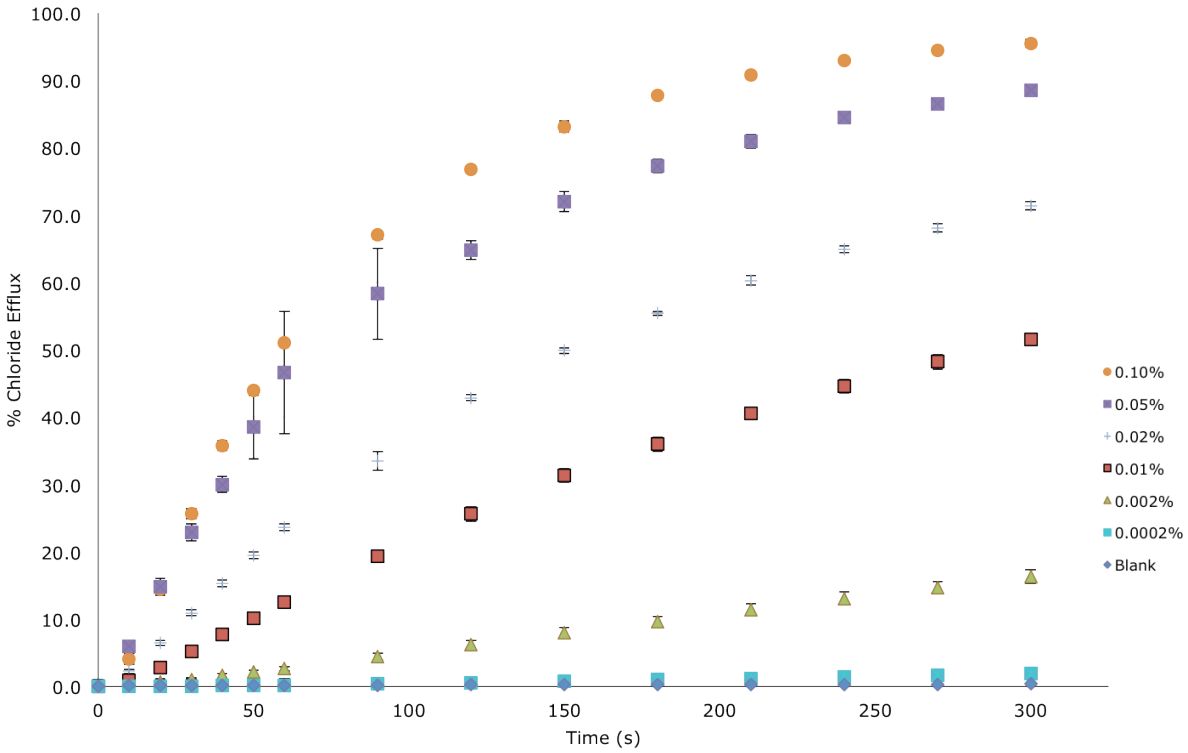

Figure S 27: Chloride efflux as a function of time, promoted by the addition of various concentrations of receptor **2**, from unilamellar POPC vesicles containing 489 mM NaCl buffered to pH 7.2 with 5 mM sodium phosphate salts. The vesicles were dispersed in 489 mM $NaNO_3$ buffered to pH 7.2 with 5 mM sodium phosphate salts. The receptor was loaded as a DMSO solution at 0 s. At the end of the experiment the vesicles were lysed to calibrate the chloride selective electrode to 100% chloride efflux.

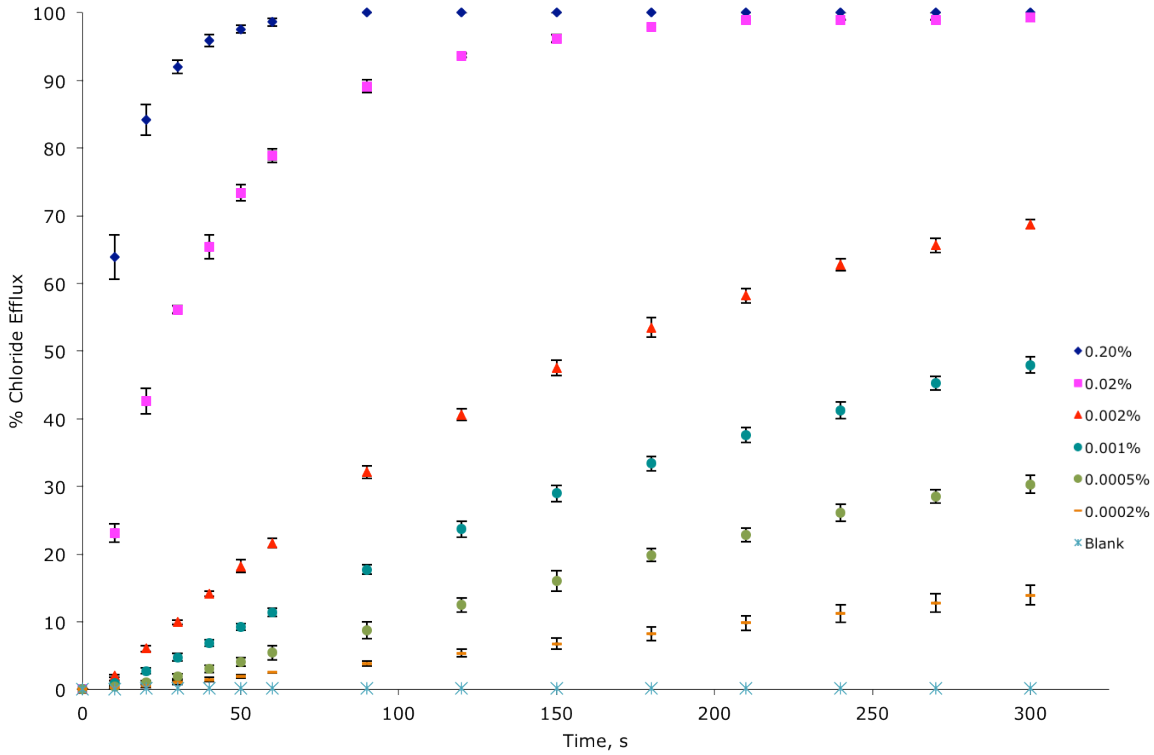

Figure S 28: Chloride efflux as a function of time, promoted by the addition of various concentrations of receptor **3,** from unilamellar POPC vesicles containing 489 mM NaCl buffered to pH 7.2 with 5 mM sodium phosphate salts. The vesicles were dispersed in 489 mM $NaNO_3$ buffered to pH 7.2 with 5 mM sodium phosphate salts. The receptor was loaded as a DMSO solution at 0 s. At the end of the experiment the vesicles were lysed to calibrate the chloride selective electrode to 100% chloride efflux.

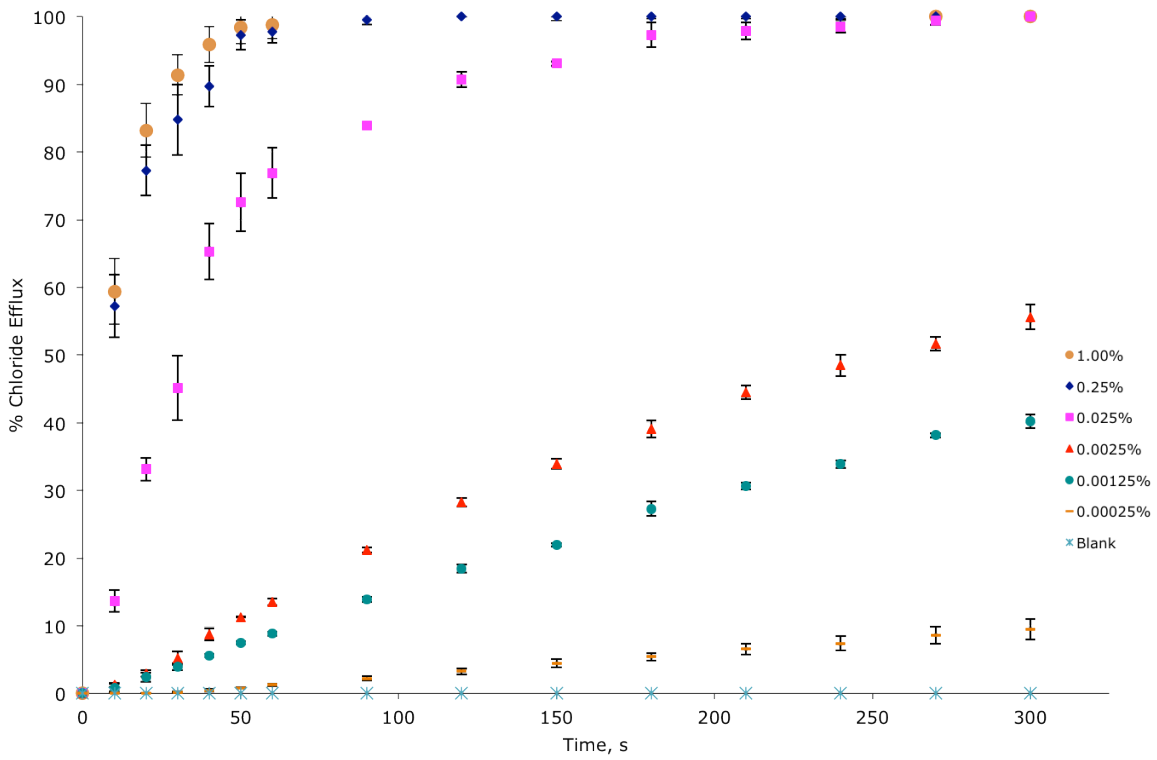

Figure S 29: Chloride efflux as a function of time, promoted by the addition of various concentrations of receptor **3**, from unilamellar POPC vesicles containing 489 mM NaCl buffered to pH 7.2 with 5 mM sodium phosphate salts. The vesicles were dispersed in 489 mM $NaNO_3$ buffered to pH 7.2 with 5 mM sodium phosphate salts. The receptor was loaded as a DMSO solution at 0 s. At the end of the experiment the vesicles were lysed to calibrate the chloride selective electrode to 100% chloride efflux.

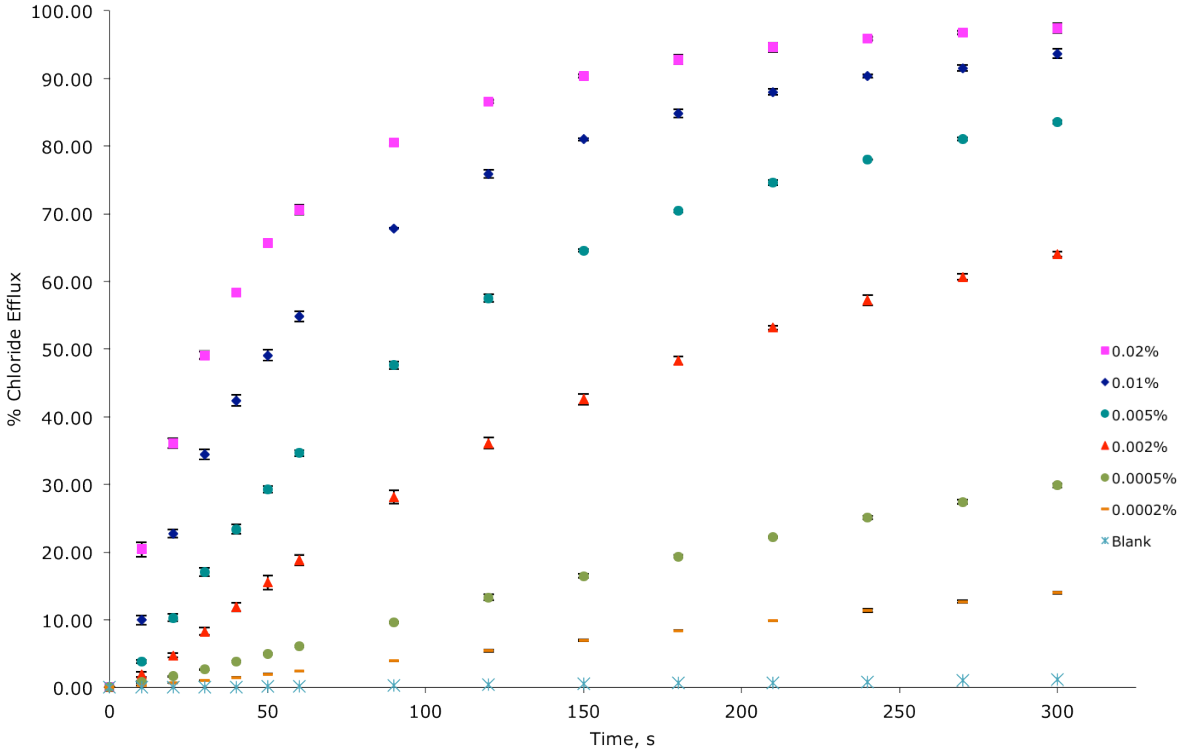

Figure S 30: Chloride efflux as a function of time, promoted by the addition of various concentrations of receptor **3,** from unilamellar POPC vesicles containing 489 mM NaCl buffered to pH 7.2 with 5 mM sodium phosphate salts. The vesicles were dispersed in 489 mM $NaNO_3$ buffered to pH 7.2 with 5 mM sodium phosphate salts. The receptor was loaded as a DMSO solution at 0 s. At the end of the experiment the vesicles were lysed to calibrate the chloride selective electrode to 100% chloride efflux.

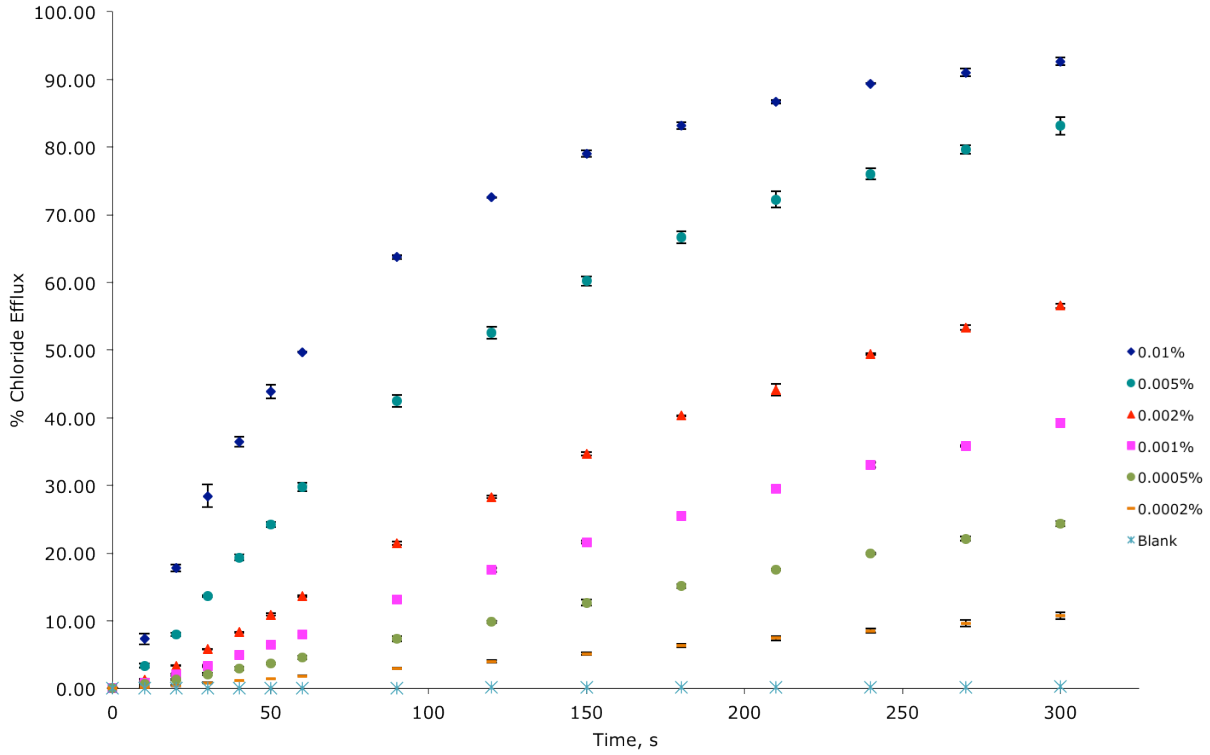

Figure S 31: Chloride efflux as a function of time, promoted by the addition of various concentrations of receptor **3,** from unilamellar POPC vesicles containing 489 mM NaCl buffered to pH 7.2 with 5 mM sodium phosphate salts. The vesicles were dispersed in 489 mM $NaNO_3$ buffered to pH 7.2 with 5 mM sodium phosphate salts. The receptor was loaded as a DMSO solution at 0 s. At the end of the experiment the vesicles were lysed to calibrate the chloride selective electrode to 100% chloride efflux.

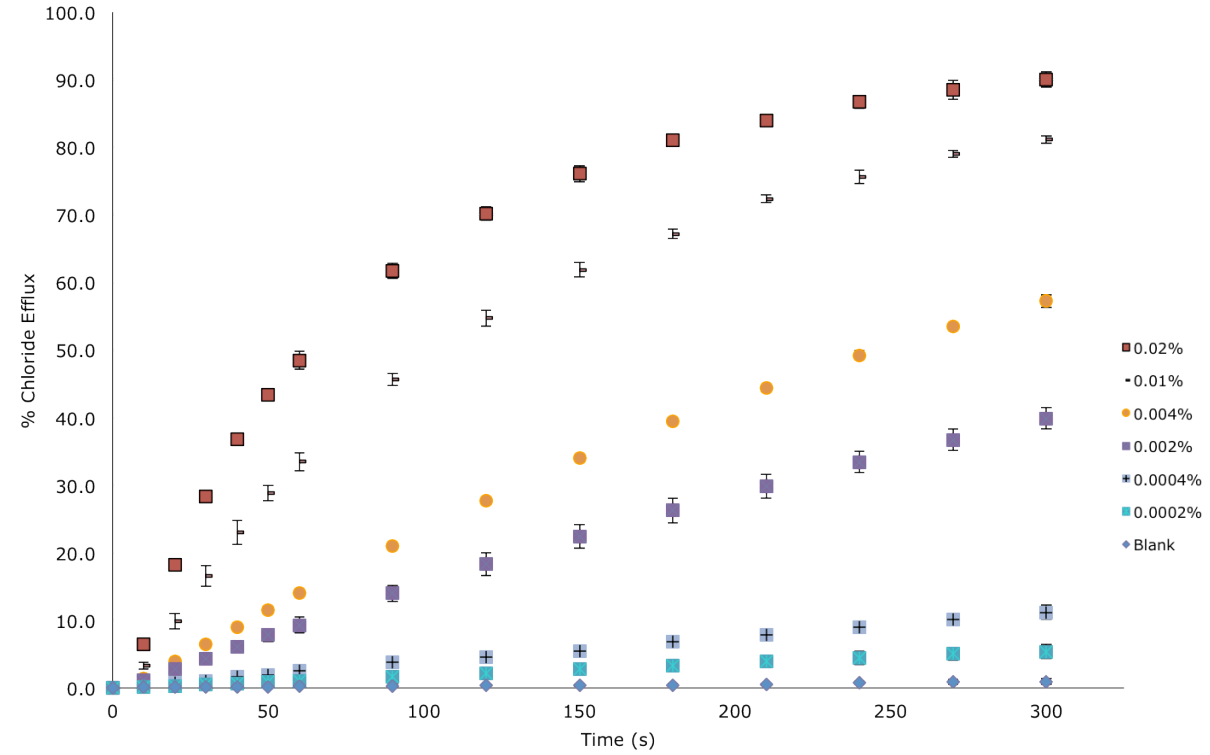

Figure S 32: Chloride efflux as a function of time, promoted by the addition of various concentrations of receptor **4**, from unilamellar POPC vesicles containing 489 mM NaCl buffered to pH 7.2 with 5 mM sodium phosphate salts. The vesicles were dispersed in 489 mM $NaNO_3$ buffered to pH 7.2 with 5 mM sodium phosphate salts. The receptor was loaded as a DMSO solution at 0 s. At the end of the experiment the vesicles were lysed to calibrate the chloride selective electrode to 100% chloride efflux.

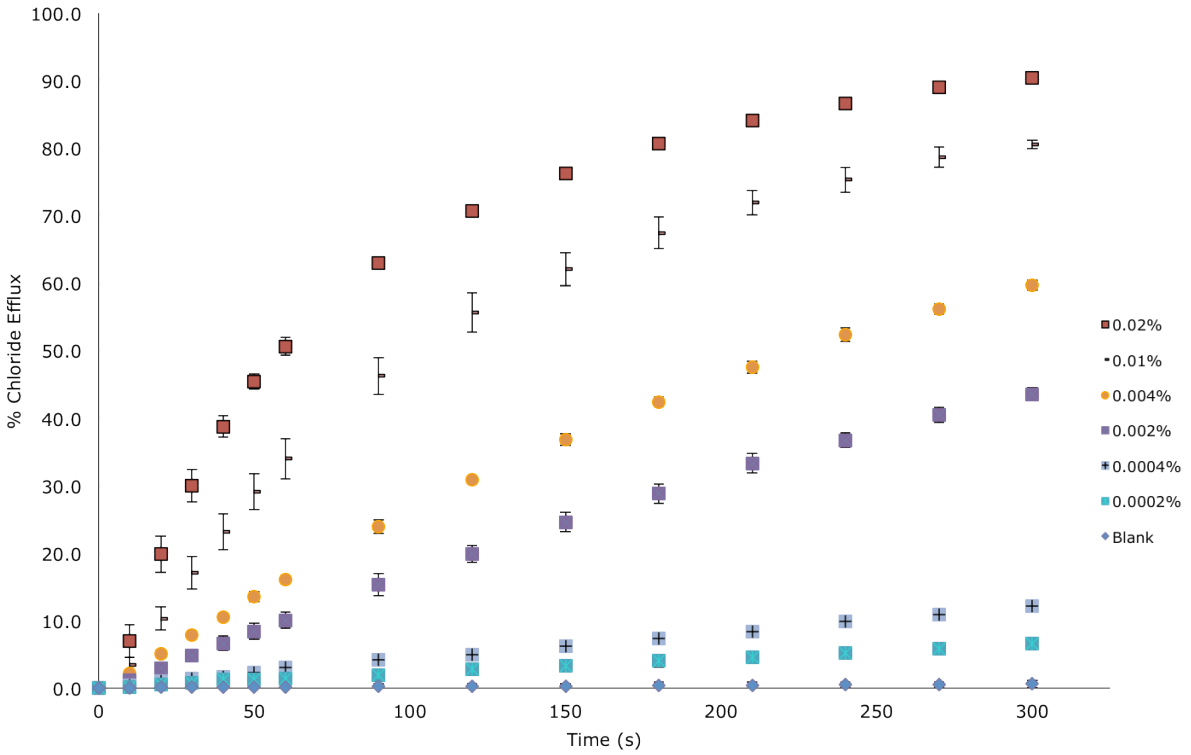

Figure S 33: Chloride efflux as a function of time, promoted by the addition of various concentrations of receptor **4,** from unilamellar POPC vesicles containing 489 mM NaCl buffered to pH 7.2 with 5 mM sodium phosphate salts. The vesicles were dispersed in 489 mM $NaNO_3$ buffered to pH 7.2 with 5 mM sodium phosphate salts. The receptor was loaded as a DMSO solution at 0 s. At the end of the experiment the vesicles were lysed to calibrate the chloride selective electrode to 100% chloride efflux.

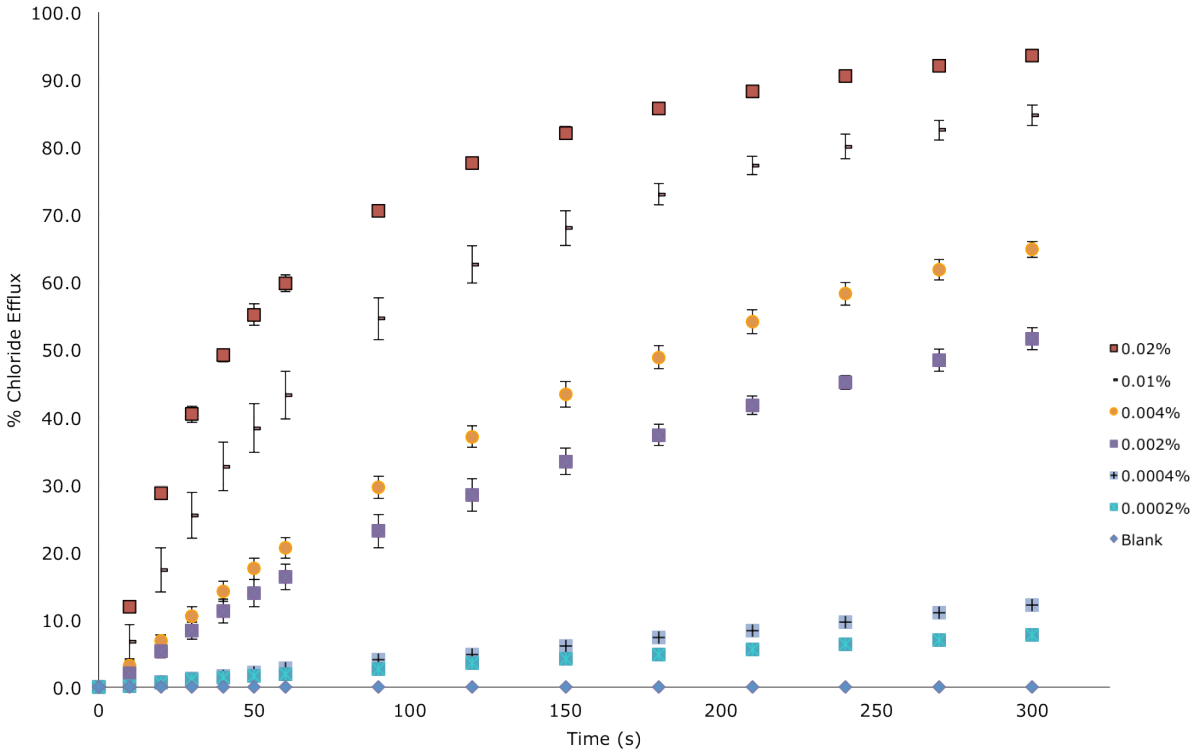

Figure S 34: Chloride efflux as a function of time, promoted by the addition of various concentrations of receptor **4**, from unilamellar POPC vesicles containing 489 mM NaCl buffered to pH 7.2 with 5 mM sodium phosphate salts. The vesicles were dispersed in 489 mM $NaNO_3$ buffered to pH 7.2 with 5 mM sodium phosphate salts. The receptor was loaded as a DMSO solution at 0 s. At the end of the experiment the vesicles were lysed to calibrate the chloride selective electrode to 100% chloride efflux.

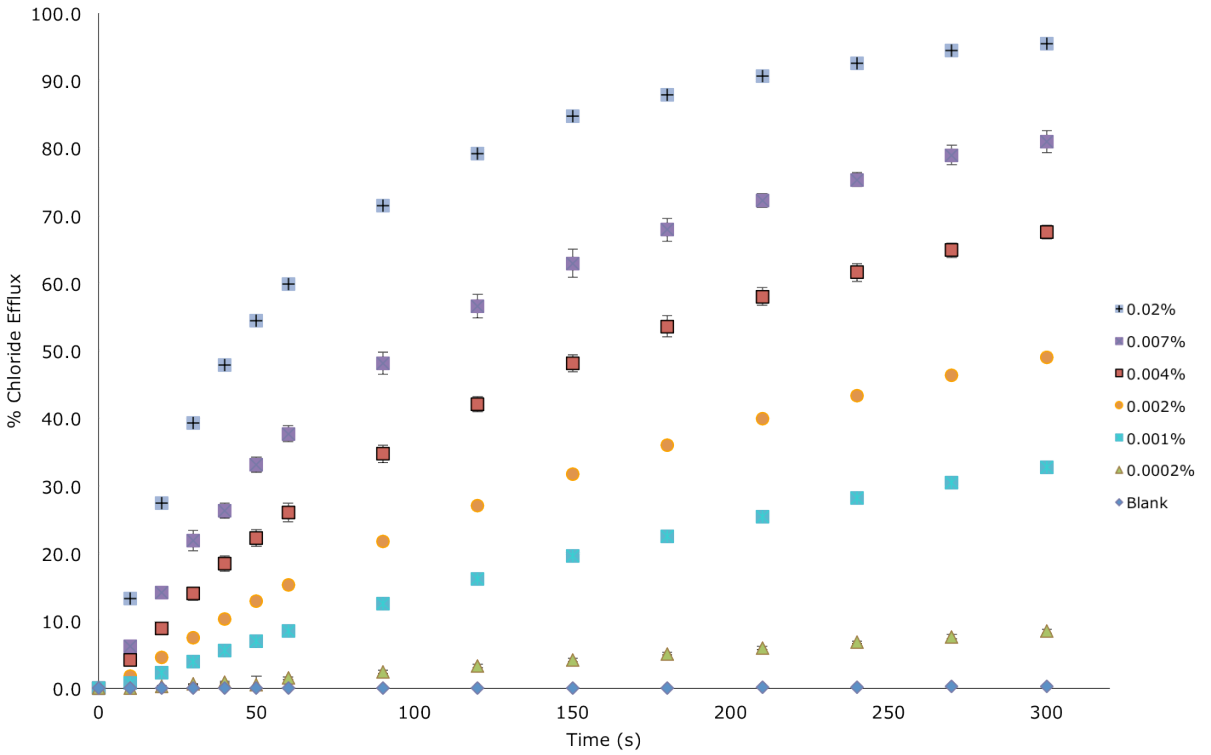

Figure S 35: Chloride efflux as a function of time, promoted by the addition of various concentrations of receptor **6**, from unilamellar POPC vesicles containing 489 mM NaCl buffered to pH 7.2 with 5 mM sodium phosphate salts. The vesicles were dispersed in 489 mM $NaNO_3$ buffered to pH 7.2 with 5 mM sodium phosphate salts. The receptor was loaded as a DMSO solution at 0 s. At the end of the experiment the vesicles were lysed to calibrate the chloride selective electrode to 100% chloride efflux.

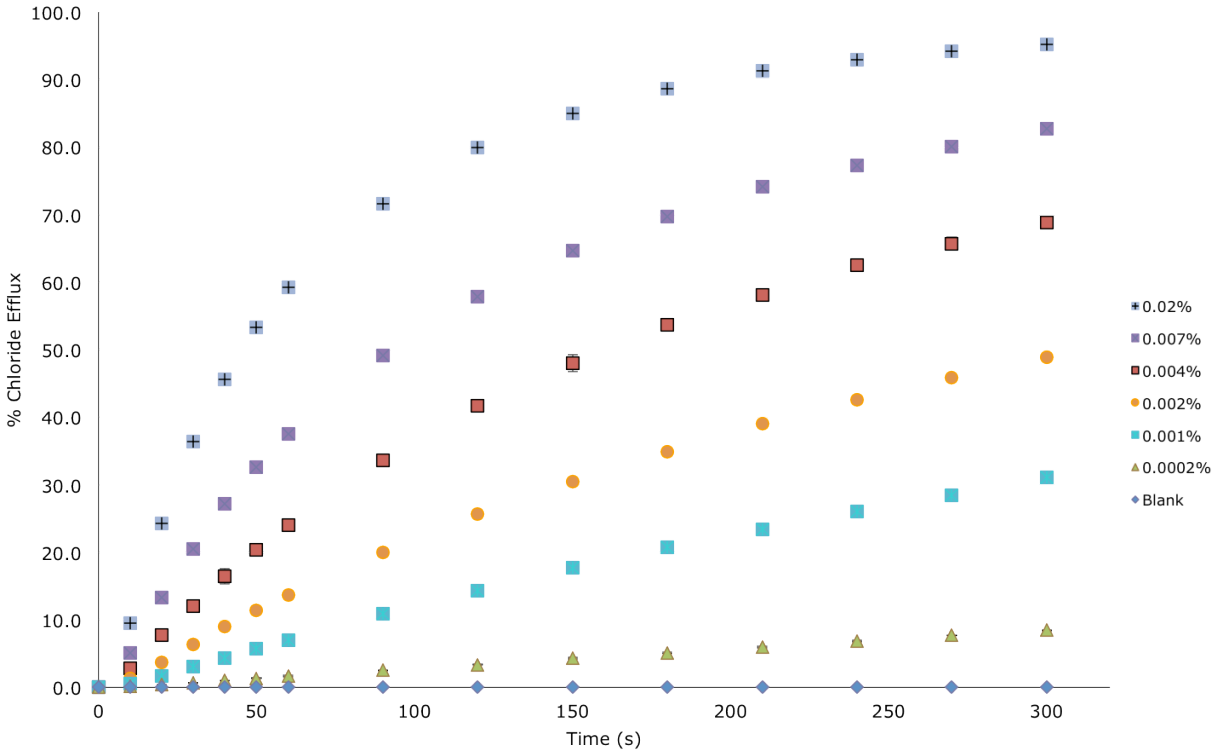

Figure S 36: Chloride efflux as a function of time, promoted by the addition of various concentrations of receptor **6**, from unilamellar POPC vesicles containing 489 mM NaCl buffered to pH 7.2 with 5 mM sodium phosphate salts. The vesicles were dispersed in 489 mM $NaNO_3$ buffered to pH 7.2 with 5 mM sodium phosphate salts. The receptor was loaded as a DMSO solution at 0 s. At the end of the experiment the vesicles were lysed to calibrate the chloride selective electrode to 100% chloride efflux.

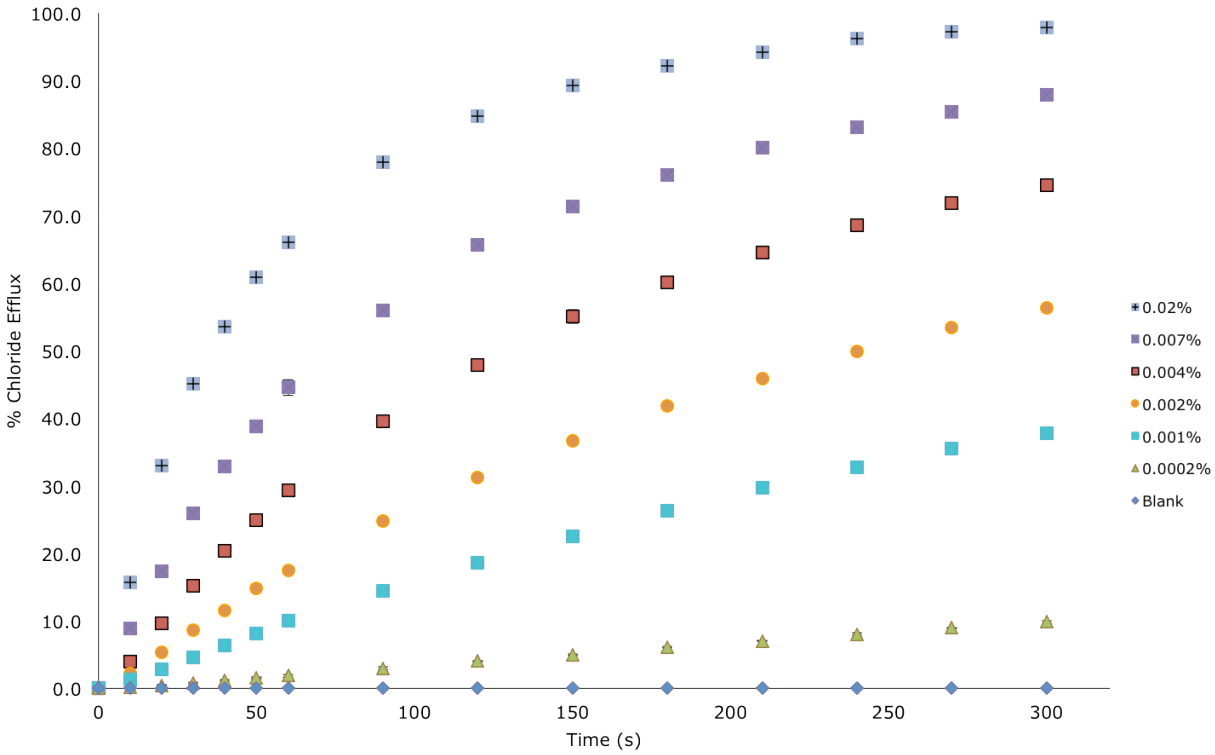

Figure S 37: Chloride efflux as a function of time, promoted by the addition of various concentrations of receptor **6,** from unilamellar POPC vesicles containing 489 mM NaCl buffered to pH 7.2 with 5 mM sodium phosphate salts. The vesicles were dispersed in 489 mM $NaNO_3$ buffered to pH 7.2 with 5 mM sodium phosphate salts. The receptor was loaded as a DMSO solution at 0 s. At the end of the experiment the vesicles were lysed to calibrate the chloride selective electrode to 100% chloride efflux.

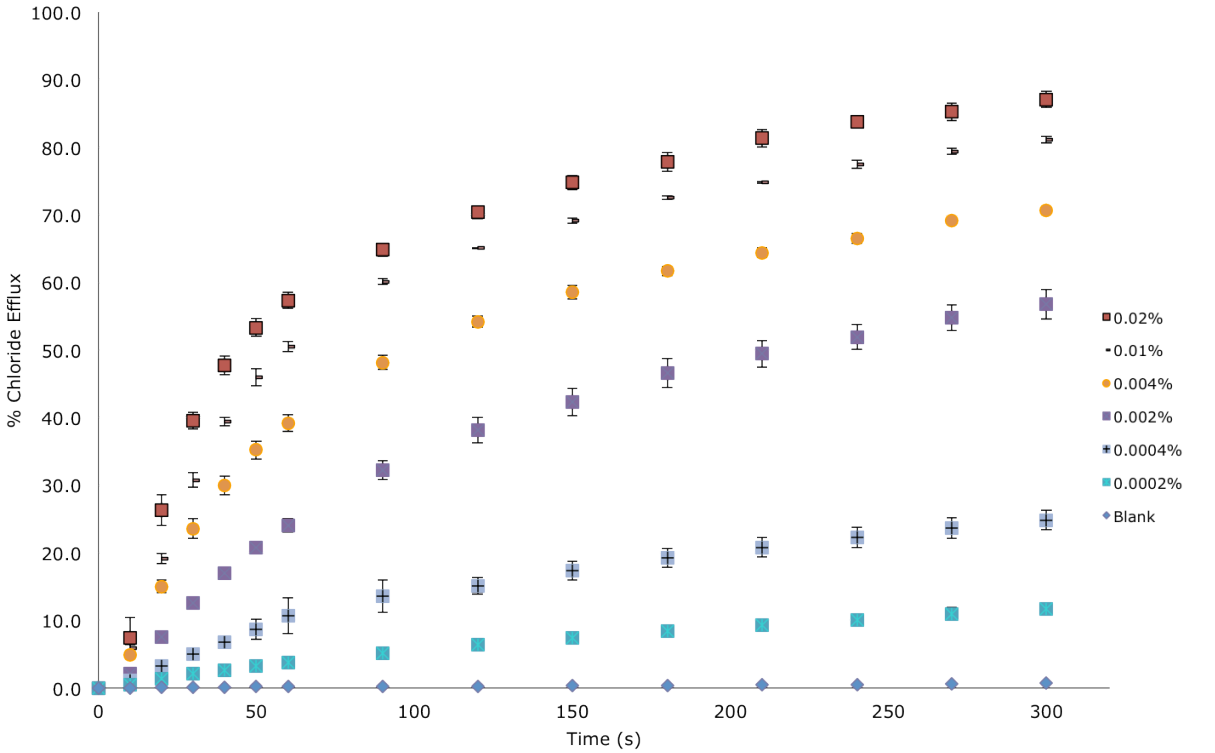

Figure S 38: Chloride efflux as a function of time, promoted by the addition of various concentrations of receptor **7**, from unilamellar POPC vesicles containing 489 mM NaCl buffered to pH 7.2 with 5 mM sodium phosphate salts. The vesicles were dispersed in 489 mM $NaNO_3$ buffered to pH 7.2 with 5 mM sodium phosphate salts. The receptor was loaded as a DMSO solution at 0 s. At the end of the experiment the vesicles were lysed to calibrate the chloride selective electrode to 100% chloride efflux.

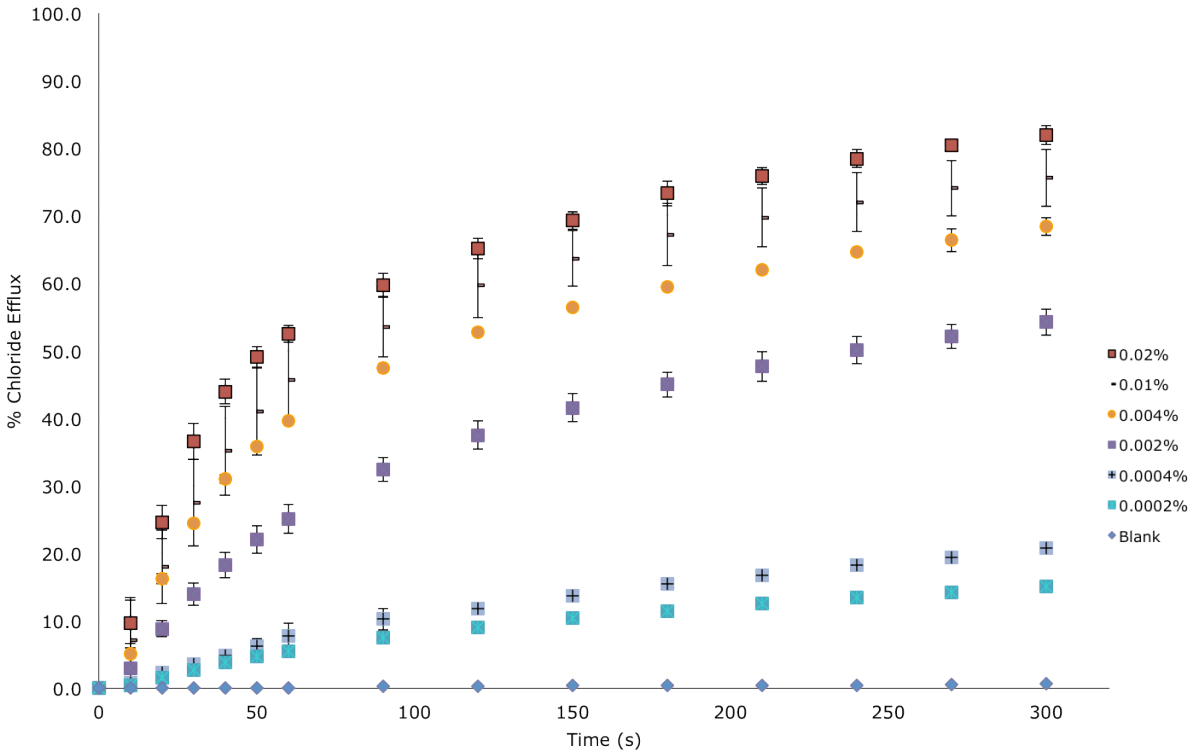

Figure S 39: Chloride efflux as a function of time, promoted by the addition of various concentrations of receptor **7,** from unilamellar POPC vesicles containing 489 mM NaCl buffered to pH 7.2 with 5 mM sodium phosphate salts. The vesicles were dispersed in 489 mM $NaNO_3$ buffered to pH 7.2 with 5 mM sodium phosphate salts. The receptor was loaded as a DMSO solution at 0 s. At the end of the experiment the vesicles were lysed to calibrate the chloride selective electrode to 100% chloride efflux.

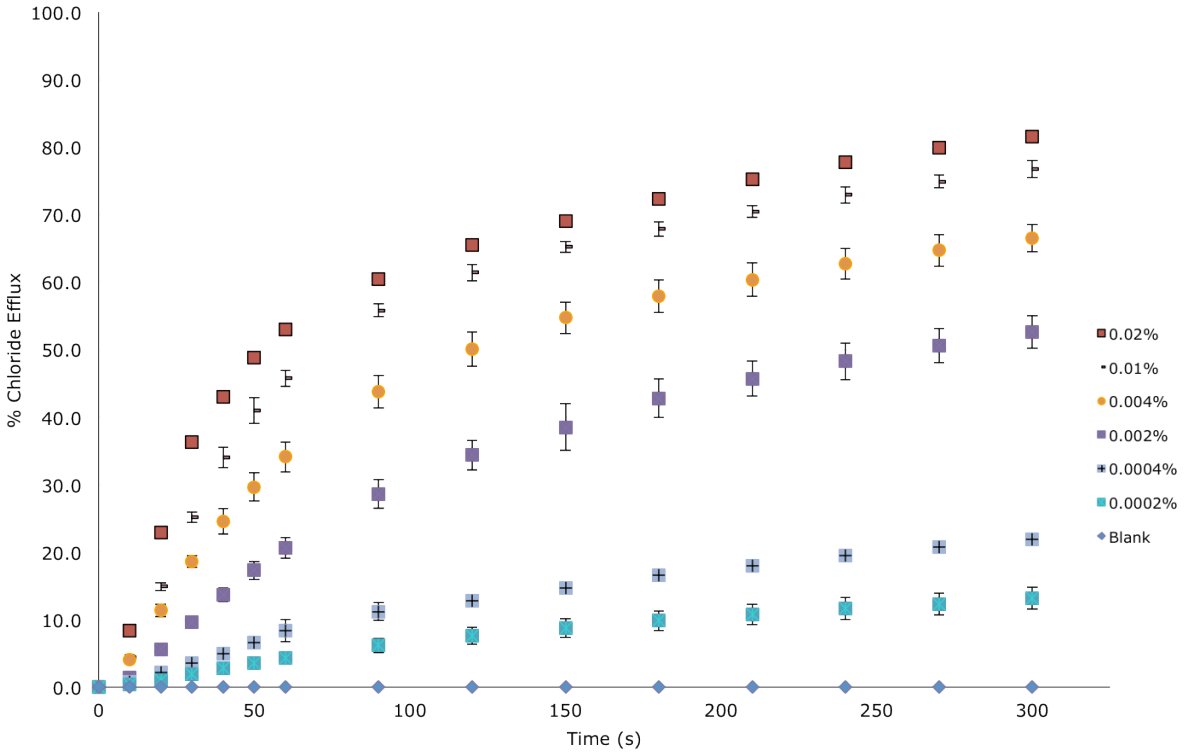

Figure S 40: Chloride efflux as a function of time, promoted by the addition of various concentrations of receptor **7**, from unilamellar POPC vesicles containing 489 mM NaCl buffered to pH 7.2 with 5 mM sodium phosphate salts. The vesicles were dispersed in 489 mM $NaNO_3$ buffered to pH 7.2 with 5 mM sodium phosphate salts. The receptor was loaded as a DMSO solution at 0 s. At the end of the experiment the vesicles were lysed to calibrate the chloride selective electrode to 100% chloride efflux.

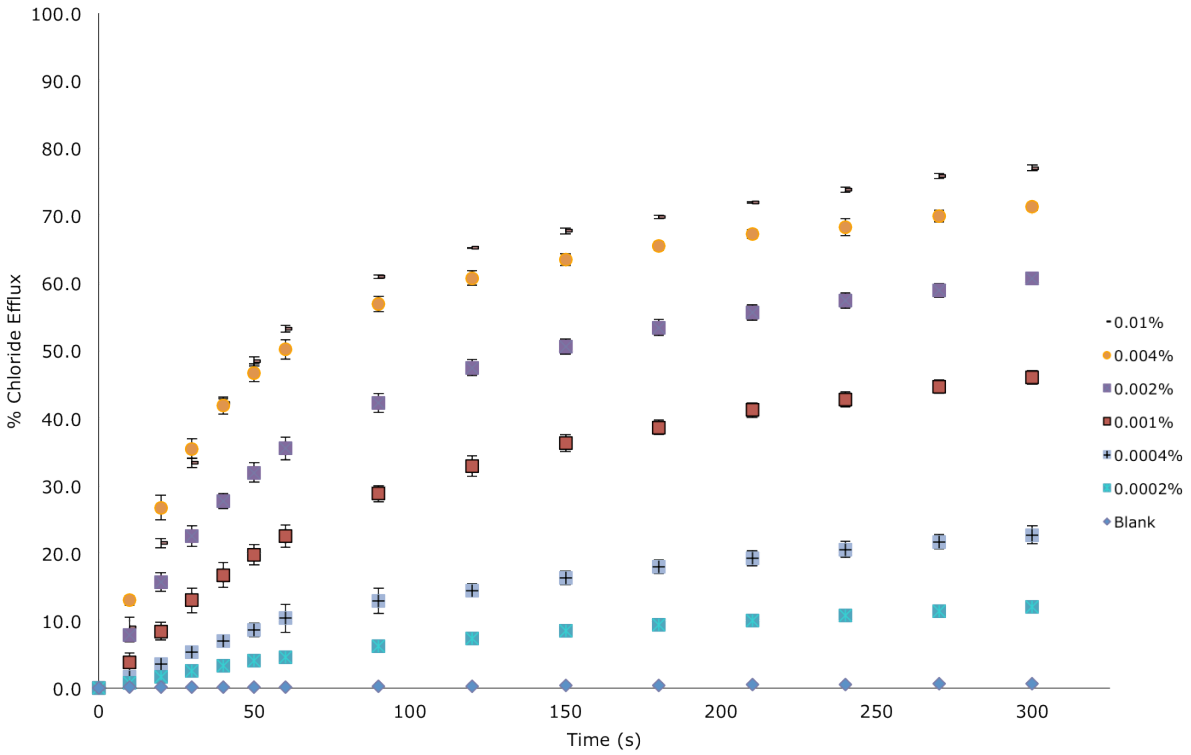

Figure S 41: Chloride efflux as a function of time, promoted by the addition of various concentrations of receptor **7,** from unilamellar POPC vesicles containing 489 mM NaCl buffered to pH 7.2 with 5 mM sodium phosphate salts. The vesicles were dispersed in 489 mM $NaNO_3$ buffered to pH 7.2 with 5 mM sodium phosphate salts. The receptor was loaded as a DMSO solution at 0 s. At the end of the experiment the vesicles were lysed to calibrate the chloride selective electrode to 100% chloride efflux.

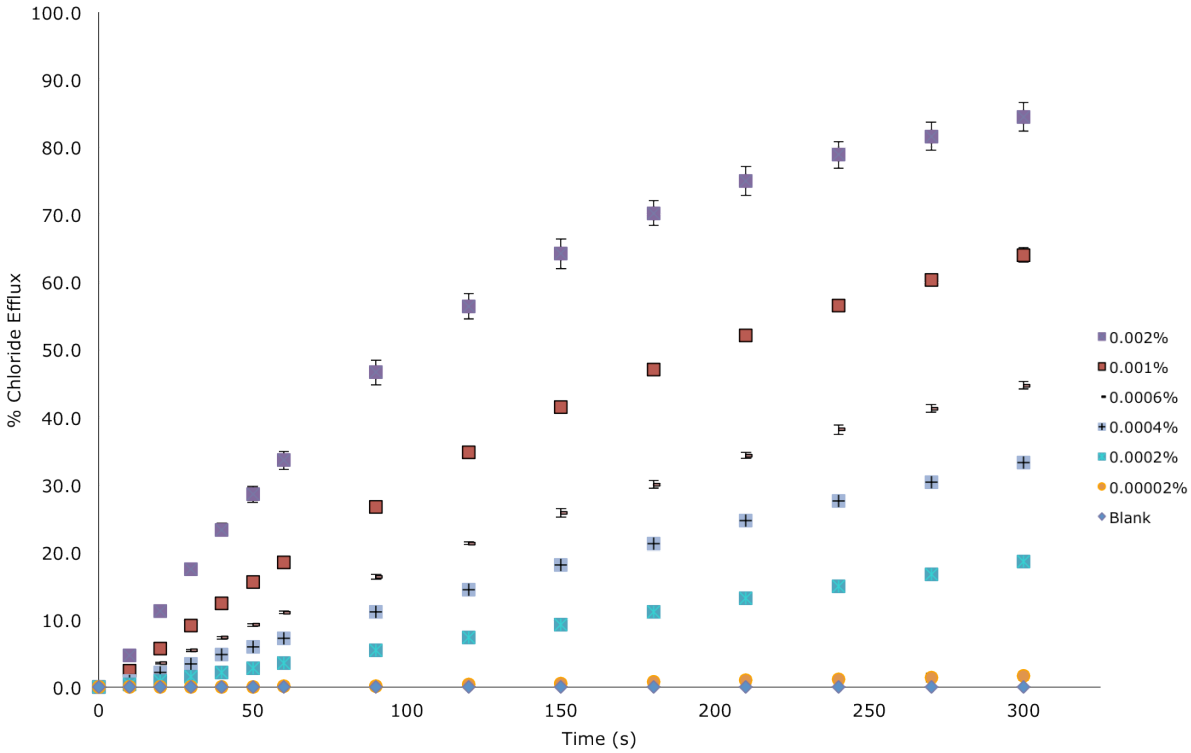

Figure S 42: Chloride efflux as a function of time, promoted by the addition of various concentrations of receptor **8,** from unilamellar POPC vesicles containing 489 mM NaCl buffered to pH 7.2 with 5 mM sodium phosphate salts. The vesicles were dispersed in 489 mM $NaNO_3$ buffered to pH 7.2 with 5 mM sodium phosphate salts. The receptor was loaded as a DMSO solution at 0 s. At the end of the experiment the vesicles were lysed to calibrate the chloride selective electrode to 100% chloride efflux.

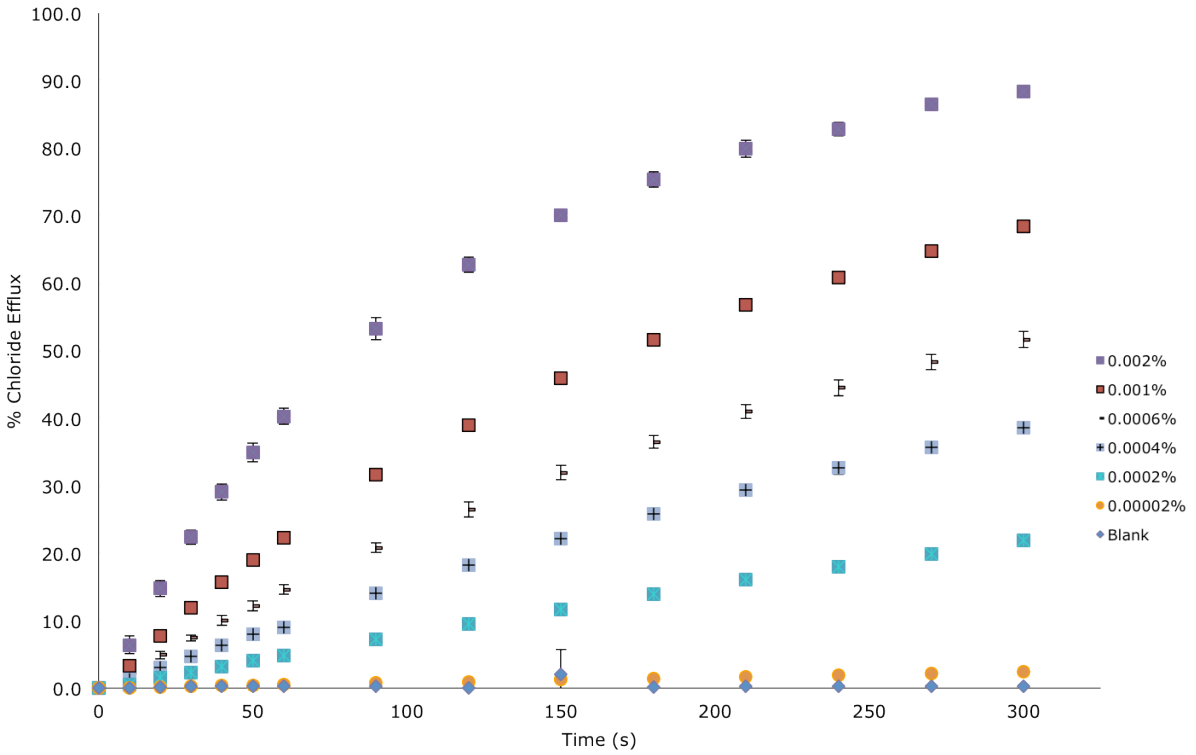

Figure S 43: Chloride efflux as a function of time, promoted by the addition of various concentrations of receptor **8**, from unilamellar POPC vesicles containing 489 mM NaCl buffered to pH 7.2 with 5 mM sodium phosphate salts. The vesicles were dispersed in 489 mM $NaNO_3$ buffered to pH 7.2 with 5 mM sodium phosphate salts. The receptor was loaded as a DMSO solution at 0 s. At the end of the experiment the vesicles were lysed to calibrate the chloride selective electrode to 100% chloride efflux.

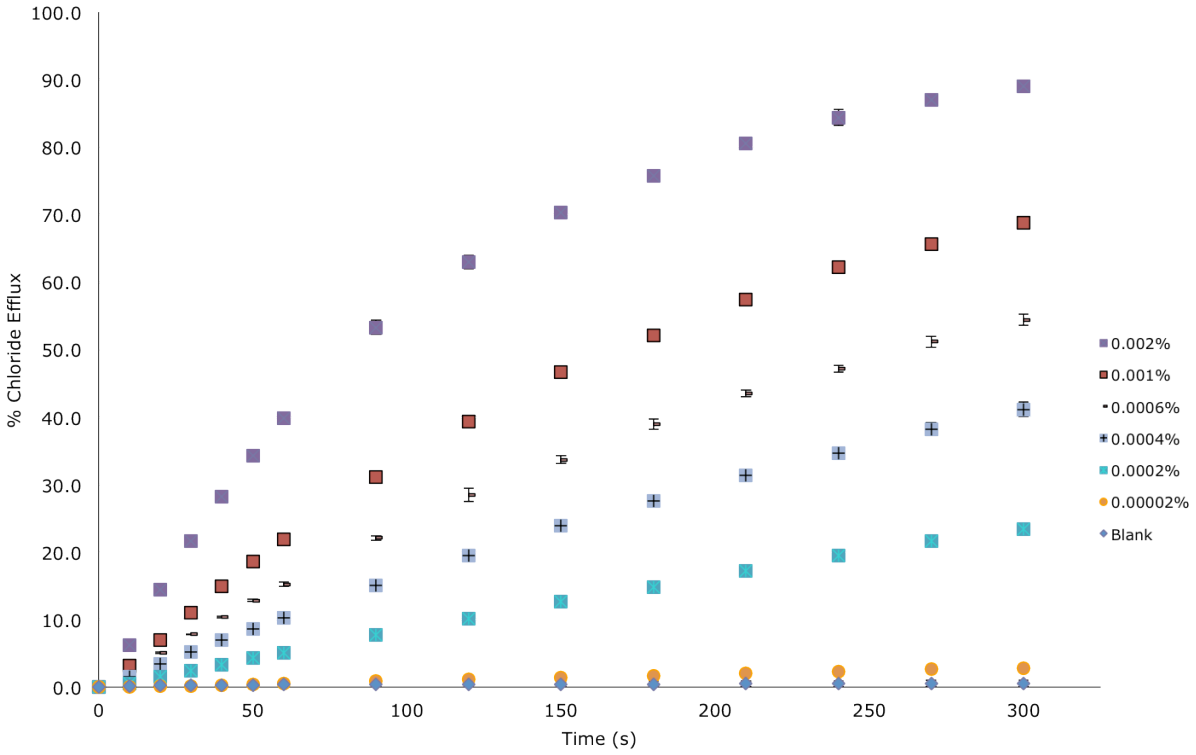

Figure S 44: Chloride efflux as a function of time, promoted by the addition of various concentrations of receptor **8,** from unilamellar POPC vesicles containing 489 mM NaCl buffered to pH 7.2 with 5 mM sodium phosphate salts. The vesicles were dispersed in 489 mM $NaNO_3$ buffered to pH 7.2 with 5 mM sodium phosphate salts. The receptor was loaded as a DMSO solution at 0 s. At the end of the experiment the vesicles were lysed to calibrate the chloride selective electrode to 100% chloride efflux.

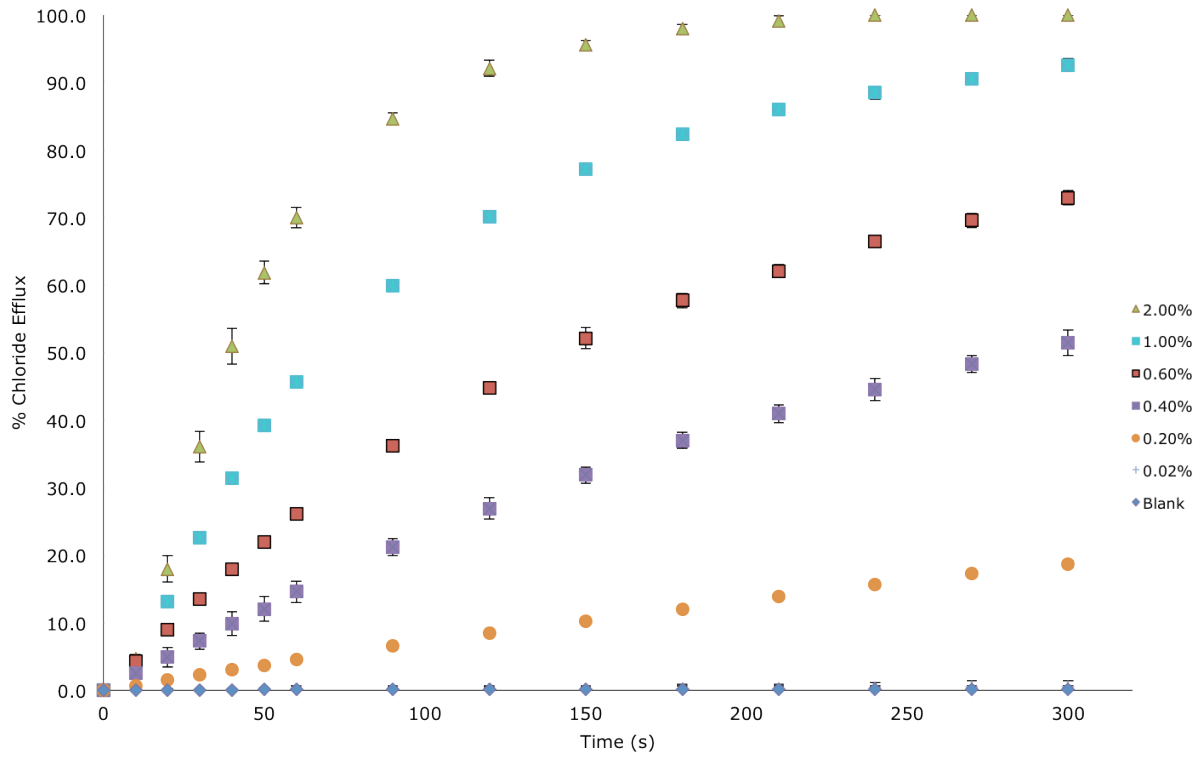

Figure S 45: Chloride efflux as a function of time, promoted by the addition of various concentrations of receptor **10**, from unilamellar POPC vesicles containing 489 mM NaCl buffered to pH 7.2 with 5 mM sodium phosphate salts. The vesicles were dispersed in 489 mM $NaNO_3$ buffered to pH 7.2 with 5 mM sodium phosphate salts. The receptor was loaded as a DMSO solution at 0 s. At the end of the experiment the vesicles were lysed to calibrate the chloride selective electrode to 100% chloride efflux.

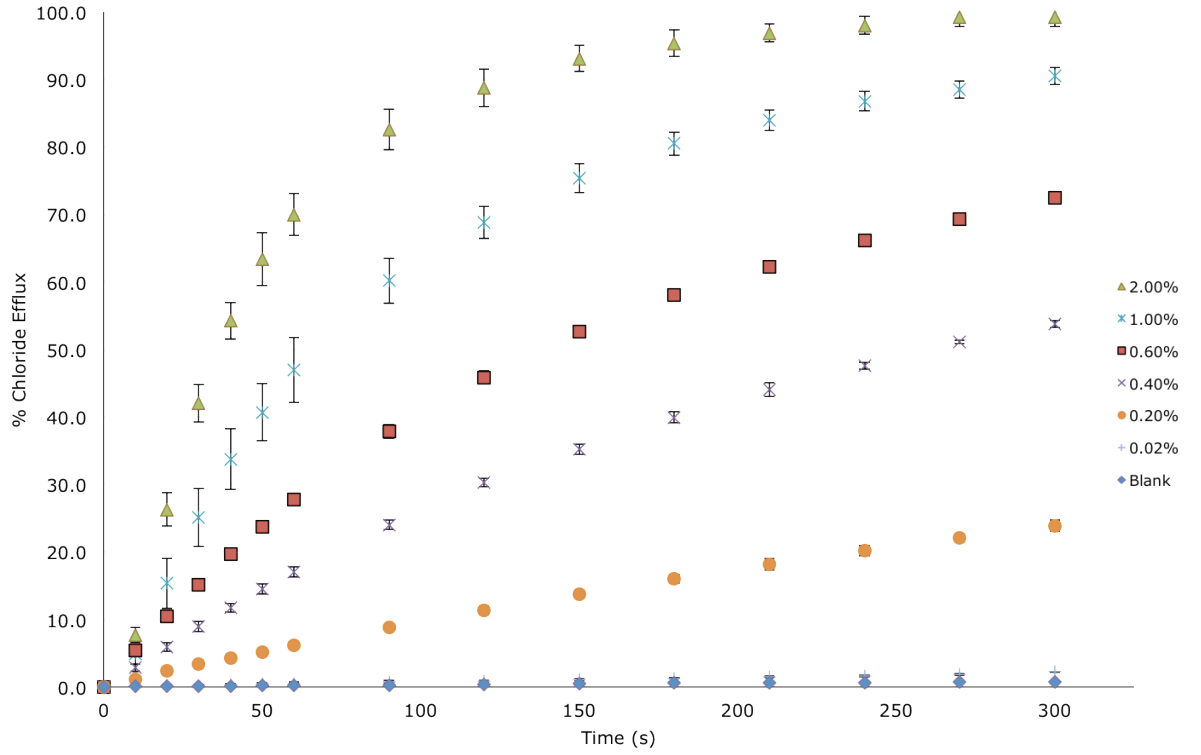

Figure S 46: Chloride efflux as a function of time, promoted by the addition of various concentrations of receptor **10**, from unilamellar POPC vesicles containing 489 mM NaCl buffered to pH 7.2 with 5 mM sodium phosphate salts. The vesicles were dispersed in 489 mM $NaNO_3$ buffered to pH 7.2 with 5 mM sodium phosphate salts. The receptor was loaded as a DMSO solution at 0 s. At the end of the experiment the vesicles were lysed to calibrate the chloride selective electrode to 100% chloride efflux.

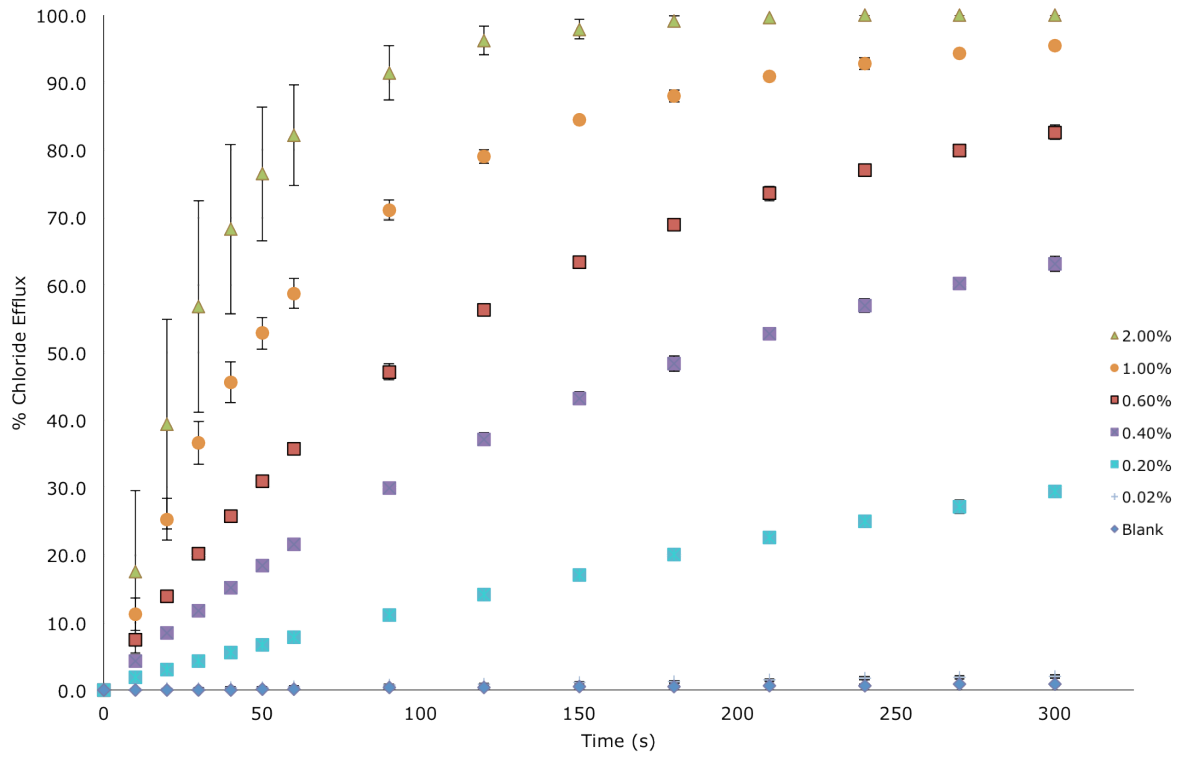

Figure S 47: Chloride efflux as a function of time, promoted by the addition of various concentrations of receptor **10,** from unilamellar POPC vesicles containing 489 mM NaCl buffered to pH 7.2 with 5 mM sodium phosphate salts. The vesicles were dispersed in 489 mM $NaNO_3$ buffered to pH 7.2 with 5 mM sodium phosphate salts. The receptor was loaded as a DMSO solution at 0 s. At the end of the experiment the vesicles were lysed to calibrate the chloride selective electrode to 100% chloride efflux.

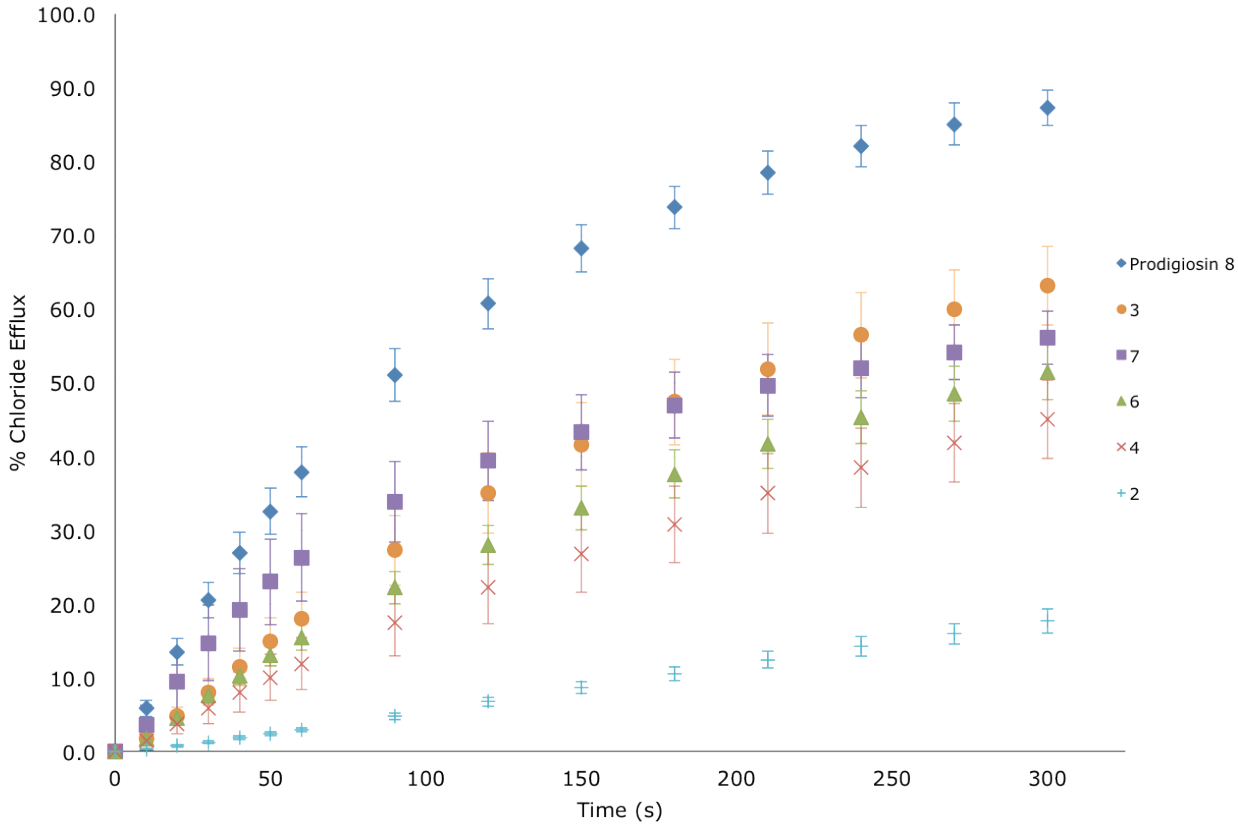

Figure S 48: Chloride efflux as a function of time, promoted by the addition of 0.002 mol% (with respect to lipid) of receptors **2**, **3**, **4**, **6**, **7** and prodigiosin **8**, from unilamellar POPC vesicles containing 489 mM NaCl buffered to pH 7.2 with 5 mM sodium phosphate salts. The vesicles were dispersed in 489 mM $NaNO_3$ buffered to pH 7.2 with 5 mM sodium phosphate salts. The receptor was loaded as a DMSO solution at 0 s. At the end of the experiment the vesicles were lysed to calibrate the chloride selective electrode to 100% chloride efflux.

S7: Anion Transport Studies: Cl^-/HCO_3^- Exchange

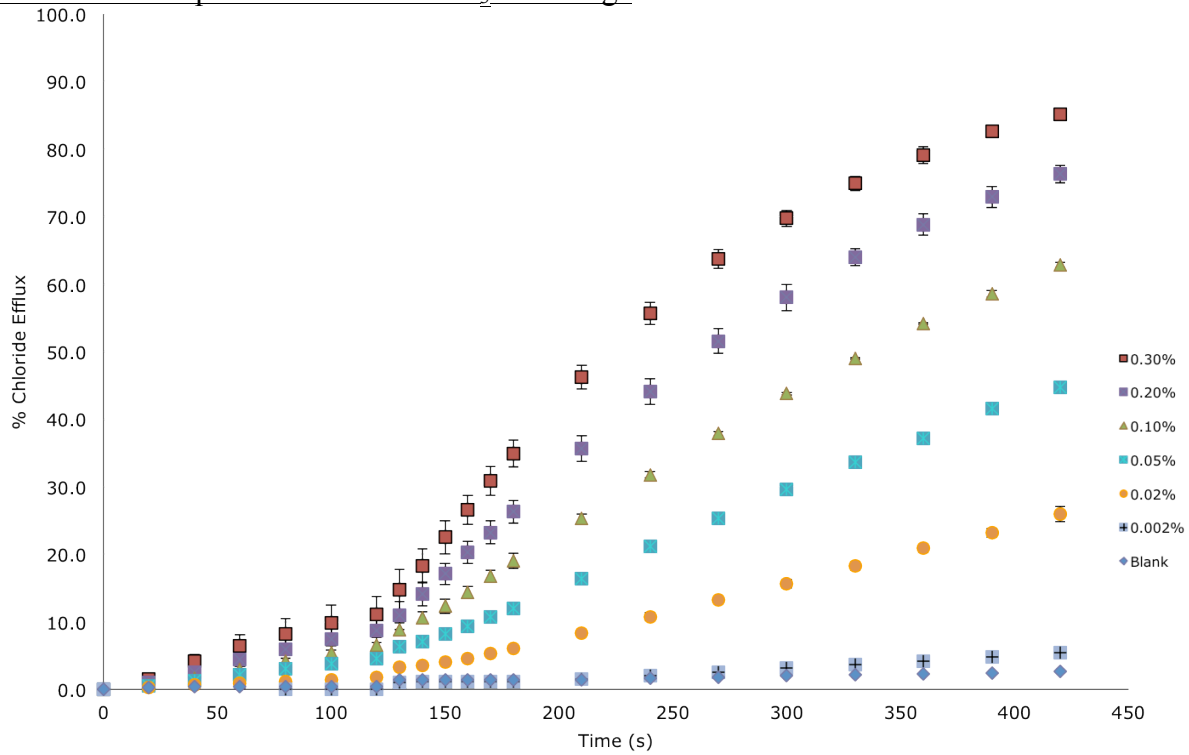

Figure S 49: Chloride efflux as a function of time, promoted by the addition of various concentration of receptor **2**, from unilamellar POPC vesicles containing 451 mM NaCl buffered to pH 7.2 with 20 mM sodium phosphate salts. The vesicles were dispersed in the external solution containing 150 mM Na_2SO_4 buffered to pH 7.2 with 20 mM sodium phosphate salts. The receptor was loaded as a DMSO solution at 0 s, and a spike of $NaHCO_3$ (33 mM) added at 120 s. At the end of the experiment the vesicles were lysed to calibrate the chloride selective electrode to 100% chloride efflux.

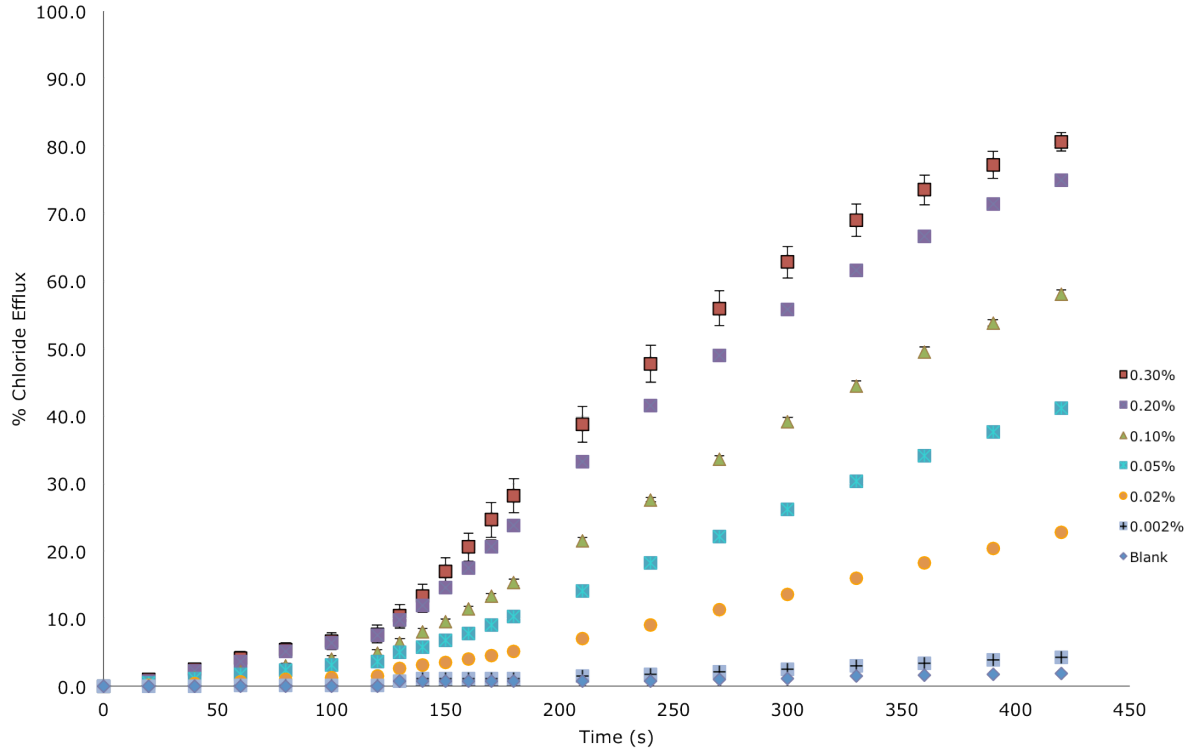

Figure S 50: Chloride efflux as a function of time, promoted by the addition of various concentrations of receptor **2**, from unilamellar POPC vesicles containing 451 mM NaCl buffered to pH 7.2 with 20 mM sodium phosphate salts. The vesicles were dispersed in the external solution containing 150 mM Na_2SO_4 buffered to pH 7.2 with 20 mM sodium phosphate salts. The receptor was loaded as a DMSO solution at 0 s, and a spike of $NaHCO_3$ (33 mM) added at 120 s. At the end of the experiment the vesicles were lysed to calibrate the chloride selective electrode to 100% chloride efflux.

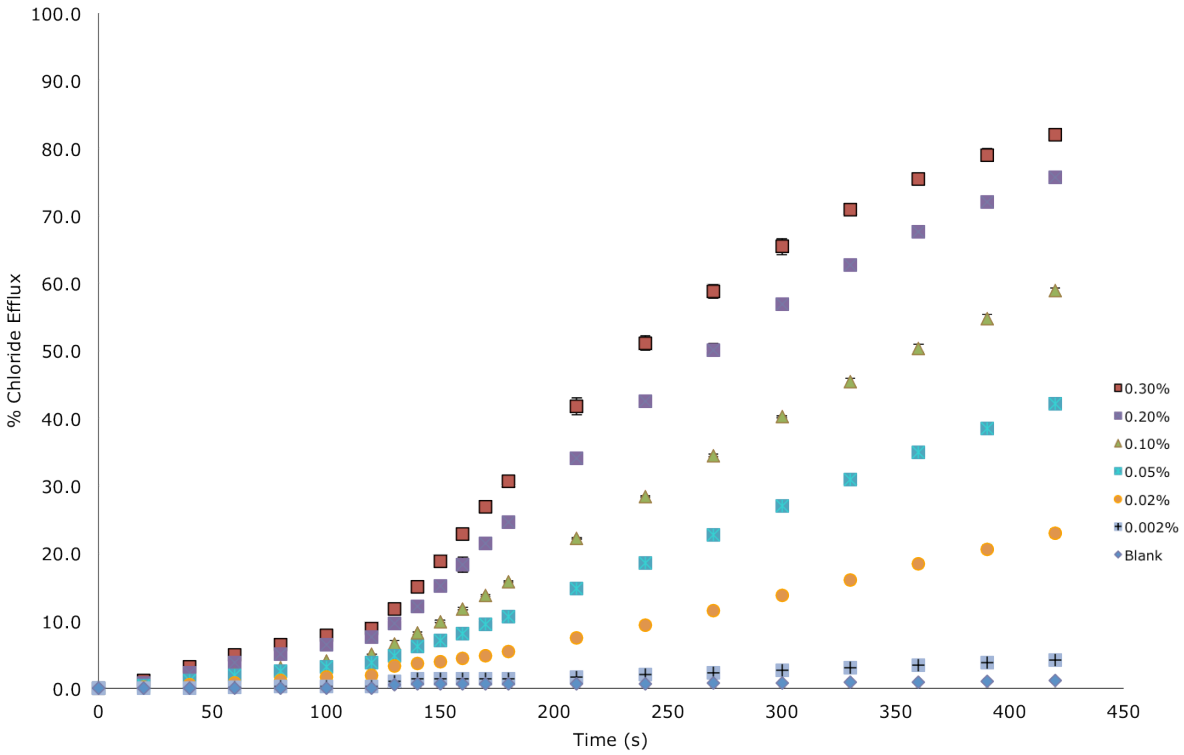

Figure S 51: Chloride efflux as a function of time, promoted by the addition of various concentrations of receptor **2**, from unilamellar POPC vesicles containing 451 mM NaCl buffered to pH 7.2 with 20 mM sodium phosphate salts. The vesicles were dispersed in the external solution containing 150 mM Na_2SO_4 buffered to pH 7.2 with 20 mM sodium phosphate salts. The receptor was loaded as a DMSO solution at 0 s, and a spike of $NaHCO_3$ (33 mM) added at 120 s. At the end of the experiment the vesicles were lysed to calibrate the chloride selective electrode to 100% chloride efflux.

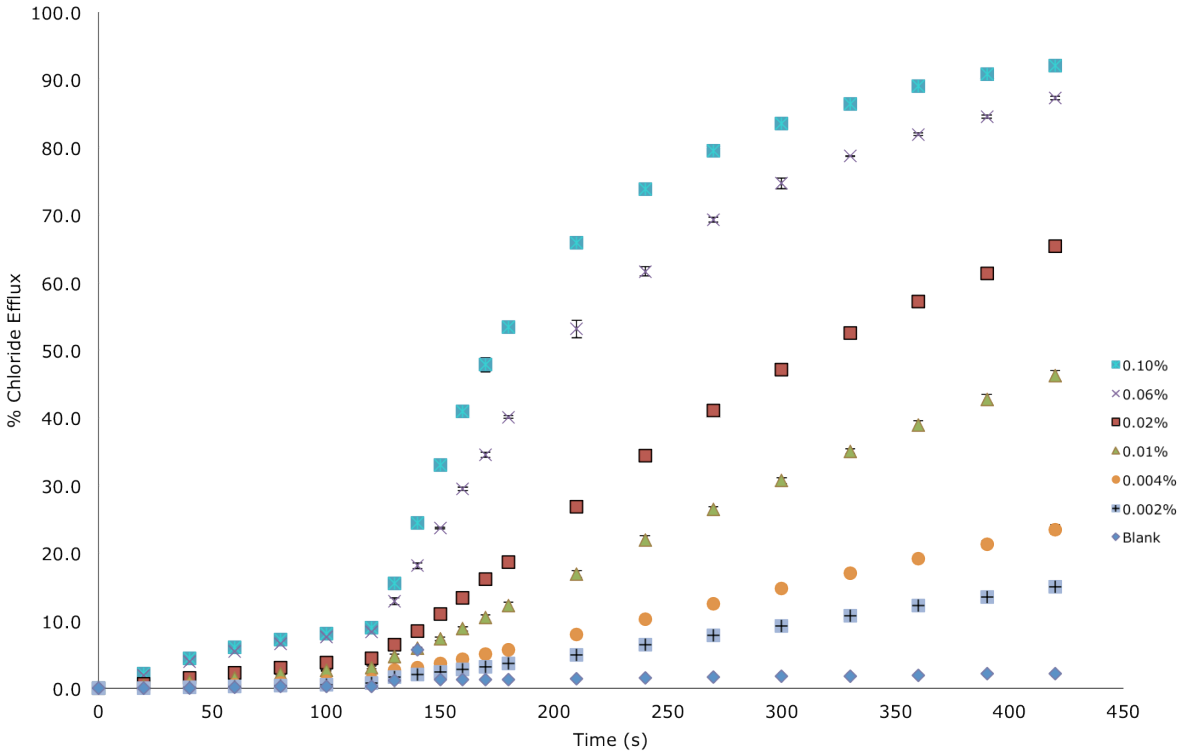

Figure S 52: Chloride efflux as a function of time, promoted by the addition of various concentration of receptor **3**, from unilamellar POPC vesicles containing 451 mM NaCl buffered to pH 7.2 with 20 mM sodium phosphate salts. The vesicles were dispersed in the external solution containing 150 mM Na_2SO_4 buffered to pH 7.2 with 20 mM sodium phosphate salts. The receptor was loaded as a DMSO solution at 0 s, and a spike of $NaHCO_3$ (33 mM) added at 120 s. At the end of the experiment the vesicles were lysed to calibrate the chloride selective electrode to 100% chloride efflux.

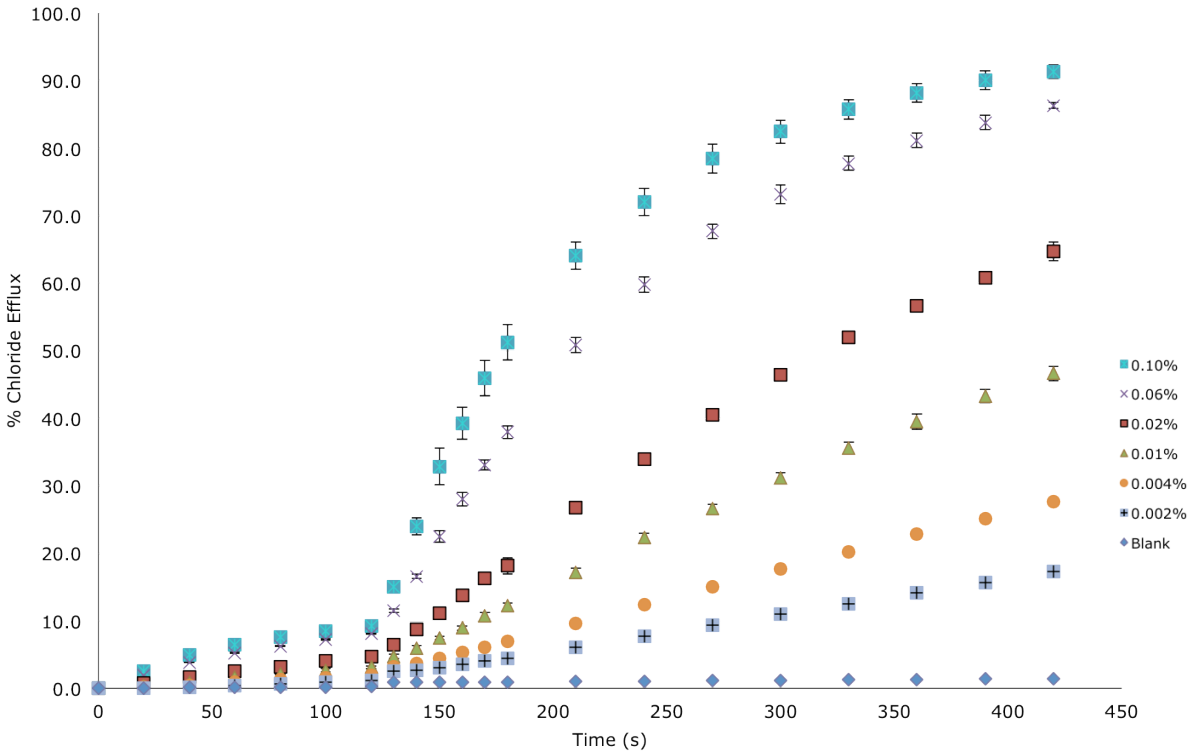

Figure S 53: Chloride efflux as a function of time, promoted by the addition of various concentrations of receptor **3**, from unilamellar POPC vesicles containing 451 mM NaCl buffered to pH 7.2 with 20 mM sodium phosphate salts. The vesicles were dispersed in the external solution containing 150 mM Na_2SO_4 buffered to pH 7.2 with 20 mM sodium phosphate salts. The receptor was loaded as a DMSO solution at 0 s, and a spike of $NaHCO_3$ (33 mM) added at 120 s. At the end of the experiment the vesicles were lysed to calibrate the chloride selective electrode to 100% chloride efflux.

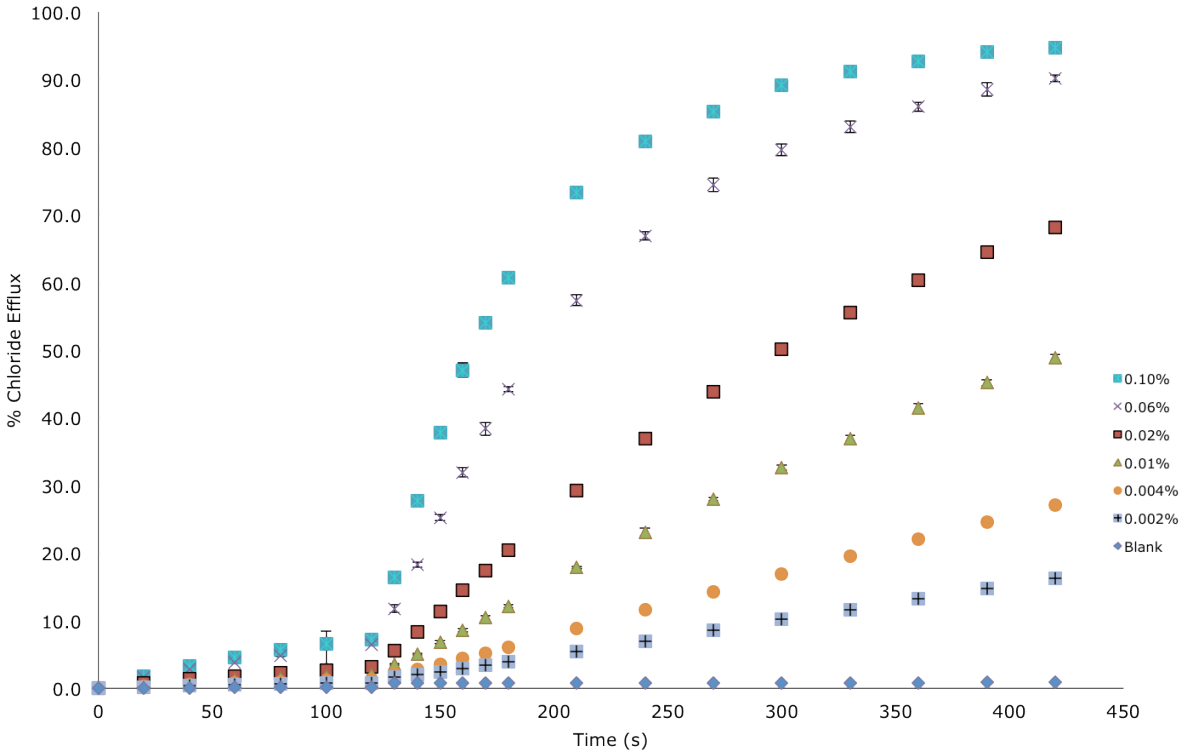

Figure S 54: Chloride efflux as a function of time, promoted by the addition of various concentrations of receptor **3**, from unilamellar POPC vesicles containing 451 mM NaCl buffered to pH 7.2 with 20 mM sodium phosphate salts. The vesicles were dispersed in the external solution containing 150 mM Na_2SO_4 buffered to pH 7.2 with 20 mM sodium phosphate salts. The receptor was loaded as a DMSO solution at 0 s, and a spike of $NaHCO_3$ (33 mM) added at 120 s. At the end of the experiment the vesicles were lysed to calibrate the chloride selective electrode to 100% chloride efflux.

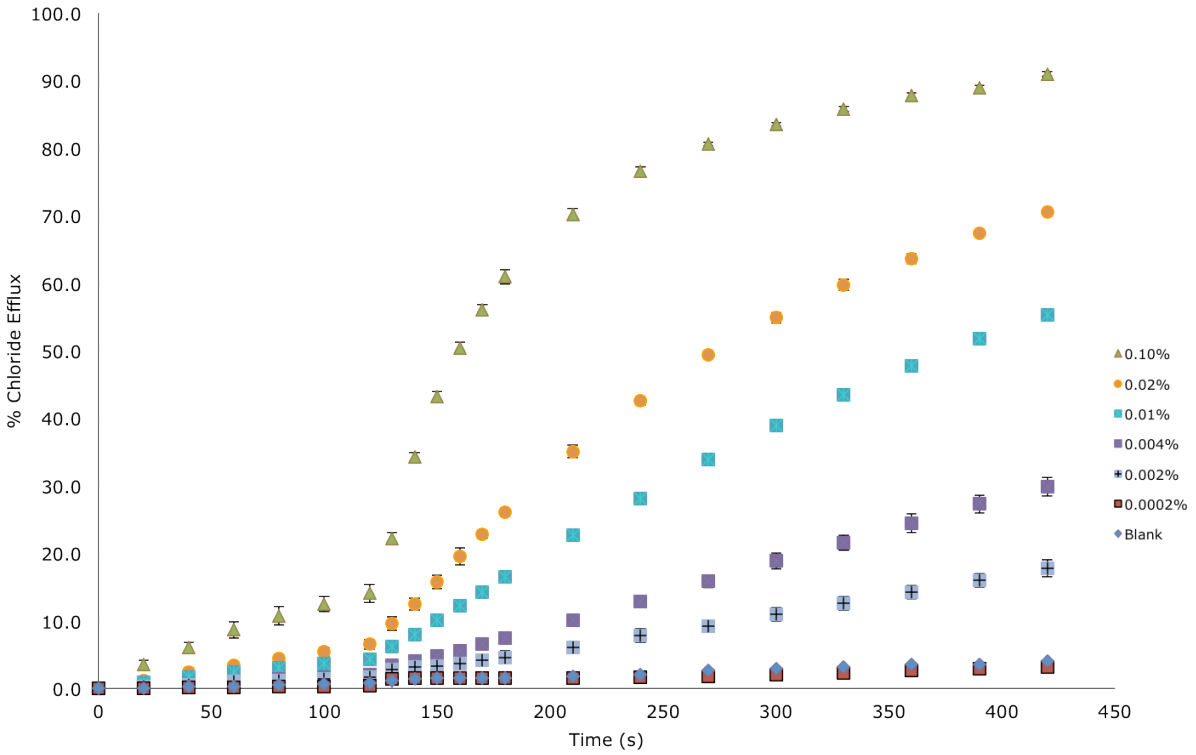

Figure S 55: Chloride efflux as a function of time, promoted by the addition of various concentration of receptor **4**, from unilamellar POPC vesicles containing 451 mM NaCl buffered to pH 7.2 with 20 mM sodium phosphate salts. The vesicles were dispersed in the external solution containing 150 mM Na_2SO_4 buffered to pH 7.2 with 20 mM sodium phosphate salts. The receptor was loaded as a DMSO solution at 0 s, and a spike of $NaHCO_3$ (33 mM) added at 120 s. At the end of the experiment the vesicles were lysed to calibrate the chloride selective electrode to 100% chloride efflux.

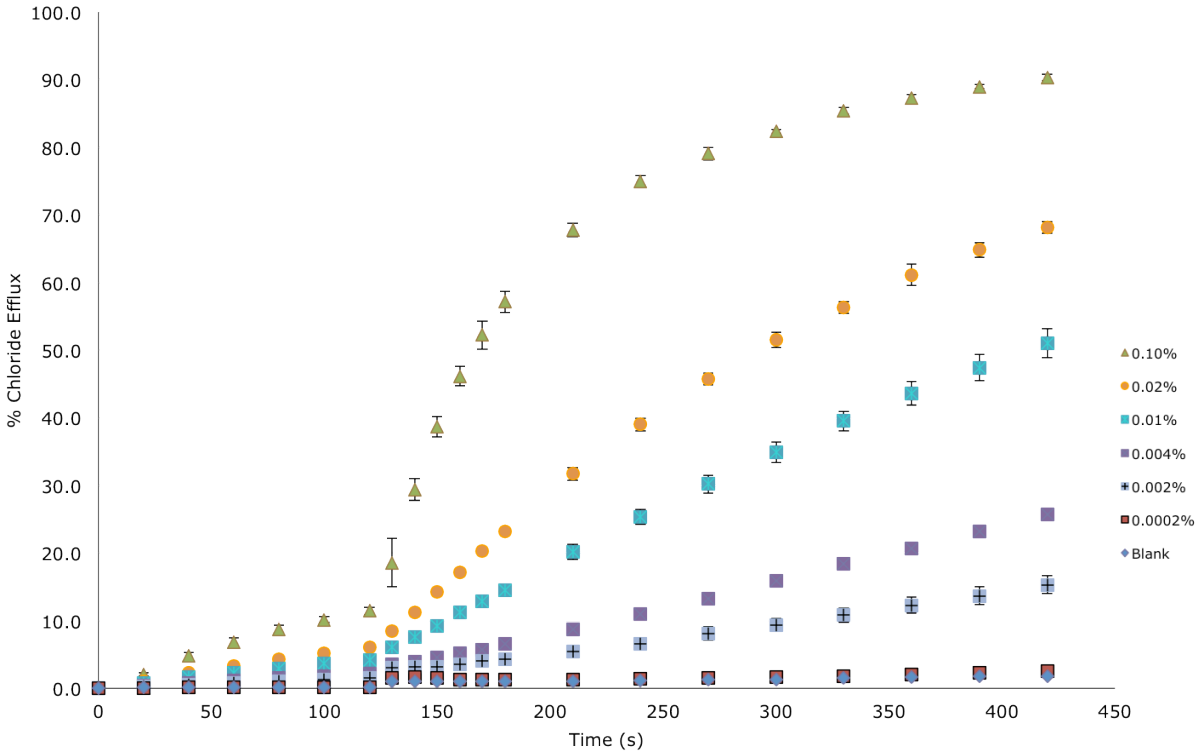

Figure S 56: Chloride efflux as a function of time, promoted by the addition of various concentrations of receptor **4**, from unilamellar POPC vesicles containing 451 mM NaCl buffered to pH 7.2 with 20 mM sodium phosphate salts. The vesicles were dispersed in the external solution containing 150 mM Na_2SO_4 buffered to pH 7.2 with 20 mM sodium phosphate salts. The receptor was loaded as a DMSO solution at 0 s, and a spike of $NaHCO_3$ (33 mM) added at 120 s. At the end of the experiment the vesicles were lysed to calibrate the chloride selective electrode to 100% chloride efflux.

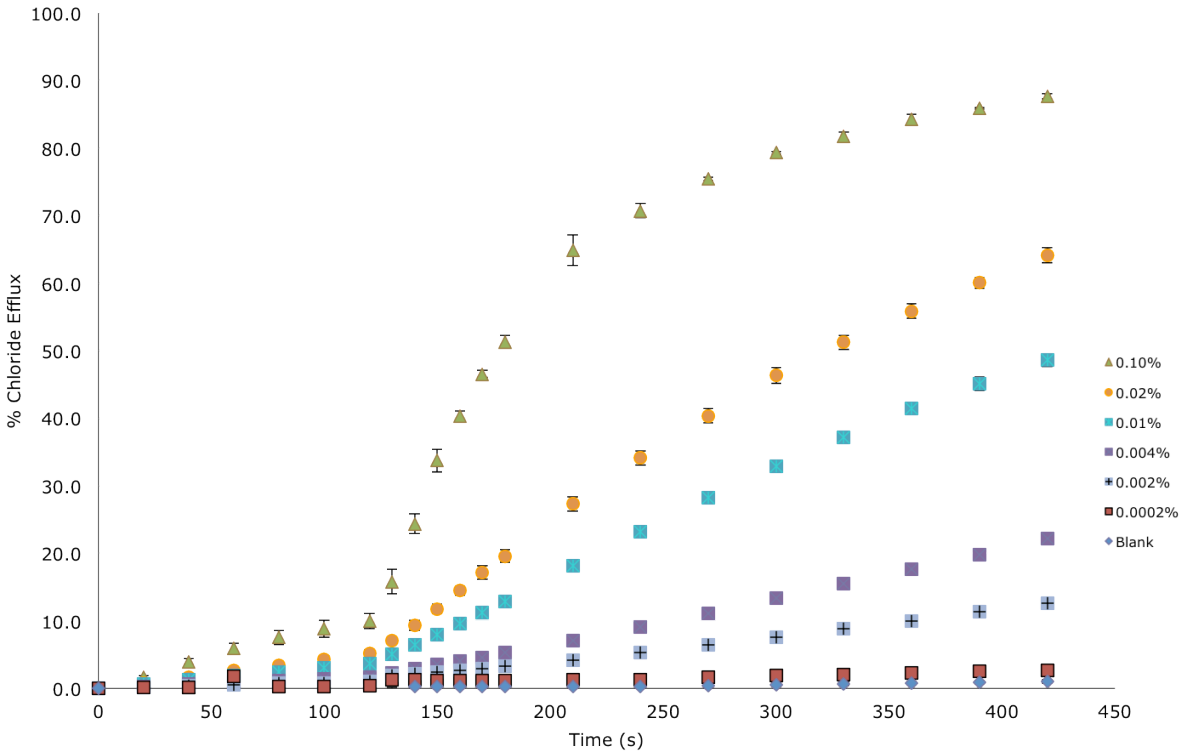

Figure S 57: Chloride efflux as a function of time, promoted by the addition of various concentrations of receptor **4**, from unilamellar POPC vesicles containing 451 mM NaCl buffered to pH 7.2 with 20 mM sodium phosphate salts. The vesicles were dispersed in the external solution containing 150 mM Na_2SO_4 buffered to pH 7.2 with 20 mM sodium phosphate salts. The receptor was loaded as a DMSO solution at 0 s, and a spike of $NaHCO_3$ (33 mM) added at 120 s. At the end of the experiment the vesicles were lysed to calibrate the chloride selective electrode to 100% chloride efflux.

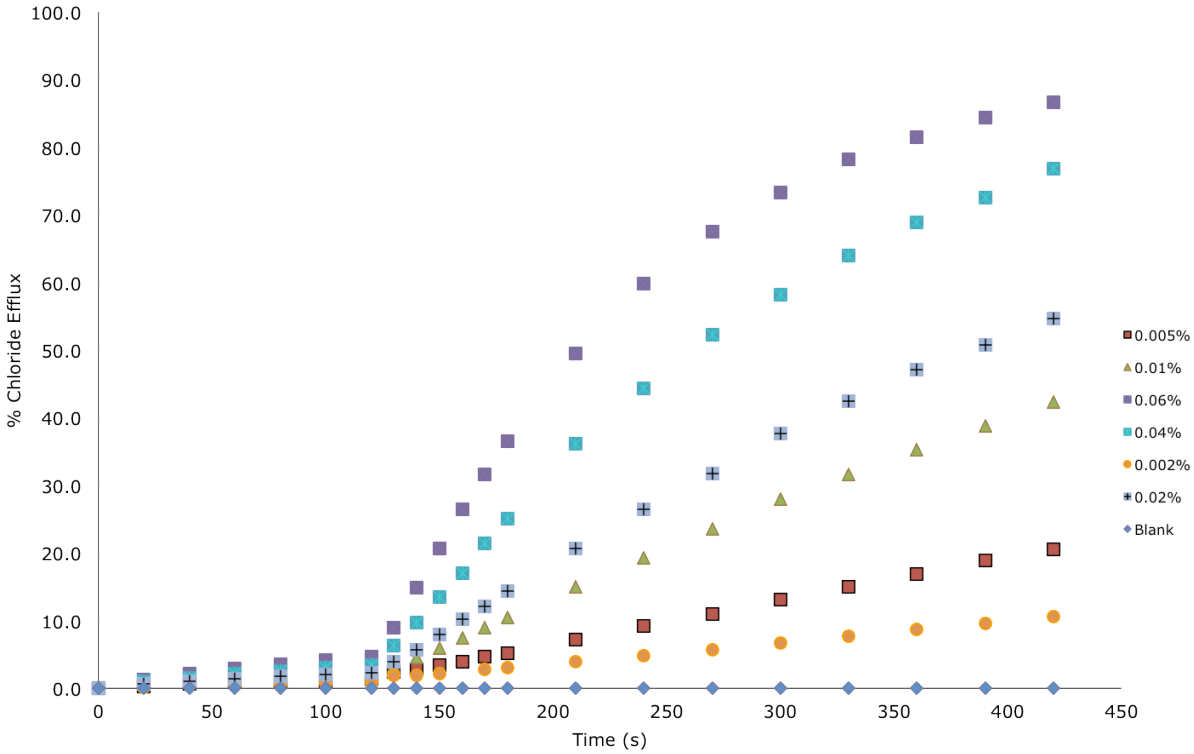

Figure S 58: Chloride efflux as a function of time, promoted by the addition of various concentrations of receptor **6**, from unilamellar POPC vesicles containing 451 mM NaCl buffered to pH 7.2 with 20 mM sodium phosphate salts. The vesicles were dispersed in the external solution containing 150 mM Na_2SO_4 buffered to pH 7.2 with 20 mM sodium phosphate salts. The receptor was loaded as a DMSO solution at 0 s, and a spike of $NaHCO_3$ (33 mM) added at 120 s. At the end of the experiment the vesicles were lysed to calibrate the chloride selective electrode to 100% chloride efflux.

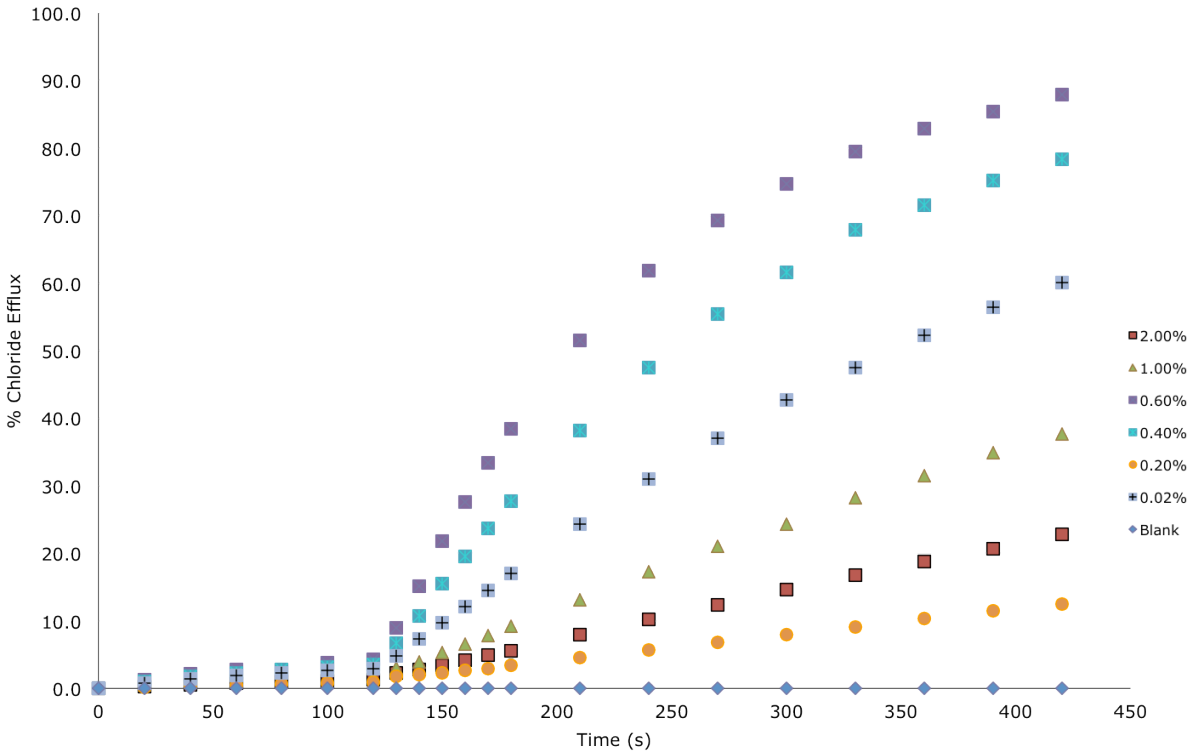

Figure S 59: Chloride efflux as a function of time, promoted by the addition of various concentrations of receptor **6**, from unilamellar POPC vesicles containing 451 mM NaCl buffered to pH 7.2 with 20 mM sodium phosphate salts. The vesicles were dispersed in the external solution containing 150 mM Na_2SO_4 buffered to pH 7.2 with 20 mM sodium phosphate salts. The receptor was loaded as a DMSO solution at 0 s, and a spike of $NaHCO_3$ (33 mM) added at 120 s. At the end of the experiment the vesicles were lysed to calibrate the chloride selective electrode to 100% chloride efflux.

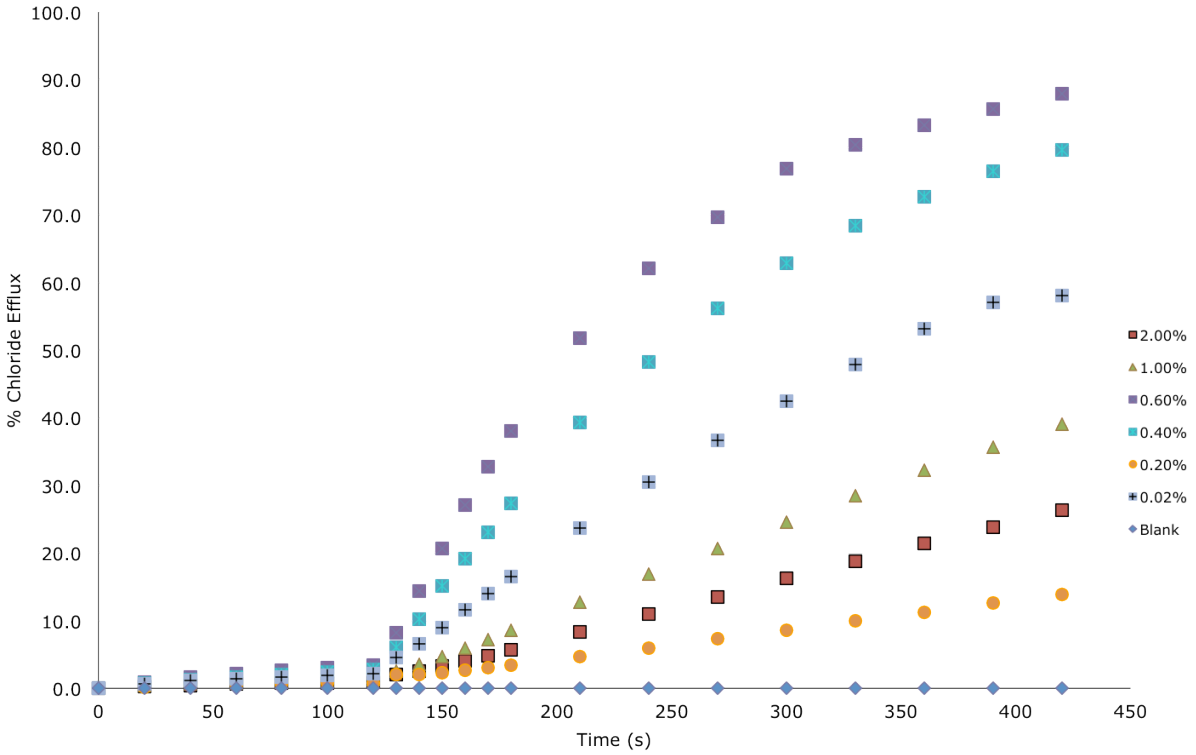

Figure S 60: Chloride efflux as a function of time, promoted by the addition of various concentrations of receptor **6**, from unilamellar POPC vesicles containing 451 mM NaCl buffered to pH 7.2 with 20 mM sodium phosphate salts. The vesicles were dispersed in the external solution containing 150 mM Na_2SO_4 buffered to pH 7.2 with 20 mM sodium phosphate salts. The receptor was loaded as a DMSO solution at 0 s, and a spike of $NaHCO_3$ (33 mM) added at 120 s. At the end of the experiment the vesicles were lysed to calibrate the chloride selective electrode to 100% chloride efflux.

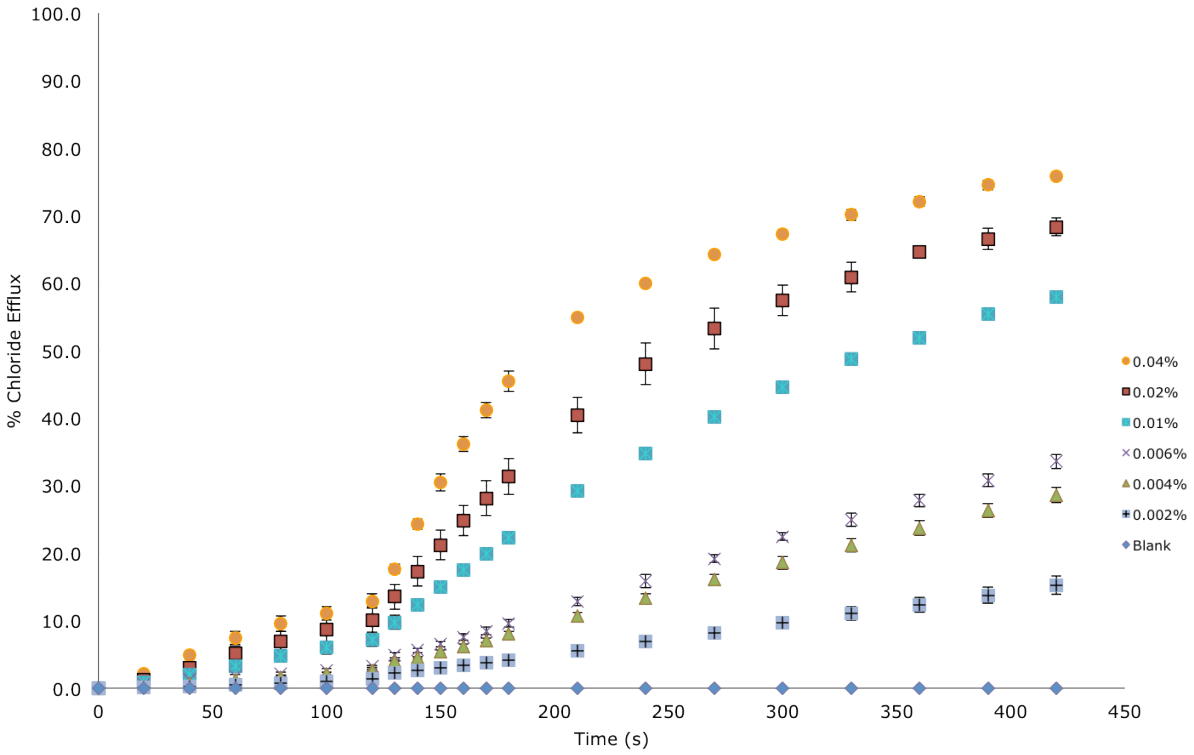

Figure S 61: Chloride efflux as a function of time, promoted by the addition of various concentration of receptor **7**, from unilamellar POPC vesicles containing 451 mM NaCl buffered to pH 7.2 with 20 mM sodium phosphate salts. The vesicles were dispersed in the external solution containing 150 mM Na_2SO_4 buffered to pH 7.2 with 20 mM sodium phosphate salts. The receptor was loaded as a DMSO solution at 0 s, and a spike of $NaHCO_3$ (33 mM) added at 120 s. At the end of the experiment the vesicles were lysed to calibrate the chloride selective electrode to 100% chloride efflux.

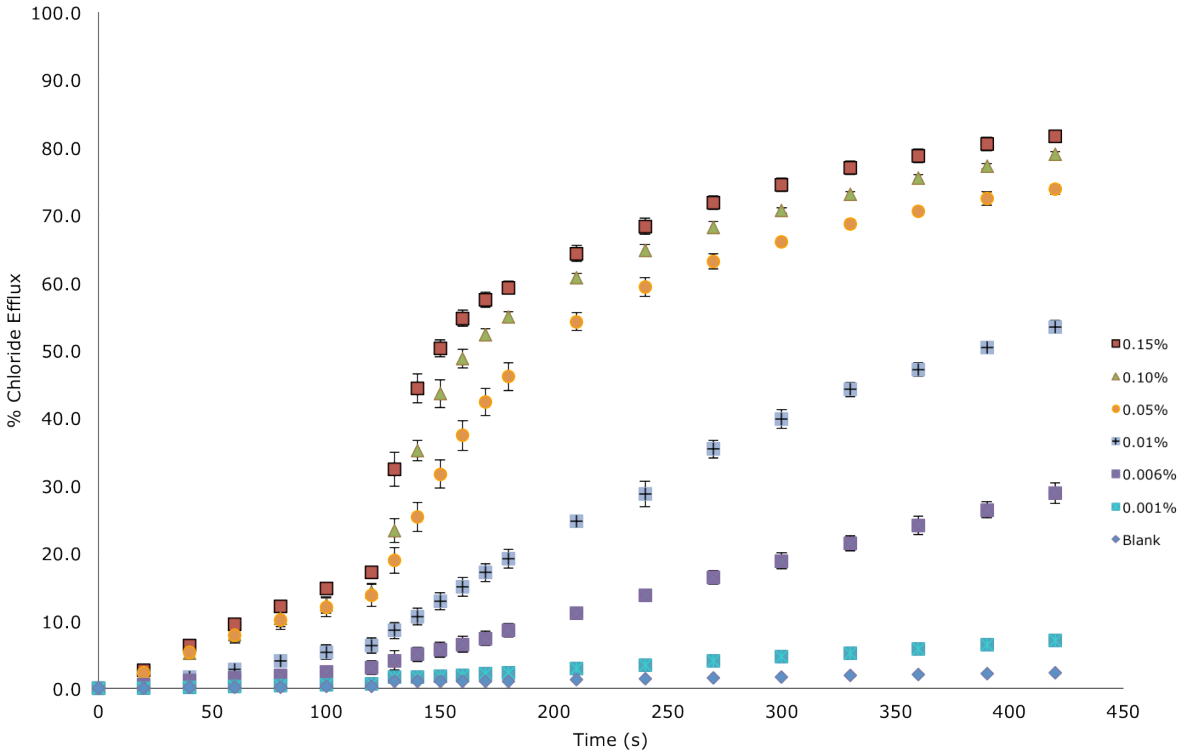

Figure S 62: Chloride efflux as a function of time, promoted by the addition of various concentrations of receptor **7**, from unilamellar POPC vesicles containing 451 mM NaCl buffered to pH 7.2 with 20 mM sodium phosphate salts. The vesicles were dispersed in the external solution containing 150 mM Na_2SO_4 buffered to pH 7.2 with 20 mM sodium phosphate salts. The receptor was loaded as a DMSO solution at 0 s, and a spike of $NaHCO_3$ (33 mM) added at 120 s. At the end of the experiment the vesicles were lysed to calibrate the chloride selective electrode to 100% chloride efflux.

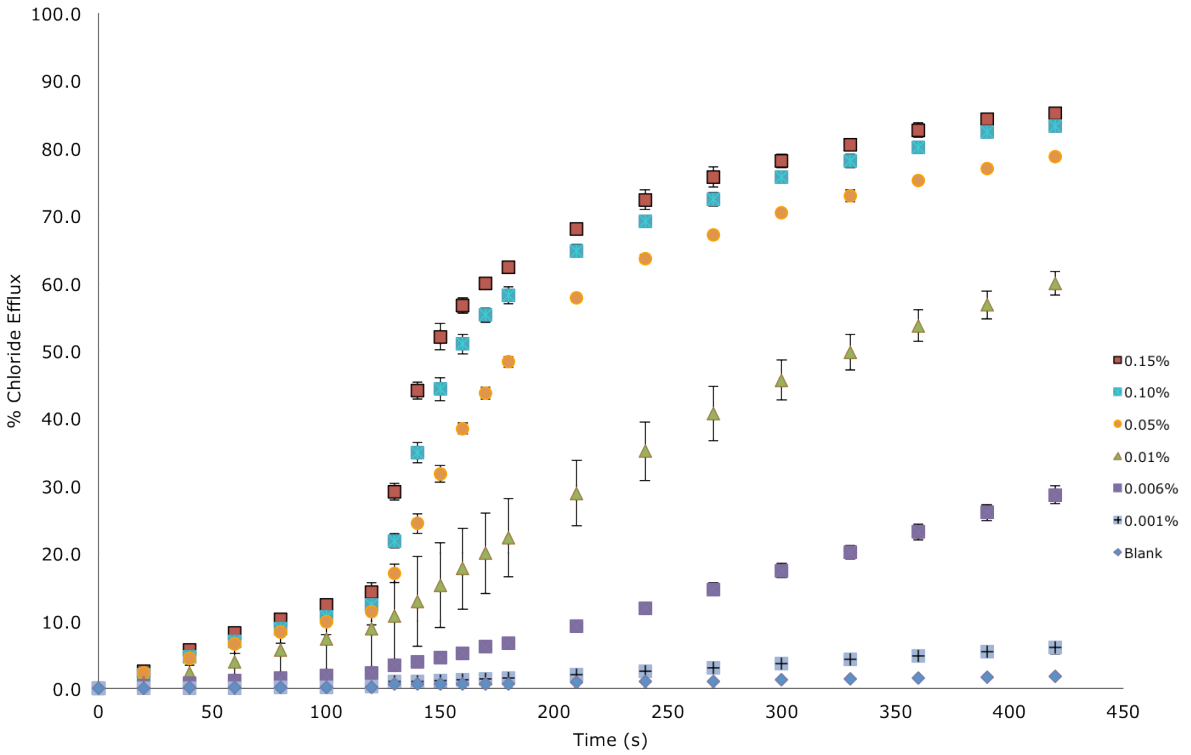

Figure S 63: Chloride efflux as a function of time, promoted by the addition of various concentration of receptor **7**, from unilamellar POPC vesicles containing 451 mM NaCl buffered to pH 7.2 with 20 mM sodium phosphate salts. The vesicles were dispersed in the external solution containing 150 mM Na_2SO_4 buffered to pH 7.2 with 20 mM sodium phosphate salts. The receptor was loaded as a DMSO solution at 0 s, and a spike of $NaHCO_3$ (33 mM) added at 120 s. At the end of the experiment the vesicles were lysed to calibrate the chloride selective electrode to 100% chloride efflux.

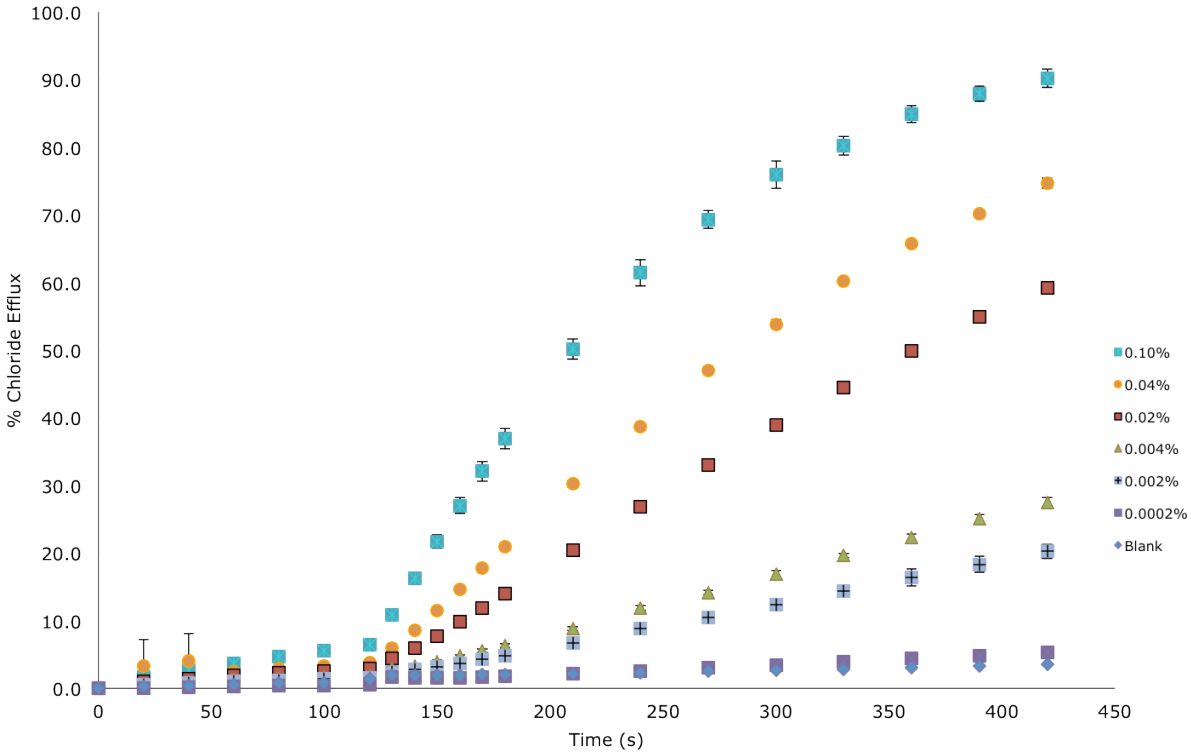

Figure S 64: Chloride efflux as a function of time, promoted by the addition of various concentrations of receptor **8**, from unilamellar POPC vesicles containing 451 mM NaCl buffered to pH 7.2 with 20 mM sodium phosphate salts. The vesicles were dispersed in the external solution containing 150 mM Na_2SO_4 buffered to pH 7.2 with 20 mM sodium phosphate salts. The receptor was loaded as a DMSO solution at 0 s, and a spike of $NaHCO_3$ (33 mM) added at 120 s. At the end of the experiment the vesicles were lysed to calibrate the chloride selective electrode to 100% chloride efflux.

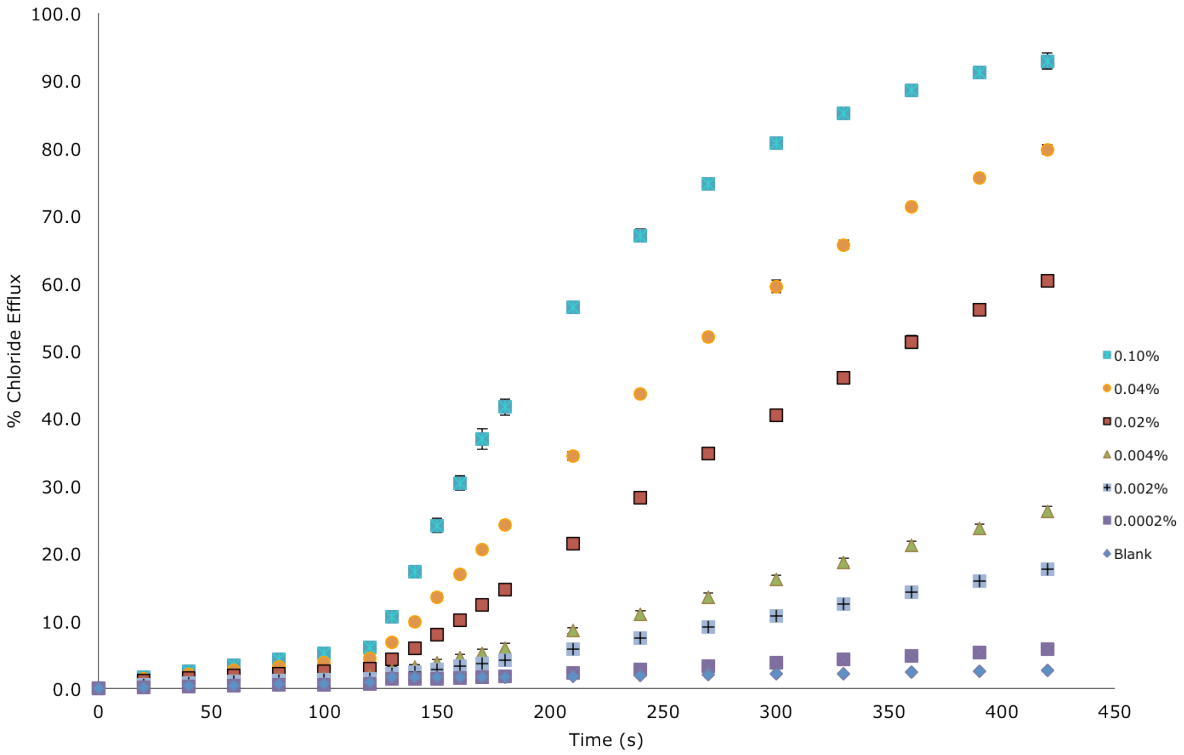

Figure S 65: Chloride efflux as a function of time, promoted by the addition of various concentrations of receptor **8**, from unilamellar POPC vesicles containing 451 mM NaCl buffered to pH 7.2 with 20 mM sodium phosphate salts. The vesicles were dispersed in the external solution containing 150 mM Na_2SO_4 buffered to pH 7.2 with 20 mM sodium phosphate salts. The receptor was loaded as a DMSO solution at 0 s, and a spike of $NaHCO_3$ (33 mM) added at 120 s. At the end of the experiment the vesicles were lysed to calibrate the chloride selective electrode to 100% chloride efflux.

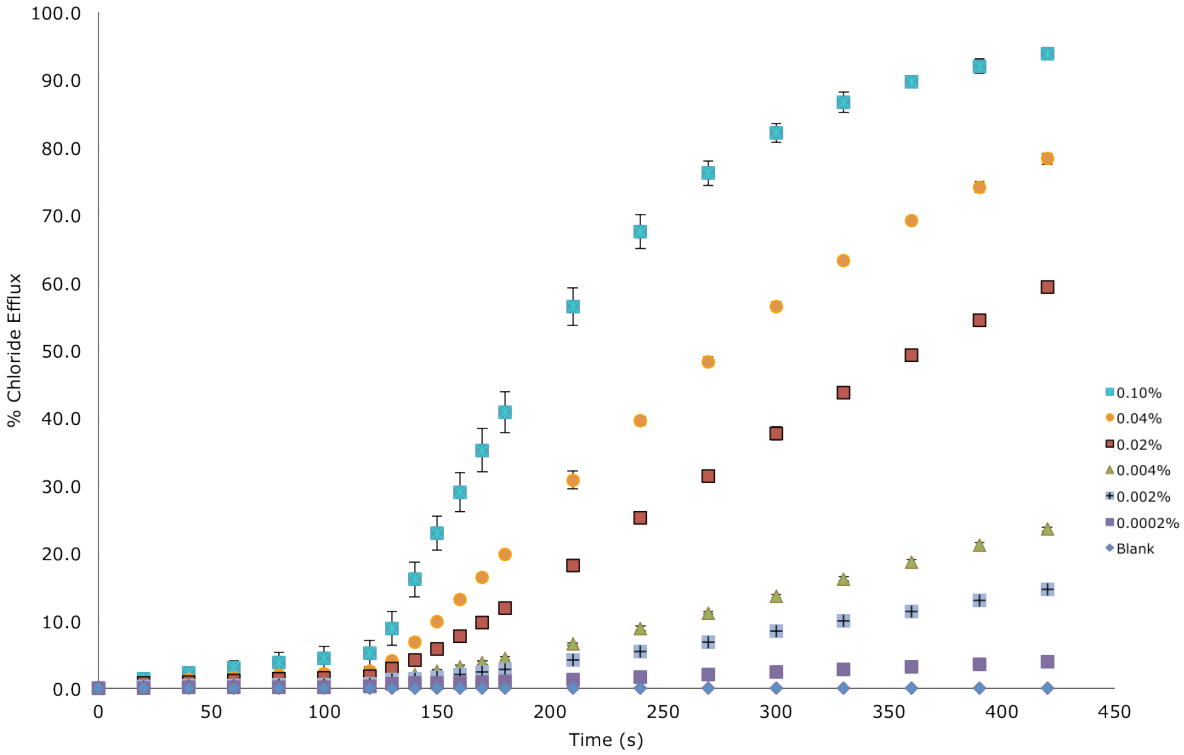

Figure S 66: Chloride efflux as a function of time, promoted by the addition of various concentrations of receptor **8**, from unilamellar POPC vesicles containing 451 mM NaCl buffered to pH 7.2 with 20 mM sodium phosphate salts. The vesicles were dispersed in the external solution containing 150 mM Na_2SO_4 buffered to pH 7.2 with 20 mM sodium phosphate salts. The receptor was loaded as a DMSO solution at 0 s, and a spike of $NaHCO_3$ (33 mM) added at 120 s. At the end of the experiment the vesicles were lysed to calibrate the chloride selective electrode to 100% chloride efflux.

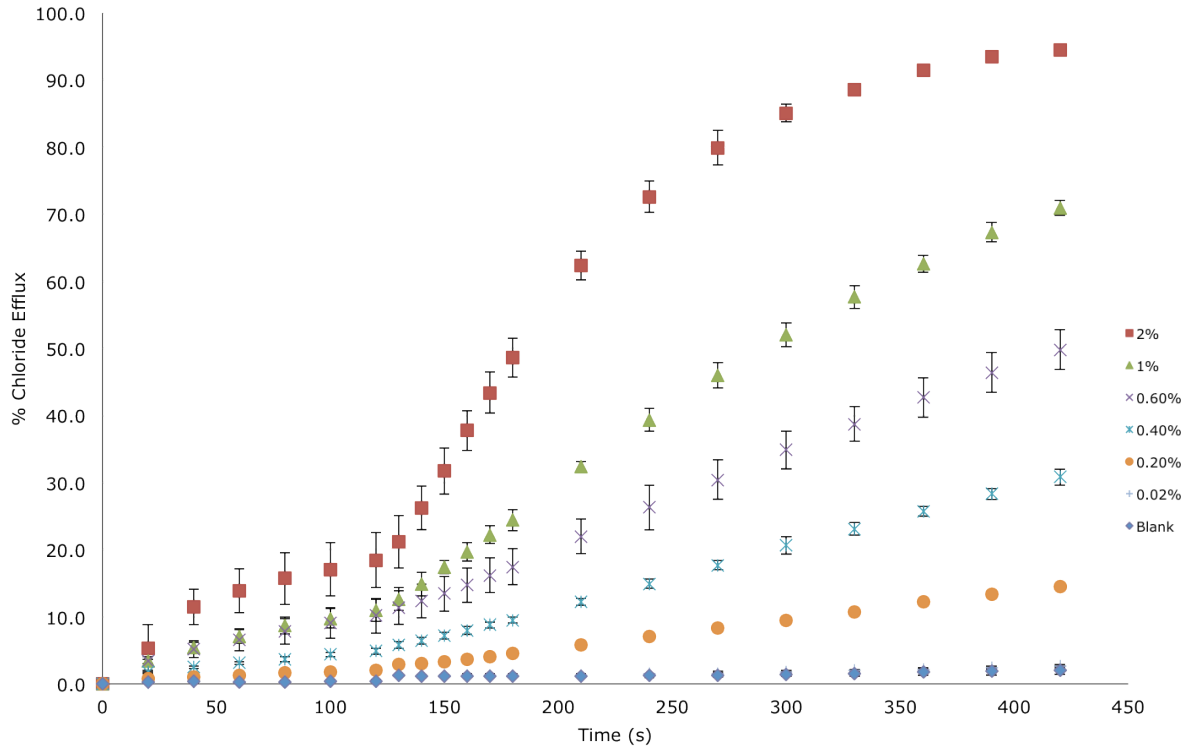

Figure S 67: Chloride efflux as a function of time, promoted by the addition of various concentration of receptor **10**, from unilamellar POPC vesicles containing 451 mM NaCl buffered to pH 7.2 with 20 mM sodium phosphate salts. The vesicles were dispersed in the external solution containing 150 mM Na_2SO_4 buffered to pH 7.2 with 20 mM sodium phosphate salts. The receptor was loaded as a DMSO solution at 0 s, and a spike of $NaHCO_3$ (33 mM) added at 120 s. At the end of the experiment the vesicles were lysed to calibrate the chloride selective electrode to 100% chloride efflux.

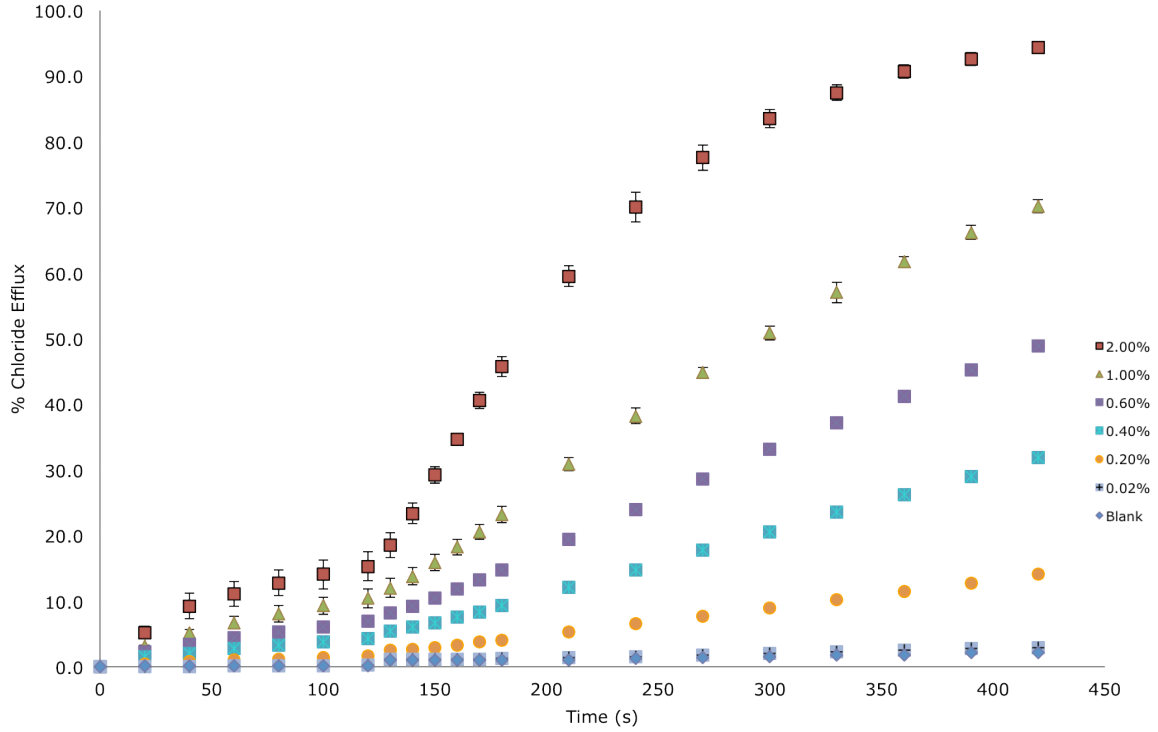

Figure S 68: Chloride efflux as a function of time, promoted by the addition of various concentrations of receptor **10**, from unilamellar POPC vesicles containing 451 mM NaCl buffered to pH 7.2 with 20 mM sodium phosphate salts. The vesicles were dispersed in the external solution containing 150 mM Na_2SO_4 buffered to pH 7.2 with 20 mM sodium phosphate salts. The receptor was loaded as a DMSO solution at 0 s, and a spike of $NaHCO_3$ (33 mM) added at 120 s. At the end of the experiment the vesicles were lysed to calibrate the chloride selective electrode to 100% chloride efflux.

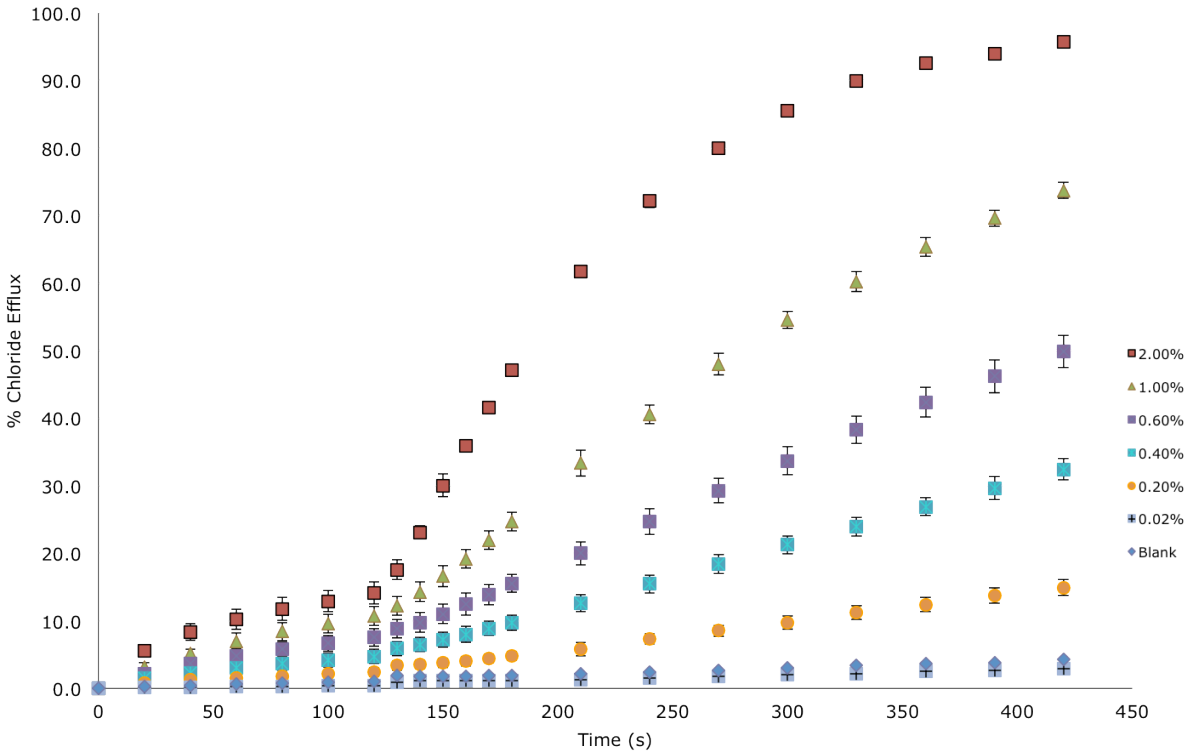

Figure S 69: Chloride efflux as a function of time, promoted by the addition of various concentrations of receptor **10**, from unilamellar POPC vesicles containing 451 mM NaCl buffered to pH 7.2 with 20 mM sodium phosphate salts. The vesicles were dispersed in the external solution containing 150 mM Na_2SO_4 buffered to pH 7.2 with 20 mM sodium phosphate salts. The receptor was loaded as a DMSO solution at 0 s, and a spike of $NaHCO_3$ (33 mM) added at 120 s. At the end of the experiment the vesicles were lysed to calibrate the chloride selective electrode to 100% chloride efflux.

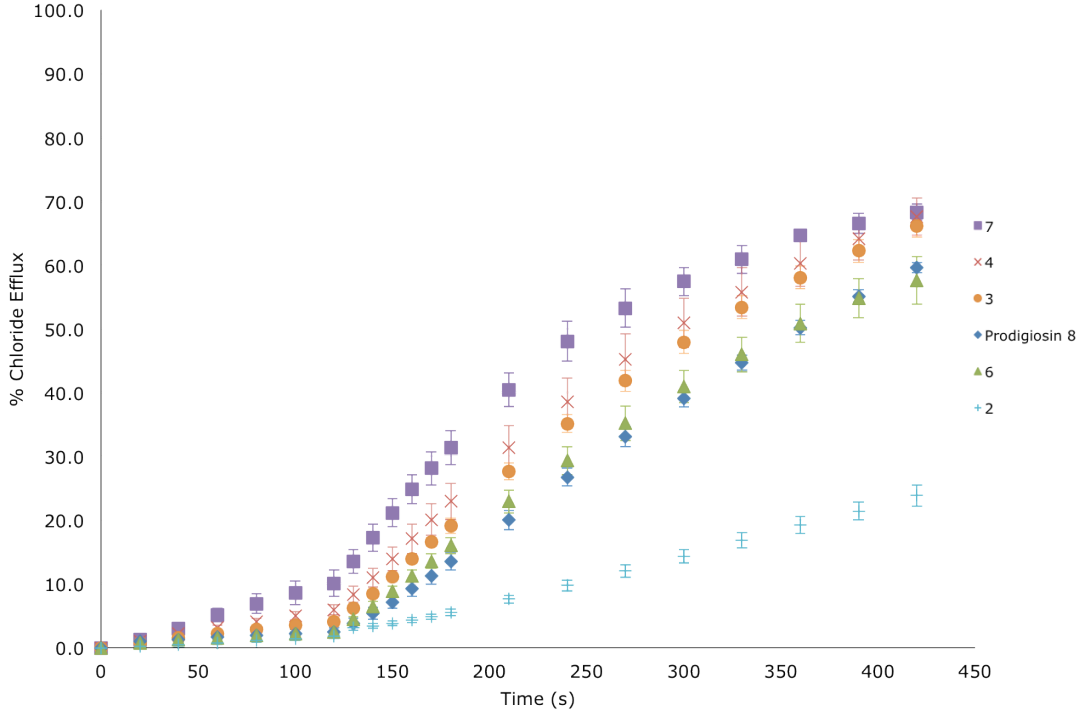

Figure S 70: Chloride efflux as a function of time, promoted by the addition of 0.02 mol% (with respect to lipid) of receptors **2**, **3**, **4**, **6**, **7** and prodigiosin **8**, from unilamellar POPC vesicles containing 451 mM NaCl buffered to pH 7.2 with 20 mM sodium phosphate salts. The vesicles were dispersed in the external solution containing 150 mM Na_2SO_4 buffered to pH 7.2 with 20 mM sodium phosphate salts. The receptor was loaded as a DMSO solution at 0 s, and a spike of $NaHCO_3$ (33 mM) added at 120 s. At the end of the experiment the vesicles were lysed to calibrate the chloride selective electrode to 100% chloride efflux.

S8: Hill Plots

During the Hill plots the chloride/nitrate transport assays were performed for various concentrations of carrier. The chloride efflux (%) 270 s after the addition of carrier was plotted as a function of the carrier concentration. Data points were fitted to the Hill equation using Origin 8.1:

$$y = V_{\max} \frac{x^n}{k^n + x^n} = 100\% \frac{x^n}{(EC_{50})^n + x^n}$$

where y is the chloride efflux at 270 s (%) and x is the carrier concentration (mol% carrier to lipid). Vmax, k and n are the parameters to be fitted. Vmax is the maximum efflux possible (this was fixed to 100%, as this is physically the maximum chloride efflux possible), n is the Hill coefficient and k is the carrier concentration needed to reach Vmax/2 (when Vmax is fixed to 100%, k equals EC50).

Hill Plots: Cl^-/NO_3^- Exchange

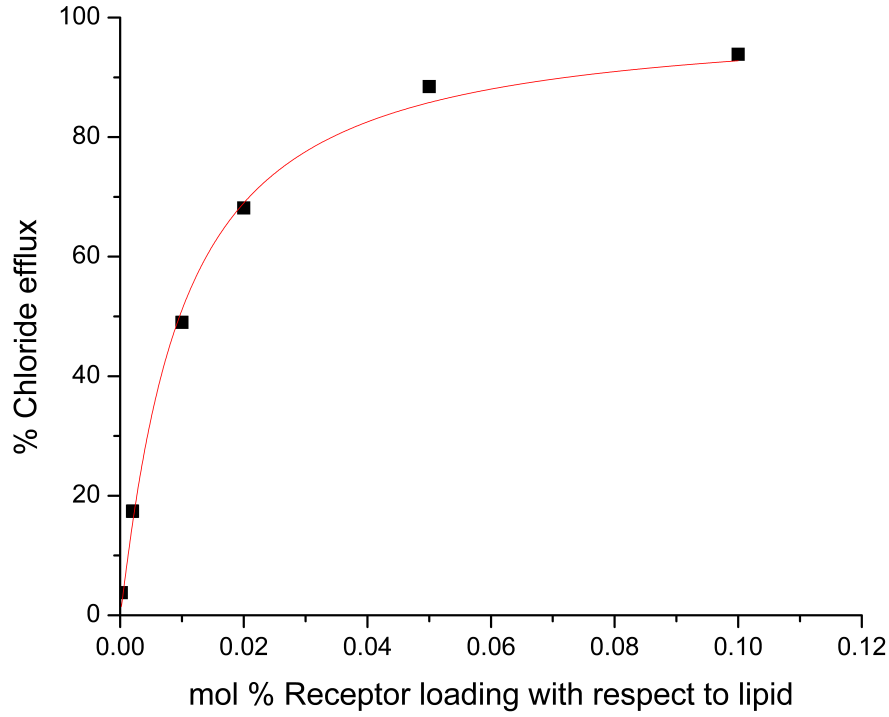

Figure S 71: Hill analysis for Cl^-/NO_3^- antiport mediated by **2**. Data was fitted to the Hill equation using Origin. $R^2 = 0.99578$, $EC_{50} = 0.00960$ mol%, n = 1.08913±0.06914.

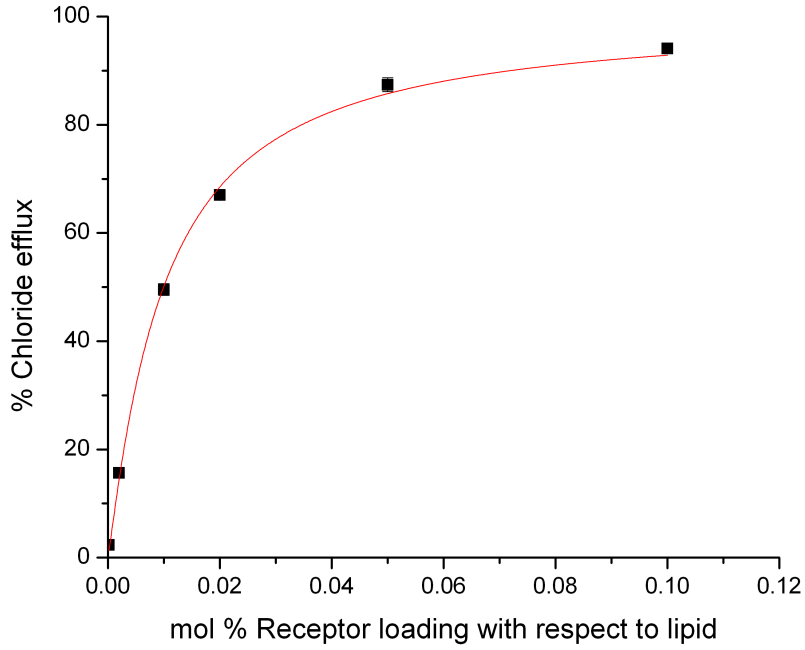

Figure S 72: Hill analysis for Cl^-/NO_3^- antiport mediated by **2**. Data was fitted to the Hill equation using Origin. $R^2 = 0.99832$, $EC_{50} = 0.00995$ mol%, n = 1.11189±0.04551.

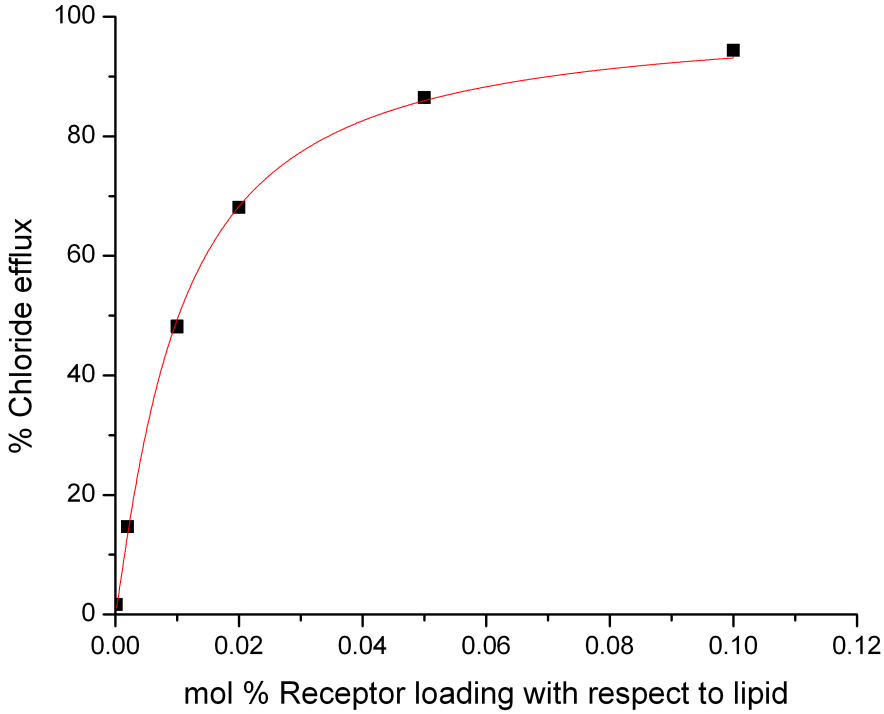

Figure S 73: Hill analysis for Cl^-/NO_3^- antiport mediated by **2**. Data was fitted to the Hill equation using Origin. $R^2 = 0.99909$, $EC_{50} = 0.01025$ mol%, n = 1.14323±0.03531.

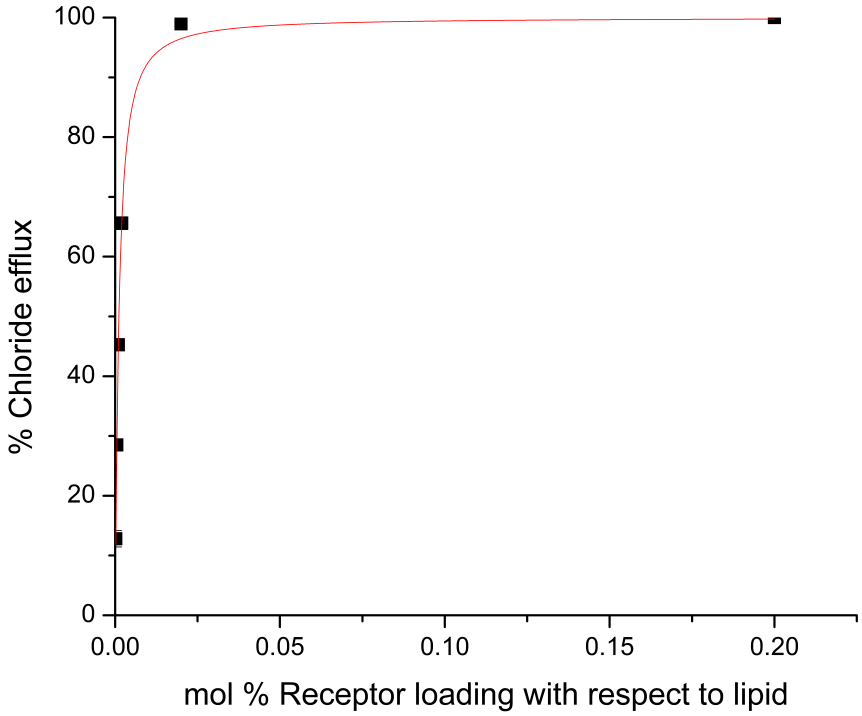

Figure S 74: Hill analysis for Cl^-/NO_3^- antiport mediated by **3**. Data was fitted to the Hill equation using Origin. $R^2 = 0.99839$, $EC_{50} = 0.00114$ mol%, n = 1.15384±0.05073.

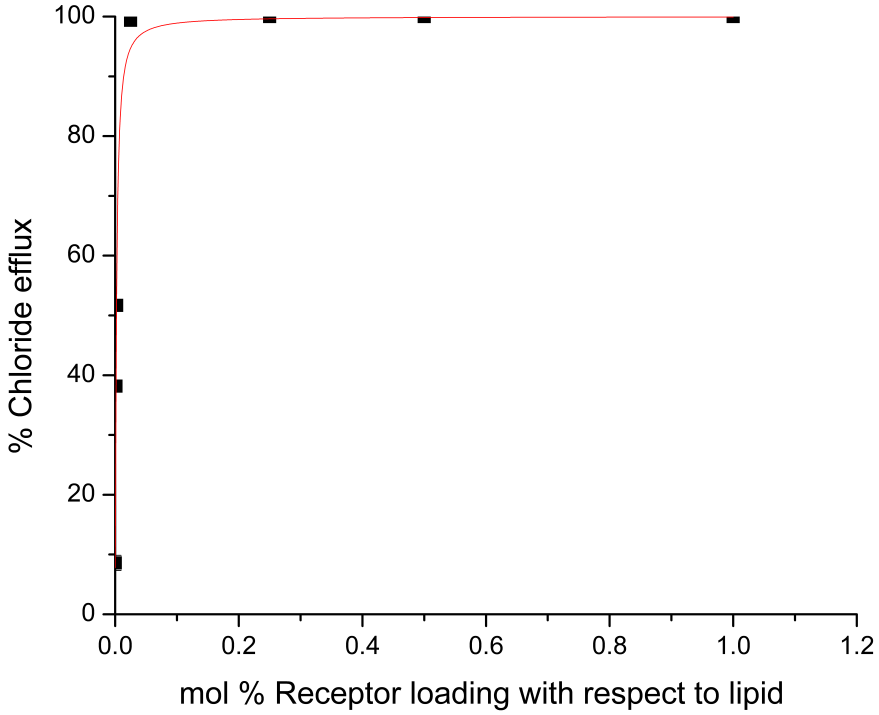

Figure S 75: Hill analysis for Cl^-/NO_3^- antiport mediated by **3**. Data was fitted to the Hill equation using Origin. $R^2 = 0.99419$, $EC_{50} = 0.00208$ mol%, n = 1.16304±0.12769.

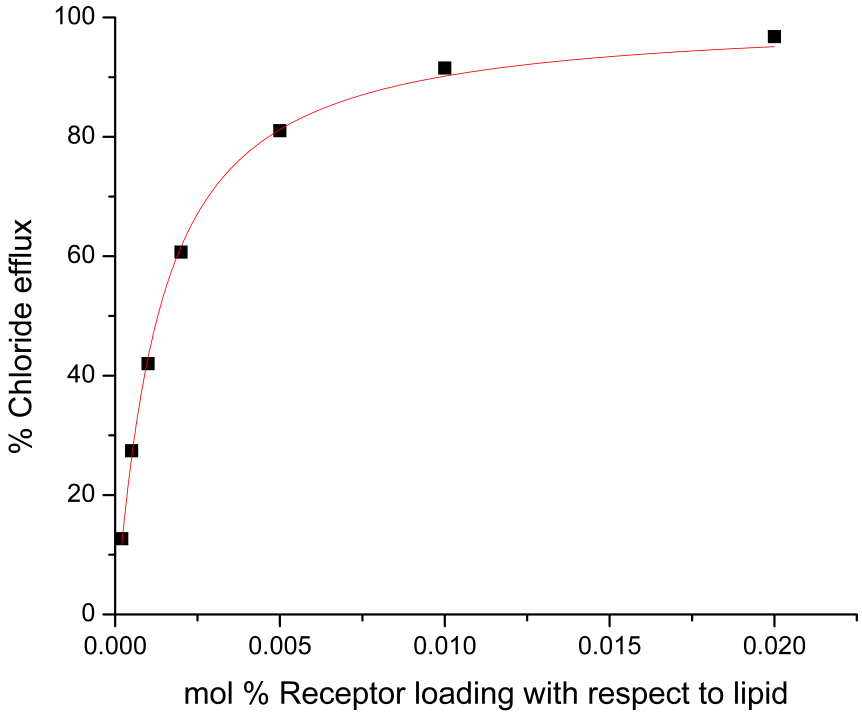

Figure S 76: Hill analysis for Cl^-/NO_3^- antiport mediated by **3**. Data was fitted to the Hill equation using Origin. $R^2 = 0.99833$, $EC_{50} = 0.00129$ mol%, n = 1.08331±0.03168.

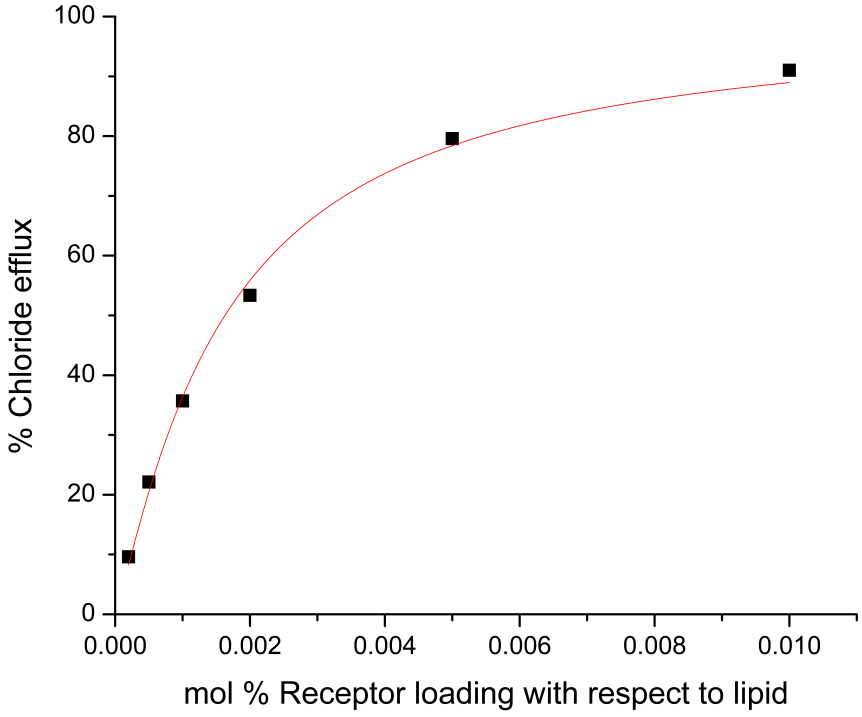

Figure S 77: Hill analysis for Cl^-/NO_3^- antiport mediated by **3**. Data was fitted to the Hill equation using Origin. $R^2 = 0.99588$, $EC_{50} = 0.00163$ mol%, n = 1.14902±0.05415.

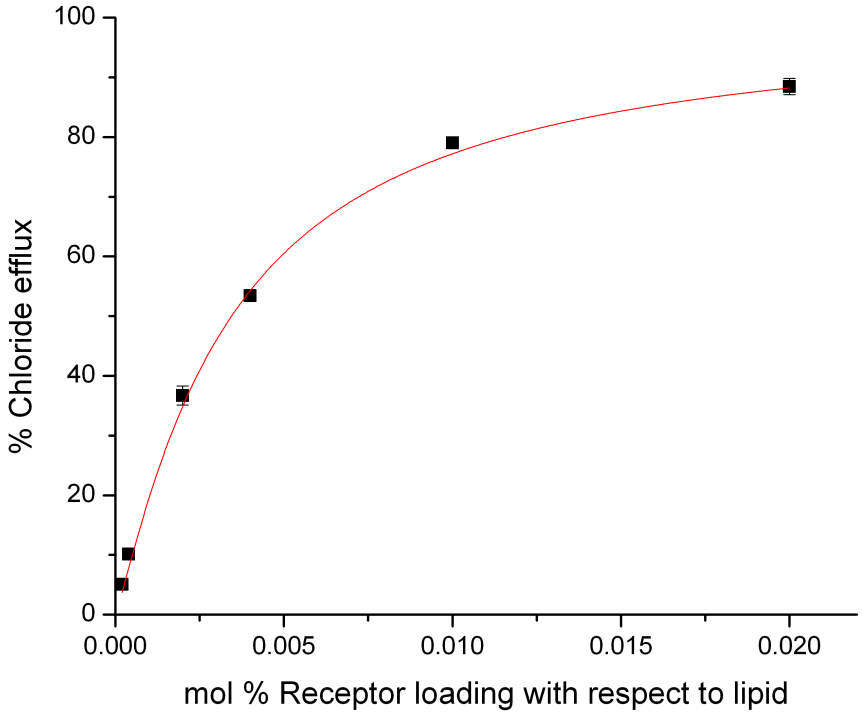

Figure S 78: Hill analysis for Cl^-/NO_3^- antiport mediated by **4**. Data was fitted to the Hill equation using Origin. $R^2 = 0.99581$, $EC_{50} = 0.00345$ mol%, n = 1.14567±0.06650.

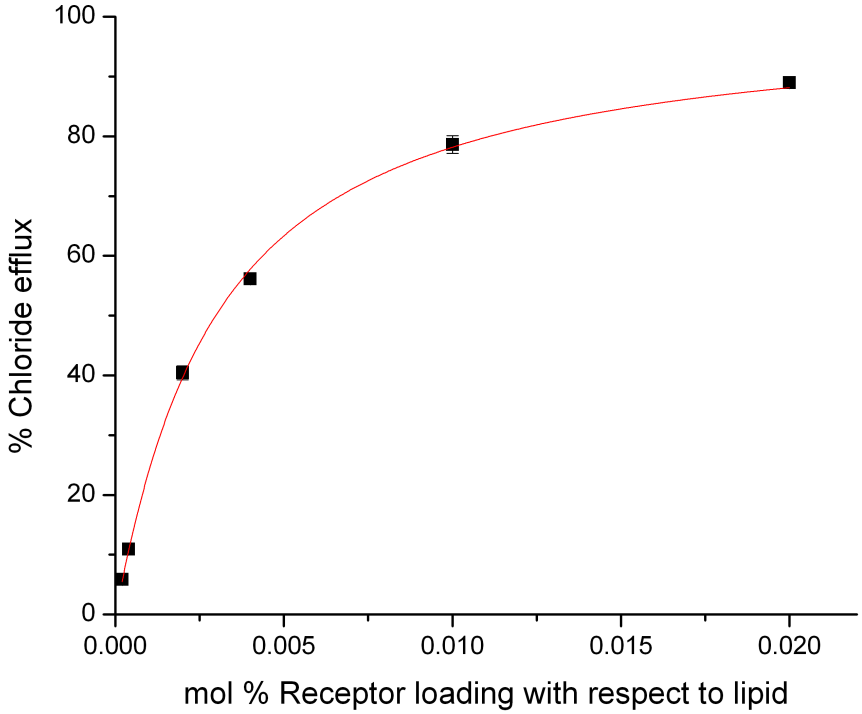

Figure S 79: Hill analysis for Cl^-/NO_3^- antiport mediated by **4**. Data was fitted to the Hill equation using Origin. $R^2 = 0.99913$, $EC_{50} = 0.00298$ mol%, n = 1.05333±0.02620.

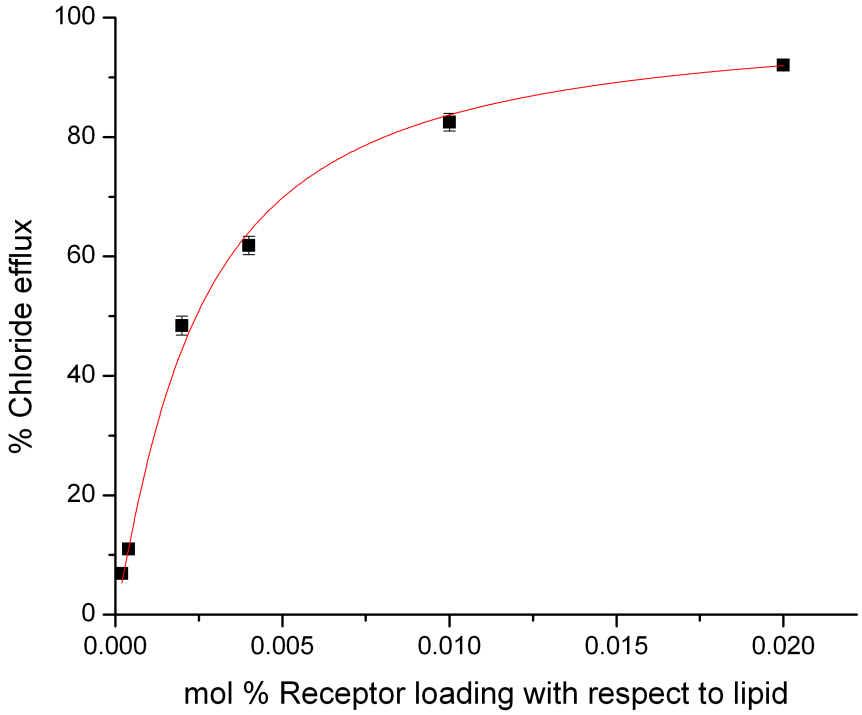

Figure S 80: Hill analysis for Cl^-/NO_3^- antiport mediated by **4**. Data was fitted to the Hill equation using Origin. $R^2 = 0.99967$, $EC_{50} = 0.00242$ mol%, n = 1.15561±0.02024.

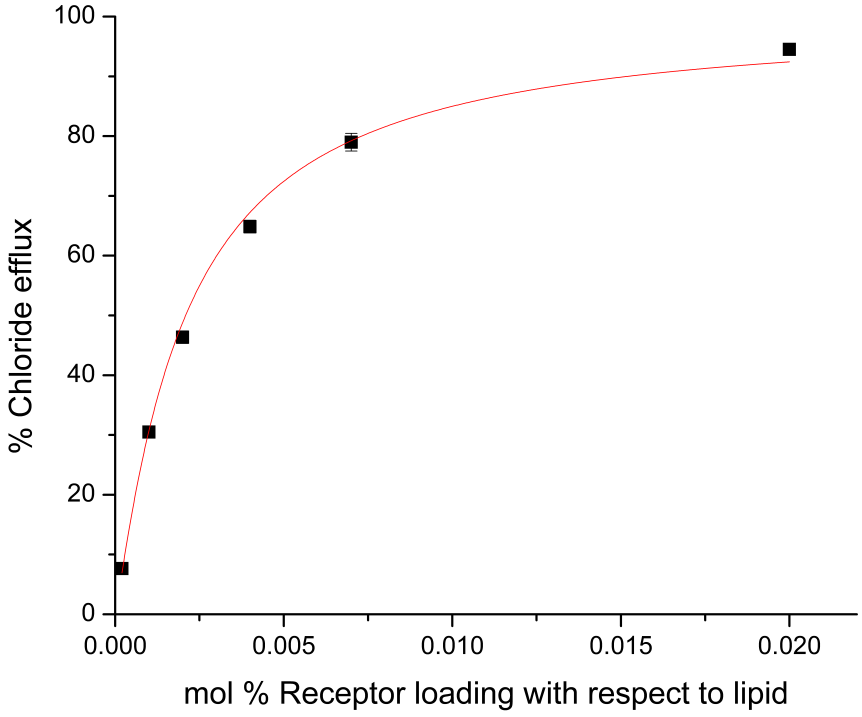

Figure S 81: Hill analysis for Cl^-/NO_3^- antiport mediated by **6**. Data was fitted to the Hill equation using Origin. R^2 = 1.10717, EC_{50} = 0.00209 mol%, n = 1.10717±0.04542.

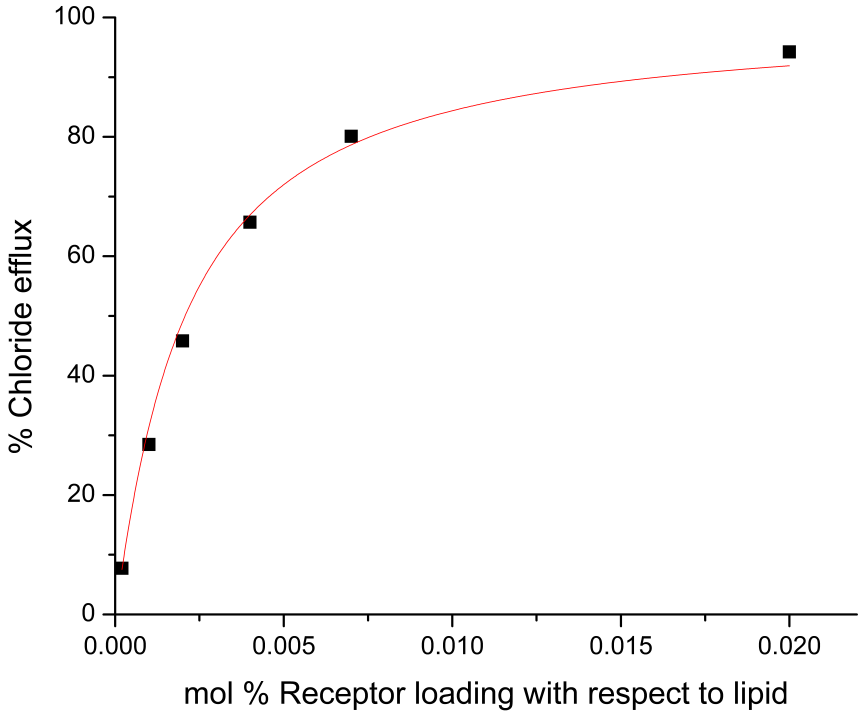

Figure S 82: Hill analysis for Cl^-/NO_3^- antiport mediated by **6**. Data was fitted to the Hill equation using Origin. R^2 = 0.99811, EC_{50} = 0.00207 mol%, n = 1.07185±0.03564.

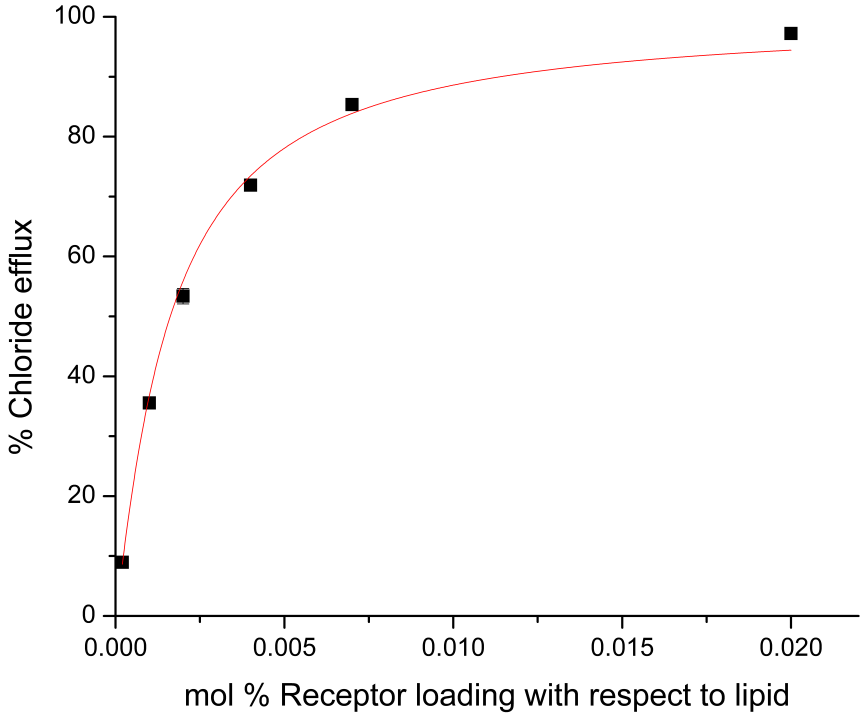

Figure S 83: Hill analysis for Cl^-/NO_3^- antiport mediated by **6**. Data was fitted to the Hill equation using Origin. $R^2 = 0.99839$, $EC_{50} = 0.00162$ mol%, n = 1.12642±0.03952.

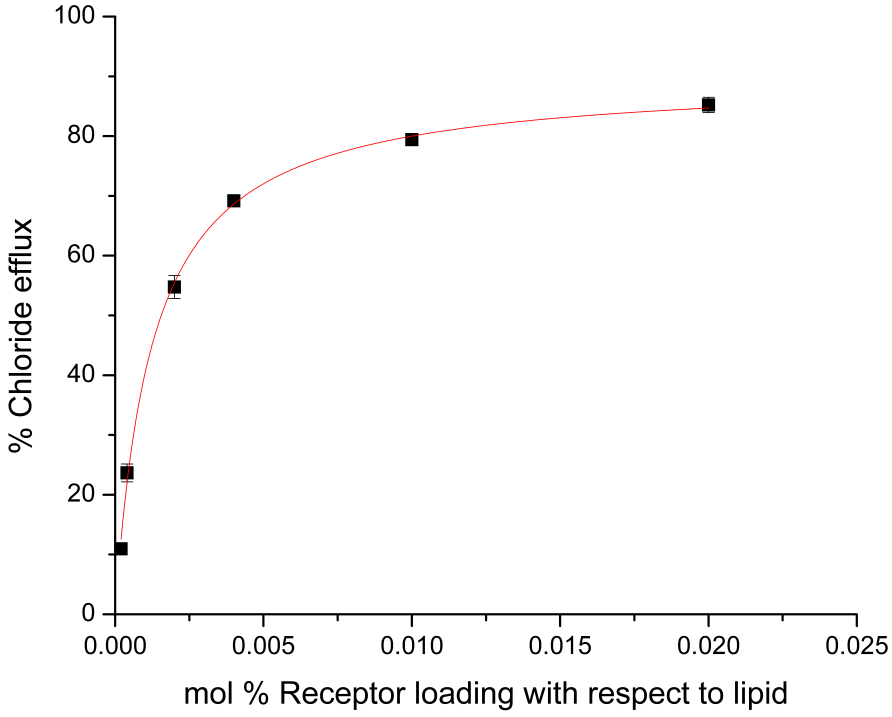

Figure S 84: Hill analysis for Cl^-/NO_3^- antiport mediated by **7**. Data was fitted to the Hill equation using Origin. $R^2 = 0.99817$, $EC_{50} = 0.00124$ mol%, n = 0.99635±0.03156.

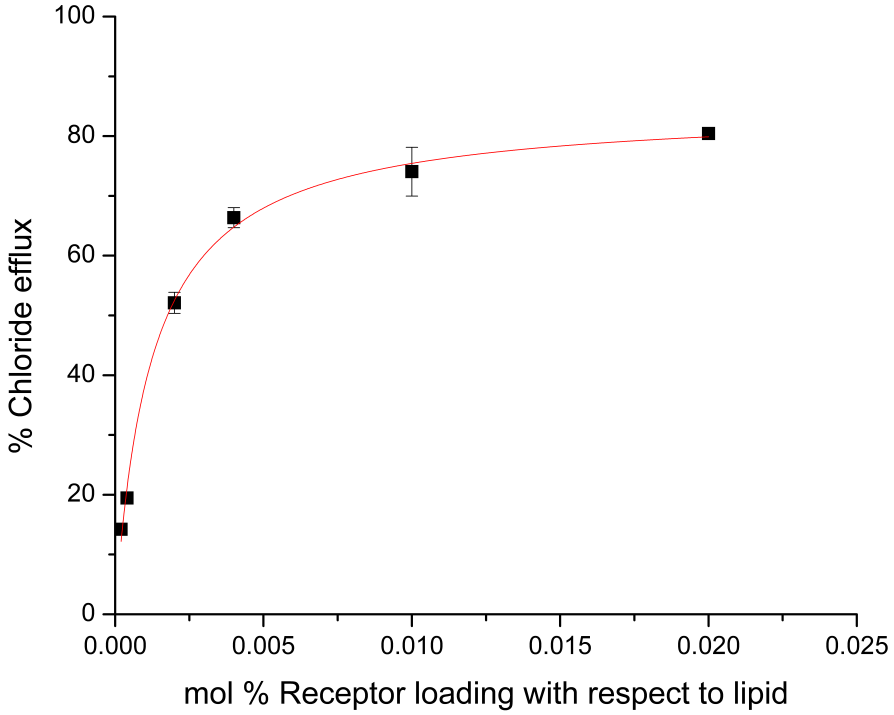

Figure S 85: Hill analysis for Cl^-/NO_3^- antiport mediated by **7**. Data was fitted to the Hill equation using Origin. $R^2 = 0.99623$, $EC_{50} = 0.00123$ mol%, n = 0.98425±0.04383.

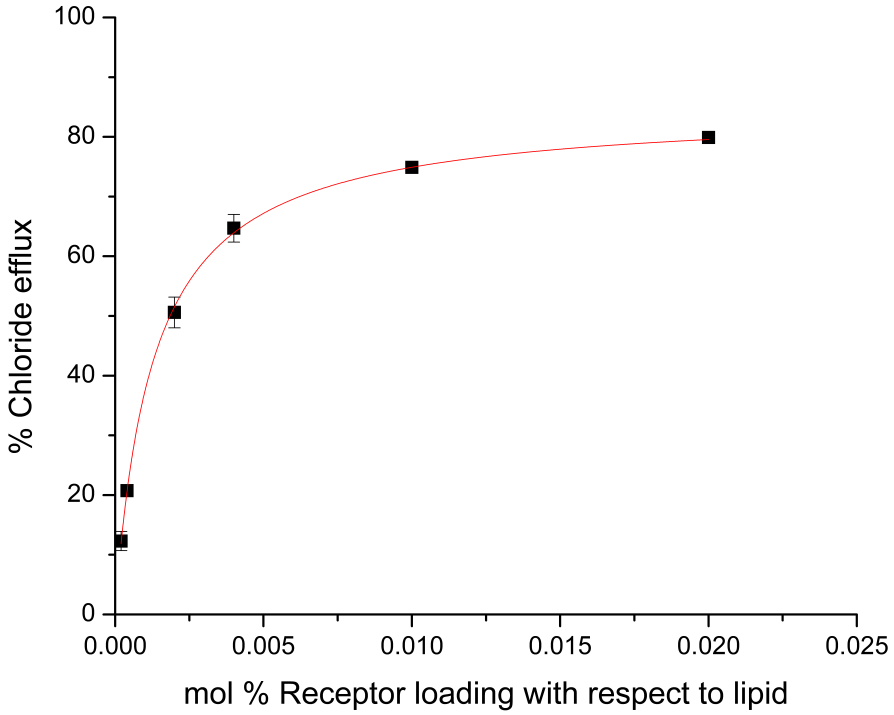

Figure S 86: Hill analysis for Cl^-/NO_3^- antiport mediated by **7**. Data was fitted to the Hill equation using Origin. $R^2 = 0.99943$, $EC_{50} = 0.00128$ mol%, n = 0.97638±0.01693.

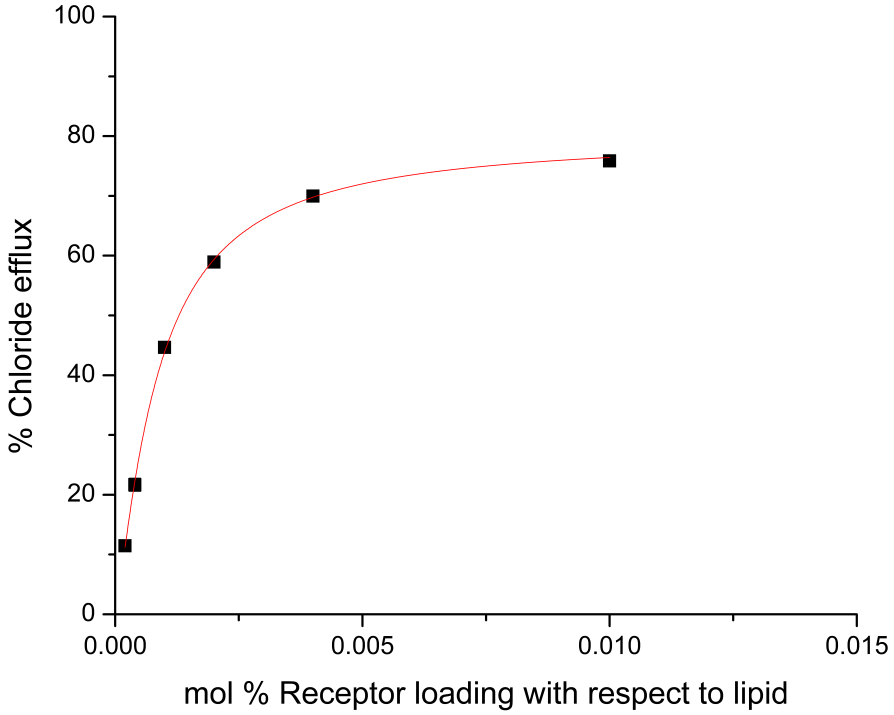

Figure S 87: Hill analysis for Cl^-/NO_3^- antiport mediated by **7**. Data was fitted to the Hill equation using Origin. $R^2 = 0.99938$, $EC_{50} = 0.00086$ mol%, n = 1.24557±0.02321.

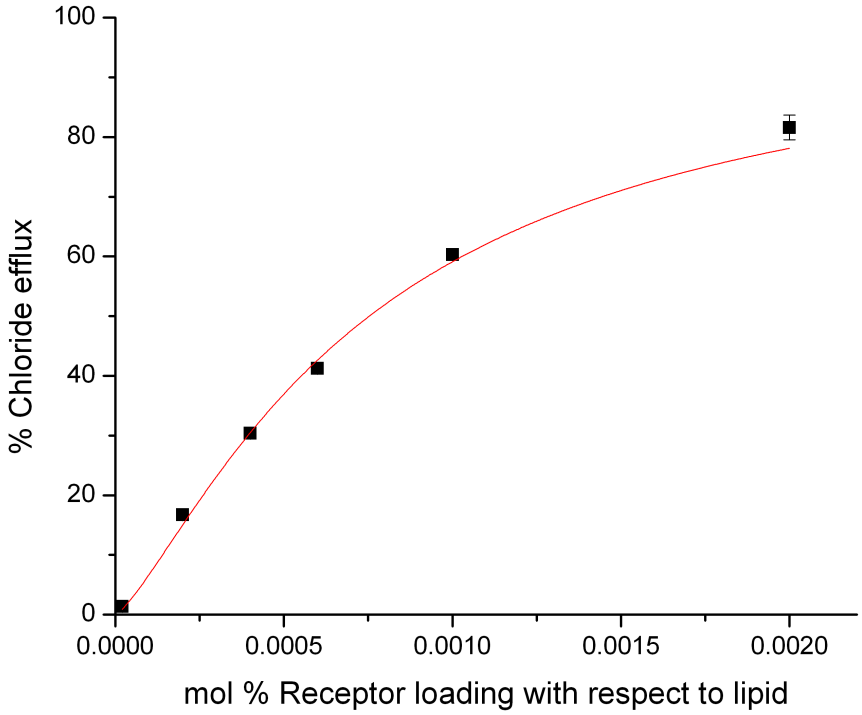

Figure S 88: Hill analysis for Cl^-/NO_3^- antiport mediated by **8**. Data was fitted to the Hill equation using Origin. $R^2 = 0.99598$, $EC_{50} = 0.00075$ mol%, n = 1.30454±0.06802.

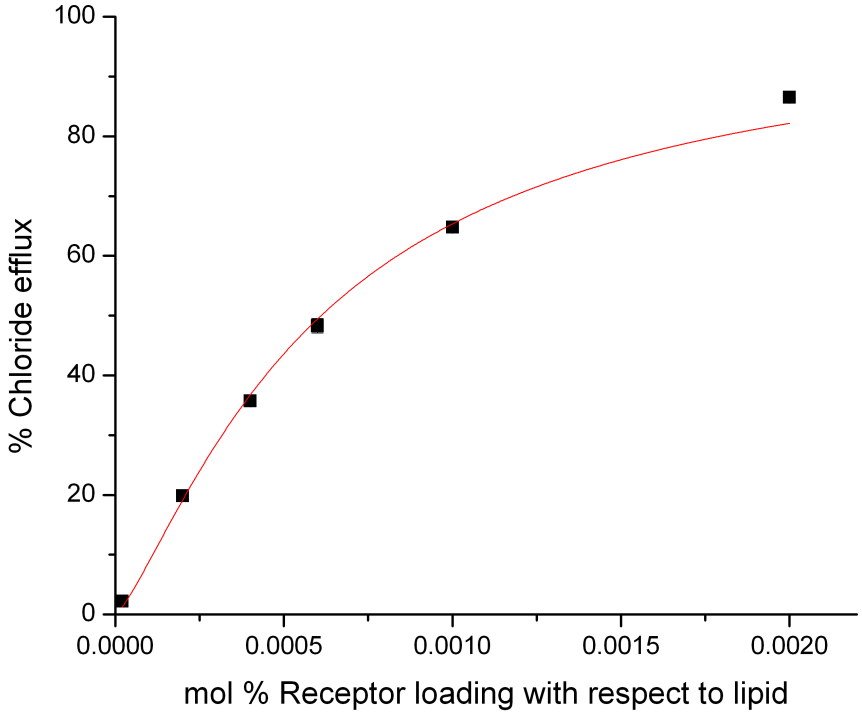

Figure S 89: Hill analysis for Cl^-/NO_3^- antiport mediated by **8**. Data was fitted to the Hill equation using Origin. $R^2 = 0.99736$, $EC_{50} = 0.00061$ mol%, n = 1.28867±0.06370.

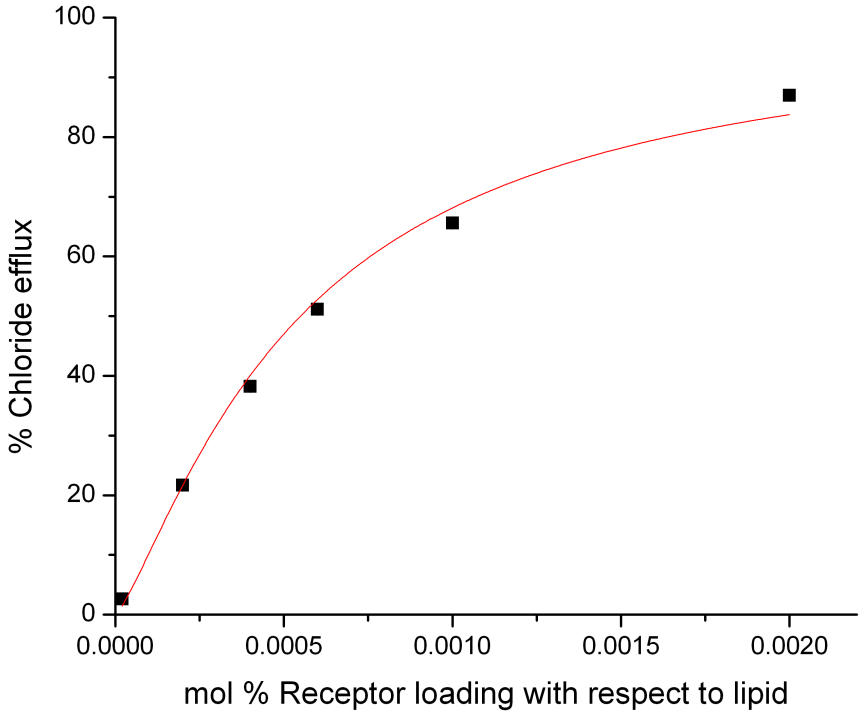

Figure S 90: Hill analysis for Cl^-/NO_3^- antiport mediated by **8**. Data was fitted to the Hill equation using Origin. $R^2 = 0.99622$, $EC_{50} = 0.00055$ mol%, n = 1.27050±0.10625.

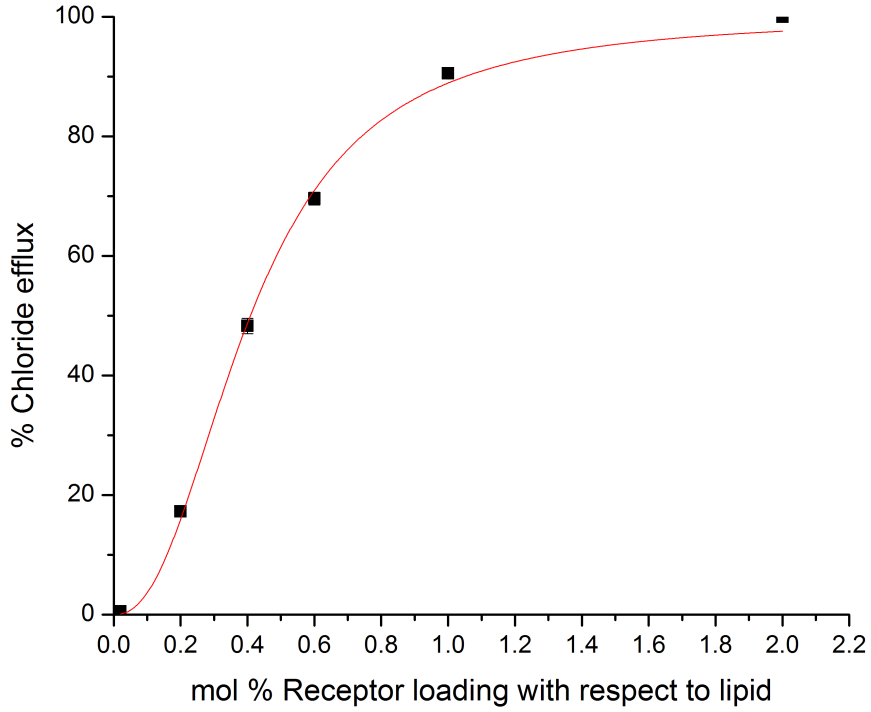

Figure S 91: Hill analysis for Cl^-/NO_3^- antiport mediated by **10**. Data was fitted to the Hill equation using Origin. $R^2 = 0.99803$, $EC_{50} = 0.40874$ mol%, n = 2.32671±0.11514.

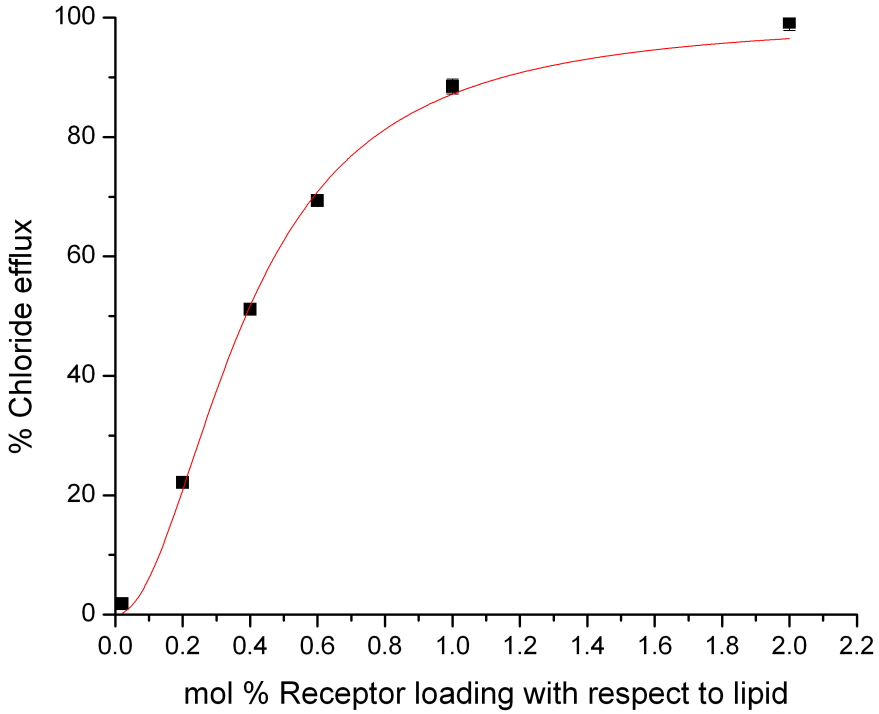

Figure S 92: Hill analysis for Cl^-/NO_3^- antiport mediated by **10**. Data was fitted to the Hill equation using Origin. $R^2 = 0.99727$, $EC_{50} = 0.38675$ mol%, n = 2.01827±0.10959.

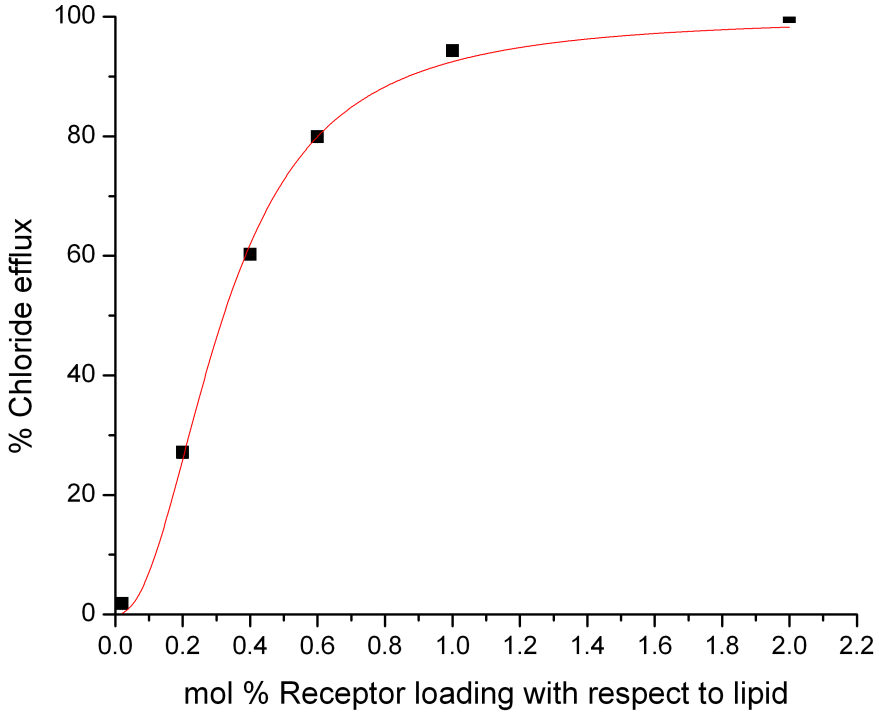

Figure S 93: Hill analysis for Cl^-/NO_3^- antiport mediated by **10**. Data was fitted to the Hill equation using Origin. $R^2 = 0.99787$, $EC_{50} = 0.32125$ mol%, n = 2.21118±0.11192.

S9: Hill Plots: Cl^-/HCO_3^- Exchange

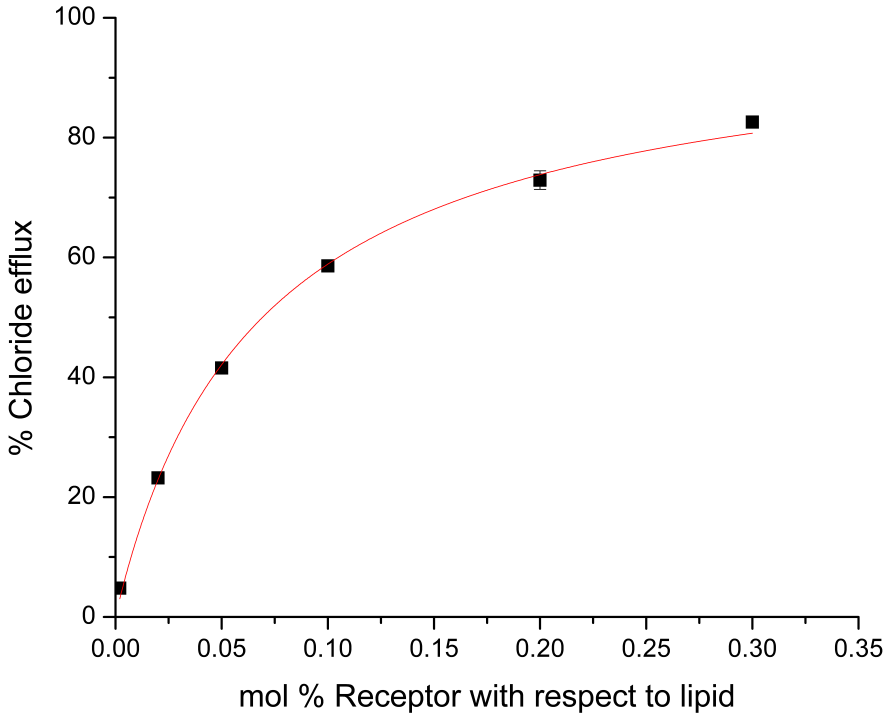

Figure S 94: Hill analysis for Cl^-/HCO_3^- antiport mediated by **2**. Data was fitted to the Hill equation using Origin. $R^2 = 0.99775$, $EC_{50} = 0.06922$ mol%, n = 0.97738±0.03525.

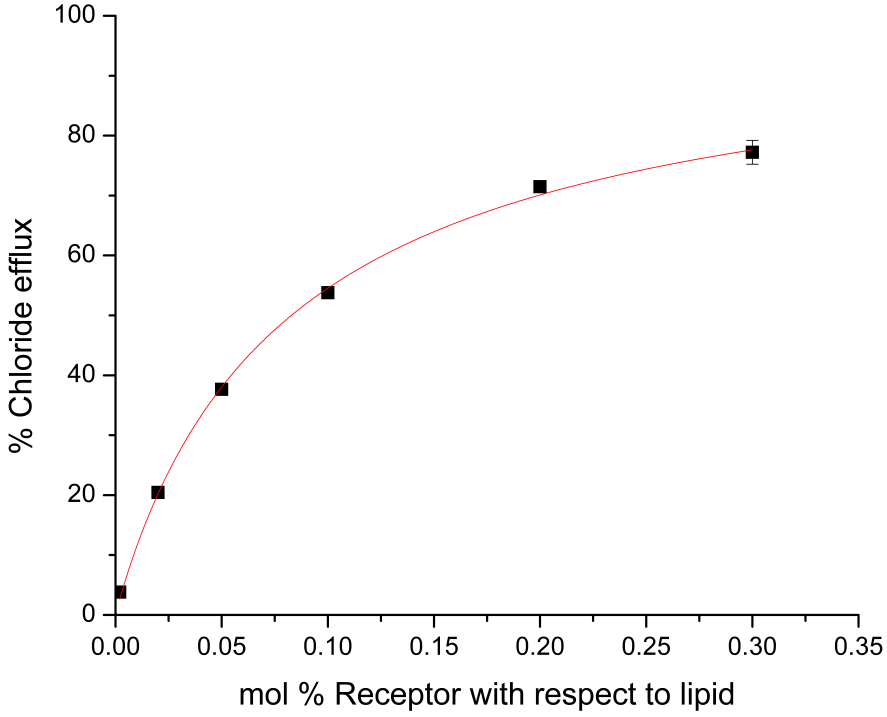

Figure S 95: Hill analysis for Cl^-/HCO_3^- antiport mediated by **2**. Data was fitted to the Hill equation using Origin. $R^2 = 0.99875$, $EC_{50} = 0.08284$ mol%, n = 0.96678±0.02550.

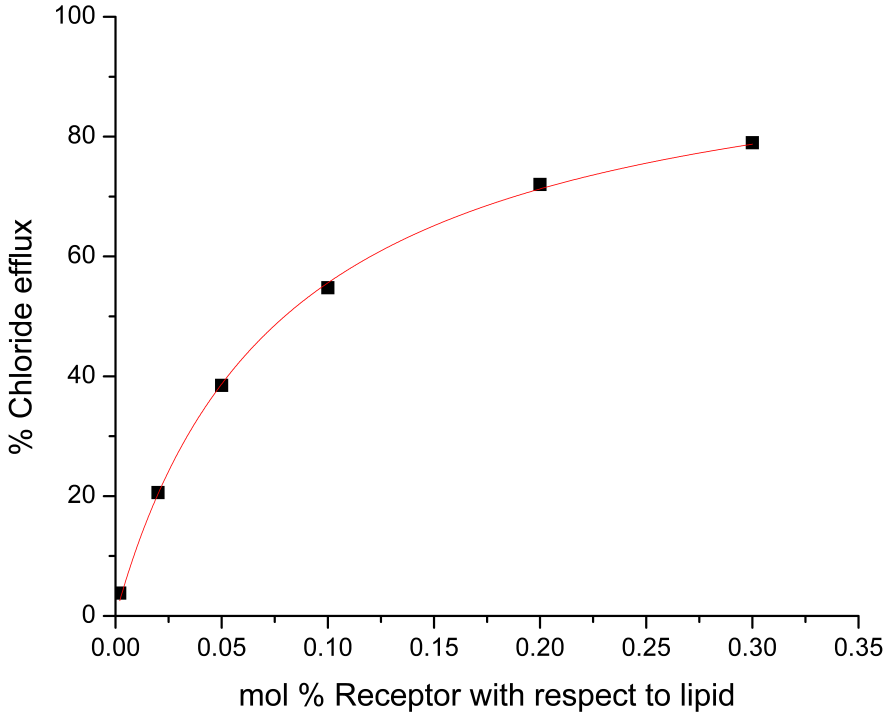

Figure S 96: Hill analysis for Cl^-/HCO_3^- antiport mediated by **2**. Data was fitted to the Hill equation using Origin. $R^2 = 0.99916$, $EC_{50} = 0.07964$ mol%, n = 0.98722±0.02159.

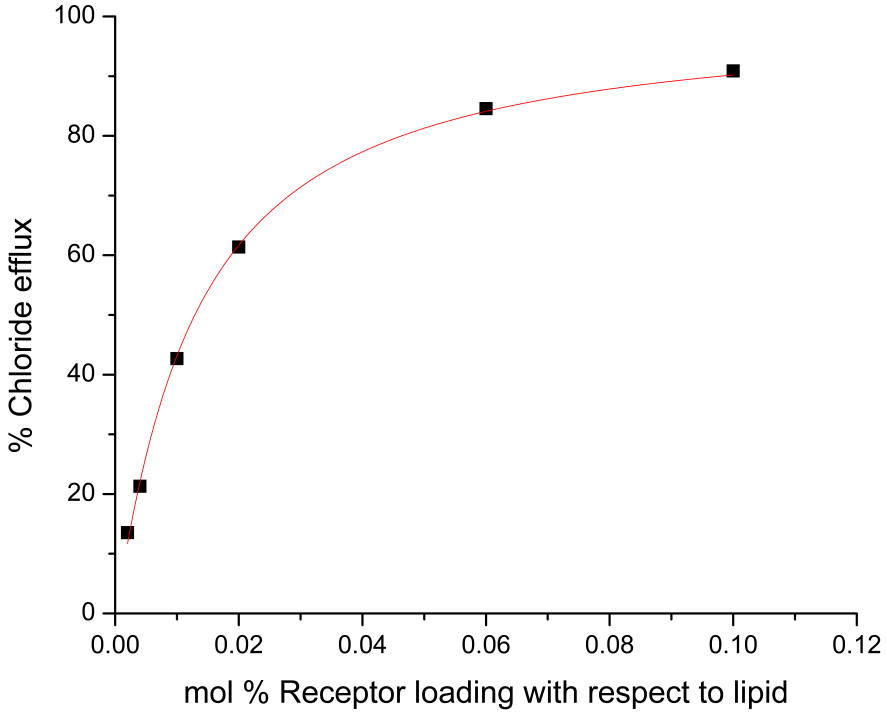

Figure S 97: Hill analysis for Cl^-/HCO_3^- antiport mediated by **3**. Data was fitted to the Hill equation using Origin. $R^2 = 0.99887$, $EC_{50} = 0.01289$ mol%, n = 1.08331±0.02641.

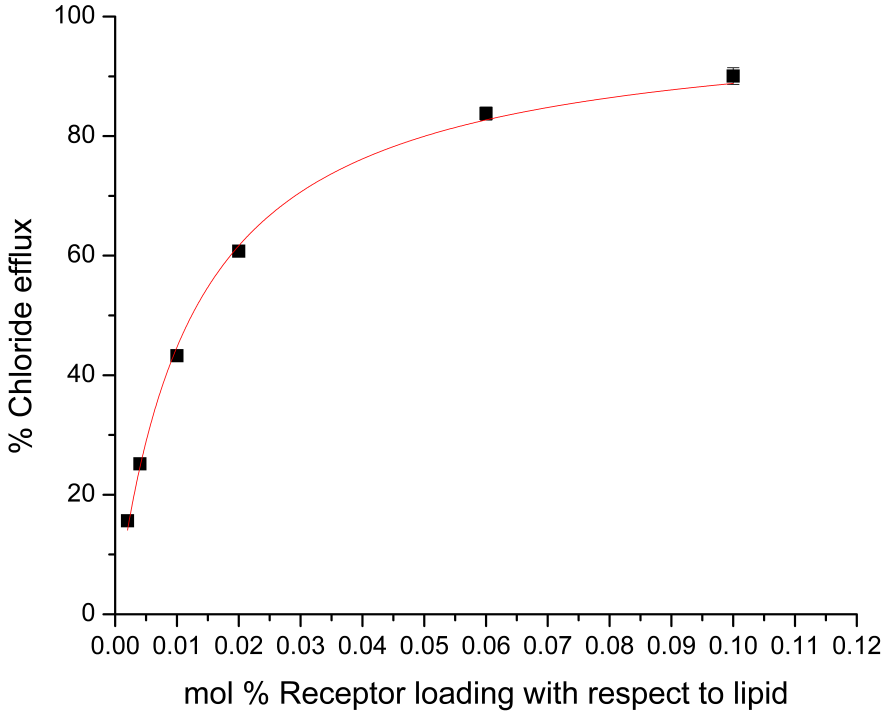

Figure S 98: Hill analysis for Cl^-/HCO_3^- antiport mediated by **3**. Data was fitted to the Hill equation using Origin. $R^2 = 0.99773$, $EC_{50} = 0.01239$ mol%, n = 0.99205±0.03227.

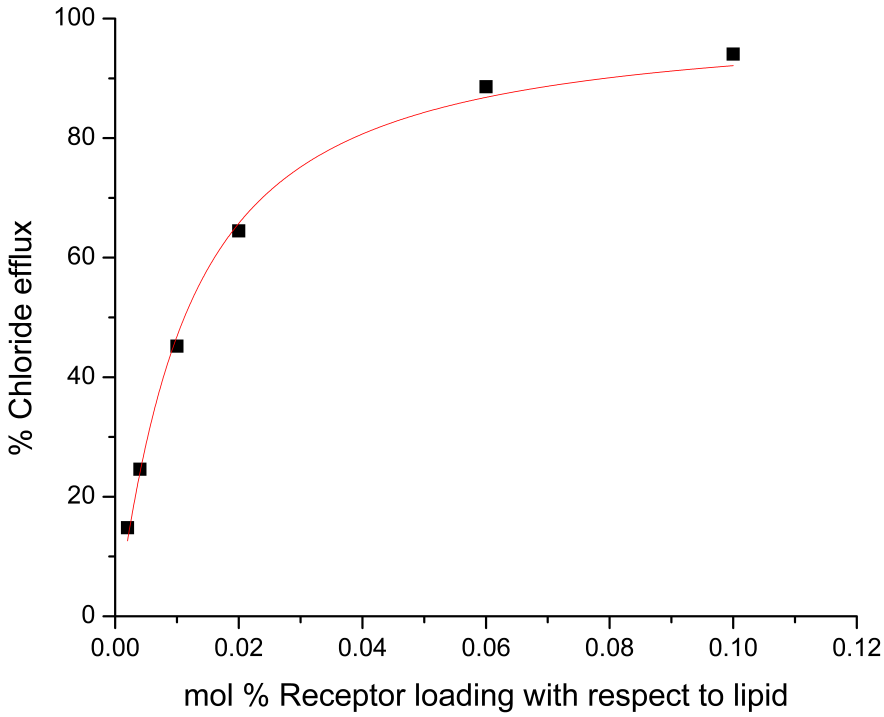

Figure S 99: Hill analysis for Cl^-/HCO_3^- antiport mediated by **3**. Data was fitted to the Hill equation using Origin. $R^2 = 0.99619$, $EC_{50} = 0.01119$ mol%, n = 1.12271±0.05206.

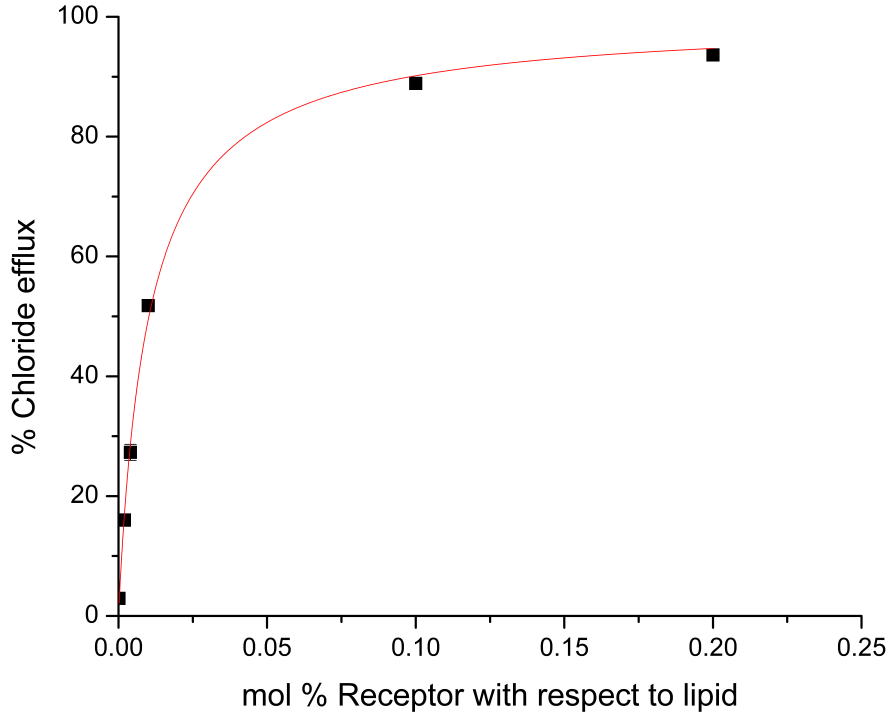

Figure S 100: Hill analysis for Cl^-/HCO_3^- antiport mediated by **4**. Data was fitted to the Hill equation using Origin. $R^2 = 0.99798$, $EC_{50} = 0.01022$ mol%, n = 0.97116±0.04544.

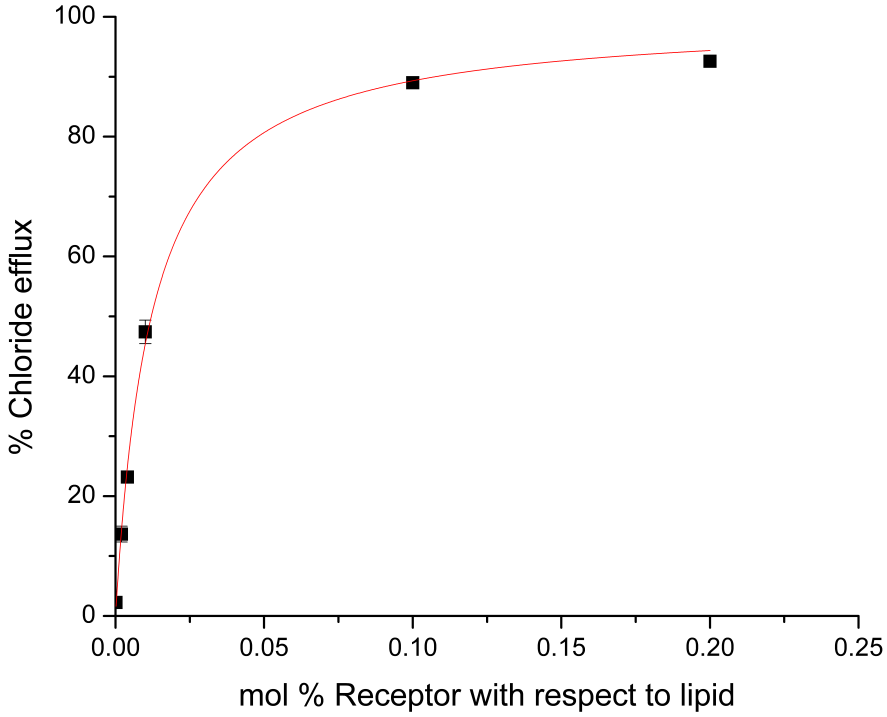

Figure S 101: Hill analysis for Cl^-/HCO_3^- antiport mediated by **4**. Data was fitted to the Hill equation using Origin. $R^2 = 0.99815$, $EC_{50} = 0.01203$ mol%, n = 1.00300±0.04459.

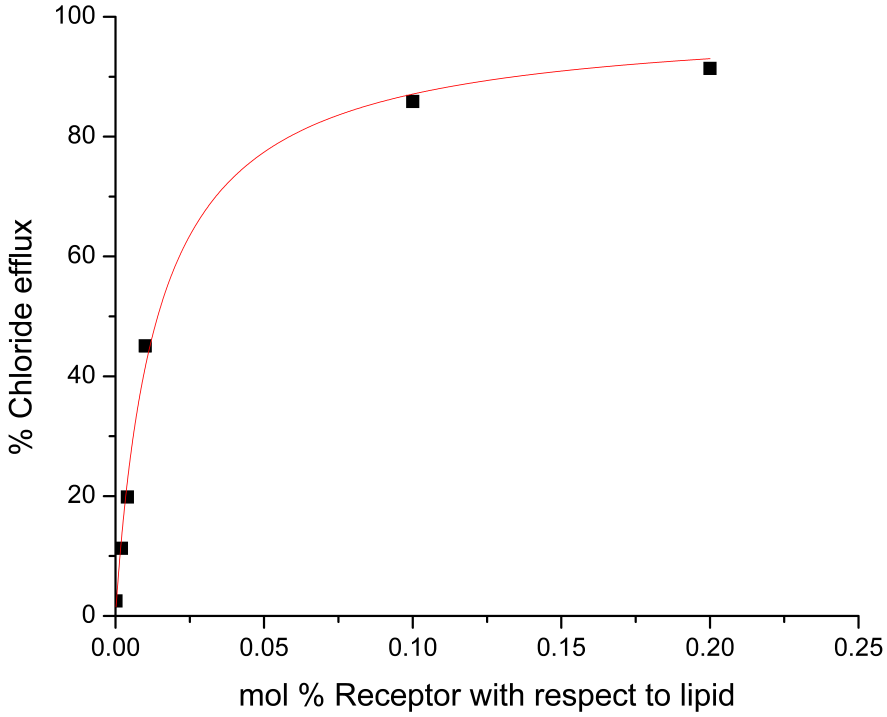

Figure S 102: Hill analysis for Cl^-/HCO_3^- antiport mediated by **4**. Data was fitted to the Hill equation using Origin. $R^2 = 0.99543$, $EC_{50} = 0.01419$ mol%, n = 0.97814±0.06372.

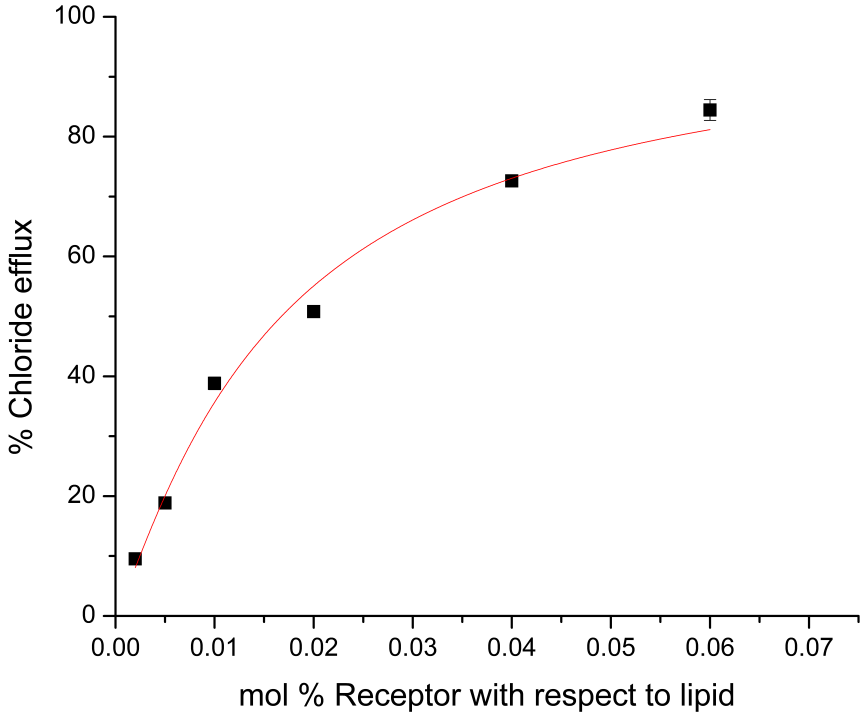

Figure S 103: Hill analysis for Cl^-/HCO_3^- antiport mediated by **6**. Data was fitted to the Hill equation using Origin. $R^2 = 0.98769$, $EC_{50} = 0.01674$ mol%, n = 1.14481±0.08553.

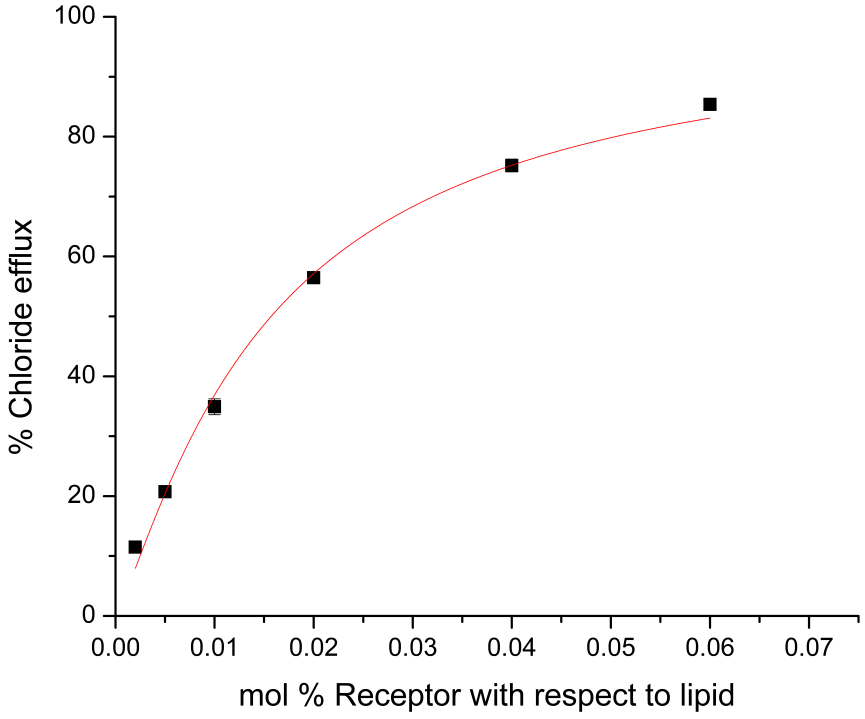

Figure S 104: Hill analysis for Cl^-/HCO_3^- antiport mediated by **6**. Data was fitted to the Hill equation using Origin. $R^2 = 0.99377$, $EC_{50} = 0.01571$ mol%, n = 1.18819±0.06354.

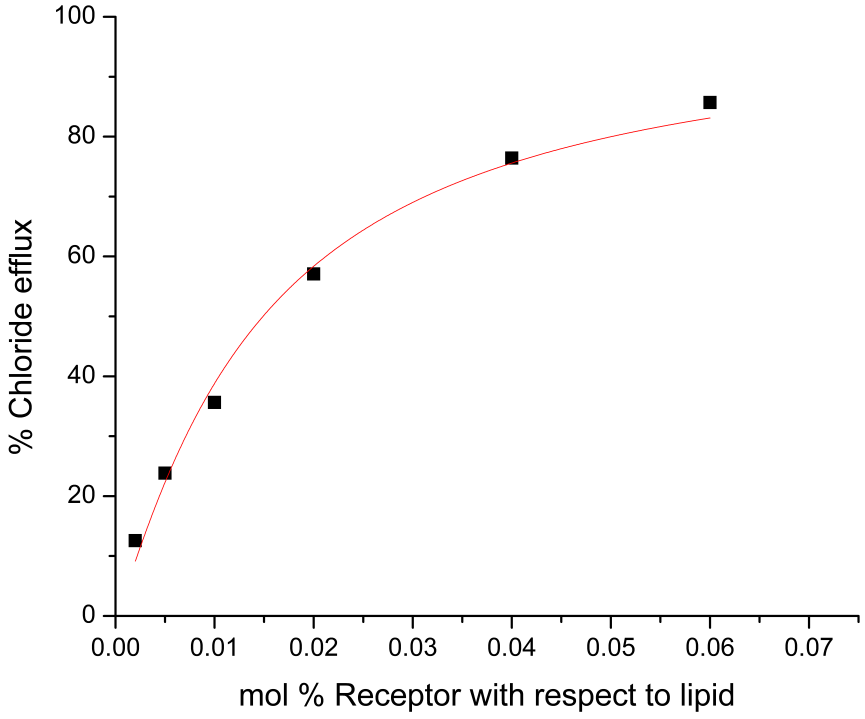

Figure S 105: Hill analysis for Cl^-/HCO_3^- antiport mediated by **6**. Data was fitted to the Hill equation using Origin. $R^2 = 0.99039$, $EC_{50} = 0.01489$ mol%, n = 1.14349±0.07452.

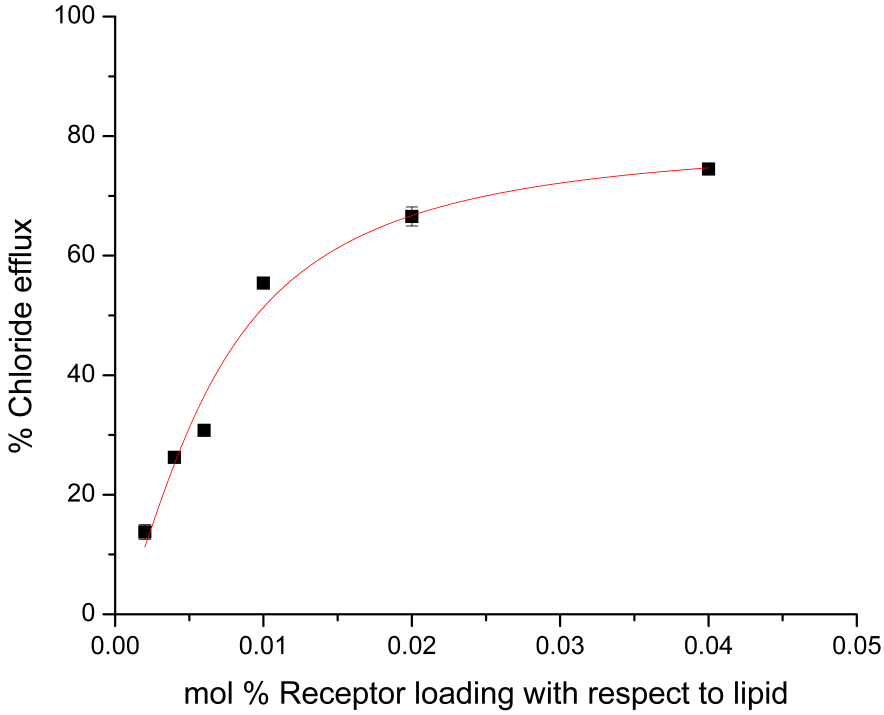

Figure S 106: Hill analysis for Cl^-/HCO_3^- antiport mediated by **7**. Data was fitted to the Hill equation using Origin. $R^2 = 0.97616$, $EC_{50} = 0.00952$ mol%, n =1.48602±0.16824.

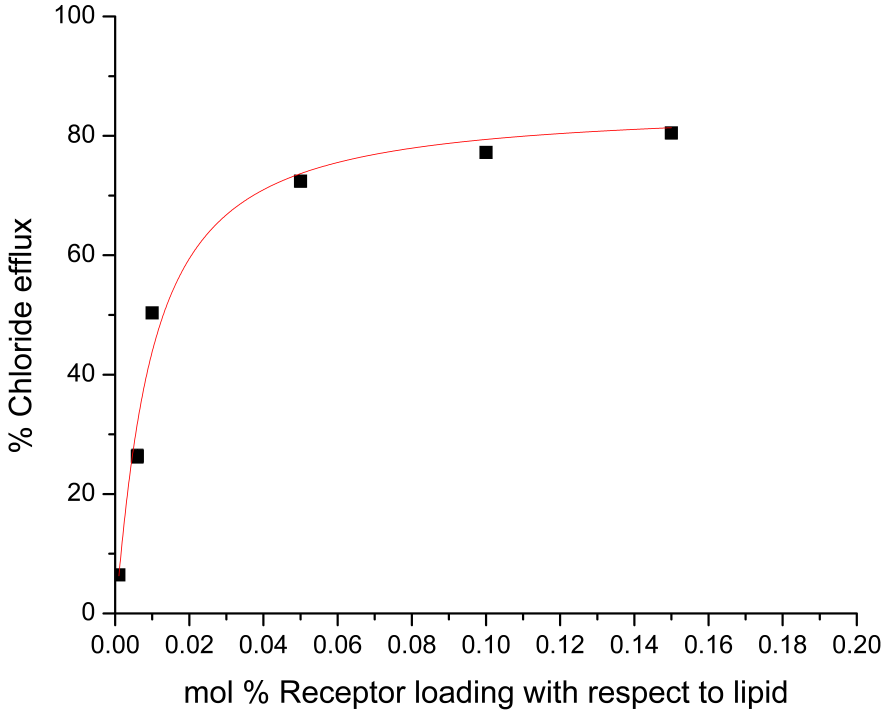

Figure S 107:: Hill analysis for Cl^-/HCO_3^- antiport mediated by **7**. Data was fitted to the Hill equation using Origin. $R^2 = 0.97824$, $EC_{50} = 0.01297$ mol%, n = 1.12323±0.16141.

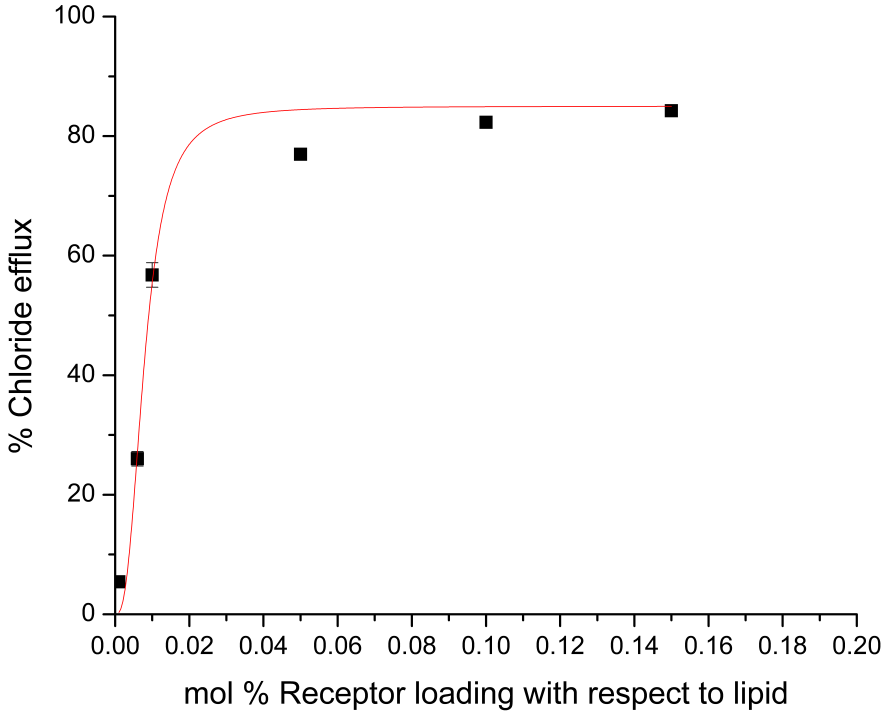

Figure S 108: Hill analysis for Cl^-/HCO_3^- antiport mediated by **7**. Data was fitted to the Hill equation using Origin. $R^2 = 0.97851$, $EC_{50} = 0.00903$ mol%, n = 2.71294±0.69415.

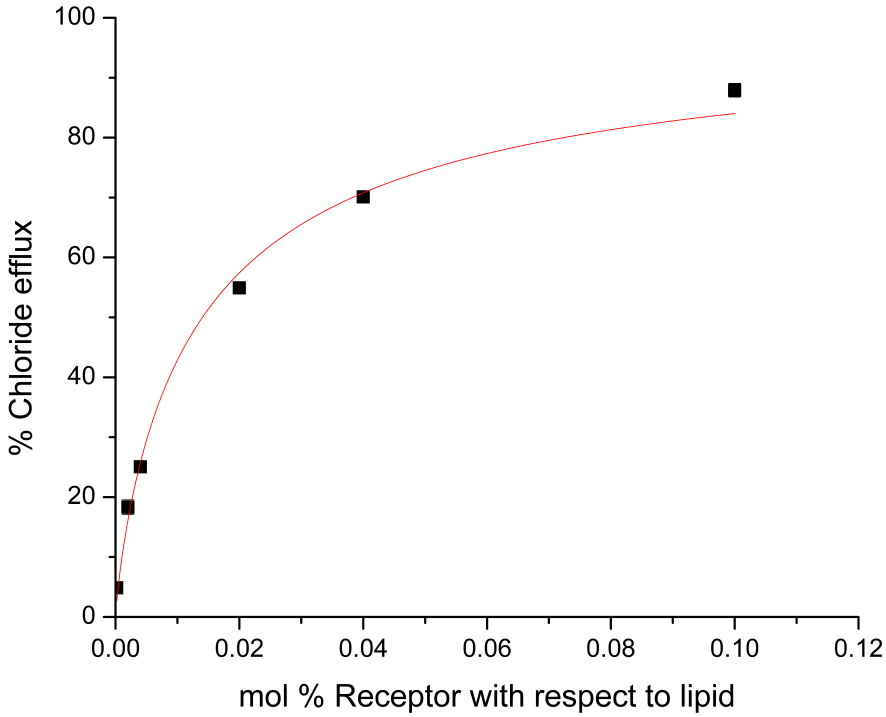

Figure S 109: Hill analysis for Cl^-/HCO_3^- antiport mediated by **8**. Data was fitted to the Hill equation using Origin. $R^2 = 0.99245$, $EC_{50} = 0.01404$ mol%, n = 0.84540±0.05519.

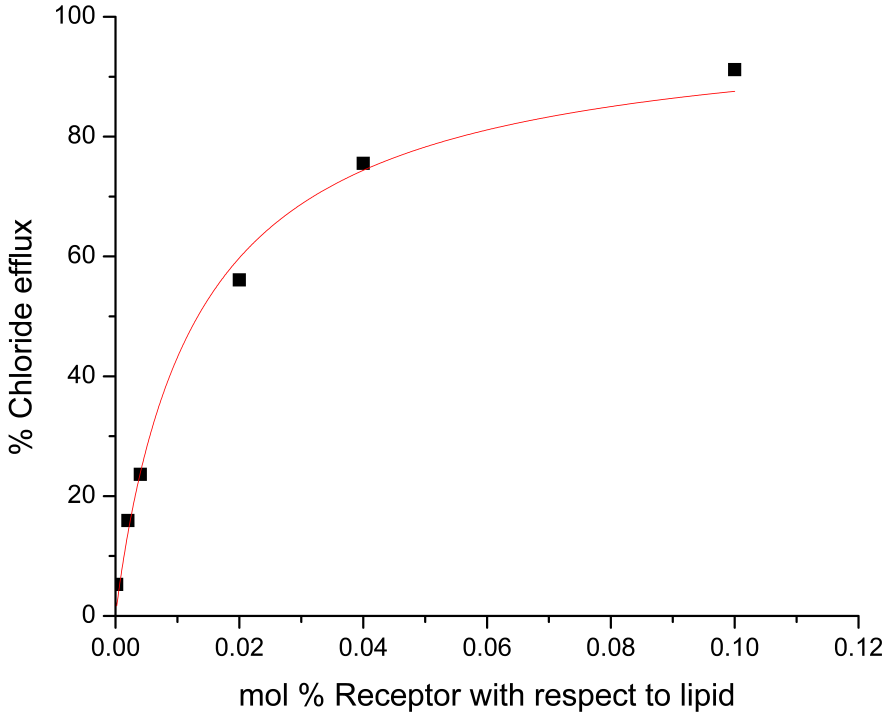

Figure S 110: Hill analysis for Cl^-/HCO_3^- antiport mediated by **8**. Data was fitted to the Hill equation using Origin. $R^2 = 0.99072$, $EC_{50} = 0.01328$ mol%, n = 0.96687±0.07453.

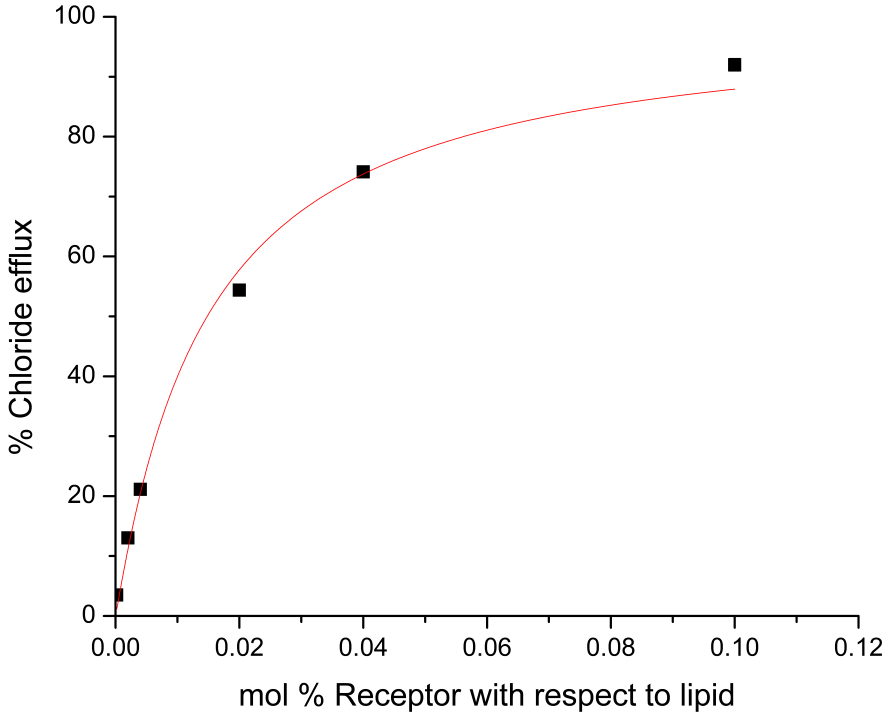

Figure S 111: Hill analysis for Cl^-/HCO_3^- antiport mediated by **8**. Data was fitted to the Hill equation using Origin. $R^2 = 0.99263$, $EC_{50} = 0.01480$ mol%, n = 1.03936±0.07542.

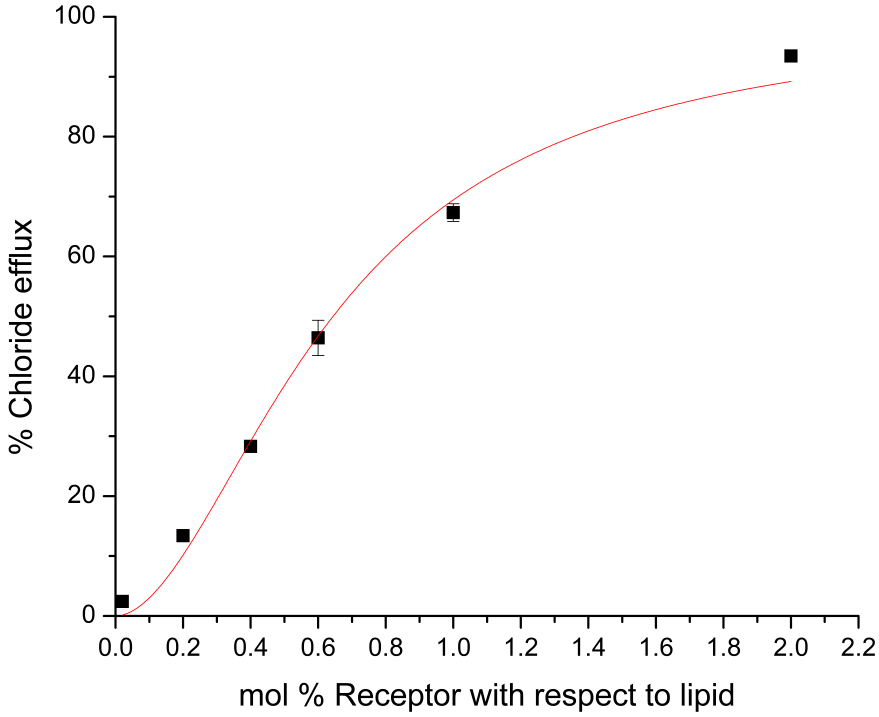

Figure S 112: Hill analysis for Cl^-/HCO_3^- antiport mediated by **10**. Data was fitted to the Hill equation using Origin. $R^2 = 0.99172$, $EC_{50} = 0.64376$ mol%, n = 1.86335±0.15237.

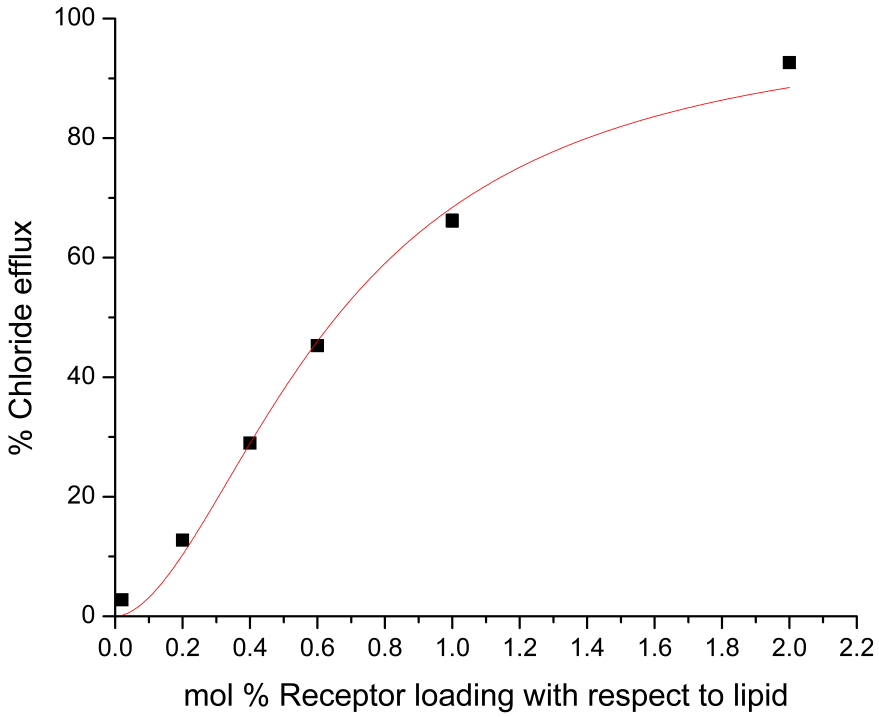

Figure S 113: Hill analysis for Cl^-/HCO_3^- antiport mediated by **10**. Data was fitted to the Hill equation using Origin. $R^2 = 0.99227$, $EC_{50} = 0.65478$ mol%, n = 1.82442±0.14185.

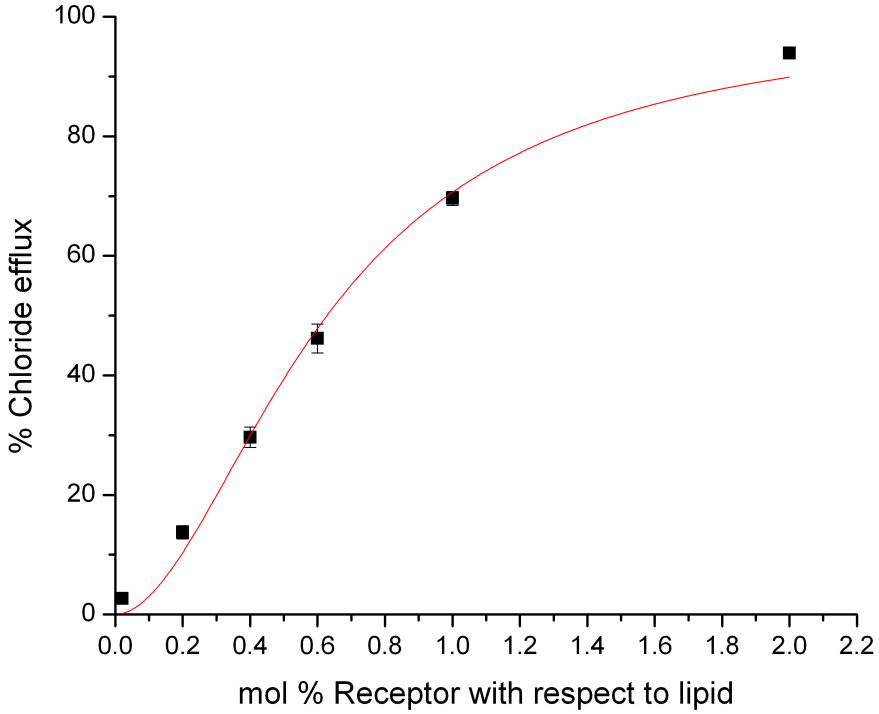

Figure S 114: Hill analysis for Cl^-/HCO_3^- antiport mediated by **10**. Data was fitted to the Hill equation using Origin. $R^2 = 0.99196$, $EC_{50} = 0.62794$ mol%, n = 1.88677±0.15356.

S10: Binding Studies

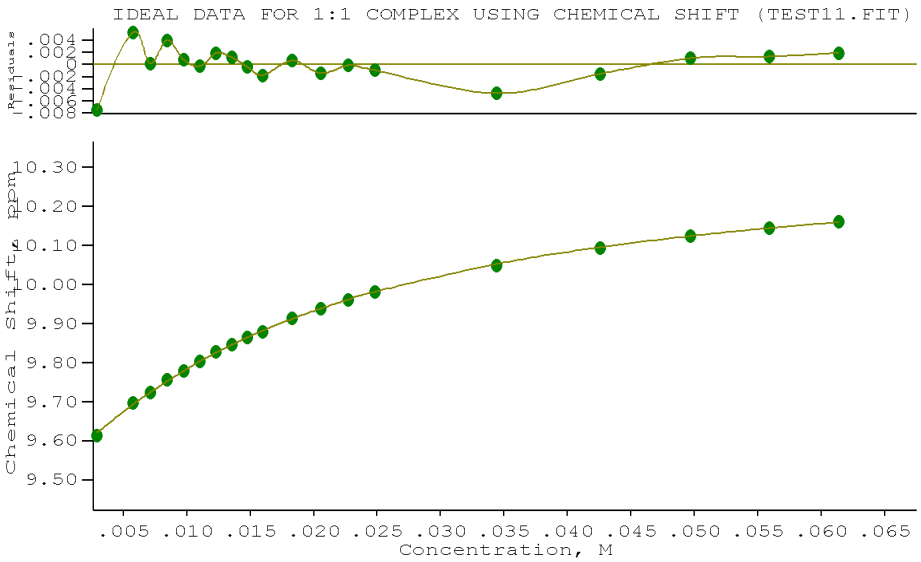

$K_1 = 65\ M^{-1} \pm 3\%$

Figure S 115: Binding curve generated from the ^{1}H NMR titration of **2** with TBACl in DMSO-d_6/H_2O 0.5%. The data was fitted to a 1:1 receptor:anion binding model using WinEQNMR2.

a)

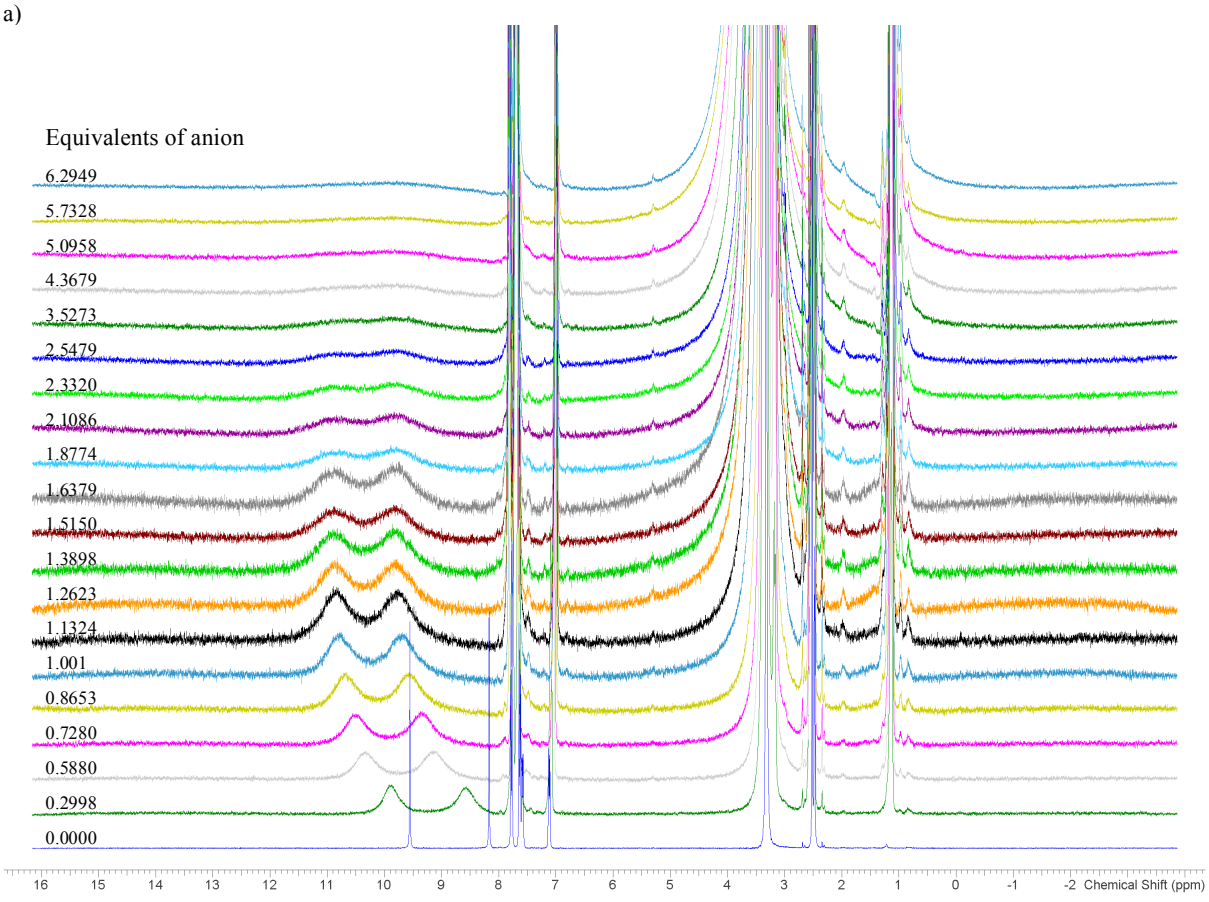

b)

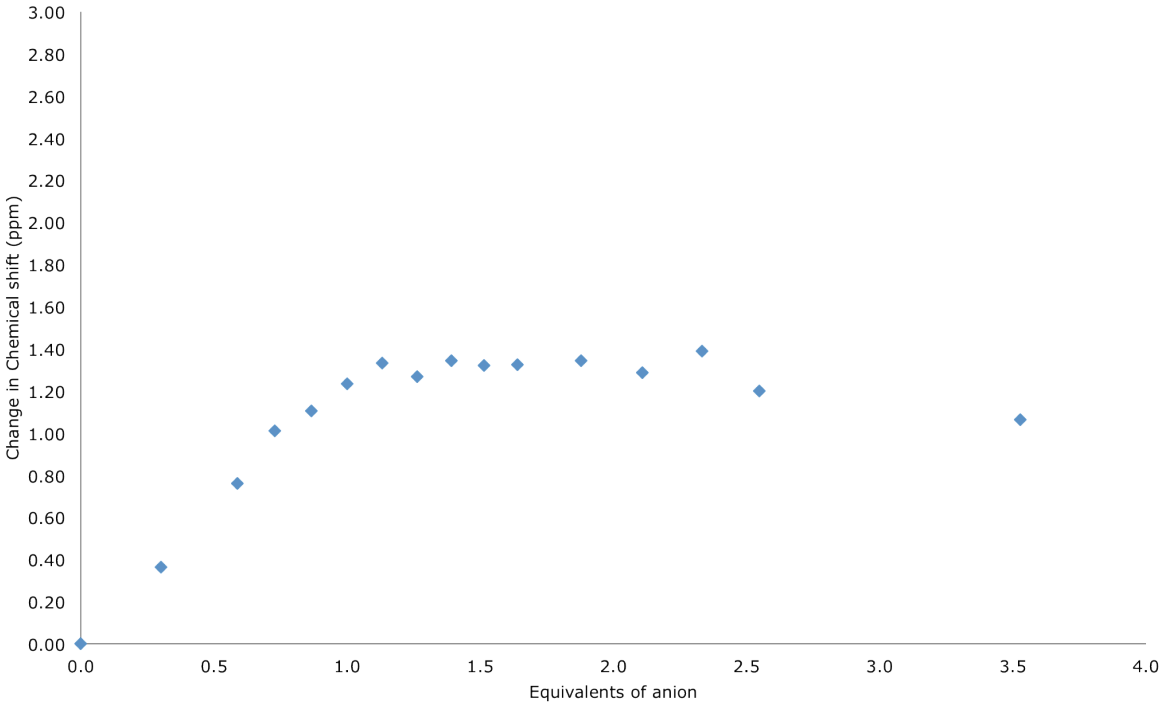
Change in Chemical shift (ppm)
3.00
2.80
2.60
2.40
2.20
2.00
1.80
1.60
1.40
1.20
1.00
0.80
0.60
0.40
0.20
0.00
0.0
0.5
1.0
1.5
2.0
2.5
3.0
3.5
4.0
Equivalents of anion

c)

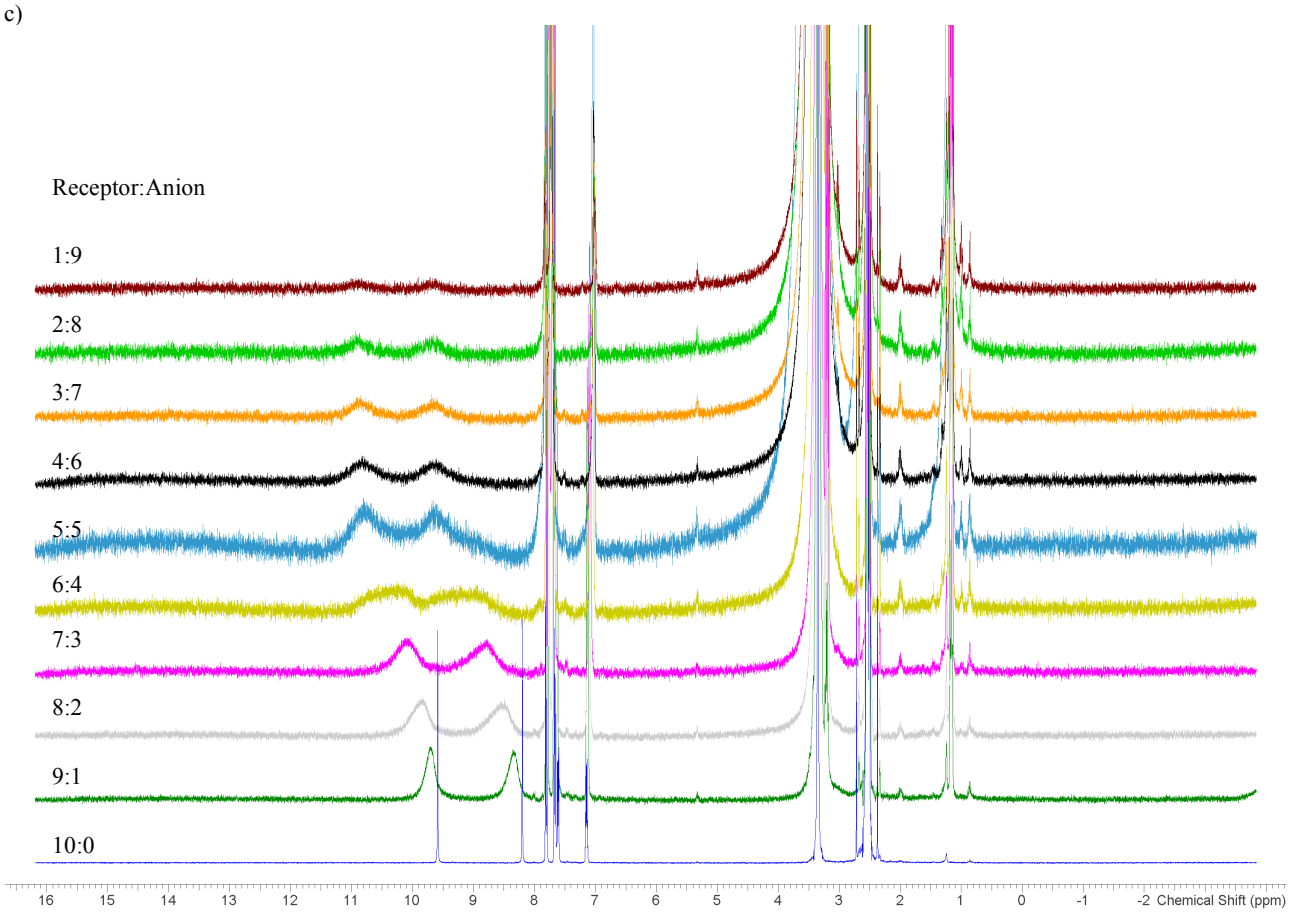
Receptor:Anion
1:9
2:8
3:7
4:6
5:5
6:4
7:3
8:2
9:1
10:0
16
15
14
13
12
11
10
9
8
7
6
5
4
3
2
1
0
-1
-2 Chemical Shift (ppm)

d)

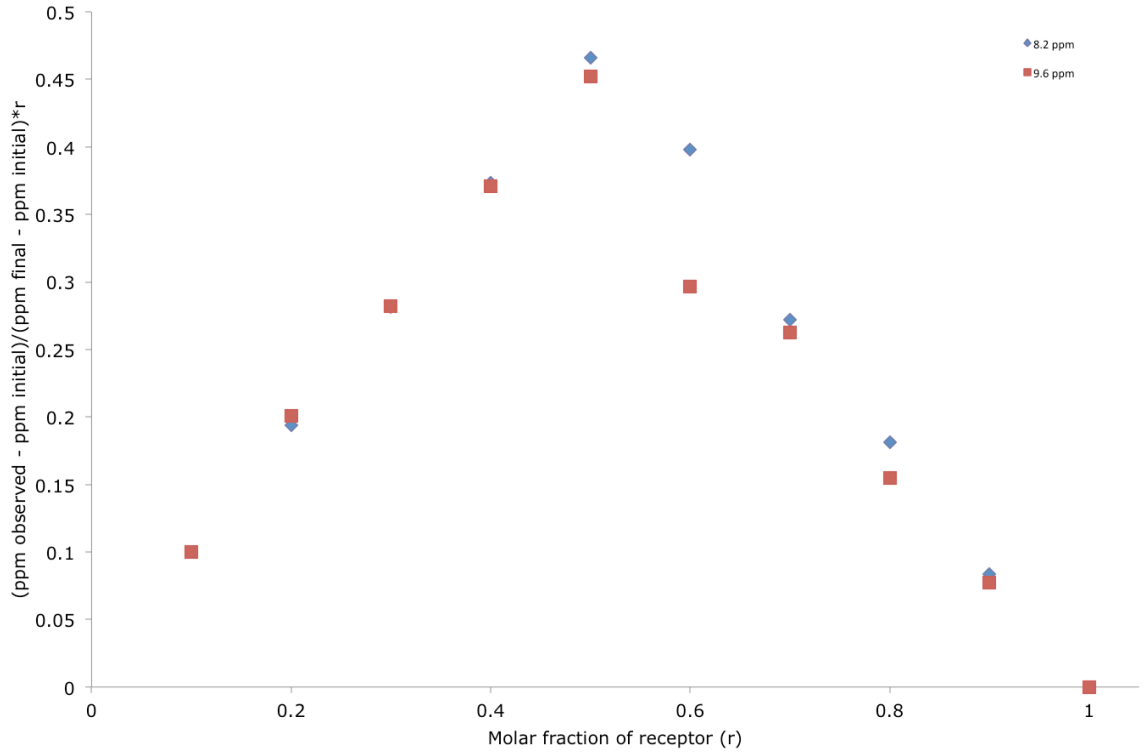

Figure S 116: a) Stack plot generated from the ^{1}H NMR titration data of **2** with $TEAHCO_3$ in DMSO-d_6/H_2O 0.5%. b) Change in chemical shift as a function of anion equivalents, of the most deshielded N-H peak, as measured from the ^{1}H NMR titration data of **2** with $TEAHCO_3$ in DMSO-d_6/H_2O 0.5%. Data could not be fit to a 1:1 (receptor:anion) binding isotherm using WinWENMR2 as it was not possible to accurately peak pick the N-H proton signals due to peak broadening. c) Stack plot generated from the ^{1}H NMR Job plot data of **2** with $TEAHCO_3$ in DMSO-d_6/H_2O 0.5%. d) Job plot of **2** with $TEAHCO_3$ in DMSO-d_6/H_2O 0.5%, showing the change in chemical shift of N-H resonances. Job plot analysis indicates a 1:1 receptor:anion binding interaction.

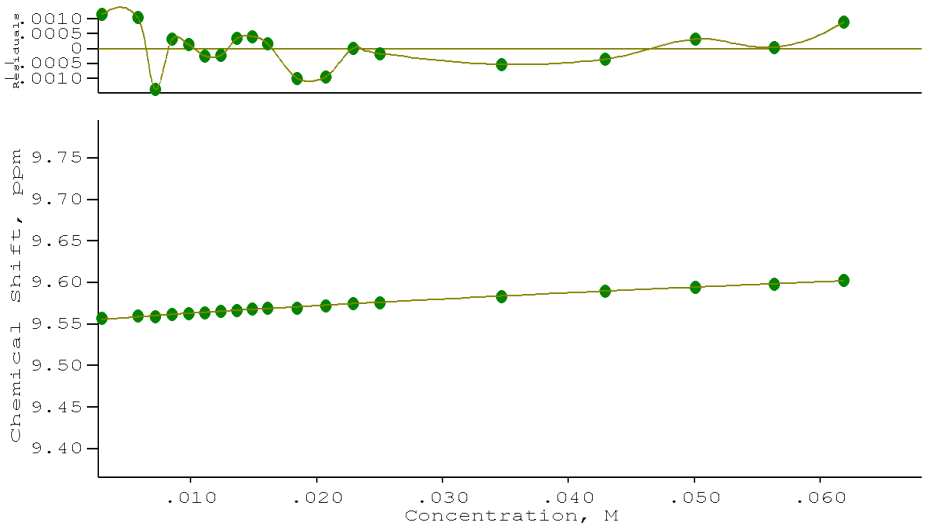

K_1 = 6 M^{-1} ± 10%

Figure S 117: Binding curve generated from the ^{1}H NMR titration of **2** with $TBANO_3$ in DMSO-d_6/H_2O 0.5%. The data was fitted to a 1:1 receptor:anion binding model using WinEQNMR2.

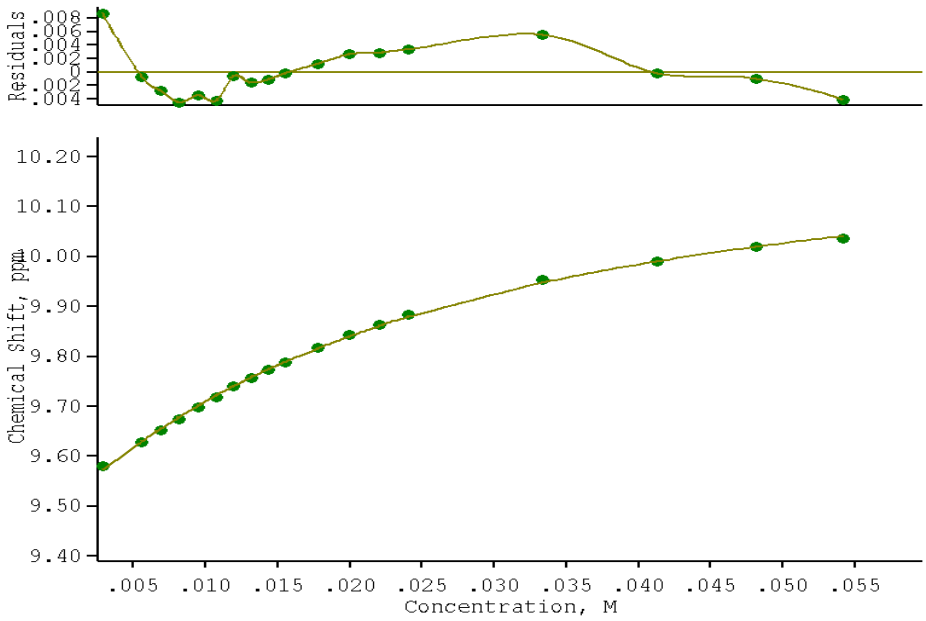

$K_1 = 50\ M^{-1} \pm 5\%$

Figure S 118: Binding curve generated from the ^1H NMR titration of **3** with TBACl in DMSO-d_6/H_2O 0.5%. The data was fitted to a 1:1 receptor:anion binding model using WinEQNMR2.

a)

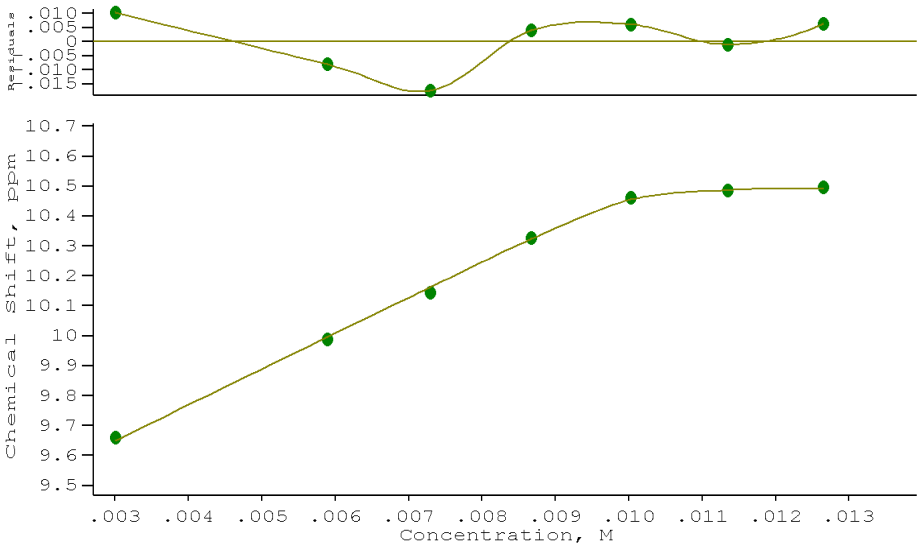

K_1 = 80868 M^{-1} ± 7%

b)

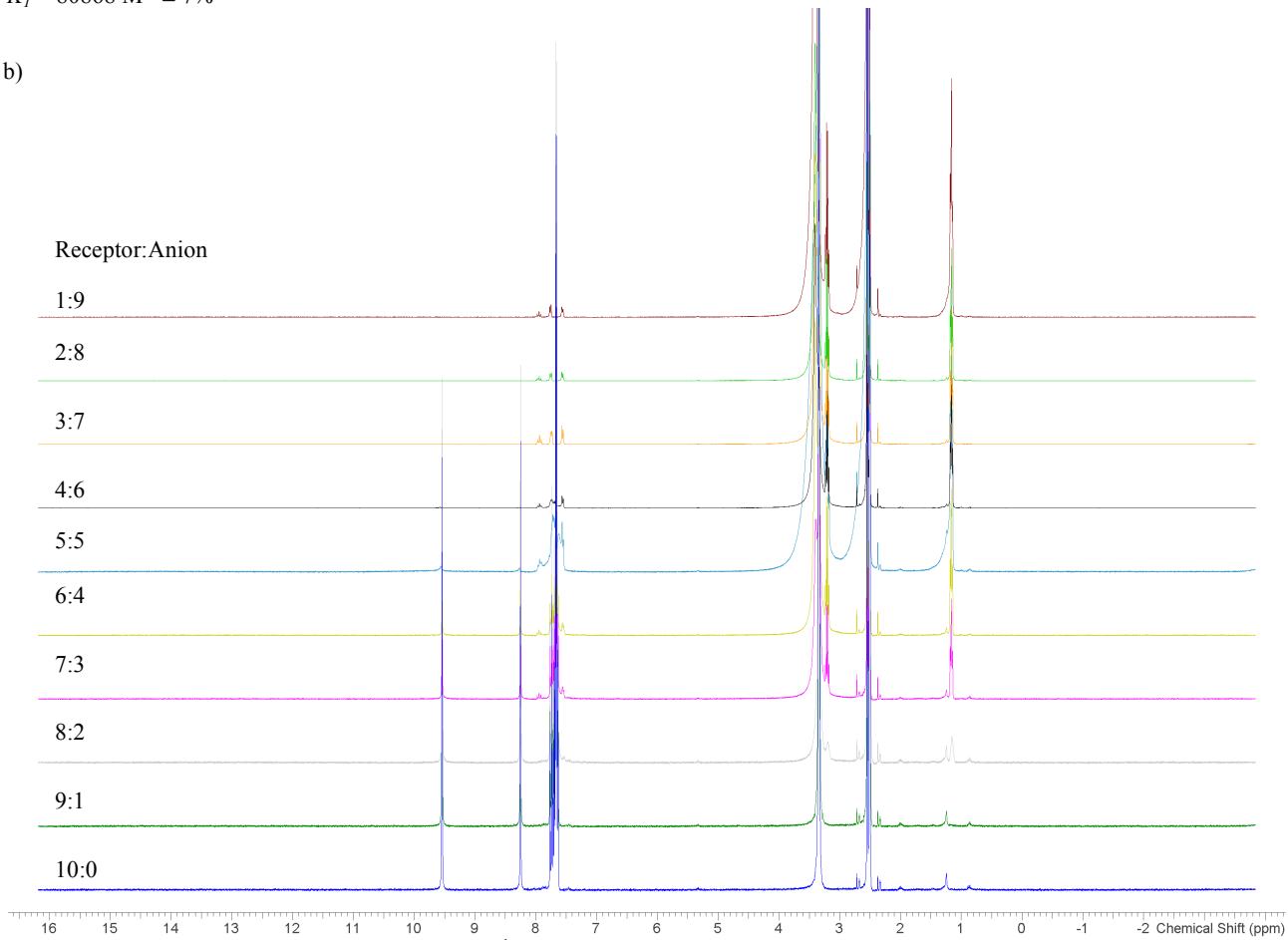

Figure S 119: a) Binding curve generated from the ^{1}H NMR titration of **3** with $TEAHCO_3$ in DMSO-d_6/H_2O 0.5%. The data was fitted to a 1:1 receptor:anion binding model using WinEQNMR2. N-H signals broadened with the addition of large equivalents of anion hence the fit was generated using fewer data points than usual. b) Stack plot generated from the ^{1}H NMR Job plot data of **3** with $TEAHCO_3$ in DMSO-d_6/H_2O 0.5%. Higher concentrations of anion lead to peak broadening, hence data could not be fitted to a Job plot.

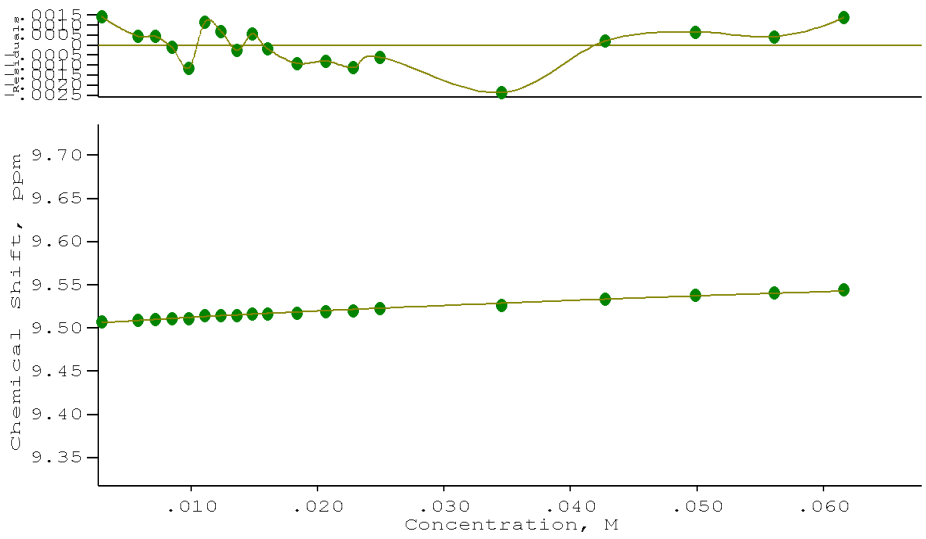

K_1 = 7 M^{-1} ± 20%

Figure S 120: Binding curve generated from the ^{1}H NMR titration of **3** with $TBANO_3$ in DMSO-d_6/H_2O 0.5%. The data was fitted to a 1:1 receptor:anion binding model using WinEQNMR2.

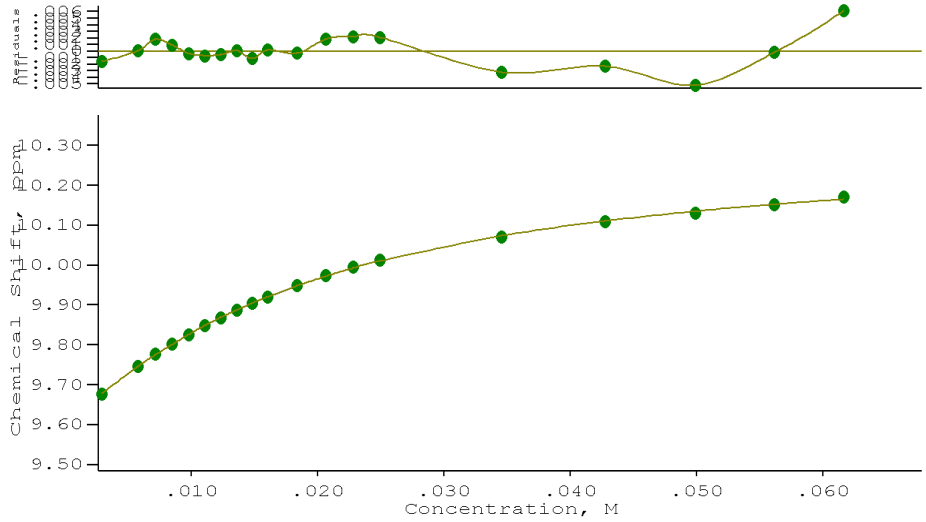

K_1 = 71 M^{-1} ± 3%

Figure S 121: Binding curve generated from the ^{1}H NMR titration of **4** with TBACl in DMSO-d_6/H_2O 0.5%. The data was fitted to a 1:1 receptor:anion binding model using WinEQNMR2.

a)

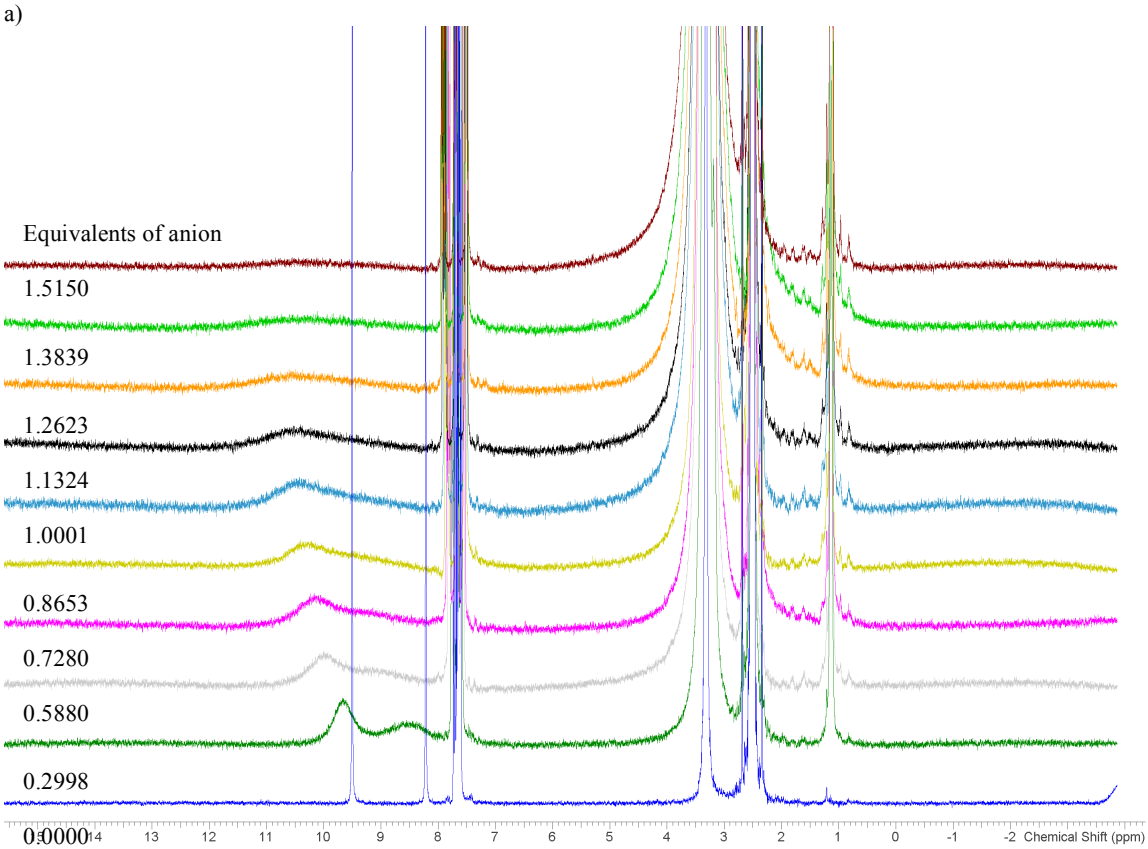

b)

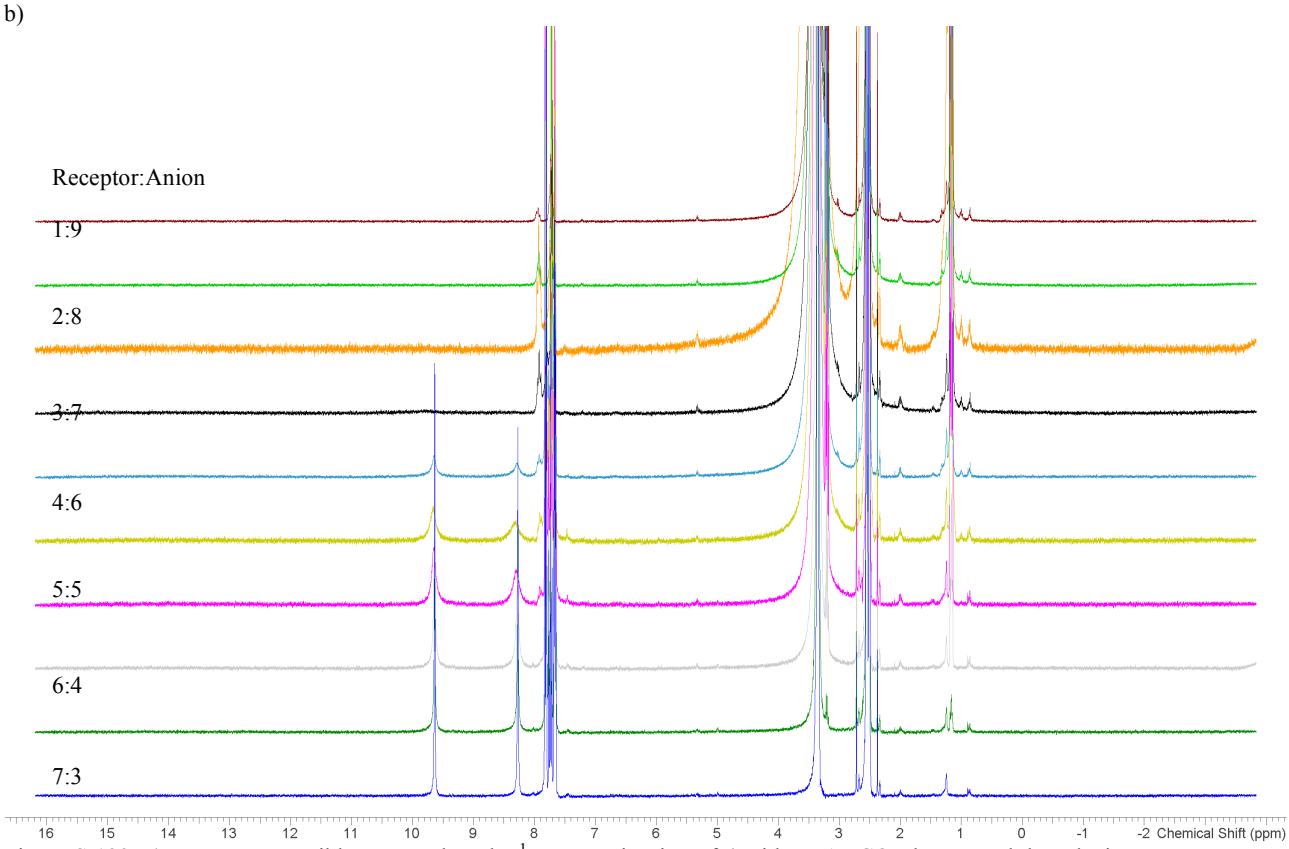

Figure S 122: a) It was not possible to complete the ^{1}H NMR titration of **4** with $TEAHCO_3$ due to peak broadening. It was not possible to accurately peak pick the N-H proton signals. b)Stack plot generated from the ^{1}H NMR Job plot data of **4** with $TEAHCO_3$ in DMSO-d_6/H_2O 0.5%. It was not possible to fit the titration data to a binding isotherm due to peak broadening. Hence Job plot analysis was done. This was also subject to peak broadening beyond the point of 1:1 receptor:anion, suggesting a possible 1:1 receptor:anion binding interaction.

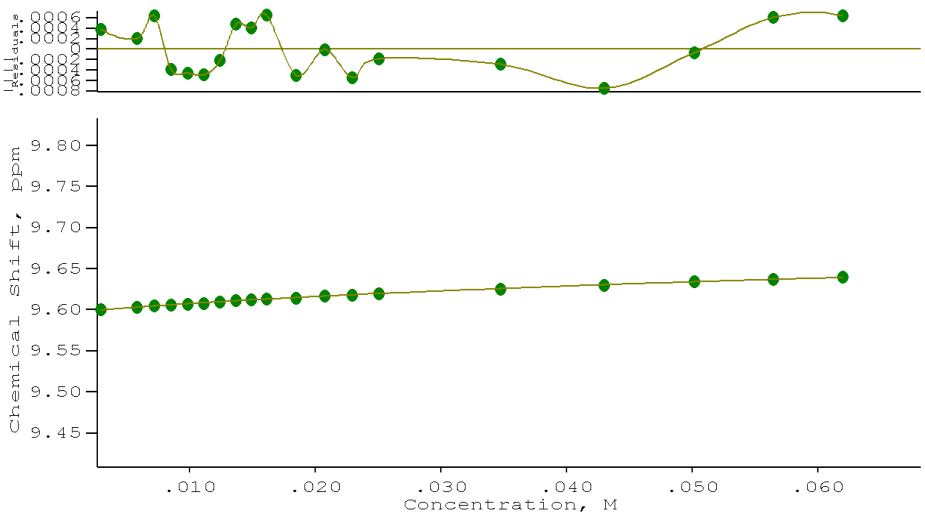

$K_1 = 13\ M^{-1} \pm 4\%$

Figure S 123: Binding curve generated from the ^1H NMR titration of **4** with $TBANO_3$ in DMSO-d_6/H_2O 0.5%. The data was fitted to a 1:1 receptor:anion binding model using WinEQNMR2.

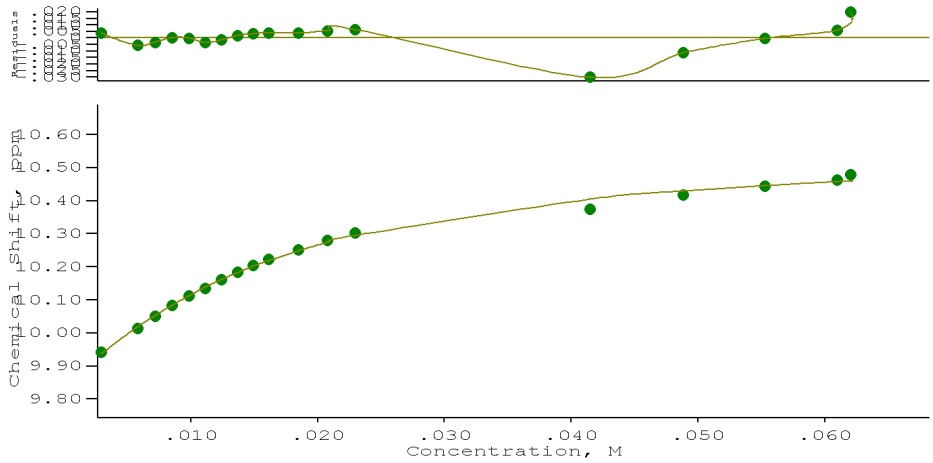

$K_1 = 94\ M^{-1} \pm 9\%$

Figure S 124: Binding curve generated from the ^1H NMR titration of **6** with TBACl in DMSO-d_6/H_2O 0.5%. The data was fitted to a 1:1 receptor:anion binding model using WinEQNMR2.

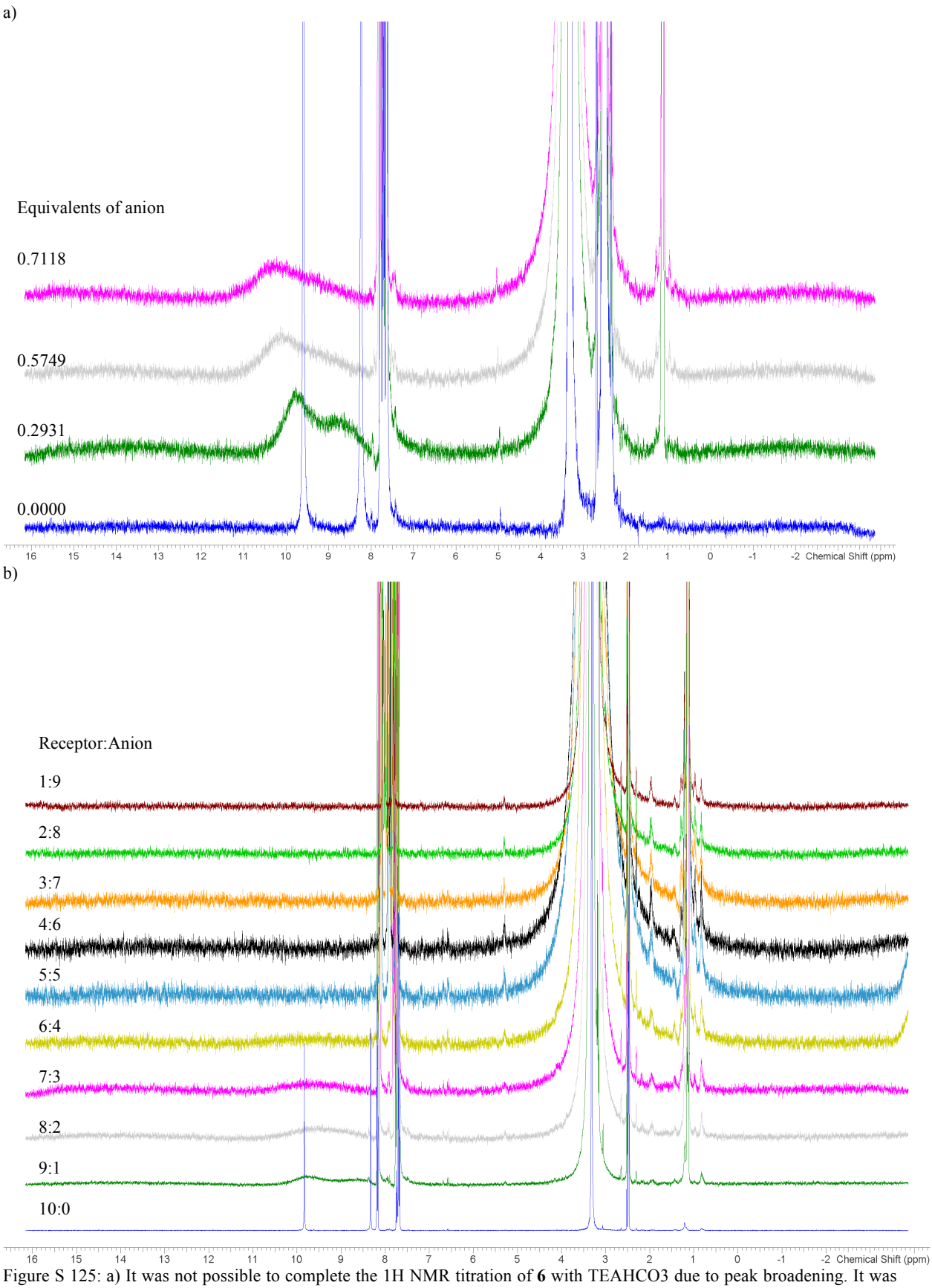

Figure S 125: a) It was not possible to complete the 1H NMR titration of **6** with TEAHCO3 due to peak broadening. It was not possible to accurately peak pick the N-H proton signals b) Stack plot generated from the 1H NMR Job plot data of **6** with TEAHCO3 in DMSO-d6/H2O 0.5%. It was not possible to fit the titration data to a binding isotherm due to peak broadening. Hence Job plot analysis was attempted. This was also subject to significant peak broadening at low anion concentrations, suggesting a possible deprotonation event.

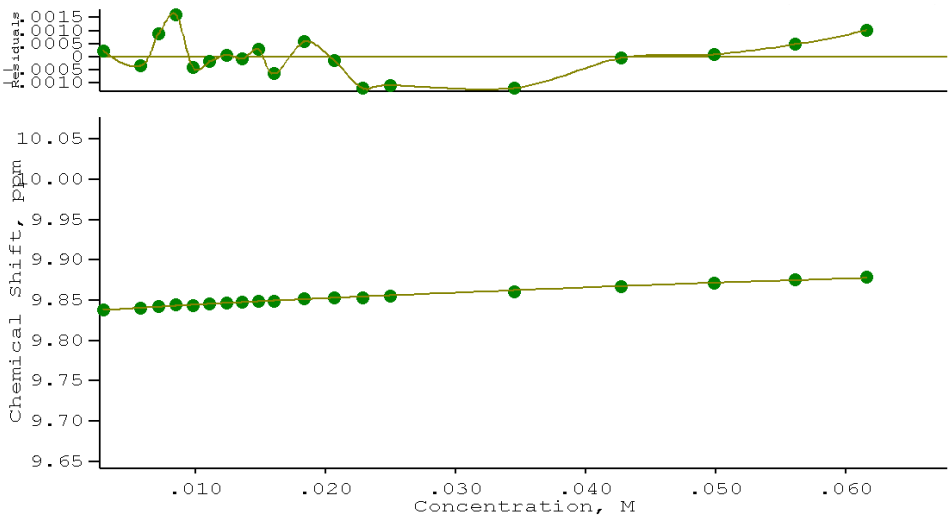

$K_1 = 7\ M^{-1} \pm 15\%$

Figure S 126: Binding curve generated from the ^1H NMR titration of **6** with $TBANO_3$ in DMSO-d_6/H_2O 0.5%. The data was fitted to a 1:1 receptor:anion binding model using WinEQNMR2.

a)

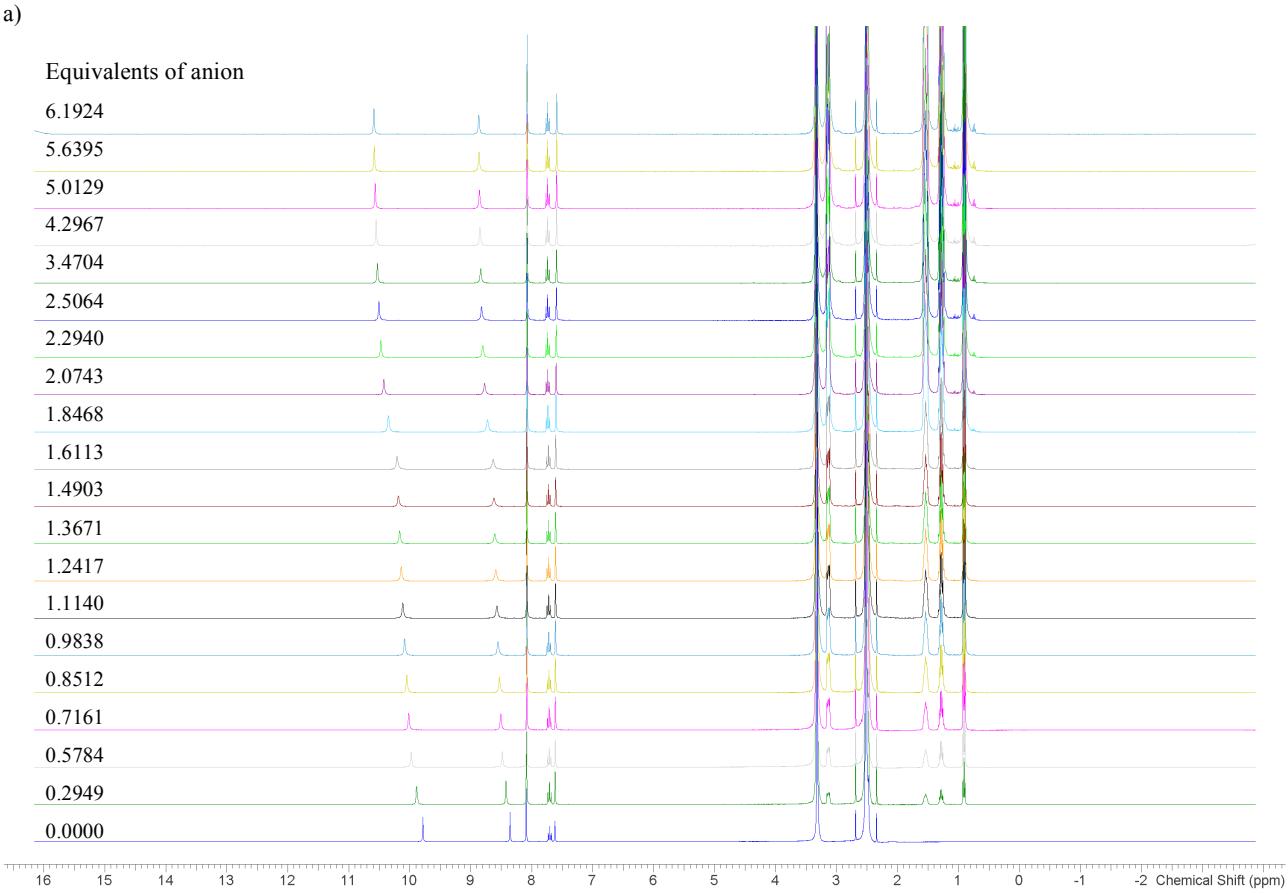
Equivalents of anion
6.1924
5.6395
5.0129
4.2967
3.4704
2.5064
2.2940
2.0743
1.8468
1.6113
1.4903
1.3671
1.2417
1.1140
0.9838
0.8512
0.7161
0.5784
0.2949
0.0000
16 15 14 13 12 11 10 9 8 7 6 5 4 3 2 1 0 -1 -2 Chemical Shift (ppm)

b)

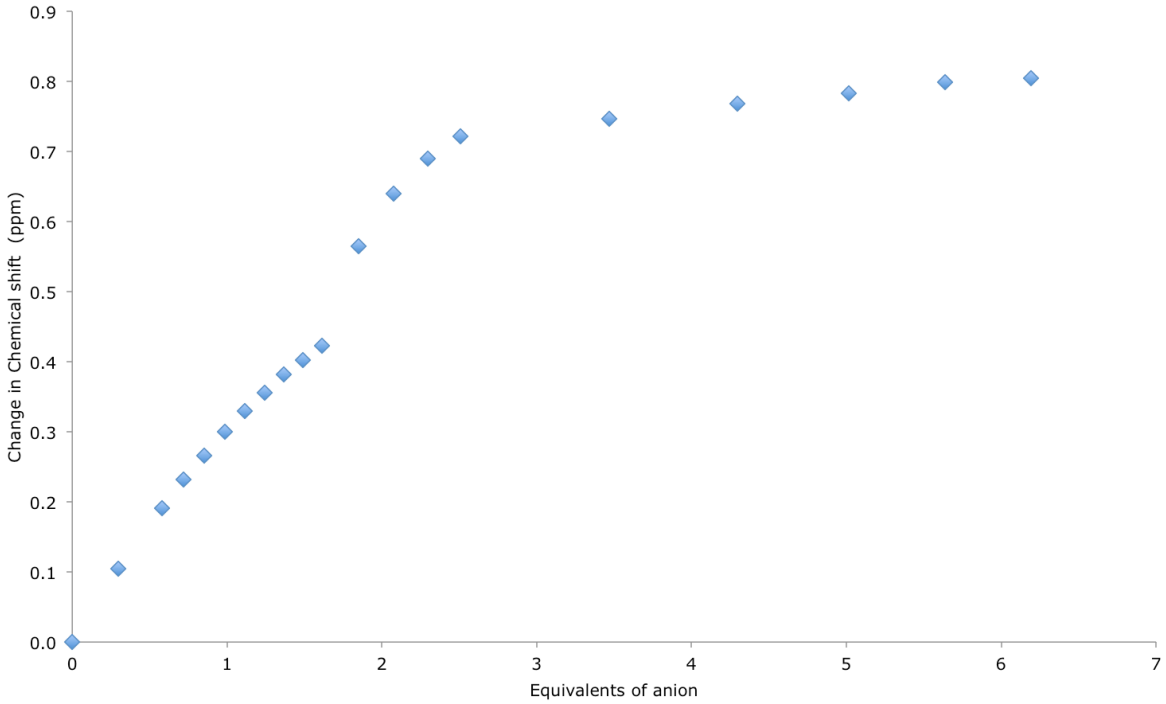
Change in Chemical shift (ppm)
0.0 0.1 0.2 0.3 0.4 0.5 0.6 0.7 0.8 0.9
0 1 2 3 4 5 6 7
Equivalents of anion

c)

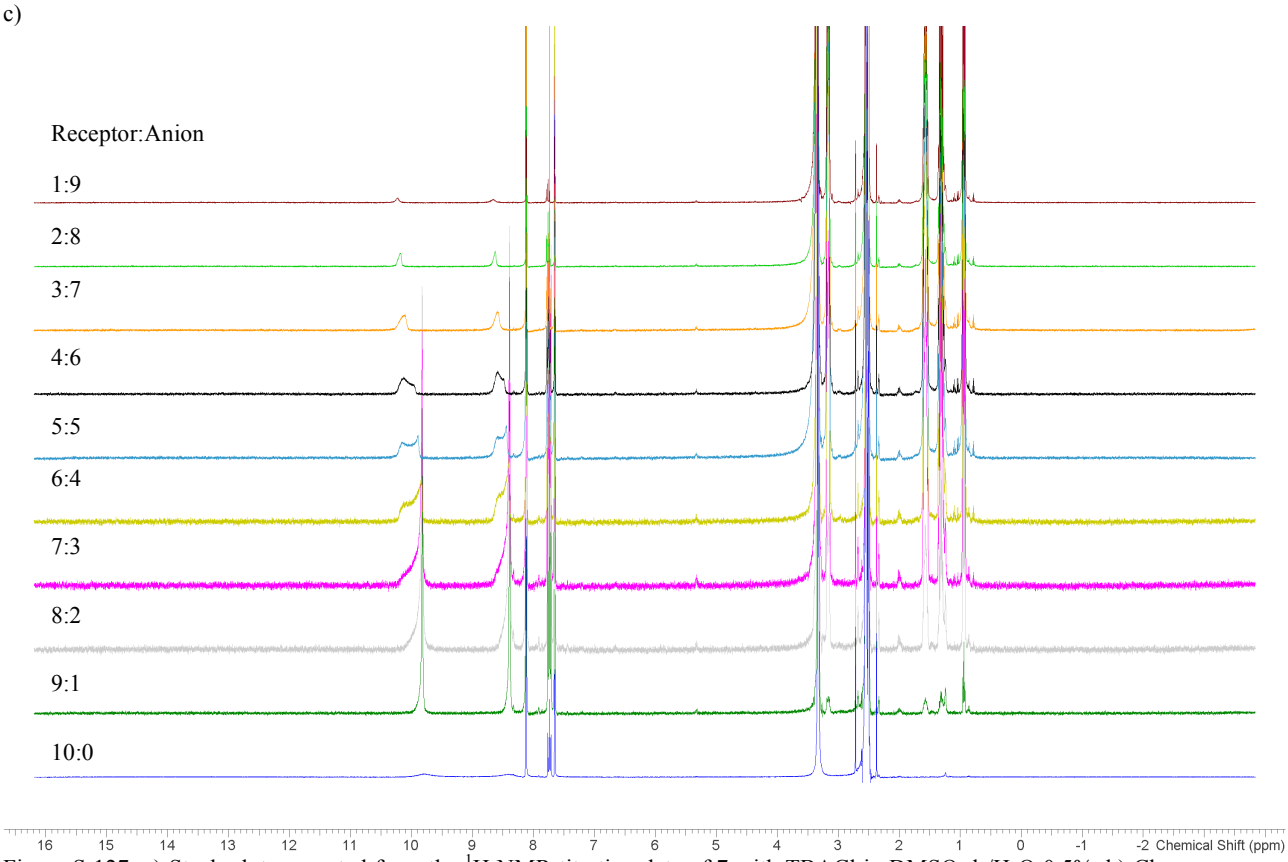

Figure S 127: a) Stack plot generated from the ^{1}H NMR titration data of **7** with TBACl in DMSO-d_6/H_2O 0.5%. b) Change in chemical shift as a function of anion equivalents, of the most deshielded N-H peak, as measured from the ^{1}H NMR titration data of **7** with TBACl in DMSO-d_6/H_2O 0.5%. Data could not be fit to a 1:1 or 1:2 (receptor:anion) binding isotherm using WinEQNMR2. c) Stack plot generated from the ^{1}H NMR Job plot data of **7** with TBACl in DMSO-d_6/H_2O 0.5%. Data could not be fitted due to slow exchange process.

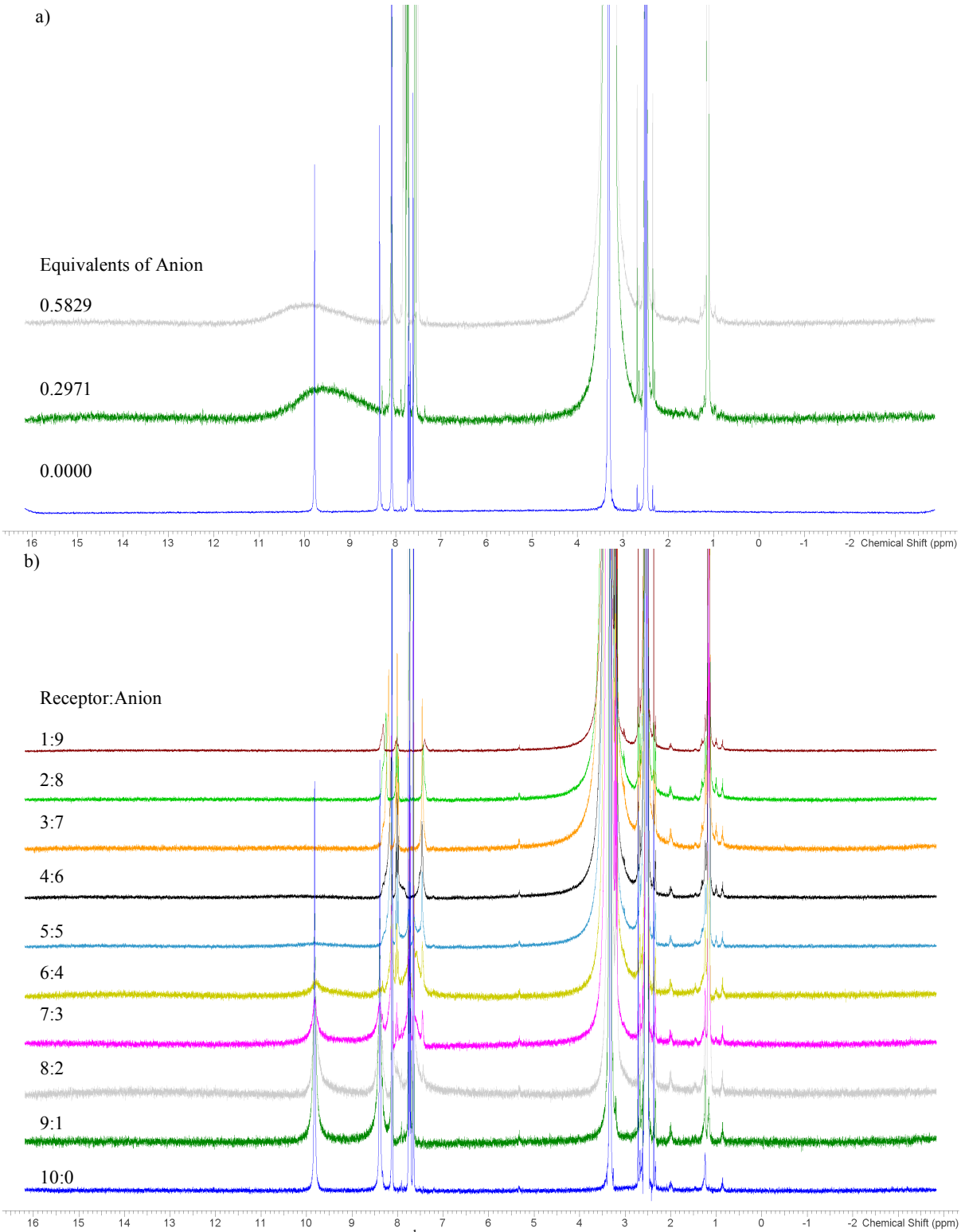

Figure S 128: a) It was not possible to complete the ^{1}H NMR titration of **7** with $TEAHCO_3$ due to peak broadening. It was not possible to accurately peak pick the N-H proton signals. b) Stack plot generated from the ^{1}H NMR Job plot data of **7** with $TEAHCO_3$ in DMSO-d_6/H_2O 0.5%. Higher concentrations of anion lead to peak broadening in the Job plot data also, hence data could not be fitted to a Job plot. Peak broadening beyond the point of 1:1 receptor:anion suggests a possible 1:1 receptor:anion binding interaction.

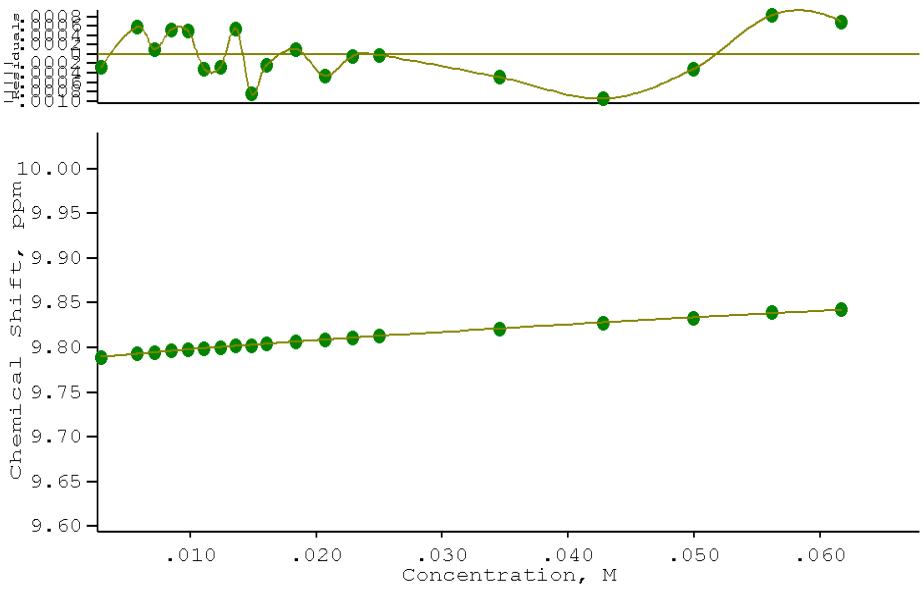

K_1 = 5 M^{-1} ± 9%

Figure S 129: Binding curve generated from the ^{1}H NMR titration of **7** with $TBANO_3$ in DMSO-d_6/H_2O 0.5%. The data was fitted to a 1:1 receptor:anion binding model using WinEQNMR2.

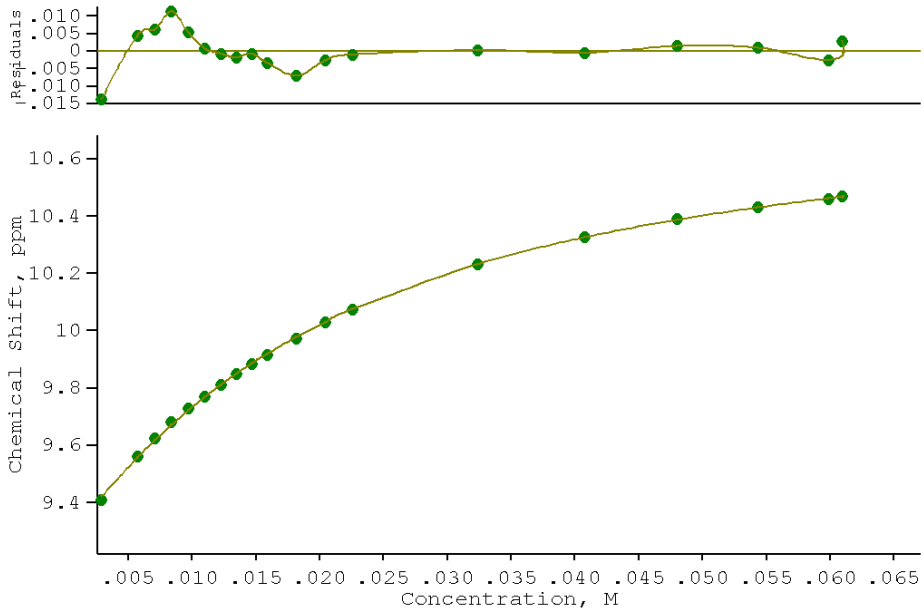

K_1 = 62 M^{-1} ± 3%

Figure S 130: Binding curve generated from the ^{1}H NMR titration of **10** with TBACl in DMSO-d_6/H_2O 0.5%. The data was fitted to a 1:1 receptor:anion binding isotherm using WinEQNMR2.

a)

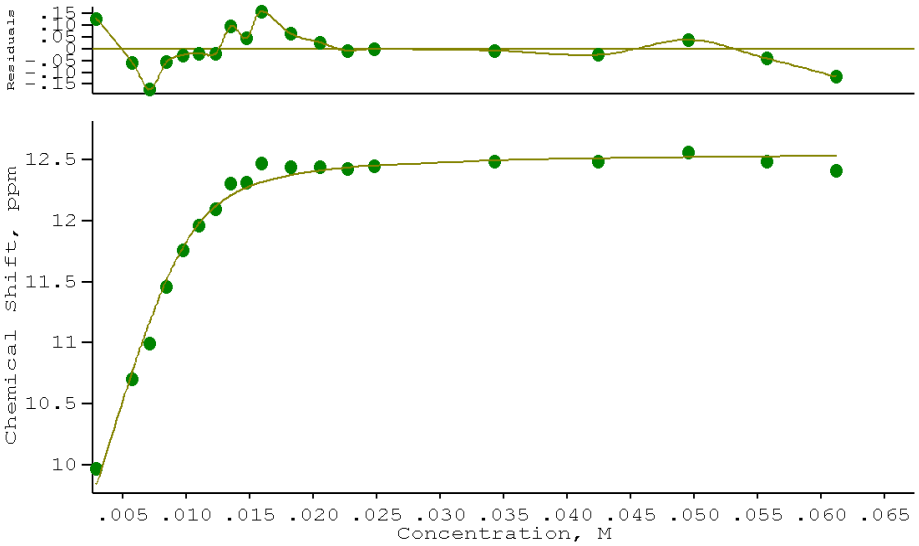

K_1 = 216 M^{-1} ± 19%

b)

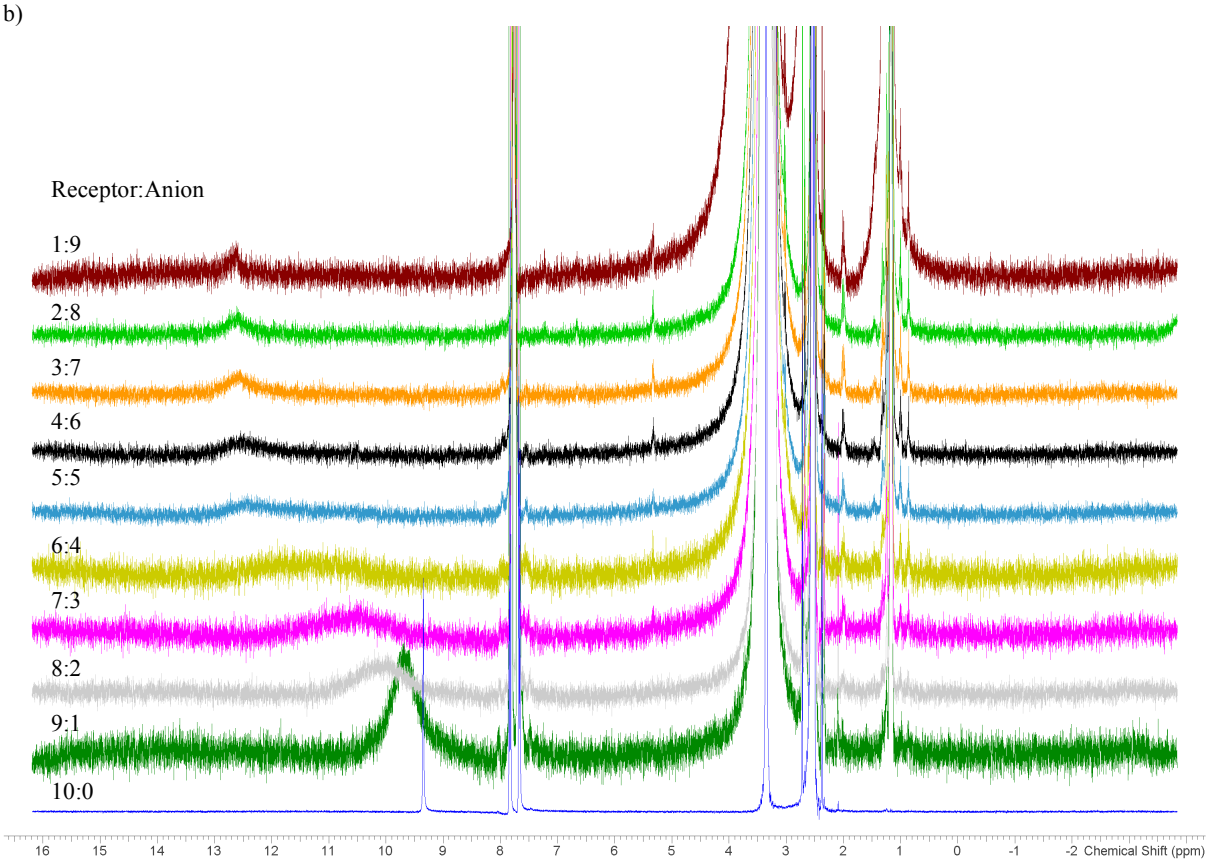

c)

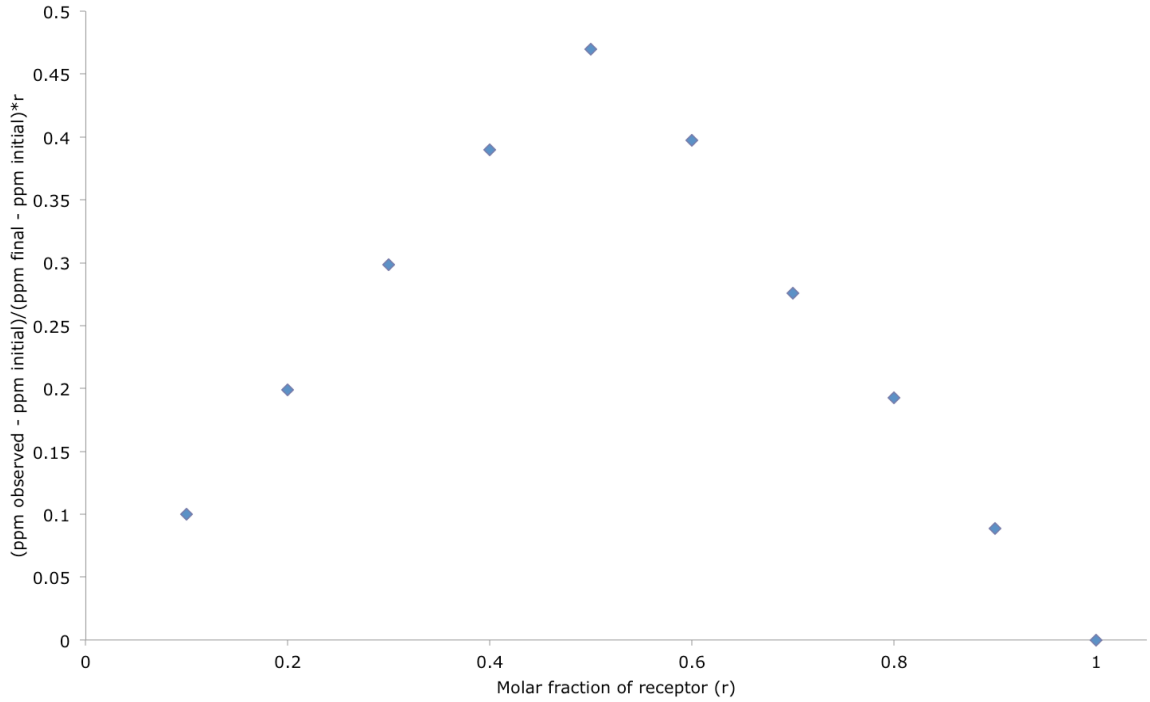

Figure S 131: a) Binding curve generated from the ^{1}H NMR titration of **10** with $TEAHCO_3$ in DMSO-d_6/H_2O 0.5%. The data was fitted to a 1:1 receptor:anion binding isotherm using WinEQNMR2. b) Stack plot generated from the ^{1}H NMR Job plot data of **10** with $TEAHCO_3$ in DMSO-d_6/H_2O 0.5%. c) The binding ratio was confirmed to be 1:1 receptor:anion by Job plot analysis of **10** with $TEAHCO_3$ in DMSO-d_6/H_2O 0.5%, despite the large error in the titration fitting.

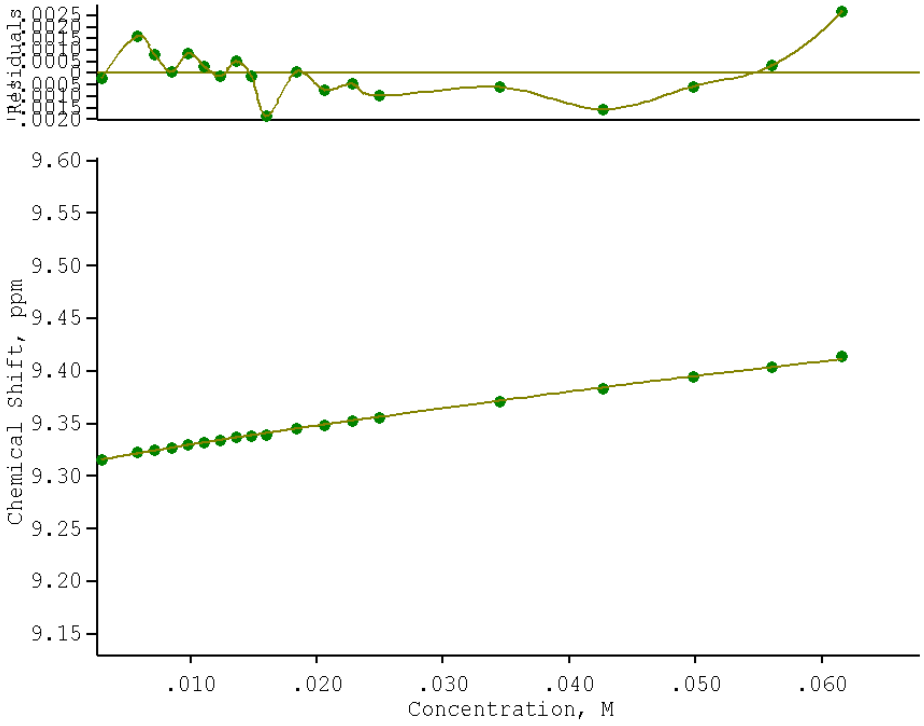

$K_1 = 4\ M^{-1} \pm 17\%$

Figure S 132: Binding curve generated from the ^{1}H NMR titration of **10** with $TBANO_3$ in DMSO-d_6/H_2O 0.5%. The data was fitted to a 1:1 receptor:anion binding model using WinEQNMR2.

S11: Crystal Structures

X-ray data for the chloride complex of **10** (TBA salt) were collected on Rigaku AFC12 goniometer equipped with an enhanced sensitivity (HG) Saturn 724+ detector mounted at the window of an FR-E+ Superbright MoKα (λ=0.71075Å) rotating anode generator with VHF Varimax optics.[3] X-ray data for the chloride complexes of **2** (TBA salt) and **6** (TMA salt) were collected on Rigaku AFC12 goniometer equipped with an enhanced sensitivity (HG) Saturn 724+ detector mounted at the window of an FR-E+ Superbright MoKα (λ=0.71075Å) rotating anode generator with HF Varimax optics. Data sets for all three structures were collected at 100 K. Empirical absorption corrections were carried out using CrystalClear software. The crystal structures were solved by direct methods as implemented in SHELXS-97.[4] Structures were refined on Fo^2 by full-matrix least-squares refinements using SHELX-97 software.[4]

All non-hydrogen atoms were refined with anisotropic displacement parameters. All hydrogen atoms were added at calculated positions and refined using a riding model with isotropic displacement parameters based on the equivalent isotropic displacement parameters (U_{eq}) of the parent atom. In the chloride complex of **2** a disorder model was included for the DMSO molecule and one of the butyl chains of one of the TBA cations present.

Crystal data for **10.TBACl**: $C_{29}H_{46}ClF_{10}N_3OS_2$, Mr = 742.26, orthorhombic, space group = P*bca*, a = 26.1622 (18), b = 17.7752 (11), c = 15.1251 (11), α = 90, β = 90, γ = 90, V = 7033.8 (8), Z = 8, μ = 0.308 mm^{-1}, D = 1.402 gcm^{-3}, Reflections collected = 44323, Unique = 8032 [R(int) = 0.0561], final R_1 = 0.0334, wR_2 = 0.0804, GoF = 0.990, data/restraints/parameters = 8032/ 0/ 415, CCDC: 1004419.

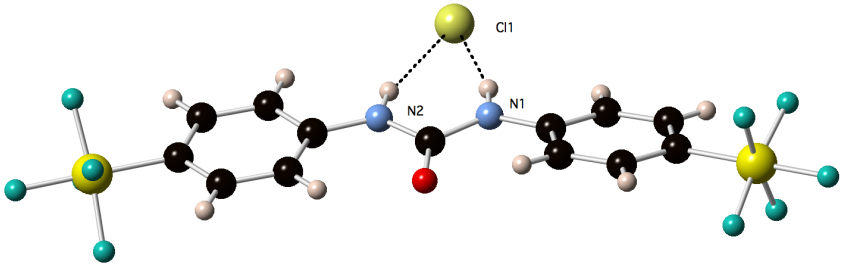

Figure S 133: **10.TBACl.**

Crystal data for **2.TBACl**: $C_{74}H_{110}Cl_2F_{20}N_{10}O_5S_5$, Mr = 1830.92, triclinic, space group = P -*1*, a = 15.6225 (11), b = 17.6830 (12), c = 18.4051 (13), α = 71.341 (5), β = 69.884 (5), γ = 67.950 (5), V = 4317.4 (5), Z = 2, μ = 0.293 mm^{-1}, D = 1.408 gcm^{-3}, Reflections collected = 32098, Unique = 15037 [R(int) = 0.0602], final R_1 = 0.0581, wR_2 = 0.1090, GoF = 0.988, data/restraints/parameters = 15037/ 18/ 1062, CCDC: 1004420.

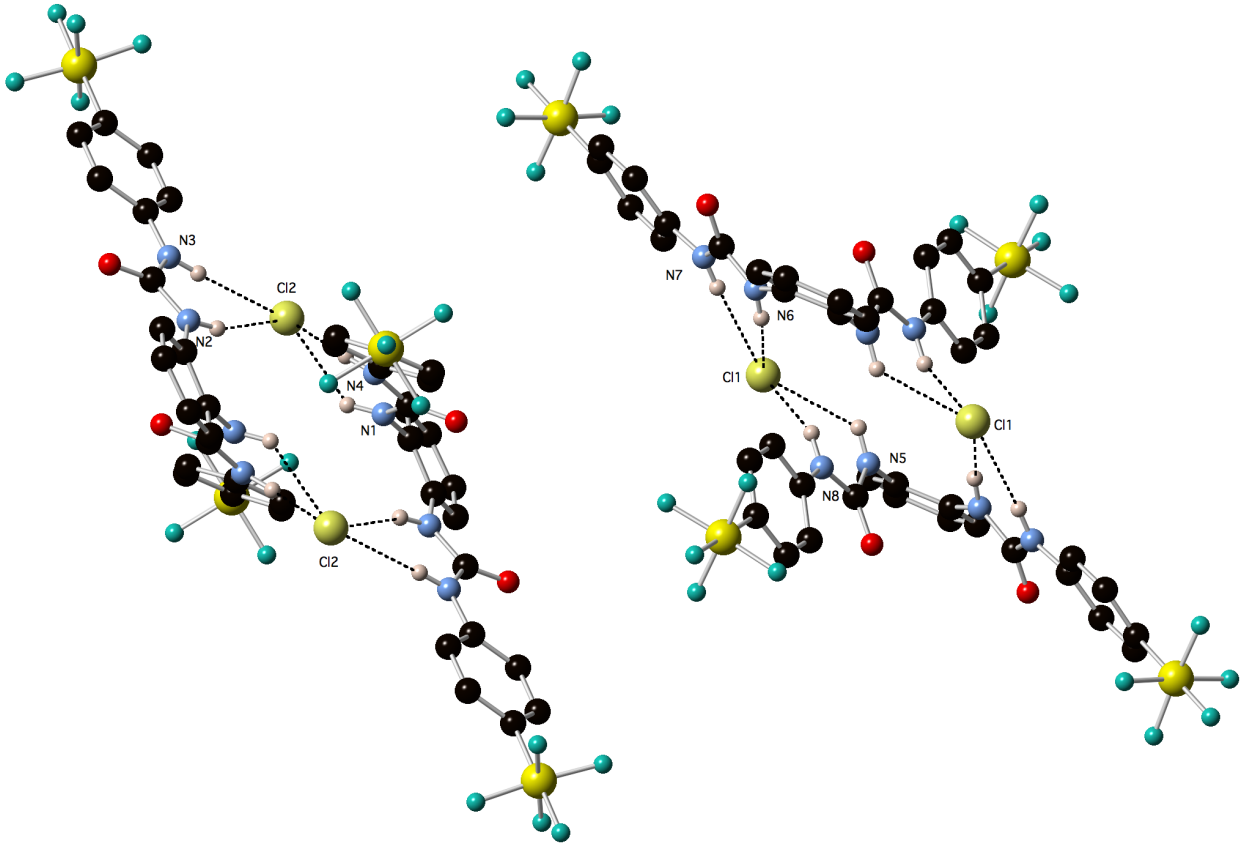

Figure S 134: Packing arrangement for **2.TBACl.**

Crystal data for **6.TMACl**: $C_{24}H_{26}ClF_2N_7O_6$, Mr = 581.97, monoclinic, space group = $P2_1/c$, a = 7.3305 (19), b = 23.581 (6), c = 15.409 (4), α = 90, β = 97.282 (4), γ = 90, V = 2642.1 (12), Z = 4, μ = 0.213 mm^{-1}, D = 1.463 gcm^{-3}, Reflections collected = 34443, Unique = 6057 [R(int) = 0.0373], final R_1 = 0.0548, wR_2 = 0.1113, GoF = 1170, data/restraints/parameters = 6057/ 0/ 361, CCDC: 1004421.

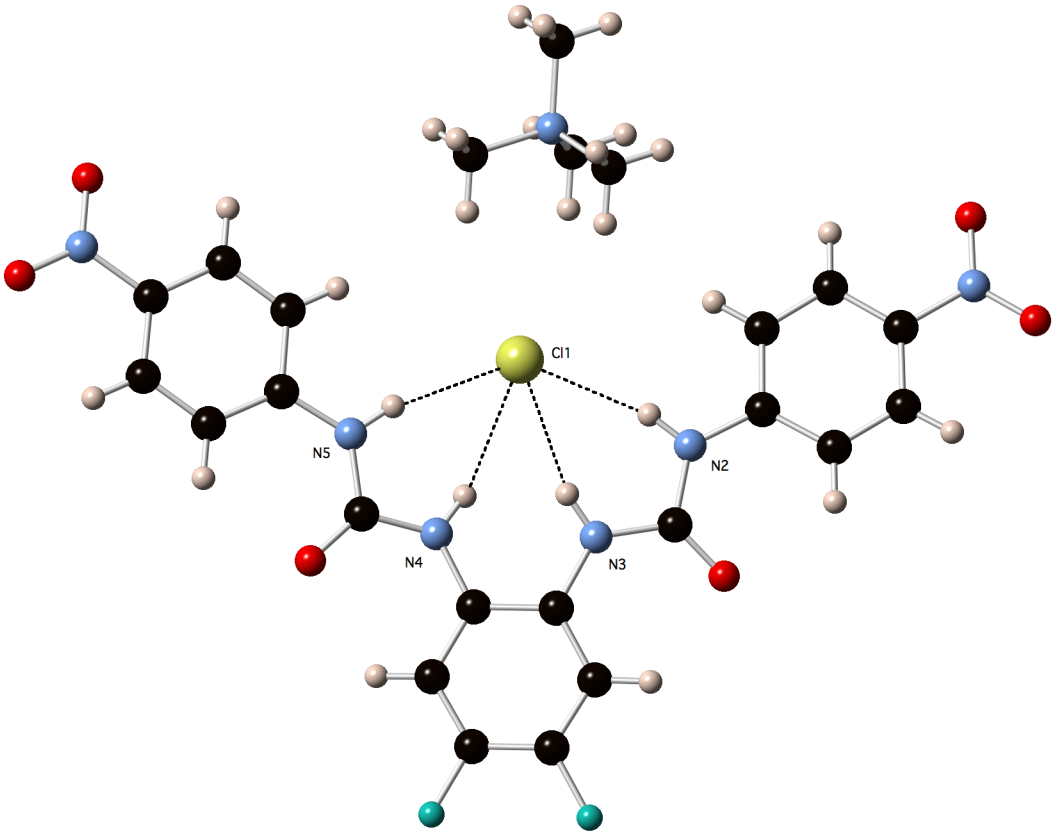

Figure S 135: Asymmetric unit cell for **6.TMACl.**

S12: References

1. MacDonald, R. C.; MacDonald, R. I.; Menco, B. P. M.; Takeshita, K.; Subbarao, N. K.; Hu, L.-r., Small-volume extrusion apparatus for preparation of large, unilamellar vesicles. *Biochimica et Biophysica Acta (BBA) - Biomembranes* **1991,** *1061* (2), 297-303.

2. Hynes, M. J., EQNMR: a computer program for the calculation of stability constants from nuclear magnetic resonance chemical shift data. *J. Chem. Soc., Dalton Trans.* **1993,** *0* (2), 311-312.

3. Coles, S. J. and Gale, P. A., Changing and challenging times for service crystallography. *Chem. Sci.*, **2012**, *3*, 683-689.

4. Sheldrick, G. M., A short history of SHELX. *Acta Cryst.*, **2008**, *A64*, 112-122.